

ABSTRACT BOOK

# RESEARCH OUTPUT 2015

By CIIT Lahore Faculty Membrs

**Library Inforamtion Services**

COMSATS INSTITUTE OF INFORMATION TECHNOLOGY LAHORE

# Table of Contents

✦ Preface: -----	02
✦ Summary/ Table: -----	03
✦ Department of Chemical Engineering: -----	04
Journal Articles: -----	04
✦ Department of Computer Science: -----	39
Journal Articles: -----	39
✦ Department of Electrical Engineering: -----	52
Journal Articles: -----	52
✦ Department of Humanities: -----	57
Journal Articles: -----	57
✦ Department of IRCBM: -----	72
Journal Articles: -----	72
✦ Department of Management Sciences: -----	122
Journal Articles: -----	122
✦ Department of Mathematics: -----	169
Journal Articles: -----	169
✦ Department of Physics: -----	205
Journal Articles: -----	205
✦ Department of Statistics: -----	268
Journal Articles: -----	268
✦ Miscellaneous: -----	277
Journal Articles: -----	277
✦ Author Index: -----	280

## ***Preface:***

CIIT is not only providing quality education, but also producing valued research publications. Due to this research work, the CIIT got its better ranking in Pakistan and Higher Education Commission declared CIIT at top ranking among Pakistani Universities. The credit goes to the researchers of CIIT, who, as usual, produced lots of papers in the year 2015. For this accomplishment, the contribution of researchers of CIIT Lahore is also extraordinary. They produced 408 journal papers during the year 2015. The compilation in your hands consists of the papers which published during the year 2015 and at CIIT platform. We only included journal papers for this anthology. The purpose of this compilation is to record the research work of our faculty members and also to facilitate the users to get all the research papers of all departments in one binding. Apart from the record, I am also sure that this compilation will provide the guidelines to new researchers of CIIT and to the researchers of other institutes, as well. I am very much thankful to worthy Director CIIT-Lahore Dr. Qaiser Abbas and Dr. Robbina Farooq, Convener Library Affairs Committee, they not only provided the guidelines, but also encourage us to prepare this compilation in appropriate form. I am also very much thankful to ORIC, which provided the data to compile this report. Without this help, it was very difficult to prepare this collection of research articles. Mr. Sajjad Ahmad Library Assistant also did a very good job to convert the data into information. He is really a good asset of the library.

With Regards

**Muhammad Tariq Najmi Incharge**

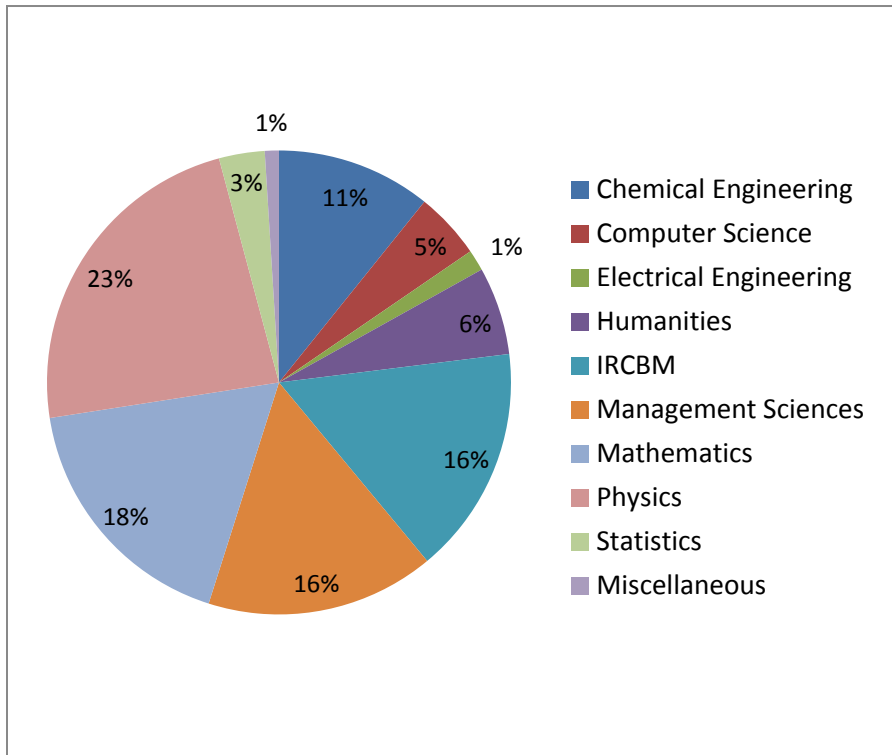
Library Information Services

CIIT-Lahore

August 30, 2016

## SUMMARY

DEPARTMENTS	JOURNAL PAPERS
CHEMICAL ENGINEERING	44
COMPUTER SCIENCE	19
ELECTRICAL ENGINEERING	6
HUMANITIES	25
IRCBM	65
MANAGEMENT SCIENCES	65
MATHEMATICS	72
PHYSICS	95
STATISTICS	13
MISCELLANEOUS	4
<b>Total</b>	<b>408</b>



# DEPARTMENT OF CHEMICAL ENGINEERING

## Journal Papers

1. Abbas, S., Hashmi, I., Rehman, M. S. U., Qazi, I. A., Awan, M. A., & Nasir, H. (2015). Monitoring of chlorination disinfection by-products and their associated health risks in drinking water of Pakistan. *Journal of water and health*, 13(1), 270-284.

### **ABSTRACT:**

This study reports the baseline data of chlorination disinfection by-products such as trihalomethanes (THMs) and their associated health risks in the water distribution network of Islamabad and Rawalpindi, Pakistan. THM monitoring was carried out at 30 different sampling sites across the twin cities for 6 months. The average concentration of total trihalomethanes (TTHMs) and chloroform ranged between 575 and 595  $\mu\text{g/L}$  which exceeded the permissible US (80  $\mu\text{g/L}$ ) and EU (100  $\mu\text{g/L}$ ) limits. Chloroform was one of the major contributors to the TTHMs concentration (>85%). The occurrence of THMs was found in the following order: chloroform, bromodichloromethane > dibromochloromethane > bromoform. Lifetime cancer risk assessment of THMs for both males and females was carried out using prediction models via different exposure routes (ingestion, inhalation, and dermal). Total lifetime cancer risk assessment for different exposure routes (ingestion, inhalation, and skin) was carried out. The highest cancer risk expected from THMs seems to be from the inhalation route followed by ingestion and dermal contacts. The average lifetime cancer risk for males and females was found to be  $0.51 \times 10^{-3}$  and  $1.22 \times 10^{-3}$ , respectively. The expected number of cancer risks per year could reach two to three cases for each city.

**Web URL:** <http://jwh.iwaponline.com/content/13/1/270.abstract>

2. Rehman, F., Medley, G. J., Bandulasena, H., & Zimmerman, W. B. (2015). Fluidic oscillator-mediated microbubble generation to provide cost effective mass transfer and mixing efficiency to the wastewater treatment plants. *Environmental research*, 137, 32-39.

**ABSTRACT:**

Aeration is one of the most energy intensive processes in the waste water treatment plants and any improvement in it is likely to enhance the overall efficiency of the overall process. In the current study, a fluidic oscillator has been used to produce microbubbles in the order of 100  $\mu\text{m}$  in diameter by oscillating the inlet gas stream to a pair of membrane diffusers. Volumetric mass transfer coefficient was measured for steady state flow and oscillatory flow in the range of 40–100 l/min. The highest improvement of 55% was observed at the flow rates of 60, 90 and 100 l/min respectively. Standard oxygen transfer rate and efficiency were also calculated. Both standard oxygen transfer rate and efficiency were found to be considerably higher under oscillatory air flow conditions compared to steady state airflow. The bubble size distributions and bubble densities were measured using an acoustic bubble spectrometer and confirmed production of monodisperse bubbles with approximately 100  $\mu\text{m}$  diameters with fluidic oscillation. The higher number density of microbubbles under oscillatory flow indicated the effect of the fluidic oscillation in microbubble production. Visual observations and dissolved oxygen measurements suggested that the bubble cloud generated by the fluidic oscillator was sufficient enough to provide good mixing and to maintain uniform aerobic conditions. Overall, improved mass transfer coefficients, mixing efficiency and energy efficiency of the novel microbubble generation method could offer significant savings to the water treatment plants as well as reduction in the carbon footprint.

**Web URL:** <http://www.sciencedirect.com/science/article/pii/S0013935114004320>

**3. Ahmad, F., Lau, K. K., Lock, S. S. M., Rafiq, S., Khan, A. U., & Lee, M. (2015). Hollow fiber membrane model for gas separation: Process simulation, experimental validation and module characteristics study. *Journal of Industrial and Engineering Chemistry*, 21, 1246-1257.**

**ABSTRACT:**

Conceptual process simulations and optimization are essential in the design, operation and troubleshooting stages of a membrane-based gas separation system. Despite this, there are few mathematical models/tools associated with a hollow fiber membrane module available in a

commercial process simulator. A mathematical model dealing with the hollow fiber module characteristics that can be included within a commercial process simulator is needed to examine the performance and economics of a gas separation system. In this study, a hollow fiber membrane model was incorporated in Aspen HYSYS as a user defined unit operation for the study of carbon dioxide separation from methane. The hollow fiber membrane model was validated experimentally. The study of a double stage membrane module with a permeate recycle, which was proposed to be the optimal configuration in previous studies, was extended to consider the effects of the module characteristics (such as the fiber length, radius of the fiber bundle, diameter of the fibers, and porosity) on the process performance and economics. The gas processing cost (GPC) increased with increasing fiber length and bundle radius, and decreased with increasing outer diameter of the fibers and porosity. At the same time, the separation efficiency (product quality) was also dependent on these module parameters. Therefore, the tradeoff for the hollow fiber membrane module characteristics needs to be determined based on the minimum GPC with respect to the desired product purity

**WEB URL:** <http://165.229.69.151/Publications/International%20Journal/2014JIECP1246.pdf>

**4. Rafiq, S., Maulud, A., Man, Z., Mutalib, M. I. A., Ahmad, F., Khan, A. U., ... & Muhammad, N. (2015). Modelling in mixed matrix membranes for gas separation. *The Canadian Journal of Chemical Engineering*, 93(1), 88-95.**

**ABSTRACT:**

Various gas permeation models including Maxwell model, Bruggeman model, Lewis-Nielson model and Pal model were compared via a modelling approach with the relative permeance of CO<sub>2</sub> against published experimental data on silica filled polysulfone/polyimide (PSF/PI) mixed matrix membranes (MMMs). However, none of the tested models were able to predict the data with good accuracy. A closer look at the cross-sectional image by scanning electron microscopy (SEM) indicated that the fillers were actually prolate ellipsoids dispersed within the matrix. Maxwell-Wagner-Sillars model was then employed to investigate the prolate effect and it was observed that the optimization curves of maximum packing ( $f_m$ ) and shape factor ( $n$ )

showed least deviations. The percentage average absolute relative error (AARE %) value for fitted shape factor ( $n_f$ ) was found to be in the range of 1.12–2.17 at 2–10 bar pressure which showed its robustness. A further evaluation from SEM image showed that the shape factor along z-direction ( $n_z$ ) displayed a minimum deviation of 17.52 % for prolates at 0.102 0.01. By using  $n_z$  as upper limit and estimated shape factor  $n_e$  through generalization, the error was reduced to 6.01 %. The AAR % deviation was found in the order of  $n_f < n_z$ , which indicated the importance of shape factor parameter for estimating true CO<sub>2</sub> permeance.

**WEB URL:**

[https://www.researchgate.net/profile/Nawshad\\_Muhammad/publication/266857328\\_Modelling\\_in\\_Mixed\\_Matrix\\_Membranes\\_for\\_Gas\\_Separation/links/54dd77c90cf28a3d93f94bfa.pdf](https://www.researchgate.net/profile/Nawshad_Muhammad/publication/266857328_Modelling_in_Mixed_Matrix_Membranes_for_Gas_Separation/links/54dd77c90cf28a3d93f94bfa.pdf)

**5. Lock, S. S. M., Lau, K. K., Ahmad, F., & Shariff, A. M. (2015) *International Journal of Greenhouse Gas Control*, 36. 114-135.**

**ABSTRACT:**

A mathematical model has been developed to characterize the multi-component CO<sub>2</sub> capture from natural gas adapting hollow fiber membrane module for the radial crossflow, countercurrent and cocurrent flow. The solution procedure can also be incorporated in a versatile manner within the Aspen HYSYS process simulator to constitute the entire CO<sub>2</sub>/natural gas separation plant in order to assist in the process design and optimization. The study of the separation performance and process economics of the different flow mechanisms has been conducted along with parameter sensitivity of typical membrane selectivity and CO<sub>2</sub> feed composition in industrial application. Based on the study's findings, ideally the countercurrent configuration exhibits a slightly higher separative performance in comparison to the radial crossflow, while both being superior to the cocurrent. It is also found that flow with the most effective separative performance is not always the most economical. Under circumstances of excessive permeation, it can lead to extra membrane area, auxiliary equipment power and hydrocarbon lost that increase the gas processing cost. Therefore, a tradeoff must be determined among these parameters to determine the optimal flow configuration for efficient CO<sub>2</sub> removal under different operating conditions.

**WEB URL:**

[https://www.researchgate.net/profile/Ssm\\_Lock/publication/273480379\\_Modeling\\_simulation\\_and\\_economic\\_analysis\\_of\\_CO2\\_capture\\_from\\_natural\\_gas\\_using\\_cocurrent\\_counter-current\\_and\\_radial\\_crossflow\\_hollow\\_fiber\\_membrane/links/563ab5b208ae45b5d284b5b5.pdf](https://www.researchgate.net/profile/Ssm_Lock/publication/273480379_Modeling_simulation_and_economic_analysis_of_CO2_capture_from_natural_gas_using_cocurrent_counter-current_and_radial_crossflow_hollow_fiber_membrane/links/563ab5b208ae45b5d284b5b5.pdf)

**6. Dong, R., Yang, W., Wu, P., Hussain, M., Wu, G., & Jiang, L. (2015). High content SiC nanowires reinforced Al composite with high strength and plasticity. *Materials Science and Engineering: A*, 630, 8-12.**

**ABSTRACT:**

Al matrix composites reinforced with one-dimensional nano-materials (for instance nanotubes, nanowires and nanofibres) have been widely investigated in the past decade. However, the preparation, microstructure and mechanical behavior of high content (>10 vol%) SiC nanowires reinforced Al (SiCnw/Al) has not been reported yet. In the present work, 15 vol% SiCnw/6061Al composite was prepared by the pressure infiltration method. SiCnw/6061Al composite demonstrated good machining performance since continuous chip was obtained after cut by carbide turning tools. SiC nanowires were uniformly distributed without any observance of SiC agglomerates. Long SiC nanowires were observed after etching, implying that the preparation process had shown minor damage to the SiC nanowires and therefore, the pressure infiltration method is a feasible and successful way to prepare high content SiCnw/Al composites. The interface between SiC nanowires and Al was well bonded, and no significant interfacial product was found. After aging treatment, 15 vol% SiCnw/6061Al composite demonstrated high strength (over 1000 MPa), while a comparable plasticity as Al matrix was retained. The strengthening effect of SiC nanowires could be fully utilized through the fracture of SiC nanowires. Moreover, the grain size of Al matrix in SiCnw/6061Al composite was significantly refined and polycrystalline diffraction rings were observed. Therefore, supplemented to previous results in one-dimensional nano-materials reinforced Al matrix composites, fine-grain was also found as another main strengthening mechanism.

**7. Piumetti, M., Hussain, M., Fino, D., & Russo, N. (2015). Mesoporous silica supported Rh catalysts for high concentration N<sub>2</sub>O decomposition. *Applied Catalysis B: Environmental*, 165, 158-168.**

**ABSTRACT:**

A set of Rh-containing catalysts (Rh-MCM-41, Rh-SBA-15, Rh-KIT-6 and Rh-MCF, nominal Rh content = 1 wt.%) has been prepared by wet impregnation of mesoporous silicas and tested for high concentration N<sub>2</sub>O abatement. The physico-chemical properties of the materials have been investigated by means of complementary techniques. The best performances, in terms of N<sub>2</sub>O decomposition, have been achieved for the Rh-MCF catalyst, due to the better textural properties of the MCF silica. In fact, the MCF-type support exhibits three-dimensional mesoporosity with ultra-large cells (up to 40 nm), which allow a uniform distribution of small RhO<sub>x</sub> particles (≈1 nm) over the high (internal) surface area of the MCF. Moreover, the Rh active sites are also readily accessible to N<sub>2</sub>O molecules. The most promising catalyst has shown the highest amount of Rh<sup>1+</sup> species, the easiest rhodium reducibility and the greatest abundance of Rh surface sites. These important features reflect the different Rh particle sizes and play a role in catalytic activity. A remarkable relationship between the catalytic activity and the dimension of the RhO<sub>x</sub> particles has been observed in the 1–2.5 nm size domain, thus confirming the dispersion-sensitivity of N<sub>2</sub>O decomposition over RhO<sub>x</sub> nanoparticles.

**WEB URL:**

[https://www.researchgate.net/publication/267226366\\_Mesoporous\\_silica\\_supported\\_Rh\\_catalysts\\_for\\_high\\_concentration\\_N2O\\_decomposition](https://www.researchgate.net/publication/267226366_Mesoporous_silica_supported_Rh_catalysts_for_high_concentration_N2O_decomposition)

**8. Xiu, Z., Yang, W., Dong, R., Hussain, M., Jiang, L., Liu, Y., & Wu, G. (2015). Microstructure and Mechanical Properties of 45 vol.% SiC p/7075Al Composite. *Journal of Materials Science & Technology*, 31(9), 930-934.**

**ABSTRACT:**

Microstructure and mechanical behavior of high volume content SiC<sub>p</sub>/7xxxAl composites have not been explored yet. Therefore, in the present work, 45 vol.% SiC<sub>p</sub>/7075Al composite has been prepared by pressure infiltration method. High density dislocations were found around SiC/Al interface in SiC<sub>p</sub>/7075Al composite after water-quenching and aging treatment. Fine dispersed nano-η' phases were observed after the aging treatment. Adverse to other SiC<sub>p</sub>/Al composites prepared by the pressure infiltration method, an interface layer was observed between SiC particles and Al matrix. Furthermore, high-resolution transmission electron microscopy (HRTEM) observation indicated that this interface layer was coherent/semi-coherent with that of the SiC particles. 45 vol.% SiC<sub>p</sub>/7075Al composite demonstrated high tensile strength (630 MPa) and micro-ductility. Compared to aged SiC<sub>p</sub>/2024Al composite, the aged SiC<sub>p</sub>/7075Al composite showed an increase of about 200% in the tensile strain and 90% in the tensile strength, respectively. It is speculated that nano-η' phases in the Al matrix significantly contributed to the strengthening effect while the interface layer between SiC and Al matrix might be beneficial to the strength and plasticity of SiC<sub>p</sub>/7075Al composite.

**WEB URL:** <http://www.sciencedirect.com/science/article/pii/S100503021500081X>

**9. Dong, R., Yang, W., Wu, P., Hussain, M., Xiu, Z., Wu, G., & Wang, P. (2015). Microstructure characterization of SiC nanowires as reinforcements in composites. *Materials Characterization*, 103, 37-41.**

**ABSTRACT:**

SiC nanowires have been rarely investigated or explored along their axial direction by transmission electron microscopy (TEM). Here we report the investigation of the cross-section microstructure of SiC nanowires by embedding them into Al matrix. Morphology of SiC nanowires was cylindrical with smooth surface or bamboo shape. Cubic (3C-SiC) and hexagonal structure (2H-SiC) phases were detected by X-ray diffraction (XRD) analysis. High density stacking faults were observed in both the cylindrical and bamboo shaped nanowires which were perpendicular to their axial direction. Selected area electron diffraction (SAED) patterns of

the cylindrical and bamboo shaped SiC nanowires both in the perpendicular and parallel direction to the axial direction were equivalent in the structure. After calculation and remodeling, it has been found that the SAED patterns were composed of two sets of diffraction patterns, corresponding to 2H-SiC and 3C-SiC, respectively. Therefore, it could be concluded that the SiC nanowires are composed of a large number of small fragments that are formed by hybrid 3C-SiC and 2H-SiC structures.

**WEB URL:** <http://www.sciencedirect.com/science/article/pii/S1044580315000728>

**10. Akhter, P., Hussain, M., Saracco, G., & Russo, N. (2015). Novel nanostructured-TiO<sub>2</sub> materials for the photocatalytic reduction of CO<sub>2</sub> greenhouse gas to hydrocarbons and syngas. *Fuel*, 149, 55-65.**

**ABSTRACT:**

In the current work an attempt has been made to synthesize novel high surface area nano-TiO<sub>2</sub> materials (titanium dioxide nanoparticles/TNPs and nanostructured or mesoporous titanium dioxide using KIT-6 silica template/Meso. TiO<sub>2</sub>) in order to establish the photocatalytic reduction of CO<sub>2</sub> greenhouse gas in the presence of H<sub>2</sub>O vapor to produce hydrocarbons and syngas. The synthesized materials have been characterized through N<sub>2</sub>-adsorption/desorption, X-ray diffraction (XRD), field emission scanning electron microscopy (FE-SEM) and ultraviolet-visible (UV-Vis) spectroscopy analysis techniques. The TNPs consists of an average 11 nm of TiO<sub>2</sub> particles, shows a higher surface area of 151 m<sup>2</sup>/g than the commercial Aeroxide P25 TiO<sub>2</sub> (53 m<sup>2</sup>/g), and also demonstrates an enhanced adsorption capacity. However, the Meso. TiO<sub>2</sub> has shown a higher surface area (190 m<sup>2</sup>/g) and mesoporosity (4 nm pores) than the TNPs and Aeroxide P25 TiO<sub>2</sub>, as confirmed by the characterizations. In the reaction, the TNPs with the enhanced adsorption capability, due to the high surface area and smaller nano-sized particle morphology, showed a higher syngas (CO, H<sub>2</sub>) production than the commercial Aeroxide P25 TiO<sub>2</sub>. However, the novel Meso. TiO<sub>2</sub> showed more hydrocarbons (CH<sub>4</sub>, CH<sub>3</sub>OH) and a higher syngas production together with better reaction kinetics and stability due to its better characteristics than the commercial Aeroxide P25 TiO<sub>2</sub>. The key parameters that affect the

activity have been optimized to increase fuel production. The reaction mechanism indicates competitive adsorption of CO<sub>2</sub> and H<sub>2</sub>O vapors on the catalyst surface. The key parameters including the UV light source and UV intensity, H<sub>2</sub>O/CO<sub>2</sub> ratios and catalyst shapes influence the catalytic performance, and therefore, these parameters have been optimized to increase the fuel products. Partial saturation of the active adsorption sites and the oxygen produced are the possible causes of the deactivation, however, the catalysts can be regenerated quickly through a simple evaporation technique.

**WEB URL:** <http://www.sciencedirect.com/science/article/pii/S001623611400948X>

**11. Hussain, M., Deorsola, F. A., Russo, N., Fino, D., & Pirone, R. (2015). Abatement of CH<sub>4</sub> emitted by CNG vehicles using Pd-SBA-15 and Pd-KIT-6 catalysts. *Fuel*, 149, 2-7.**

**ABSTRACT:**

Compressed Natural Gas (CNG) engines are growing in interest in the car market due to their ability in the limitation of NO<sub>x</sub> and CO<sub>2</sub> emissions. Unburned methane is harder to oxidize than gasoline-derived unconverted HCs and its strong greenhouse effect induces the development of tailored after treatment technologies. In this work, SBA-15 and in particular KIT-6 have been used as supports for Pd catalysts for the abatement of methane emitted by CNG engines. The synthesized materials have been characterized through XRD, N<sub>2</sub>-adsorption/desorption, EDX, STEM, and TEM analysis techniques. The influence of different pore structure and size of the mesoporous supports as well as of different Pd loading (in the range 0.25–0.7 wt%) on the activity has been investigated. All mesoporous silica supported Pd catalysts showed almost complete conversion of methane, although catalysts with the lowest Pd loadings reached 90% of conversion over 650 °C, whereas the maximum Pd loadings allowed to decrease the temperature of complete conversion, with T<sub>90</sub> at 405 °C by employing the KIT-6 mesoporous silica support.

**WEB URL:** <http://www.sciencedirect.com/science/article/pii/S0016236114012332>

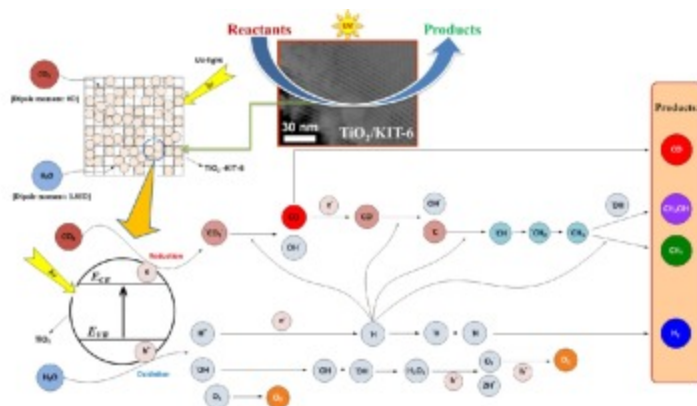
12. Hussain, M., Akhter, P., Saracco, G., & Russo, N. (2015). Nanostructured TiO<sub>2</sub>/KIT-6 catalysts for improved photocatalytic reduction of CO<sub>2</sub> to tunable energy products. *Applied Catalysis B: Environmental*, 170, 53-65.

**ABSTRACT:**

Nanostructured TiO<sub>2</sub>/KIT-6 catalysts with different concentrations of incorporated TiO<sub>2</sub>, have been synthesized, characterized, and examined in order to improve the photocatalytic reduction of carbon dioxide (CO<sub>2</sub>) feedstock with water vapor (H<sub>2</sub>O) to produce tunable value-added energy products. Nanostructured TiO<sub>2</sub>, dispersed on KIT-6 (three-dimensional mesoporous silica), was found to be present in both the silica framework and on the surface, where it produced large surface area photocatalysts with enhanced adsorption capability of the reactants to photocatalytically convert into CH<sub>4</sub>, CH<sub>3</sub>OH (hydrocarbons) and CO, H<sub>2</sub> (similar to syngas). The formed products were influenced directly by the dispersed TiO<sub>2</sub> concentration as well as by the calcination temperature. Hydrocarbon and CO formation as well as the reaction kinetics improved as the TiO<sub>2</sub> concentration was increased from 1 to 20 wt%. However, a further increase in TiO<sub>2</sub> loadings (to 90%) decreased the hydrocarbon and CO, and increased H<sub>2</sub> formation. The highest optimization toward hydrocarbon selectivity was shown by 20 wt% TiO<sub>2</sub>, while a 90 wt% TiO<sub>2</sub> loading was more selective for H<sub>2</sub> formation. This was likely due to the uniform dispersion and stabilization of the anatase TiO<sub>2</sub> with 20 wt% on KIT-6, which in turn allowed more CO<sub>2</sub> adsorption and a better light penetration than 90% TiO<sub>2</sub>/KIT-6 in which it showed a bulk phase and large agglomerates with light penetration limitations that were more favorable for H<sub>2</sub>O adsorption. A reaction mechanism, which has helped to understand these findings, has been proposed. Moreover, a 24 h activity test with the optimized 20 wt% TiO<sub>2</sub>/KIT-6 showed an increase in the product yield but only a minor, gradual decrease in the reaction rate, which points out that these photocatalysts could be promising for turning CO<sub>2</sub> greenhouse gas feedstock into selective renewable energy products.

---

Graphical abstract



**WEB URL:** <http://www.sciencedirect.com/science/article/pii/S0926337315000120>

**13. Khan, Z., Inayat, A., Yusup, S., & Ahmad, M. M. (2015). Kinetic parameters determination using optimization approach in integrated catalytic adsorption steam gasification for hydrogen production. *International Journal of Hydrogen Energy*, 40(29), 8824-8832.**

**ABSTRACT:**

Integrated catalytic adsorption (ICA) gasification provides an efficient mean to produce hydrogen rich gas. This article presents the prospect of ICA steam gasification of palm kernel shell. The effect of temperature, steam to biomass ratio and adsorbent to biomass are investigated for H<sub>2</sub>, CO, CO<sub>2</sub> and CH<sub>4</sub> composition to determine kinetic parameters by minimizing the error between experimental and modelling results. Based on the evaluated kinetic parameters, the model predicts the product gas composition for the effect of temperature, steam to biomass ratio and adsorbent to biomass ratio. A significant fitting of model predicted values to the experimental results is achieved. Furthermore, it is also found that the water gas shift reaction is non-spontaneous and far away from the equilibrium at a temperature range of 600 Ce675 C which may be due to strong CO<sub>2</sub> adsorption reaction.

**WEB URL:**

[https://www.researchgate.net/profile/Zakir\\_Khan6/publication/278743802\\_Kinetic\\_parameters\\_determination\\_using\\_optimization\\_approach\\_in\\_integrated\\_catalytic\\_adsorption\\_steam\\_gasification\\_for\\_hydrogen\\_production/links/55d7081e08ae9d65948c28e2.pdf](https://www.researchgate.net/profile/Zakir_Khan6/publication/278743802_Kinetic_parameters_determination_using_optimization_approach_in_integrated_catalytic_adsorption_steam_gasification_for_hydrogen_production/links/55d7081e08ae9d65948c28e2.pdf)

**14. Choi, K. H., Siddiqui, G. U., Yang, B. S., & Mustafa, M. (2015). Synthesis of ZnSnO<sub>3</sub> nanocubes and thin film fabrication of (ZnSnO<sub>3</sub>/PMMA) composite through electrospray deposition. *Journal of Materials Science: Materials in Electronics*, 26(8), 5690-5696.**

**ABSTRACT:**

A composite of zinc stannate (ZnSnO<sub>3</sub>) nanocubes and poly(methyl methacrylate) (PMMA) has been prepared and deposited on a flexible substrate polyethylene terephthalate (PET) through electrospray deposition (ESD). This fabrication technique has been found very effective for deposition of this composite as thin film. ZnSnO<sub>3</sub> is an inorganic biocompatible and piezoelectric material while PMMA is a transparent and durable organic polymer material. ZnSnO<sub>3</sub> nanocubes have been synthesized via an aqueous solution method and ZnSnO<sub>3</sub>/PMMA composite has been deposited as thin film on PET through ESD. The average layer thickness of the as deposited ZnSnO<sub>3</sub>/PMMA composite film on PET was found to be 149 nm. Morphological and structural characterization of ZnSnO<sub>3</sub> nanocubes through FESEM and XRD showed its size uniformity and crystalline nature. The size of the ZnSnO<sub>3</sub> nanocubes was estimated by FESEM analysis which was around 50–70 nm. The chemical composition has been investigated with the help of FTIR and Raman spectroscopy. The optical characterization of as deposited ZnSnO<sub>3</sub>/PMMA composite film through UV/Vis spectroscopy showed an average transmittance of around 92 % and electrical characterization exhibited resistivity of approximately  $50 \times 10^5 \Omega \text{ cm}$ . This dielectric nature of ZnSnO<sub>3</sub>/PMMA composite film indicates that this composite material can be employed as dielectric layer in printed electronics.

**WEB URL:** <http://link.springer.com/article/10.1007/s10854-015-3121-1>

**15. Mustafa, M., Sherin, L., Kim, H. C., Lee, Y. W., & Choi, K. H. (2015). Fabrication and conduction mechanism evaluation of polyfluorene polymeric Schottky diode. *Polymers for Advanced Technologies*, 26(9), 1109-1113.**

**ABSTRACT:**

A thin film of polyfluorene polymer was sandwiched between a conductive polymer deposited on silver nanowire and metal electrode to form a multilayer polymer-based diode device. The electrical properties of fabricated polymeric diode have been studied by current–voltage method. The current–voltage characteristics of the fabricated device exhibited non-ideal, asymmetrical, and rectifying behavior. Ohmic current conduction mechanism was observed in the device at low voltage. At higher voltage values, the space-charge-limited current conduction mechanism was found to be dominated. The values of the Schottky barrier height, ideality factor, and saturation current density were extracted according to the standard thermionic emission model and discussed. The barrier height and ideality factor were calculated as 0.72 eV and 2.53, respectively. Copyright © 2015 John Wiley & Sons, Ltd.

**WEB URL:** <http://onlinelibrary.wiley.com/doi/10.1002/pat.3542/full>

**16. Muhammad, N., Gao, Y., Khan, M. I., Khan, Z., Rahim, A., Iqbal, F., & Iqbal, J. (2015). Effect of ionic liquid on thermo-physical properties of bamboo biomass. *Wood Science and Technology*, 49(5), 897-913.**

**ABSTRACT:**

In this work, [Emim]Gly ionic liquid was used for the pretreatment of bamboo biomass followed by regeneration of cellulose-rich material. Thermal degradation study of untreated bamboo and cellulose-rich material was carried out under dynamic condition using thermogravimetric analysis. Free kinetics models of Kissinger, Ozawa, Flynn–Wall–Ozawa, and Kissinger–Akahira–Sunose were used to determine the kinetic parameters of thermal degradation process. The pattern of activation energy ( $E_a$ ) values with respect to % conversion values was noted different for the aforementioned models. The  $E_a$  calculated using the Kissinger method were 184 and 156 kJ mol<sup>-1</sup>, and Ozawa method were 185 and 157 kJ mol<sup>-1</sup> of untreated and treated sample of bamboo, respectively, while the values of  $E_a$  calculated by Flynn–Wall–Ozawa and Kissinger–Akahira–Sunose were 71.7–203.4 kJ mol<sup>-1</sup> and 281.7–230.7 kJ mol<sup>-1</sup> for untreated and treated sample of bamboo, respectively. Calorific and CHNS values of both untreated and

regenerated cellulose-rich material were measured by bomb calorimeter and elemental analyzer (CHNS), respectively. Both the calorific value and carbon content of the regenerated cellulose-rich material (15.62 J/kg, 37.86 %, respectively) were found to be less than those of untreated bamboo (17.40 J/kg and 43.14 %, respectively). The bamboo and regenerated cellulose-rich material were investigated by X-ray diffraction and X-ray Photoelectron Spectroscopy, and changes in the cellulose crystalline structure were correlated with thermal degradation behavior and kinetics parameters.

**WEB URL:** <http://link.springer.com/article/10.1007/s00226-015-0736-6>

**17. Ajmal, M., Yunus, U., Matin, A., & Haq, N. U. (2015). Synthesis, characterization and in vitro evaluation of methotrexate conjugated fluorescent carbon nanoparticles as drug delivery system for human lung cancer targeting. *Journal of Photochemistry and Photobiology B: Biology*, 153, 111-120.**

**ABSTRACT:**

Nanotechnology based cancer therapeutics have rapidly advanced towards the solution of many limitations associated with other drug delivery agents such as nonspecific distribution within the body, low water solubility and non-biocompatibility. Carbon nanoparticles have demonstrated unique properties that are useful to combat with these issues, including their properties dependent on size, high stability in different solvents, compatible size for drug delivery and ease of surface modifications. Fluorescent carbon nanoparticles with good water solubility were obtained from a carbohydrate source by acid assisted ultrasonic treatment at 35 kHz for 4 h. This simple and economical method can be used for large scale production. Electron microscopic, spectroscopic and thermo gravimetric analysis techniques were used to characterize these carbon nanoparticles. Functionalized CNPs were further conjugated with anticancer drug-methotrexate and used as fluorescent nano-carriers. In this research work, we determined the in vitro bioactivity of CNPs-methotrexate conjugates by lactate dehydrogenase assay, cell adhesion assay and sulforhodamine B assay in human lung carcinoma cell line

(H157). The CNPs showed promising biocompatibility and CNPs-MTX conjugates demonstrated potent cytotoxic effects and high anticancer activities in human lung cancer cell line.

**WEB URL:**

[https://www.researchgate.net/profile/Abdul\\_Matin5/publication/282126582\\_Synthesis\\_characterization\\_and\\_in\\_vitro\\_evaluation\\_of\\_methotrexate\\_conjugated\\_fluorescent\\_carbon\\_nanoparticles\\_as\\_drug\\_delivery\\_system\\_for\\_human\\_lung\\_cancer\\_targeting/links/562cec9508aef25a24431220.pdf](https://www.researchgate.net/profile/Abdul_Matin5/publication/282126582_Synthesis_characterization_and_in_vitro_evaluation_of_methotrexate_conjugated_fluorescent_carbon_nanoparticles_as_drug_delivery_system_for_human_lung_cancer_targeting/links/562cec9508aef25a24431220.pdf)

**18. Khan, A. L., Sree, S. P., Martens, J. A., Raza, M. T., & Vankelecom, I. F. (2015). Mixed matrix membranes comprising of matrimid and mesoporous COK-12: Preparation and gas separation properties. *Journal of Membrane Science*, 495, 471-478.**

**ABSTRACT:**

Novel ordered mesoporous COK-12 type silica particles were used as fillers in polyimide (Matrimid) based mixed-matrix membranes (MMMs). The highly ordered 2D hexagonal structured filler materials with short and straight pores were synthesized at room temperature under quasi-neutral pH. The gas permeation and SEM results of the MMMs confirmed a homogenous filler dispersion and defect free synthesis of membranes. The presence of large mesopores in the fillers leading to faster diffusion of penetrant gas resulted in higher gas permeabilities in comparison to pristine Matrimid membrane. The potential of the membrane under mixed-gas conditions and different operating temperatures was also evaluated. The membranes showed decreasing trend of activation energy of permeation with the addition of filler. The ease of synthesis, highly ordered structure with short and straight pore channels and improved gas permeation properties makes COK-12a promising filler for industrial gas separations.

**WEB URL:** <http://www.sciencedirect.com/science/article/pii/S0376738815301022>

**19. Anjum, M. W., de Clippel, F., Didden, J., Khan, A. L., Couck, S., Baron, G. V., ... & Vankelecom, I. F. J. (2015). Polyimide mixed matrix membranes for CO<sub>2</sub> separations using carbon-silica nanocomposite fillers. *Journal of Membrane Science*, 495, 121-129.**

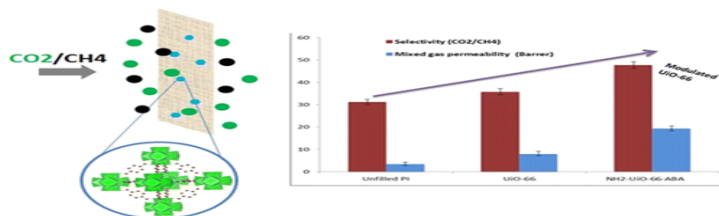
## ABSTRACT:

Mixed matrix membranes (MMMs) have a potential to improve the separation performance of polymeric membranes while maintaining their advantages of easy processing and lower costs. In this work, series of MMMs were developed via solution casting by adding porous carbon–silica nanocomposite (CSM) fillers to a readily available Matrimid® membrane. CSMs were prepared by a hard template synthesis technique to get a tuneable porosity and surface chemistry which is controlled by the optimization of the filler porosity using carbon deposition, the pyrolysis conditions, and the maximization of polarity via oxygen functional groups. SEM images of the synthesized MMMs confirmed the good adhesion and dispersion of the fillers within the polymer matrix. The separation results demonstrate that the overall separation efficiency is increased by the addition of a carbon phase, providing an increased affinity for the CO<sub>2</sub> gas molecules next to the creation of extra porosity and free volume. It was showed that significantly improved CO<sub>2</sub> mixed gas selectivity and permeability for CO<sub>2</sub>:N<sub>2</sub> and CO<sub>2</sub>:CH<sub>4</sub> gas mixtures at 9 bar and 308 K was achieved. For gas mixtures with a 50:50 (CO<sub>2</sub>:N<sub>2</sub>) feed composition, a 2-fold and 6-fold increase of the mixed gas selectivity (up to 42.5) and permeability (up to 27 Barrer) compared to unfilled PI was achieved, respectively. The performance of the membranes was compared to the existing literature data.

**WEB URL:** <http://www.sciencedirect.com/science/article/pii/S0376738815301010?np=y>

20. Anjum, M. W., Vermoortele, F., Khan, A. L., Bueken, B., De Vos, D. E., & Vankelecom, I. F. (2015). Modulated UiO-66-Based Mixed-Matrix Membranes for CO<sub>2</sub> Separation. *ACS applied materials & interfaces*, 7(45), 25193-25201.

## ABSTRACT:



Mixed-matrix membranes (MMMs) composed of polyimide (PI) and metal–organic frameworks (MOFs) were synthesized using Matrimid as the polymer and zirconium terephthalate UiO-66 as the filler. The modulation approach, combined with the use of amine-functionalized linkers, was used for synthesis of the MOF fillers in order to enhance the intrinsic separation performance of the MOF and improve the particle–PI compatibility. The presence of amine groups on the MOF outer surface introduced either through the linker, through the modulator, or through both led to covalent linking between the fillers and Matrimid, which resulted in very stable membranes. In addition, the presence of amine groups inside the pores of the MOFs and the presence of linker vacancies inside the MOFs positively influenced CO<sub>2</sub> transport. MMMs with 30 wt % loading showed excellent separation performance for CO<sub>2</sub>/CH<sub>4</sub> mixtures. A significant increase in the mixed-gas selectivity (47.7) and permeability (19.4 barrer) compared to the unfilled Matrimid membrane (i.e., 50% more selective and 540% more permeable) was thus achieved for the MMM containing the MOF prepared from 2-aminoterephthalic acid and 4-aminobenzoic acid, respectively used as the linker and as the modulator.

**WEB URL:** <http://pubs.acs.org/doi/abs/10.1021/acsami.5b08964>

**21. Dong, R., Yang, W., Wu, P., Hussain, M., Yu, Z., Jiang, L., & Wu, G. (2015). Effect of reinforcement shape on the stress–strain behavior of aluminum reinforced with SiC nanowire. *Materials & Design*, 88, 1015-1020.**

**ABSTRACT:**

The effect of surface morphology of SiC nanowires on mechanical properties of Al matrix composite was investigated. Four kinds of SiC nanowires (bamboo shaped SiC nanowires contents were 14.6%, 24.9%, 36.2% and 45.3%, respectively) have been selected to prepare composites by pressure infiltration method with the same volume fraction (15 vol.%). The SiC nanowires and Al matrix were well bonded and no significant interfacial product was found in the composites. With the increase of bamboo shaped nanowires content (from 14.6% to 45.3%), the tensile strength and elongation were increased 8% and 57%, respectively. Different

to cylindrical with smooth surface, negligible pull-out of bamboo shaped SiC nanowires was observed. The effect of bamboo shaped SiC nanowires on the mechanical properties of composites has been discussed in detailed. It is suggested that the improvement in the tensile strength and elongation of the SiC NWs/6061Al composites could be attributed mainly to the improvement of the interfacial bonding and the increased of interfacial area.

**WEB URL:** <http://www.sciencedirect.com/science/article/pii/S0264127515305104>

**22. Dong, R., Yang, W., Yu, Z., Wu, P., Hussain, M., Jiang, L., & Wu, G. (2015). Aging behavior of 6061Al matrix composite reinforced with high content SiC nanowires. *Journal of Alloys and Compounds*, 649, 1037-1042.**

**ABSTRACT:**

The aging behavior of Al matrix composites reinforced with high content nano-reinforcements has been rarely reported. In the present work, the aging behavior of 15 vol.% SiCnw/6061Al composite prepared by pressure infiltration method has been investigated. GP zones,  $\beta''$  ( $Mg_5Si_6$ ) and B' ( $MgSi_{>1}$ ) were observed as the main precipitates in under-aged, peak-aged and over-aged SiCnw/6061Al composite, respectively. After addition of high content SiC nanowires, the precipitation sequence of 6061Al has changed from "GP zones  $\rightarrow$   $\beta''$  ( $Mg_5Si_6$ )  $\rightarrow$   $\beta'$  ( $Mg_{1.8}Si$ )  $\rightarrow$   $\beta$  ( $Mg_2Si$ )" to "GP zones  $\rightarrow$   $\beta''$  ( $Mg_5Si_6$ )  $\rightarrow$  B' ( $MgSi_{>1}$ )". Due to their higher surface energy and larger surface areas of SiC nanowires, the segregation of Mg element is very serious, leading to insufficient Mg amount to form high Mg precipitates. Moreover, the hardness of SiCnw/6061Al composite was decreased much faster than that of 6061Al alloy in the over-aging period, which might be due to the inferior strengthening effect and/or low dispersivity of B' phase.

**WEB URL:** <http://www.sciencedirect.com/science/article/pii/S0925838815306319>

**23. Yang, W., Dong, R., Yu, Z., Wu, P., Hussain, M., & Wu, G. (2015). Strengthening behavior in high content SiC nanowires reinforced Al composite. *Materials Science and Engineering: A*, 648, 41-46.**

**ABSTRACT:**

Recently, it has been found that the larger surface areas of SiC nanowires have significant effect on the microstructure and performance of composites. The strengthening effect of SiC nanowires is preceded to the traditional micron-scale reinforcements. However, the strengthening behavior and corresponding model of the SiCnw/6061Al composite has not been understood yet. Therefore, in the present work, SiCnw/6061Al composites with different fractions (10, 15 and 20 vol%) have been prepared by pressure infiltration method. The effect of SiC nanowires' amount on the microstructure and the mechanical properties of SiCnw/Al composites has been investigated. The interface between SiC nanowires and Al matrix was well bonded and free of interfacial reaction products regardless of heat treatments. The tensile strength of annealed SiCnw/6061Al composites was increased with the content of SiC nanowires. However, the tensile strength of aged SiCnw/6061Al composite was reached to its maximum at 15 vol%, which should be attributed to the higher porosity of the composites. The yield strength was increased with the content of SiC nanowires, and the strengthening behavior of SiCnw/6061Al composites could be described by the modified shear-lag model. The strengthening factor (the slope of  $\sigma_{cy}-Vr$  curves) of SiCnw/6061Al composites is much higher than that of Al composite reinforced with particulates and short whiskers.

WEB URL: <http://www.sciencedirect.com/science/article/pii/S0921509315303816>

**24. Yang, W., Dong, R., Jiang, L., Wu, G., & Hussain, M. (2015). Unstable stacking faults in submicron/micron Al grammings in multi-SiCp/multi-Al nanocomposite. *Vacuum*, 122, 1-5.**

**ABSTRACT:**

It is difficult to obtain planar defects in aluminum due to its high stacking fault energy, in particular in submicron/micron Al grains. In this work we provide evidence for planar defects in submicron/micron Al grain of composites with multi nano-particles by transmission electron microscope observations. Nano-SiC particles (<100 nm) were found within micron-Al grains (>2  $\mu\text{m}$ ), while submicron SiC particles (200–500 nm) were present at the boundary of ultrafine Al grains (100–500 nm). Zigzag defects and linear defects were observed in both the micron-Al grains and ultrafine Al grains. These defects are made up of distortion areas, edge dislocations, stacking faults which contain Frank partial dislocations and twinning. Therefore, these defects are in a state of extreme instability, which would “disappear” under the electron beam irradiation in a few seconds. These results highlight that the increase of interface could lead to the formation of stacking faults, even in the micron Al grains.

**WEB URL:** <http://www.sciencedirect.com/science/article/pii/S0042207X15300555>

**25. Riaz, S., Nasir, M., Iqbal, J., & Nawaz, M. H. (2015). Polystyrenic porphyrins as catalysts for alkane oxidation. *Research on Chemical Intermediates*, 41(9), 6283-6287.**

**ABSTRACT:**

We report herein the catalytic effect of metalloporphyrins (MnP–PS, CoP–PS, ZnP–PS) covalently bonded with one or four arms of polystyrene. These metalloporphyrins were employed as active catalysts for oxidation of ethylbenzene in the presence of freshly prepared  $\text{O}_2$ . Our results show that one-arm polystyrenic porphyrins demonstrate enhanced catalytic efficiency, with better yield as compared with four-arm polystyrenic porphyrins. In addition, the catalytic efficiencies of the studied metalloporphyrins, calculated from gas chromatography–mass spectrometry (GC–MS) analysis, were found to be dependent on the central metal in the order  $\text{Mn} > \text{Co} > \text{Zn}$ . We also found that these catalysts have advantages of higher stability, facile separation, and good recyclability with comparable efficiencies.

**WEB URL:** <http://link.springer.com/article/10.1007/s11164-014-1739-x>

**26. Ullah, S., Khan, A. Z., Ullah, A., Muhammad, S., Iqbal, Z., Ali, Z., ... & Hussain, H. (2015). Synthesis and characterization of pentablock copolymers based on Pluronic® L64 and poly (methyl methacrylate). *Polymer Science Series B*, 57(6), 659-668.**

**ABSTRACT:**

The synthesis and characterization of amphiphilic pentablock copolymers based on Pluronic® L64 (PEO<sub>13</sub>-PPO<sub>30</sub>-PEO<sub>13</sub>) and poly(methyl methacrylate) (PMMA), synthesized via atom transfer radical polymerization (ATRP) is reported. The L64 is first transformed into a bifunctional ATRP macroinitiator which was subsequently chain extended with MMA by ATRP to afford PMMA-*b*-L64-*b*-PMMA pentablock copolymers. The chemical structure of the synthesized amphiphilic block copolymers is characterized by FTIR, <sup>1</sup>H NMR spectroscopy, and gel permeation chromatography (GPC). The GPC profiles of the block copolymers clearly show an increase in molar mass after the ATRP of MMA and monomodal molecular weight distributions for all the samples. Finally, preliminary studies on their aggregation behavior in aqueous solution have also been investigated by measuring the scattering light intensity as function of block copolymer concentration to estimate the critical aggregation concentration (CAC). The CAC decreases with increasing of hydrophobic content in copolymer, i.e., ~25 and ~15 mg/mL, respectively, is estimated for the pure L64 and PMMA<sub>13</sub>-*b*-L64-*b*-PMMA<sub>13</sub>. Further, with increase in temperature, the CAC is found to decrease that is attributed to the dehydration of the PEO segments at higher temperatures.

**WEB URL:** <http://link.springer.com/article/10.1134/S1560090415070052>

**27. Zhang, S., Chen, G., Pei, R., Hussain, M., Wang, Y., Li, D., ... & Wu, G. (2015). Effect of Gd content on interfacial microstructures and mechanical properties of C f/Mg composite. *Materials & Design*, 65, 567-574.**

**ABSTRACT:**

Matrix alloying is an effective and convenient method to improve the interface bonding strength for continuous carbon fiber reinforced magnesium matrix composites. In this work, rare earth metal Gd was selected as an alloying element to improve the interface bonding of C<sub>f</sub>/Mg composite. C<sub>f</sub>/Mg composites with different Gd content were fabricated by pressure infiltration method. The effect of Gd addition on the interfacial microstructures and mechanical properties of the composites were investigated. The results showed that the rare earth Gd tended to segregate at interface area to form Gd<sub>2</sub>O<sub>3</sub> layer and particle phase Mg<sub>7</sub>Gd. Both the interfacial products enhanced the interface bonding strength which can be identified by the increase of interlaminar shear strength (ILSS). In particular, the Gd addition promoted the ILSS and bending strength greatly, with an increase by 60.4% and 25.3% compared with C<sub>f</sub>/Mg composite, respectively. The fracture surfaces of the composites were examined by scanning electron microscopy and micrographs were employed to explain the inherent relation between interface characterization and mechanical properties.

**WEB URL:** <http://www.sciencedirect.com/science/article/pii/S026130691400747X?np=y>

**28. Sheikh, R., Shao, G. N., Khan, Z., Abbas, N., Kim, H. T., & Park, Y. H. (2015). Esterification of oleic acid by heteropolyacid/TiO<sub>2</sub>–SiO<sub>2</sub> catalysts synthesized from less expensive precursors. *Asia-Pacific Journal of Chemical Engineering*, 10(3), 339-346.**

**ABSTRACT:**

A series of 12-tungstophosphoric acid [HPW, H<sub>3</sub>PW<sub>12</sub>O<sub>40</sub> (HPW)] catalysts supported on mesoporous titania–silica composite (TSC) were prepared by impregnation method. Primarily, TSC with mesostructure was successfully prepared by a modified sol–gel process using a less expensive silica precursor (sodium silicate) and titanium oxychloride as a titania source. In order to develop catalysts with various properties, the HPW loading over mesoporous TSC was controlled between 5 and 50 wt%. The surface morphology and structural properties of the prepared catalysts were characterized using N<sub>2</sub> gas physisorption analysis, Fourier transform

infrared spectroscopy, X-ray diffraction, ultraviolet spectroscopy, transmission electron microscopy, and scanning electron microscopy analysis. The X-ray diffraction and ultraviolet spectroscopy results were useful in determining the HPW dispersion on the support material. The catalytic activities of the samples were tested in liquid phase esterification of oleic acid with methanol. The results suggested that HPW dispersion on the support material was essential for the stability and performance of the catalysts during the esterification reaction. Even though the activity of the synthesized catalysts increased with increasing HPW loading, the homogeneity decreased in the samples with higher HPW content (30–50 wt%). The 20%HPW/TSC sample was found to be an active and catalytically stable catalyst, which was successfully regenerated and recycled for three consecutive runs. Copyright © 2015 Curtin University of Technology and John Wiley & Sons, Ltd.

**WEB URL:** <http://onlinelibrary.wiley.com/doi/10.1002/apj.1871/full>

**29. Rashid, N., Rehman, M. S., & Han, J. I. (2015). Enhanced growth rate and lipid production of freshwater microalgae by adopting two-stage cultivation system under diverse light and nutrients conditions. *Water and Environment Journal*, 29(4), 533-540.**

**ABSTRACT:**

This study aims to investigate the growth behaviour and lipid production of *Chlorella vulgaris* (a microalga) by manipulating the effect of light and nutrients. In our presumptive two-staged growth model, *C. vulgaris* was first grown under low levels of light and nutrients in stage 1 and then in stage 2 under several combinations of light and nutrients, Nt-/Lt- minimum nutrients and minimum light as control; Nt+/Lt+ maximum light and maximum nutrients; Nt+/Lt- maximum nutrients and minimum light, and Nt-/Lt+ minimum nutrients and maximum light. Doubling time reduced from  $46.8 \pm 02$  hours in control (Nt-/Lt-) to  $36.1 \pm 04$  in Nt-/Lt+ and  $37.7 \pm 0.9$  in Nt+/Lt- and further down to  $25.2 \pm 03$  h in Nt+/Lt+. The highest lipid contents were found in Nt-/Lt+ ( $9.5 \pm 0.14\%$ ) followed by Nt+/Lt+ ( $8.6 \pm 0.2\%$ ), Nt+/Lt- ( $6.4 \pm 0.12\%$ ) and Nt-/Lt- ( $6.1 \pm 0.22\%$ ), respectively. The maximum biomass (909 mg/L) was found in Nt+/Lt+ likely suggesting that limited growth in control was attributed to the limitation of nutrients and

light. Incremental addition of light and nutrients is suggested for enhanced growth rate, biomass and lipid production.

**WEB URL:** <http://onlinelibrary.wiley.com/doi/10.1111/wej.12110/abstract>

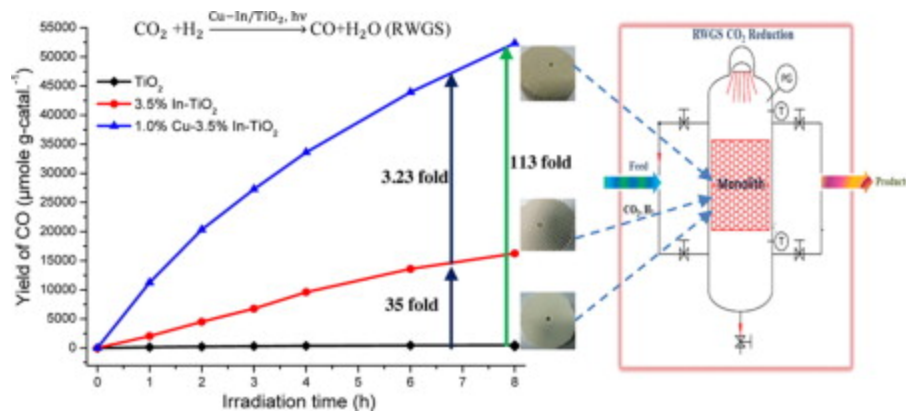
**30. Tahir, M., & Amin, N. S. (2015). Photocatalytic CO<sub>2</sub> reduction with H<sub>2</sub> as reductant over copper and indium co-doped TiO<sub>2</sub> nanocatalysts in a monolith photoreactor. *Applied Catalysis A: General*, 493, 90-102.**

**ABSTRACT:**

The photocatalytic CO<sub>2</sub> reduction with H<sub>2</sub> over copper (Cu) and indium (In) co-doped TiO<sub>2</sub> nanocatalysts in a monolith photoreactor has been investigated. The catalysts, prepared via modified sol–gel method, were dip-coated onto the monolith channels. The structure and properties of nanocatalysts with various metal and co-metal doping levels were characterized by XRD, SEM, TEM, N<sub>2</sub> adsorption–desorption, XPS, and UV–vis spectroscopy. The anatase-phase mesoporous TiO<sub>2</sub>, with Cu and In deposited as Cu<sup>+</sup> and In<sup>3+</sup> ions over TiO<sub>2</sub>, suppressed photogenerated electron–hole pair recombination. CO was the major photoreduction product with a maximum yield rate of 6540 μmol g<sup>-1</sup> h<sup>-1</sup> at 99.27% selectivity and 9.57% CO<sub>2</sub> conversion over 1.0 wt% Cu–3.5 wt% In co-doped TiO<sub>2</sub> at 120 °C and CO<sub>2</sub>/H<sub>2</sub> ratio of 1.5. The photoactivity of Cu–In co-doped TiO<sub>2</sub> monolithic catalyst for CO production was 3.23 times higher than a single ion (In)-doped TiO<sub>2</sub> and 113 times higher than un-doped TiO<sub>2</sub>. The performance of the monolith photoreactor for CO production over Cu–In co-doped TiO<sub>2</sub> catalyst was 12-fold higher than the cell-type photoreactor. More importantly, the quantum efficiency of the monolith photoreactor was significantly improved over Cu–In co-doped TiO<sub>2</sub> nanocatalyst using H<sub>2</sub> as a reductant. The stability of the monolithic Cu–In co-doped TiO<sub>2</sub> catalyst for CO partially reduced after the third run, but retained for hydrocarbons.

---

Graphical abstract



**WEB URL:** <http://www.sciencedirect.com/science/article/pii/S0926860X15000101>

**31. Tahir, M., Tahir, B., & Amin, N. S. (2015). Photocatalytic CO<sub>2</sub> reduction by CH<sub>4</sub> over montmorillonite modified TiO<sub>2</sub> nanocomposites in a continuous monolith photoreactor. *Materials Research Bulletin*, 63, 13-23.**

**ABSTRACT:**

In this study, the performance of montmorillonite (MMT) modified TiO<sub>2</sub> nanocomposites for photocatalytic CO<sub>2</sub> reduction with CH<sub>4</sub> in a continuous monolith photoreactor has been investigated. The MMT modified TiO<sub>2</sub> nanocomposites were dip-coated over monolith channels and were characterized by XRD, SEM, TEM, XPS, N<sub>2</sub>-adsorption-desorption and UV-vis spectroscopy. The MMT produced anatase phase of TiO<sub>2</sub> and reduced TiO<sub>2</sub> crystallite size from 19 nm to 13 nm. CO was the major reduction product with a yield rate of 237.5 μmol g-catal.<sup>-1</sup> h<sup>-1</sup> over 10 wt.% MMT-loaded TiO<sub>2</sub> at 100 °C, and CO<sub>2</sub>/CH<sub>4</sub> feed ratio 1.0. The photoactivity of MMT-loaded TiO<sub>2</sub> monolithic catalyst was 2.52 times higher than bare TiO<sub>2</sub>. Likewise, low concentrations of C<sub>2</sub>H<sub>6</sub>, CH<sub>3</sub>OH, C<sub>3</sub>H<sub>6</sub> and C<sub>3</sub>H<sub>8</sub> were detected in the products mixture. These results inferred MMT modified TiO<sub>2</sub> and monolith photoreactor were beneficial for enhancing photocatalysis process with appreciable productivity. The stability test revealed photoactivity of MMT-loaded TiO<sub>2</sub> nanocomposites partially diminished in recycle runs.

**WEB URL:** <http://www.sciencedirect.com/science/article/pii/S0025540814007302>

**32. Nasibi, M., Shishesaz, M. R., Sarpoushi, M. R., Borhani, M. R., & Ahmad, Z. (2015). Fabrication of a novel graphene nano-sheet electrode embedded with nano-particles of zirconium dioxide for electrochemical capacitors: Ions-redeposition on the surface of nanoporous electrode. *Materials Science in Semiconductor Processing*, 30, 625-630.**

**ABSTRACT:**

In this paper, the effect of charge/discharge cycles on the electrode containing nano-zirconium oxide, nanoporous carbon black and graphene nanosheets in electrochemical capacitors has been described. Surface morphology and electrochemical performance of the prepared electrode have also been conducted. The electrode prepared from graphene nanosheets (GNS), nanoporous carbon black (NCB), zirconium oxide ( $ZrO_2$ ), and polytetrafluoroethylene (PTFE) in molar ratio of 54:09:27:10 respectively showed a maximum specific capacitance as high as  $11.84 \text{ F g}^{-1}$  in the potential range between  $-0.45$  and  $0.35 \text{ V}$  (V vs. SCE) at a scan rate of  $10 \text{ mV s}^{-1}$  in a  $3 \text{ M NaCl}$  electrolyte. The electrochemical results show the low ratio of the outer to total charge ( $q^{\text{O}}/q^{\text{T}}$ ) which confirms the low current response and higher voltage reversal at the end potentials. SEM images confirms the ions re-deposit as agglomerates and accompanied by a drastic decrease in the surface area on the surface of the electrode after one charge/discharge cycle.

**WEB URL:** <http://www.sciencedirect.com/science/article/pii/S1369800114006258>

**33. Shahzad, K., Saleem, M., Ghauri, M., Akhtar, J., Ali, N., & Akhtar, N. A. (2015). Emissions of  $NO_x$ ,  $SO_2$ , and  $CO$  from Co-Combustion of Wheat Straw and Coal Under Fast Fluidized Bed Condition. *Combustion Science and Technology*, 187(7), 1079-1092.**

**ABSTRACT:**

Fuel diversity and reduction in pollutant emissions are driving the increased utilization of  $CO_2$  neutral biomass. Effects of operating conditions, such as bed temperature; excess air ratio; and secondary to primary air ratio on emissions of  $NO_x$ ,  $SO_2$ , and  $CO$  for burning different blends of wheat straw and Salt Range coal under fast fluidized bed conditions in a pilot scale

test facility, are reported in this study. Emissions of NO<sub>x</sub> were found to decrease with an increase in wheat straw ratio and secondary to primary air ratio. SO<sub>2</sub> and CO emissions were observed to decrease with an increase in excess air ratio and wheat straw ratio.

**Web URL:** <http://www.tandfonline.com/doi/abs/10.1080/00102202.2014.1002561>

**34. Bazmi, A A., Gholamreza Z., and Haslenda H (2015)"Design of decentralized biopower generation and distribution system for developing countries." *Journal of Cleaner Production* 86 (2015): 209-220.**

**ABSTRACT:**

This paper presents a general decentralized energy generation optimization model for developing countries. A mixed integer nonlinear programming model has been formulated and implemented, representing decisions regarding (1) the optimal number, locations, and sizes of various types of processing plants, (2) the amounts of biomass transported, and electricity to be transmitted between the selected locations over a selected period, and minimizes the objective function of overall generation cost. The model has been applied first for designing a decentralized energy generation system using palm oil biomass for Iskandar Malaysia region of the state of Johor, Malaysia and then extended to entire state. We investigated the benefits of more distributed types of processing networks, in terms of the overall economics and the robustness to demand variations. No change in designed decentralized energy generation system and distribution network was observed when the demand was lowered to 90%, 75% and 60% of original demand.

**WEB URL:** <http://www.sciencedirect.com/science/article/pii/S095965261400907X>

**35. Tahir, M., & Amin, N. S. (2015). Indium-doped TiO<sub>2</sub> nanoparticles for photocatalytic CO<sub>2</sub> reduction with H<sub>2</sub>O vapors to CH<sub>4</sub>. *Applied Catalysis B: Environmental*, 162, 98-109.**

**ABSTRACT:**

Indium (In)-doped titanium dioxide (TiO<sub>2</sub>) nanoparticles were synthesized using a controlled sol-gel method. The structures and properties of the catalysts were characterized by XRD, FE-SEM, TEM, XPS, BET, UV-vis and PL spectroscopy. Indium, present over the TiO<sub>2</sub> in metal state, inhibited crystal growth and produced anatase phase of mesoporous TiO<sub>2</sub> nanoparticles. Doping In in TiO<sub>2</sub> also increased the surface area and enlarged the band gap. The photocatalytic activities of In-doped TiO<sub>2</sub> nanoparticles were considerably improved for CO<sub>2</sub> reduction with H<sub>2</sub>O vapors in a cell type photoreactor. CO was observed as the main product over TiO<sub>2</sub>, but doping In in TiO<sub>2</sub> remarkably increased the CH<sub>4</sub> yield. CH<sub>4</sub> production rate over 10 wt.% In-doped TiO<sub>2</sub> was 7.9-fold higher than the bare TiO<sub>2</sub> at 100 °C and CO<sub>2</sub>/H<sub>2</sub>O ratio of 1.43. In addition, C<sub>1-3</sub> higher hydrocarbons namely C<sub>2</sub>H<sub>4</sub>, C<sub>2</sub>H<sub>6</sub>, C<sub>3</sub>H<sub>6</sub> and C<sub>3</sub>H<sub>8</sub> were detected in the product mixture. The enhanced photoactivity in mesoporous In-doped TiO<sub>2</sub> nanoparticles can be attributed to interfacial transfer of photogenerated charges, which led to effective charge separation and inhibited recombination of photogenerated electron-hole (e<sup>-</sup>/h<sup>+</sup>) pairs. Langmuir-Hinshelwood model, developed to investigate reaction rate parameters, fitted well with the experimental data.

**WEB URL:** <http://www.sciencedirect.com/science/article/pii/S0926337314003762>

**36. Hurain, S. S., Habib, A., Hussain, S. M., & Ul-Haq, N. (2015). Ultrasound-Assisted Synthesis of Titania Nanoparticles, Characterization of Their Thin Films, and Activity in Photooxidation of β-Naphthol. *Journal of Electronic Materials*, 44(11), 4622-4627.**

**ABSTRACT:**

Nanosized titania (TiO<sub>2</sub>) films and powders were prepared from titanium isopropoxide by ultrasonication then ultrasonic aerosol-assisted chemical vapor deposition (UAACVD). X-ray diffraction (XRD), used to study the crystal structure, phase, and crystallite size of TiO<sub>2</sub> samples annealed at 500°C, revealed anatase was the main crystalline phase. Scanning electron microscopy and atomic force microscopy revealed the quasi-spherical morphology of the TiO<sub>2</sub> nanoparticles; average size distribution was in the range 20–35 nm. Ultraviolet-visible

spectroscopy was used to evaluate the photocatalytic activity of the anatase TiO<sub>2</sub>, on the basis of efficiency of degradation of  $\beta$ -naphthol. Pure TiO<sub>2</sub> nanoparticles synthesized by use of sonication–UAACVD then calcination at 500°C enabled effective photodegradation under UV light. This method of synthesis of TiO<sub>2</sub> is superior to the reflux–UAACVD method with titanium isopropoxide as precursor.

**WEB URL:** <http://link.springer.com/article/10.1007/s11664-015-3996-x>

**37. Xiu, Z., Yang, W., Dong, R., Hussain, M., Jiang, L., Liu, Y., & Wu, G. (2015). Microstructure and Mechanical Properties of 45 vol.% SiC p/7075Al Composite. *Journal of Materials Science & Technology*, 31(9), 930-934.**

**ABSTRACT:**

Microstructure and mechanical behavior of high volume content SiC<sub>p</sub>/7xxxAl composites have not been explored yet. Therefore, in the present work, 45 vol.% SiC<sub>p</sub>/7075Al composite has been prepared by pressure infiltration method. High density dislocations were found around SiC/Al interface in SiC<sub>p</sub>/7075Al composite after water-quenching and aging treatment. Fine dispersed nano- $\eta'$  phases were observed after the aging treatment. Adverse to other SiC<sub>p</sub>/Al composites prepared by the pressure infiltration method, an interface layer was observed between SiC particles and Al matrix. Furthermore, high-resolution transmission electron microscopy (HRTEM) observation indicated that this interface layer was coherent/semi-coherent with that of the SiC particles. 45 vol.% SiC<sub>p</sub>/7075Al composite demonstrated high tensile strength (630 MPa) and micro-ductility. Compared to aged SiC<sub>p</sub>/2024Al composite, the aged SiC<sub>p</sub>/7075Al composite showed an increase of about 200% in the tensile strain and 90% in the tensile strength, respectively. It is speculated that nano- $\eta'$  phases in the Al matrix significantly contributed to the strengthening effect while the interface layer between SiC and Al matrix might be beneficial to the strength and plasticity of SiC<sub>p</sub>/7075Al composite.

**WEB URL:** <http://www.sciencedirect.com/science/article/pii/S100503021500081X>

**38. Islam, A., Yasin, T., Sabir, A., Khan, S. M., Sultan, M., Shafiq, M., ... & Jamil, T. (2015). High-temperature electrical properties of silane cross-linked chitosan/poly (vinyl alcohol) membrane: thermal, mechanical and surface characterization. *e-Polymers*, 15(4), 255-261.**

**ABSTRACT:**

Chitosan and poly(vinyl alcohol) were blended and cross-linked with tetraethoxysilane and showed conductive properties. Impedance spectroscopy was used to study the influence of temperature on the electrical properties of the membranes. The conductivity of the membranes was increased with an increase in temperature. Free water was decreased and bound water was increased with an increase in cross-linker contents. The tensile strength improved, whereas elongation at break decreased by increasing the amount of cross-linker contents. The water contact angle of the membranes lowered with time, exhibiting the hydrophilic nature of the membranes. The novel characteristics of biocompatible membranes can be used in biomedical applications including biological schemes that require smaller charge in medicinal apparatus, bioelectrode coatings, etc.

**WEB URL:** <http://www.degruyter.com/view/j/epoly.2015.15.issue-4/epoly-2015-0048/epoly-2015-0048.xml>

**39. Abdullah, M. A., Afzaal, M., Ismail, Z., Ahmad, A., Nazir, M. S., & Bhat, A. H. (2015). Comparative study on structural modification of *Ceiba pentandra* for oil sorption and palm oil mill effluent treatment. *Desalination and Water Treatment*, 54(11), 3044-3053.**

**ABSTRACT:**

The performance of raw *Ceiba pentandra* (L.) Gaertn (raw kapok fibers (RKF)) for oil sorption and palm oil mill effluent (POME) treatment was compared with structurally modified kapok (NaOH-treated (SKF) and surface-modified kapok fiber (SMKF)) and bentonite clay. Based on FTIR, kapok wax functional group at 1726/cm was not detected in SKF rendering higher hydrophilicity. The reduction in peak intensity at 473 and 523/cm upon HCl treatment of bentonite, suggests the cleavage of Si–O–Al bond layer and Si–O–Mg (Fe) bonds. For filtration

under gravity at 0.08 g/cm<sup>3</sup>, SKF showed high POME sorption of 82 g/g, but lower diesel sorption of 23 g/g. With HCl-treated bentonite, POME sorption at 69 g/g was only slightly higher than diesel sorption of 60 g/g. However, RKF and raw bentonite achieved higher removal efficiency of biological oxygen demand, chemical oxygen demand (COD), total organic carbon, and total nitrogen at 74–98% and 72–94%, respectively, than with SKF at 66–80%, and HCl-treated bentonite at 64–80%. In batch mode, SMKf at 0.08 g/cm<sup>3</sup> showed the highest oil sorption capacity of 56.7 g/g for Crude Palm Oil (CPO) and 33.7 g/g for diesel. Under continuous mode with 4000 mg/l CPO in water, 99% of COD removal was achieved at all packing densities and flow rates, regardless of kapok packing material. The dynamic oil retention was 96–99% for CPO and 99–100% for diesel at all packing densities. RKF and SMKf can both be suitable sorbent materials for CPO and diesel sorption, and for POME treatment.

**WEB URL:** <http://www.tandfonline.com/doi/abs/10.1080/19443994.2014.906326>

**40. Bhutto, A. W., Harijan, K., Qureshi, K., Bazmi, A. A., & Bahadori, A. (2015). Perspectives for the production of ethanol from lignocellulosic feedstock—A case study. *Journal of Cleaner Production*, 95, 184-193.**

**ABSTRACT:**

Pakistan has limited indigenous resources of fossil fuel and the deficit is being filled through imports of crude oil and petroleum product. The country presently produces bio ethanol predominantly from molasses, a byproduct of the refining of sugarcane. Since promotion of 1<sup>st</sup>-generation biofuels appears unsustainable because of the potential stress on food commodities, crop residues present a major opportunity for cleaner production through promotion of 2nd generation bio ethanol. Based on the evaluation of the availability of lignocellulosic biomass in Pakistan, this study forecasts the annual yield of five lignocellulosic feedstocks i.e. cotton stalks, sugarcane tops, rice straw, maize stalks and wheat straw from 2013 to 2030 in Pakistan with the help of Adaptive Neuro Fuzzy Interface System Model. Based on the availability of biomass feedstock, the study forecasts the maximum theoretical potential

for production of bio ethanol from these crop residues up to 2030. Our study also analyses the parameters affecting the basic price for the crop residue collection.

**WEB URL:** <http://www.sciencedirect.com/science/article/pii/S0959652615002188>

**41. Sarpoushi, M. R., Nasibi, M., Moshrefifar, M., Mazloum-Ardakani, M., Ahmad, Z., & Riazi, H. R. (2015). Electrochemical investigation of graphene/nanoporous carbon black for supercapacitors. *Materials Science in Semiconductor Processing*, 33, 89-93.**

**ABSTRACT:**

In this paper, mixing effect of nanoporous carbon black (NCB) and graphene nanosheets (GNS) on surface morphology and electrochemical performance of prepared electrodes were investigated. 80:10:10 (NCB:GNS:PTFE) prepared electrodes show a maximum specific capacitance as high as  $10.22 \text{ F g}^{-1}$  in 3 M NaCl electrolyte. Addition of nanoporous carbon black increases outer to total charge stored ( $q_o^*/q_T^*$ ) on the electrode from 0.024 to 0.037 which confirms the higher current response and higher voltage reversal at the end potentials.

**WEB URL:** <http://www.sciencedirect.com/science/article/pii/S1369800115000542>

**42. Hussain, M, Akhter, P., Russo, N., & Saracco, G. (2015) "New optimized mesoporous silica incorporated isolated Ti materials towards improved photocatalytic reduction of carbon dioxide to renewable fuels." *Chemical Engineering Journal* 278: 279-292.**

**ABSTRACT:**

In the present work, novel isolated Ti-SBA-15-spherical and Ti-KIT-6 (Si/Ti = 200, 100 and 50) photocatalysts have been synthesized; optimized through  $\text{N}_2$ -adsorption/desorption, SEM, EDX, UV-Vis, FT-IR, XPS and TEM analysis techniques; and explored for the photocatalytic reduction of greenhouse gas  $\text{CO}_2$  to renewable fuels. The Ti-KIT-6 (Si/Ti = 100) showed better  $\text{CH}_4$  production rate ( $4.15 \mu\text{mol gcat.}^{-1} \text{ h}^{-1}$ ) than the corresponding Ti-KIT-6-dried ( $2.63 \mu\text{mol gcat.}^{-1} \text{ h}^{-1}$ ) and the Ti-SBA-15-calcined/dried ( $1.85, 3.45 \mu\text{mol gcat.}^{-1} \text{ h}^{-1}$ ,

respectively) in the initial optimization reactions. CH<sub>3</sub>OH, CO, and H<sub>2</sub> are the other main fuel products produced by the Ti-KIT-6-calcined (Si/Ti = 100). The increased surface concentration of OH groups found in the Ti-KIT-6-calcined (Si/Ti = 100) than the other two ratios (Si/Ti = 200, 50), the presence of more accessible surface reaction active sites due to the lower number of Ti–O–Ti or TiO<sub>2</sub> agglomerates, and the more isolated Ti species which are uniformly dispersed on the 3-D KIT-6 mesoporous silica support without collapsing the mesoporous structure, have boosted the higher activity, which is even higher than the best commercial Aeroxide P25 TiO<sub>2</sub>. The reaction has been preceded by the competitive adsorption of CO<sub>2</sub> and H<sub>2</sub>O vapors. The UV light source/intensity, H<sub>2</sub>O/CO<sub>2</sub> ratios and catalyst shapes are the key factors that influence the performance of the catalyst, and therefore, these parameters have been optimized to boost the fuel products.

**WEB URL:** <http://www.sciencedirect.com/science/article/pii/S1385894714011607>

**43. Sherin, L., Mustafa, M., & Shujaat, S. (2015). Evaluation of Terminalia bellerica Roxb. Leaf Extracted in Different Solvents for Antioxidant Activities. *Asian Journal of Chemistry*, 27(12), 4527.**

**ABSTRACT:**

Terminalia bellerica, an esteemed ayurvedic plant, is employed traditionally in the management of an array of diverse pathological conditions. The present work is aimed to assess antioxidant potential of plant leaf extracts. Crude methanol extract was fractioned with different solvents and antioxidant activities along with total phenolic and flavonoid content were investigated with different antioxidant testing models, including DPPH, ABTS, anti-lipid peroxidation and total antioxidant capacity assays. Ethyl acetate (IC<sub>50</sub> = 3.48 µg mL<sup>-1</sup>) as well as chloroform (IC<sub>50</sub> = 4.55 µg mL<sup>-1</sup>) extracts exhibited persuasive DPPH radical scavenging activity, much better than standard antioxidant Trolox (IC<sub>50</sub> = 6.17 µg mL<sup>-1</sup>). In ABTS assay, ethyl acetate extract (IC<sub>50</sub> = 0.18 µg mL<sup>-1</sup>) showed enhanced potential in comparison to other extracts and standard antioxidants Trolox and n-propyl gallate. Chloroform extract offered maximum protection against lipid peroxidation (IC<sub>50</sub> = 0.28 mg mL<sup>-1</sup>) and highest total antioxidant activity (4.54 mM

g-1). All the extracts showed variable magnitude of phenolics and flavonoids content. In conclusion, ethylacetate and chloroform extracts of Terminalia bellerica leaf possess potent antioxidant potential which could be harnessed as economically viable source of natural antioxidants.

**WEB URL:** <http://search.proquest.com/openview/571639fef6b27176fb2b4e10d99d7b60/1?pq-origsite=gscholar&cbl=2030306>

**44. Jabeen, G., Farooq, R., Khan, A. U., & Khan, A. A. (2015). Acetyl-CoA pathway for biosynthesis of organics. *Asian Journal of Chemistry*, 27(1), 1.**

**ABSTRACT:**

A great diversity of microorganisms have tendency to reduce numerous organic compounds and gases. Various acetogens have potential to produce valuable organic compounds by acquiring environmentally sustainable approaches. Acetogens like *Sporomusa ovata*, *Clostridium ljungdahlii*, *Clostridium aceticum*, *Moorella thermoacetica* and *Acetobacterium woodii* are attractive species for fixing waste greenhouse gases. Acetogens utilize acetyl Co-A pathway for acetate production with small amount of butanol and alcohols. Genetic mutations, metabolic engineering and bioelectrochemical synthesis can be adopted to divert the chemical reaction pathway apart from acetate production. In bioelectrochemical synthesis, electrodes material, electrodes surface areas, kind of biofilms, ion exchange membranes, internal resistances, etc. effect electron exchange between microorganisms and electron acceptors. Adapted strains provide an insight into the mechanisms of extracellular electron exchange. There's a requirement to modify the metabolic pathways of microorganisms by sequencing their genomes to obtain ethanol, isopropanol, n-butanol, etc. This review provides insight of natural and engineered methods for scavenging greenhouse gases using acetyl Co-A metabolic pathways adopted by acetogens. The unique approach is the critical discussion leading to the selection of acetyl Co-A pathway on the basis of its energy efficiency. The research on bioelectrochemical process, metabolic engineering and their applications are being focused to give a comprehensive review on the subject.

**WEB URL:** [https://www.researchgate.net/profile/Asad\\_Khan27/publication/278390833\\_Acetyl-CoA\\_Pathway\\_for\\_Biosynthesis\\_of\\_Organics/links/557ffb3108aeea18b77a29a5.pdf](https://www.researchgate.net/profile/Asad_Khan27/publication/278390833_Acetyl-CoA_Pathway_for_Biosynthesis_of_Organics/links/557ffb3108aeea18b77a29a5.pdf)

# DEPARTMENT OF COMPUTER SCIENCE

## Journal Articles

1. Chaudhry, M. T., Ling, T. C., Hussain, S. A., & Lu, X. Z. (2015). Thermal-aware relocation of servers in green data centers. *Frontiers of Information Technology & Electronic Engineering*, 16(2), 119-134.

**ABSTRACT:**

Rise in inlet air temperature increases the corresponding outlet air temperature from the server. As an added effect of rise in inlet air temperature, some active servers may start exhaling intensely hot air to form a hotspot. Increase in hot air temperature and occasional hotspots are an added burden on the cooling mechanism and result in energy wastage in data centers. The increase in inlet air temperature may also result in failure of server hardware. Identifying and comparing the thermal sensitivity to inlet air temperature for various servers helps in the thermal-aware arrangement and location switching of servers to minimize the cooling energy wastage. The peak outlet temperature among the relocated servers can be lowered and even be homogenized to reduce the cooling load and chances of hotspots. Based upon mutual comparison of inlet temperature sensitivity of heterogeneous servers, this paper presents a proactive approach for thermal-aware relocation of data center servers. The experimental results show that each relocation operation has a cooling energy saving of as much as 2.1 kW·h and lowers the chances of hotspots by over 77%. Thus, the thermal-aware relocation of servers helps in the establishment of green data centers.

**WEB URL:** <http://link.springer.com/article/10.1631%2FFITEE.1400174>

2. Chaudhry, M. T., Ling, T. C., Manzoor, A., Hussain, S. A., & Kim, J. (2015). Thermal-aware scheduling in green data centers. *ACM Computing Surveys (CSUR)*, 47(3), 39.

**ABSTRACT:**

Data centers can go green by saving electricity in two major areas: computing and cooling. Servers in data centers require a constant supply of cold air from on-site cooling mechanisms for reliability. An increased computational load makes servers dissipate more power as heat and eventually amplifies the cooling load. In thermal-aware scheduling, computations are scheduled with the objective of reducing the data-center-wide thermal gradient, hotspots, and cooling magnitude. Complemented by heat modeling and thermal-aware monitoring and profiling, this scheduling is energy efficient and economical. A survey is presented henceforth of thermal-aware scheduling and associated techniques for green data centers.

**WEB URL:** <http://dl.acm.org/citation.cfm?id=2678278>

**3. Kaleem, M., Hussain, S. A., Raza, I., Chaudhry, S. R., & Raza, M. H. (2015). A direction and relative speed (DARS)-based routing protocol for VANETS in a highway scenario. *Journal of the Chinese Institute of Engineers*, 38(3), 399-405.**

**ABSTRACT:**

The dynamic nature of vehicular ad hoc networks (VANETs) requires efficient routing protocols for better performance. It is challenging to provide a universal routing protocol that performs well in all scenarios of VANETs. A routing protocol is challenged by vehicle speed, position, and network density. VANETs for highways are dependent on speed and direction of vehicles thus requiring customized routing protocols. This paper presents a novel direction and relative speed (DARS)-based routing protocol for highways using a single-hop packet forwarding approach. It selects the next hop using DARS of the vehicle. The experiments show significant improvement in packet delivery ratio, end-to-end delay, packet drop ratio, and Jain's fairness index for proposed protocol compared to direction-based ad hoc on demand distance vector.

**WEB URL:** <http://www.tandfonline.com/doi/abs/10.1080/02533839.2014.970354>

**4. Rasool, G., Ehsan, F., & Shahbaz, M. (2015). A systematic literature review on electricity management systems. *Renewable and Sustainable Energy Reviews*, 49, 975-989.**

**ABSTRACT:**

Many countries in the world and most importantly Pakistan is suffering from severe electricity crisis. Information Technology (IT) is being used in every field of the life and we may apply IT to overcome electricity crisis. A large number of papers are presented by different researchers on electricity management. The key motivation of this systematic literature review is to study, analyze and explore the status of different solutions presented for management of electricity throughout the world and determine requirements for the development of a new electricity management system. We apply standard systematic review method with the manual search of three digital libraries. Out of 74 primary studies, 27 studies are software contributions, 13 studies are hardware solutions, 18 studies represent the theoretical work and 16 studies contribute proposed ideas. The quality of the contributions is fair as 74 articles out of 209 were selected as candidate studies after manual peer review. Currently, the solutions presented by different researchers are limited in scope. Many researchers are working on tool contributions, but most of them are only providing solutions for specific regions and communities. There is a need to develop a generic Electricity Management System (EMS) that should be customizable and can be used as generic solution.

**WEB URL:** <http://www.sciencedirect.com/science/article/pii/S136403211500324X>

**5. Khan, N. A., Ahmad, F., & Khan, S. A. (2015). SHER: A Colored Petri Net Based Random Mobility Model for Wireless Communications. *PLoS one*,10(8), e0133634.**

**ABSTRACT:**

In wireless network research, simulation is the most imperative technique to investigate the network's behavior and validation. Wireless networks typically consist of mobile hosts; therefore, the degree of validation is influenced by the underlying mobility model, and synthetic models are implemented in simulators because real life traces are not widely available. In wireless communications, mobility is an integral part while the key role of a mobility model is to mimic the real life traveling patterns to study. The performance of routing protocols and mobility management strategies e.g. paging, registration and handoff is highly

dependent to the selected mobility model. In this paper, we devise and evaluate the Show Home and Exclusive Regions (SHER), a novel two-dimensional (2-D) Colored Petri net (CPN) based formal random mobility model, which exhibits sociological behavior of a user. The model captures hotspots where a user frequently visits and spends time. Our solution eliminates six key issues of the random mobility models, i.e., *sudden stops, memoryless movements, border effect, temporal dependency of velocity, pause time dependency, and speed decay* in a single model. The proposed model is able to predict the future location of a mobile user and ultimately improves the performance of wireless communication networks. The model follows a uniform nodal distribution and is a mini simulator, which exhibits interesting mobility patterns. The model is also helpful to those who are not familiar with the formal modeling, and users can extract meaningful information with a single mouse-click. It is noteworthy that capturing dynamic mobility patterns through CPN is the most challenging and virulent activity of the presented research. Statistical and reachability analysis techniques are presented to elucidate and validate the performance of our proposed mobility model. The state space methods allow us to algorithmically derive the system behavior and rectify the errors of our proposed model.

**WEB URL:** <http://journals.plos.org/plosone/article?id=10.1371/journal.pone.0133634>

**6. Hussain, I., Chen, L., Mirza, H. T., Chen, G., & Hassan, S. U. (2015). Right mix of speech and non-speech: hybrid auditory feedback in mobility assistance of the visually impaired. *Universal Access in the Information Society*, 14(4), 527-536.**

**ABSTRACT:**

Despite the growing awareness about mobility issues surrounding auditory interfaces used by visually impaired people, designers still face challenges while creating sound for auditory interfaces. This paper presents a new approach of hybrid auditory feedback, which converts frequently used speech instructions to non-speech (i.e., spearcons), based on users' travelled frequency and sound repetition. Using a within-subject design, twelve participants (i.e., blind people) carried out a task, using a mobility assistant application in an indoor environment. As

surfaced from the study results, the hybrid auditory feedback approach is more effective than non-speech and it is pleasant compared with repetitive speech-only. In addition, it can substantially improve user experience. Finally, these findings may help researchers and practitioners use hybrid auditory feedback, rather than using speech- or non-speech-only, when designing or creating accessibility/assistive products and systems.

**WEB URL:** <http://link.springer.com/article/10.1007/s10209-014-0350-7>

**7. Rasool, G., & Arshad, Z. (2015). A review of code smell mining techniques. *Journal of Software: Evolution and Process*, 27(11), 867-895.**

**ABSTRACT:**

Over the past 15 years, researchers presented numerous techniques and tools for mining code smells. It is imperative to classify, compare, and evaluate existing techniques and tools used for the detection of code smells because of their varying features and outcomes. This paper presents an up-to-date review on the state-of-the-art techniques and tools used for mining code smells from the source code of different software applications. We classify selected code smell detection techniques and tools based on their detection methods and analyze the results of the selected techniques. We present our observations and recommendations after our critical analysis of existing code smell techniques and tools. Our recommendations may be used by existing and new tool developers working in the field of code smell detection. The scope of this review is limited to research publications in the area of code smells that focus on detection of code smells as compared with previous reviews that cover all aspects of code smells. Copyright © 2015 John Wiley & Sons, Ltd.

**WEB URL:** <http://onlinelibrary.wiley.com/doi/10.1002/smr.1737/abstract>

**8. Ratyal, N. I., Taj, I. A., Bajwa, U. I., & Sajid, M. (2015). 3D face recognition based on pose and expression invariant alignment. *Computers & Electrical Engineering*, 46, 241-255.**

**ABSTRACT:**

In this paper we present a novel pose and expression invariant approach for 3D face registration based on intrinsic coordinate system characterized by nose tip, horizontal nose plane and vertical symmetry plane of the face. It is observed that distance of nose tip from 3D scanner is reduced after pose correction which is presented as a quantifying heuristic for proposed registration scheme. In addition, motivated by the fact that a single classifier cannot be generally efficient against all face regions, a two tier ensemble classifier based 3D face recognition approach is presented which employs Principal Component Analysis (PCA) for feature extraction and Mahalanobis Cosine (MahCos) matching score for classification of facial regions with weighted Borda Count (WBC) based combination and a re-ranking stage. The performance of proposed approach is corroborated by extensive experiments performed on two databases: GavabDB and FRGC v2.0, confirming effectiveness of fusion strategies to improve performance.

**WEB URL:** <http://www.sciencedirect.com/science/article/pii/S0045790615002116>

**9. Treur, J., & Umair, M. (2015). Emotions as a vehicle for rationality: Rational decision making models based on emotion-related valuing and Hebbian learning. *Biologically Inspired Cognitive Architectures*, 14, 40-56.**

**ABSTRACT:**

In this paper an adaptive decision model based on predictive loops through feeling states is analysed from the perspective of rationality. Hebbian learning is considered for different types of connections in the decision model. To assess the extent of rationality, a measure is introduced reflecting the environment's behaviour. Simulation results and the extents of rationality of the different models over time are presented and analysed.

**WEB URL:** <http://www.sciencedirect.com/science/article/pii/S2212683X15000201>

**10. Ullah, H., Gilanie, G., Hussain, F., & Ahmad, E. (2015). Autocorrelation optical coherence tomography for glucose quantification in blood. *Laser Physics Letters*, 12(12), 125602.**

**ABSTRACT:**

We report a new method for glucose monitoring in blood tissue based on the autocorrelation function (ACF) analysis in Fourier domain optical coherence tomography (FD-OCT). We have determined the changes in OCT monitoring signals' depth to characterize the modulations in ACFs for quantitative measurements of glucose concentrations in blood. We found that an increase in the concentration of glucose in blood results in decreased OCT monitoring signal due to the increase in the refractive index of the media.

**WEB URL:** <http://iopscience.iop.org/article/10.1088/1612-2011/12/12/125602/meta>

**11. Rathore, S., Hussain, M., Iftikhar, M. A., & Jalil, A. (2015). Novel structural descriptors for automated colon cancer detection and grading. *Computer methods and programs in biomedicine*, 121(2), 92-108.**

**ABSTRACT:**

The histopathological examination of tissue specimens is necessary for the diagnosis and grading of colon cancer. However, the process is subjective and leads to significant inter/intra observer variation in diagnosis as it mainly relies on the visual assessment of histopathologists. Therefore, a reliable computer-aided technique, which can automatically classify normal and malignant colon samples, and determine grades of malignant samples, is required. In this paper, we propose a novel colon cancer diagnostic (CCD) system, which initially classifies colon biopsy images into normal and malignant classes, and then automatically determines the grades of colon cancer for malignant images. To this end, various novel structural descriptors, which mathematically model and quantify the variation among the structure of normal colon tissues and malignant tissues of various cancer grades, have been employed. Radial basis function (RBF) kernel of support vector machines (SVM) has been employed as classifier in order to classify/grade colon samples based on these descriptors. The proposed system has been tested on 92 malignant and 82 normal colon biopsy images. The classification performance has been measured in terms of various performance measures, and quite promising performance has been observed. Compared with previous techniques, the proposed

system has demonstrated better cancer detection (classification accuracy = 95.40%) and grading (classification accuracy = 93.47%) capability. Therefore, the proposed CCD system can provide a reliable second opinion to the histopathologists.

**WEB URL:** <http://www.sciencedirect.com/science/article/pii/S0169260715001510>

**12. Abid, S. A., Othman, M., Shah, N., Sabir, O., Ali, M., Shafi, J., & Ullah, S. (2015). Merging of DHT-based logical networks in MANETs. *Transactions on Emerging Telecommunications Technologies*, 26(12), 1347-1367.**

**ABSTRACT:**

We study the challenging problem of the network partitioning and merging in context with the mismatch problem and the resilience of the logical structure in distributed hash table (DHT)-based routing protocols for mobile ad hoc networks (MANETs). The existing DHT-based approaches for routing in MANETs do not consider the merging of logical networks, which occurs because of limited transmission range and mobility of nodes. In this paper, we identify that the mismatch problem is aggravated when logical networks are merged, which directly depends upon the shape of the logical structure in which nodes are arranged according to their logical identifier. To address this problem, we first propose a leader-based approach (LA) to detect and merge logical networks. In addition, we discuss the effectiveness of a three-dimensional logical space and three-dimensional logical structure when logical networks are merged. In three-dimensional logical space and three-dimensional logical structure, we take into account the physical intra-neighbour relationship of a node and interpret that relationship in terms of logical identifiers. Simulation results show that the proposed DHT-based protocol along with LA outperforms the existing DHT-based routing protocol in terms routing overhead, end-to-end delay, path-stretch values and packet delivery ratio. Copyright © 2015 John Wiley & Sons, Ltd.

**WEB URL:** <http://onlinelibrary.wiley.com/doi/10.1002/ett.2969/abstract>

**13. Raza, I., Jabeen, S., Shabbir, F., Abbasi, M., Chaudhry, S., & Hussain, S. A. (2015). Optical Wireless Channel Characterization For Indoor Visible Light Communications. *Indian Journal of Science and Technology*, 8(22).**

**ABSTRACT:**

The visible Light Communications (VLC) has gained a lot of interest for indoor communications resulting in several research challenges. The use of Light Emitting Diodes (LEDs) as light source poses many modulation issues for Line Of Sight (LOS) Optical Wireless Channel (OWC). This paper investigates the line of sight optical wireless channel characterization for visible light communications designing a realistic indoor environment adding path loss along with Additive White Gaussian Noise (AWGN) to the channel. A comprehensive mathematical model is derived and simulated to investigate the performance of the proposed system considering the effect of different parameters such as  $E_b/N_0$ , Signal to Noise Ratio (SNR), distance between transmitter and receiver, signal power on the Bit Error Rate (BER), propagation delay, and spectral efficiency. The propose indoor OWC for VLC enhances the transmission range from 4 meters to 6 meters having optimal quality of transmission in a channel representing real indoor environment.

**WEB URL:** <http://www.indjst.org/index.php/indjst/article/view/70605>

**14. Habib, Z., Rasool, G., & Sakai, M. (2015). Admissible curvature continuous areas for fair curves using G<sup>2</sup> Hermite PH quintic polynomial. *Journal of King Saud University-Computer and Information Sciences*, 27(2), 140-146.**

**ABSTRACT:**

In this paper we derive admissible curvature continuous areas for monotonically increasing curvature continuous smooth curve by using a single Pythagorean hodograph (PH) quintic polynomial of G<sup>2</sup> contact matching Hermite end conditions. Curves with monotonically increasing or decreasing curvatures are considered highly smooth (fair) and are very useful in geometric design. Making the design by using smooth curves is a fascinating problem of

computing with significant physical and esthetic applications especially in high speed transportation and robotics. First we derive sufficient conditions for curvature continuity on a single PH quintic polynomial with given Hermite end conditions then we find the admissible area for the smooth curve with respect to the curvatures at its endpoints.

**WEB URL:** <http://www.sciencedirect.com/science/article/pii/S1319157815000129>

**15. Khalid, M., Shehzaib, U., & Asif, M. (2015). A Case of Mobile App Reviews as a Crowdsourcse. *International Journal of Information Engineering and Electronic Business (IJIEEB)*, 7(5), 39-47.**

**ABSTRACT:**

Crowdsourcing is a famous technique to get innovative ideas and soliciting contribution from a large online community particularly in e-business. This technique is contributing towards changing the current business techniques and practices. It is also equally famous in analysis and design of m-business services. Mobile app stores are providing an opportunity for its users' to participate and contribute in the growth of mobile app market. App reviews given by users usually contain active, heterogeneous and real life user experience of mobile app which can be useful to improve the quality of app. Best to our knowledge, the strength of mobile app reviews as a crowdsourcse is not fully recognized and understood by the community yet. In this paper, we have analysed a crowdsourcing reference model to find out which features of crowdsourcse are present and are related to our case of mobile app reviews as a crowdsourcse. We have analyzed and discussed each construct of the reference model from the perspective of mobile app reviews. Moreover, app reviews as a crowdsourcing technique is discussed by utilizing the four pillars of the reference model: the crowd, the crowdsourcer, the crowdsourcing, and the crowdsourcing platform. We have also identified and partially validated certain constructs of the model and highlighted the significance of app reviews as a crowdsourcse based on existing literature. In this study, only one crowdsourcing reference model is used which can be a limitation of our study. The study can be further investigated and compared with other crowdsourcing reference models to get better insights of app reviews as a crowdsourcse. We

believe that the understanding of app reviews as a crowdsourcing technique can lead to the further development of the mobile app market and can open further research opportunities.

**WEB URL:** <http://www.mecs-press.org/ijieeb/ijieeb-v7-n5/v7n5-6.html>

**16. Khalid, M., Asif, M., & Shehzaib, U. (2015). Towards Improving the Quality of Mobile App Reviews. *International Journal of Information Technology and Computer Science (IJITCS)*, 7(10), 35.**

**ABSTRACT:**

Mobile app reviews are gaining importance as a crowd source to improve the quality of mobile apps. Mobile app review systems are providing a platform for users to share their experiences and to support in decision making for a certain app. Developers, on the other side, are utilizing the review system to get real-life user experience as a source of improving their apps. This paper has analyzed existing review system and proposed few recommendations for the current review system to improve the quality of app reviews. The proposed review system can help for collection and analysis of user reviews to make it more meaningful with less intensive data mining techniques. The proposed system can help the end users to get an overview of mobile apps. The recommendations in this paper are derived from the existing literature related to app reviews and will help to improve the current review systems for better app reviews from users as well as developers perspective.

**WEB LINK:** <http://www.mecs-press.org/ijitcs/ijitcs-v7-n10/v7n10-5.html>

**17. Afzal., H. Naz T., Sadiq. A (2015). A Survey on Automatic Mapping of Ontology to Relational Database Schema. *Res. J. Recent Sci.*, 4(4), 66-70**

**ABSTRACT:**

The semantic Web is gaining significance day by day. One of the main aims of Semantic Web is to make the web work like database. Ontology plays a significant role in Semantic Web and acts as a foundation stone in a building. With the fame of ontologies, we require an effective and immediate approach to change all ontology constructs into relational database automatically so

that it could be queried effectively. The mapping of ontology information into relational database facilitates multiple operations such as information seeking and recovery. A large volume of research work has been carried out on automatic conversion of RDF/OWL notions into database. However there exist issues in automatic conversion and mapping of ontology to relational database. In this review paper, we furnish state of the art and methodologies to automatically transform ontology to relational database. We also describe their drawbacks and benefits. We finally present the future research work for lossless and automatic mapping of ontology into relational database format.

**WEB URL:** <http://www.isca.in/rjrs/v4i4.php>

**18. Ahmad, Z., Ahmad, F., & Naseer, M. (2015). Towards Z Specification Of Place Transition Nets. *Vfast Transactions on Software Engineering*, 6(2), 13-17.**

**ABSTRACT:**

Petri net formalism has dynamics and it is well suited for distributed or concurrent systems. However, it has a graphical representation in the form of a bipartite graph through which the type of data cannot be identified. This paper presents the Z specification of the net structure of place transition nets to provide the data semantics of graphical structure. This paper further addresses the Z specification of special sub classes of Petri nets, which include state machine, marked graphs and free choice nets.

**WEB URL:** <http://www.vfast.org/journals/index.php/VTSE/article/view/328>

**19. A. Khan et al. (2015). Application-based Classification and Comparison of Secure Routing Protocols in Wireless Sensor Networks: A Survey. *Smart Computing Review*, 5(3), 209-223.**

**ABSTRACT:**

Wireless Sensor Networks is an emergent field in computer network domains, and routing plays a key role in every wireless sensor network. In a wireless sensor network, an adversary can disturb the entire network by attacking routing services. These attacks are relatively easy to deploy against a wireless sensor network as opposed to traditional wired networks, because of

the unattended nature of the deployment of sensor nodes. In the case of wireless sensor networks, the compromised routing messages result in the diffusion of incorrect routing information, which can disrupt network behavior. When considering these realities, securing a routing protocol is a key objective of every wireless sensor network. In this paper, we analyze different secure routing protocols and do a comprehensive survey in terms of their application areas, key distribution schemes, authentication schemes, basic security requirements, and their defense against different attacks. To make our survey more precise, we categorized the secure routing protocols into four groups: secure data-centric, secure hierarchical, secure location-based, and secure quality-of-service routing protocols. All secure routing protocols discussed in this survey paper fall under these four categories.

**WEB URL:** [file:///C:/Users/sahmed/Downloads/smartcr\\_vol5no3p9.pdf](file:///C:/Users/sahmed/Downloads/smartcr_vol5no3p9.pdf)

# DEPARTMENT OF ELECTRICAL ENGINEERING

## Journal Papers

1. Hamayun, M. T., Edwards, C., Alwi, H., & Bajodah, A. (2015). A fault tolerant direct control allocation scheme with integral sliding modes. *International Journal of Applied Mathematics and Computer Science*, 25(1), 93-102.

**ABSTRACT:**

In this paper, integral sliding mode control ideas are combined with direct control allocation in order to create a fault tolerant control scheme. Traditional integral sliding mode control can directly handle actuator faults; however, it cannot do so with actuator failures. Therefore, a mechanism needs to be adopted to distribute the control effort amongst the remaining functioning actuators in cases of faults or failures, so that an acceptable level of closed-loop performance can be retained. This paper considers the possibility of introducing fault tolerance even if fault or failure information is not provided to the control strategy. To demonstrate the efficacy of the proposed scheme, a high fidelity nonlinear model of a large civil aircraft is considered in the simulations in the presence of wind, gusts and sensor noise.

**WEB URL:** <http://www.degruyter.com/view/j/amcs.2015.25.issue-1/amcs-2015-0007/amcs-2015-0007.xml>

2. Khan, A., Baig, S., & Nawaz, T. (2015). DWMT transceiver equalization using overlap FDE for downlink ADSL. *Turkish Journal of Electrical Engineering & Computer Sciences*, 23(3), 681-697.

**ABSTRACT:**

Discrete wavelet multitone (DWMT) modulation is a wavelet transform based technique implemented using perfect reconstruction filter banks. It has been recently proposed for

various wireline channels such as digital subscriber loops (DSLs) as a solution to the problems posed by a discrete multitone (DMT) transceiver including interblock interference (IBI) and lower spectral efficiency due to the employment of a cyclic prefix (CP) in the guard interval (GI) for DMT symbols. The greater side lobe attenuation offered by wavelet filter banks results in improved spectral containment and lower IBI in DWMT transceivers. However, no standard equalization technique exists for a DWMT based transceiver so as to remove the effect of channel on the transmitted signal in DWMT systems. This paper proposes the application of overlap frequency domain equalization (OFDE) in DWMT modulated systems and compares the bit error rate (BER) performance with time domain equalization (TDE) technique. It is shown through simulation results that minimum mean square error (MMSE) based OFDE can be applied as an equalization technique for a downlink asymmetric DSL (ADSL) channel with lower computational complexity and BER performance comparable to that of TDE.

**WEB URL:** <http://journals.tubitak.gov.tr/elektrik/abstract.htm?id=16005>

**3. Alwi, H., Edwards, C., Stroosma, O., Mulder, J. A., & Hamayun, M. T. (2015). Real-Time Implementation of an ISM Fault-Tolerant Control Scheme for LPV Plants. *Industrial Electronics, IEEE Transactions on*, 62(6), 3896-3905.**

**ABSTRACT:**

This paper proposes a fault-tolerant control (FTC) scheme for linear parameter-varying (LPV) systems based on integral sliding modes (ISMs) and control allocation (CA) and describes the implementation and evaluation of the controllers on a 6-degree-of-freedom research flight simulator called SIMONA. The FTC scheme is developed using an LPV approach to extend ideas previously developed for linear time-invariant systems, in order to cover a wide range of operating conditions. The scheme benefits from the combination of the inherent robustness properties of ISMs (to ensure sliding occurs throughout the simulation) and CA, which has the ability to redistribute control signals to all available actuators in the event of faults/failures.

**WEB URL:** <http://ieeexplore.ieee.org/xpl/articleDetails.jsp?arnumber=6998867&tag=1>

**4. Awais, M. N., & Choi, K. H. (2015). Resistive switching mechanism in printed non-volatile Ag/ZrO<sub>2</sub>/ITO sandwiched structure. *Electronics Letters*,51(25), 2147-2149.**

**ABSTRACT:**

The resistive switching mechanism in the printed sandwiched structures of Ag/zirconium oxide/indium tin oxide (ITO) is analytically demonstrated. The switching from the ON to OFF state of the fabricated device is attributed to the modulation of ohmic contact into opposite Schottky barriers following on from the electrochemical dissolution of the Ag filament from the weakest point near the ITO electrode and alteration of the Schottky barriers into an ohmic contact consequential to the reformation of the Ag filament during the transition of OFF into ON state. Physical current conduction governing laws verify the concluded transitions between ohmic contact and Schottky barriers.

**WEB URL:** [http://ieeexplore.ieee.org/xpls/abs\\_all.jsp?arnumber=7355506](http://ieeexplore.ieee.org/xpls/abs_all.jsp?arnumber=7355506)

**5. DAVIS, F., MUHAMMAD, B., CIANCA, E., & ALI, K. (2015). A Run-Time Method Based on Observable Data for the Quality Assessment of GNSS Positioning Solutions. *Selected Areas in Communications, IEEE Journal on*, 33(11), 2357-2365.**

**ABSTRACT:**

Several location-aware applications rely on the position estimated by means of Global Navigation Satellite Systems (GNSS), which are known to estimate an accurate position in an open environment. However, the quality of the estimated position is degraded in harsh environments in terms of accuracy and reliability. Liability-critical services, such as location-based charging, transportation, and road tolling, are threatened by the use of an unreliable position of the user, and the level of trust in the estimated position has to be considered to avoid a failure of the full service chain. Such an issue is faced by means of integrity monitoring methods in the field of GNSS. However, when dealing with harsh

environments, integrity monitoring techniques designed for aeronautical applications would lead to very conservative results and to the rejection of all the positions obtained. Such conservative approach is based on the theoretical error models for the estimation of the pseudorange standard deviation in open sky. The purpose of this work is to propose an innovative method for estimating the pseudorange standard deviation extrapolating it from measurements of observable data, to assess the confidence level in the obtained positions in relation to the real environment surrounding the user. While measuring the pseudorange standard deviation taking into account environment conditions and receiver accuracy, the user is able to achieve better estimation of the user equivalent range error (UERE). Estimating the UERE from raw pseudorange measurements with the proposed run-time method and its subsequent use in the computation of protection levels using the receiver autonomous integrity monitoring (RAIM) algorithm shows significant improvement in navigation system availability by deriving tight protection levels.

**WEB URL:** [http://ieeexplore.ieee.org/xpls/abs\\_all.jsp?arnumber=7102684](http://ieeexplore.ieee.org/xpls/abs_all.jsp?arnumber=7102684)

**6. Rafiq, M. A., Rafiq, M. N., & Saravanan, K. V. (2015). Dielectric and impedance spectroscopic studies of lead-free barium-calcium-zirconium-titanium oxide ceramics. *Ceramics International*, 41(9), 11436-11444.**

**ABSTRACT:**

Dielectric properties of perovskite structured  $(\text{Ba}_{0.85}\text{Ca}_{0.15})(\text{Zr}_{0.1}\text{Ti}_{0.9})\text{O}_3$ ; [BCZT], ferroelectric ceramics prepared by the conventional solid-state reaction method were investigated by AC impedance spectroscopy. To obtain high density samples, the pressed pellets were sintered at 1450 °C and 1500 °C for 4 h. Polarization–Electric field ( $P$ – $E$ ) measurements of the ceramic samples sintered at 1500 °C showed higher remnant polarization ( $P_r=12.20 \mu\text{C}/\text{cm}^2$ ) and coercive field ( $E_c=4.50 \text{ kV}/\text{cm}$ ) values when compared to  $P_r=8.02 \mu\text{C}/\text{cm}^2$  and  $E_c=3.80 \text{ kV}/\text{cm}$  respectively for the samples sintered at 1450 °C. In addition, BCZT sintered at 1500 °C showed higher dielectric constant as

compared to the one sintered at 1450 °C. However, the dielectric constant measured as a function of frequency for both the sintered samples showed single maximum value at ~105 °C, which is attributed to the structural phase transition (Curie temperature,  $T_C$ ) from ferroelectric, tetragonal phase to paraelectric, cubic phase. AC impedance analysis over the frequency range of 100 Hz to 1 MHz for the ceramic sintered at 1500 °C, showed mainly bulk contribution up to 250 °C while bulk and grain-boundary contributions were present above 250 °C. Activation energies for conductivity were found to be strongly frequency dependent. The activation energy values are attributed to the conduction of oxygen vacancies via hopping mechanism.

**WEB URL:** <http://www.sciencedirect.com/science/article/pii/S0272884215010512>

# DEPARTMENT OF HUMANITIES

## Journal Papers

1. Jibeen, T. (2015). Personality dimensions and emotional problems: The mediating role of irrational beliefs in Pakistani adult non-clinical sample. *International Journal of Psychology, 50(2)*, 93-100

**ABSTRACT:**

This study presents the first examination of the relation between the Big Five personality traits, irrational beliefs and emotional problems in Pakistan, which is an understudied country in the psychological distress literature. A total of 195 participants (aged 25–60 years), employees at COMSATS University, completed a demographic information sheet, the Big Five Personality Questionnaire, the Irrational Belief Inventory and two subscales of the Brief Symptom Inventory including depression and anxiety. Direct effects of neuroticism, openness and conscientiousness were also observed for depression and anxiety. Structural Equation Modelling demonstrated that irrational beliefs played a significant mediating role in the relationship between neuroticism and anxiety and neuroticism and depression. The results highlight the importance of cognitive beliefs in functionally linking personality traits and emotional problems.

WEB URL: <http://onlinelibrary.wiley.com/doi/10.1002/ijop.12069/abstract>

2. Idris, M., Tariq, H., & Idris, S. (2015). Home in the Dramatic World of the Father by August Strindberg. *International Journal of English Language and Literature Studies, 4(1)*, 20-26

**ABSTRACT:**

Strindberg's The Father Home, within the dramatic world of the text in question, becomes a space which the characters, especially Laura inscribes rather than just

inhabits. The metaphor of home is a popular metaphor in literature, especially in the postcolonial and social drama of Ibsen and Chekhov and other such playwrights of the modern era. House or home plays a significant role in plays like Hedda Gabler, Doll's House, The Cherry Orchard and also in other plays by Strindberg (2006) like The Dance of Death and to an extent in Miss Julie too. In The Father however, it changes its connotations, especially with respect to Laura's character as the plot develops. It becomes from a place of oppression to that of power for her and finally a Sibyl's cave where she uses her sorcery and creativity in a somewhat twisted way to mould things according to her desire. This paper seeks to critically analyze the space which defines 'home' in The Father, how it is used and consequently differed in meaning through the intervention of Laura. For this purpose it will draw upon 'The Parables of the Cave' written by Sandra M. Gilbert and Susan Gubar. This essay talks about how the simile of the cave corresponds with womb and the female abode.

**WEB URL:** <https://ideas.repec.org/a/asi/ijells/2015p20-26.html>

**3. Zubair., H. M. & Munawar., S.(2015). A Comparative Study of Distinguished English Translations concerning interpretation of Majāz in the Holy Quran *The Journal of Rotterdam Islamic and Social Sciences (Netherlands)*. 6(1). 1877-6671.**

Abstract: not found

**WEB URL:** <http://www.jriss.nl/volumes/2015-2>

**4. Mirza Muhammad Zubair Baig. (2015). Book Review of Artisans, Sufis, Shrines: Colonial Architecture in Nineteenth-Century Punjab. *Pakistan Journal of History and Culture*.35(1) 115-117.**

Abstract not found

**5. Ashraf, R. (2015). An Optimistic Evolution of Existence in Saffron Dreams by Shaila Abdullah. *Language in India*, 92.**

**ABSTRACT:**

In the realm of emerging contemporary Pakistani writers, writing in English, Shaila Abdullah's name shines as an epitome of exuberant writing style and purely Pakistani thematic considerations. Bestowed with the title of 'Word Artist' by critics, Abdullah uses her sharp and precise images to tear open the façade of the conventional practices a society nurtures. By probing into the psychology of her protagonists, Abdullah delineates different levels of struggles these women have to go through in order to establish an identity and disclose the true meaning of their existence. Arissa Illah's journey in *Saffron Dreams* is unique in its own way. She gathers up all she is left with, after facing a great tragedy. She then, joins these bits and pieces of her life not leaving even for a moment, the hold of a subtle tinge of hope and positivity. This optimism makes her stand on her feet once again and understand the real meaning and purpose of her life. Her existence evolves through stages to acceptance and negation, making her a survivor who did not succumb to the circumstances of life.

**WEB URL:**

<http://citeseerx.ist.psu.edu/viewdoc/download?doi=10.1.1.693.5493&rep=rep1&type=pdf#page=95>

**6. Fazli, S. K. (2015). The Question of Reliability in Script Scoring Practices. *European Academic Research*, 3(4) 4619-4632.**

**ABSTRACT:**

The present study analyzes the evaluation system for the compulsory subject of English at undergrad level in Bahauddin Zakariya University, Multan. The study considered how different evaluators assign scores to the same writing tasks in certain answer scripts. Mainly, the study concentrated on the reliability of scoring with reference to the paper A of the annual examination conducted for the candidates of Arts subjects at graduation level. Paper „A“ was chosen because it contained descriptive and subjective type questions and these types of questions are prone to subjective marking. This study has

been conducted with the help of randomly selected university approved examiners and answer scripts. A total of 50 scripts were marked by five examiners one after the other. This data was analyzed using the SPSS software in order to apply the ANOVA technique analysis. The analyses were made question wise as well as on the total marks awarded by the five examiners to the fifty scripts. The ANOVA technique was applied on the data in order to compare the performance of all the five examiners. The results indicated that there was no significant difference in the marking of all the five examiners on the total marks awarded. However, small differences were recorded in the marking of the individual questions.

**WEB URL:**

[https://www.researchgate.net/profile/Samar\\_Fazli/publication/280091318\\_THE\\_QUESTION\\_OF\\_RELIABILITY\\_IN\\_SCRIPT\\_SCORING\\_PRACTICES\\_Samar\\_Kamal\\_Fazli\\_Assistant\\_Professor\\_of\\_English\\_Department\\_of\\_Humanities\\_CIIT\\_Lahore\\_Pakistan/links/55d1c15808ae2496ee6580df.pdf](https://www.researchgate.net/profile/Samar_Fazli/publication/280091318_THE_QUESTION_OF_RELIABILITY_IN_SCRIPT_SCORING_PRACTICES_Samar_Kamal_Fazli_Assistant_Professor_of_English_Department_of_Humanities_CIIT_Lahore_Pakistan/links/55d1c15808ae2496ee6580df.pdf)

**7. Baig, M. M. Z. (2015) Pakistani Shades Of Humour: Finer Nuances In Patras' Humour. *European Academic Research* 3(4) 4515-4527.**

**ABSTRACT:**

This paper falls basically on my own translation of Patras Bokhari's three selected essays, first person narratives, from the source language Urdu, Pakistani national language, into the target language English in order to introduce them to the wider audience for the appraisal of humour written in Urdu. This paper also aims at the introduction of rich humour in Urdu Literature lying intact for the contemporary researchers in translation studies. Patras, known for his Urdu-ness, describes an experience as it is lived and his tone is suggestive and not conclusive. He invokes readers' imagination and demands their active participation in the reading where they correlate their schemas with that described in the writing to amplify the finer aspects of humour to the fuller blossoms. The use of situational humour in his writings has

established Patras Bokhari humourist of class in Urdu Literature and influenced his descendants and heirs in humour.

**WEB URL:**

[https://www.researchgate.net/profile/Mirza\\_Zubair\\_Baig/publication/280051777\\_Pakistani\\_Shades\\_of\\_Humour\\_Finer\\_Nuances\\_in\\_Patras\\_Humour/links/55a9606a08aea3d086803ca1.pdf](https://www.researchgate.net/profile/Mirza_Zubair_Baig/publication/280051777_Pakistani_Shades_of_Humour_Finer_Nuances_in_Patras_Humour/links/55a9606a08aea3d086803ca1.pdf)

**8. Baig, M. M. Z. (2015, June). The Desire to Rewrite Texts. In *Paper Proceedings of Second International Conference on Advances in Women's Studies* 47. 209-214.**

**ABSTRACT:**

As the canonical writings entail historical accounts which have stereotyped images of women and colonized people in the Western culture, there is desire in those who are at the margins to right/rewrite their historically doomed characters and images in order to recover the right place for their culture and selves. This establishes that something seriously went wrong in the writing of the classic texts from the perspective of the 'othered.' Here, the desire for rewriting is directly associated with the desire to re-right. My study invokes the desire to right by questioning the (re) writing process. This desire has also been intensified by Denzin's observation, "[w]riting is not an innocent practice. Men and women write culture differently". This claim refers to the genderbiased writing and observes much complicity involved in the process of writing. It also questions the writing practice which incorporates hidden motives and implicit designs.

**WEB URL:**

[http://uniqueca.com/archieves/pdf/2015/Proceeding%20\(AWS%202015\).pdf#page=209](http://uniqueca.com/archieves/pdf/2015/Proceeding%20(AWS%202015).pdf#page=209)

**9. Baig, M. M. Z. (2015). Symbiotic Feminist Postcolonial Overlapping: Understanding Theoretical Challenges and Exploring Possibilities. *European Academic Research* 3(5) 5254-5288.**

**ABSTRACT:**

Historically, the policing strategies of institutional forces in modern Western societies shaped and set limits on the representation of what are considered essentially subordinate beings. These erasures and absences hardly found their voice in the canonical texts written under the influence of patriarchy and colonialism that reinforce stereotypical representation and systematic “othering” of the characters in the institutionalized discourses of patriarchy and colonialism. Colonialism and patriarchy have been closely entwined historically. The issues of identity conform to modernist essentialist agenda, and aligned with the politics of colonization and domination, patriarchy becomes the master narrative that is uninterested in the displaced, marginalized, exploited, oppressed and, therefore, the excluded presences. An end to the physical presence of the colonial powers has not meant an end to the discourse of oppression which has affected the consciousness of the oppressed through the ages. Deconstruction of patriarchal and colonial discourses through the lenses of feminism and postcolonialism offers possibilities for the decolonization and subversion of oppressive order.

**WEB URL:**

[https://www.researchgate.net/profile/Mirza\\_Zubair\\_Baig/publication/280572533\\_Symbiotic\\_Feminist\\_Postcolonial\\_Overlapping\\_Understanding\\_Theoretical\\_Challenges\\_and\\_Exploring\\_Possibilities/links/55bf19f408ae9289a099e15a.pdf](https://www.researchgate.net/profile/Mirza_Zubair_Baig/publication/280572533_Symbiotic_Feminist_Postcolonial_Overlapping_Understanding_Theoretical_Challenges_and_Exploring_Possibilities/links/55bf19f408ae9289a099e15a.pdf)

**10. Fatima, S. Mehfooz. M. (2015). Menstruation & Menstruated One: A Study of Ancient Taboos versus Islamic Perspective and Scientific Realities in the Light of Al-Baqara 222 EUROPEAN ACADEMIC RESEARCH.3(6). 6984-7000.**

**ABSTRACT:**

Two departments of human life are of vital importance (i) Financial Resources: to survive by having basic needs of life (ii) Reproduction and good brought up of constructive group of people for the survival of humankind and progress of a civilized

state. The existence of civilized human race is impossible without the proper handling of these two institutions, so are divided equally between man and woman where man is selected as financial maintainer of his wife so that she can only focus on development and training of new generation to make them a useful individual of Islamic state. As because the human females are fixed by reproductive system so they have to go through the natural monthly menstrual process for which there exist many misogynistic traditions, myths and concepts in preislamic period but Islam recognized it as a natural biological process so only implied the restriction of sexual intercourse in the particular period and used the word (اذى) (izen for the disastrous effects of intercourse during menstruation revealed by latest scientific researches.

**WEB URL:** <http://euacademic.org/UploadArticle/1986.pdf>

**11. Baig, M. M. Z. (2015). Canon is Written Back: A Feminist/Postcolonial Critique. European Academic Research 3(6) 5987-6001.**

**ABSTRACT:**

The canonical Western narratives are reductionist, essentialist and monolithic representation(s) of the colonized and women as erased beings. Their marked absence from these texts, looked at through feminist and postcolonial lenses, asks for “critical intelligence” that questions their absence, silence or erasure, and engages us in moral critique, challenges and critiques the reductionist, essentialist and monolithic representations of the othered beings. The feminist postcolonial rewritings have been contextualized by the canonical writing, and the rewriters are not unmindful of temporal issues of voice, absences and identity which they consciously try to right in the contemporary reworks.

**WEB URL:**

[https://www.researchgate.net/profile/Mirza\\_Zubair\\_Baig/publication/281264679\\_Canon\\_is\\_Written\\_Back\\_A\\_FeministPostcolonial\\_Critique/links/55e679b008aec74dbe74e9d4.pdf](https://www.researchgate.net/profile/Mirza_Zubair_Baig/publication/281264679_Canon_is_Written_Back_A_FeministPostcolonial_Critique/links/55e679b008aec74dbe74e9d4.pdf)

**12. Naveed, A., & Aziz, S. (2015) Does schooling make a difference in English Language Proficiency? A comparison of Pakistani undergraduate students coming from English and Urdu medium schools. *European Academic Research* 3(8) 8628-8652.**

**ABSTRACT:**

The present study was undertaken to establish the level of English Language Proficiency (ELP) of first semester undergraduate students at COMSATS Institute of Information Technology, Lahore, Pakistan in the context of the established parallel system of education in the country. Students of various departments were assessed on English grammar and vocabulary. There was a significant difference in English and Urdu medium students' achievement in vocabulary use whereas no significant difference in grammar use. Percentage analysis of data revealed that majority of the students could achieve less than 50% marks in grammar and less than 50% in vocabulary. The findings identify problematic areas of ESL learning by providing insights into learners' second language errors and pinpointing areas for remedial work. The study recommends content based language learning and proficiency assessments to inform ELT and the use of communicative approaches for ELT pedagogy.

**WEB URL:**

[https://www.researchgate.net/profile/Shazia\\_Aziz/publication/283472635\\_Does\\_schooling\\_make\\_a\\_difference\\_in\\_English\\_Language\\_Proficiency\\_A\\_comparison\\_of\\_Pakistani\\_undergraduate\\_students\\_coming\\_from\\_English\\_and\\_Urdu\\_medium\\_schools/links/56398e6a08ae2da875c7a94f.pdf](https://www.researchgate.net/profile/Shazia_Aziz/publication/283472635_Does_schooling_make_a_difference_in_English_Language_Proficiency_A_comparison_of_Pakistani_undergraduate_students_coming_from_English_and_Urdu_medium_schools/links/56398e6a08ae2da875c7a94f.pdf)

**13. Fatima, S. Waseem. F. (2015). Qawāmiyat: Superiority or Responsibility? An Examination of Orientalists' Studies of Al-Nisā' 4:34 in the Light of Latest Scientific Researches. *European Academic Research* 3(7). 7802-7824.**

**ABSTRACT:**

The concept of qawāmīyat of the Holy Qurʾān which defines man's responsibility towards woman has removed all the ancient burdens of humiliation and degradation from womanhood by making her responsible for only those tasks which she can perform conveniently according to her creative design and nature. This research is based on a discussion of „qawāmīyat“ to encompass those theories by which the Qurʾānic concept of qawāmīyat has always been confused by non-Muslim researchers with ancient notions of superiority of man over woman. In contrast to the Holy Qurʾān, the holy texts of the other two most prominent Semitic and non-Semitic religions faiths, Christianity and Hinduism, regard females as inferior to man in all realms of human affairs; the notion also parallels the myths and taboos of ancient civilizations. The perception of female inferiority is so deeply rooted that the concept of qawāmīyat of the holy Qurʾān is mostly confused with these misogynistic ideas which are actually based upon gender differences and social perceptions about assignment of responsibilities.

**WEB URL:** <http://euacademic.org/UploadArticle/2040.pdf>

**14. Jibeen, T. (2015). Perceived social support and mental health problems among Pakistani university students. *Community mental health journal*, 1-5.**

**ABSTRACT:**

Despite the growing number of cross-cultural studies focusing on psychological problems, little is known about social support outside of western civilization, particularly among people in South Asian cultures. This study examined the cultural orientation regarding perceived social support and psychological problems among 912 undergraduate students (age 19–26) studying at COMSATS Institute of Information Technology, Lahore, Pakistan. The present study supported variance in cultural values regarding the relative prominence of sources of support in collectivist culture indicating that low levels of family support were related to various psychological problems. Further, low levels of peer support were related to depression, anxiety, and

interpersonal sensitivity. While familial support played a bigger role than peer support in affecting psychological problems, peer support also had a role to play. The results may help counsellors and researchers to identify more effectively the population of students at high risk for mental illness and develop culturally effective interventions to address this significant and growing public health issue.

**WEB URL:** <http://link.springer.com/article/10.1007/s10597-015-9943-8>

**15. Jibeen, T., & Khan, M. A. (2015). Internationalization of higher education: Potential benefits and costs. *International Journal of Evaluation and Research in Education*.4(4) 196-199.**

**ABSTRACT:**

Internationalization of higher education is the top stage of international relations among universities and it is no longer regarded as a goal in itself, but as a means to improve the quality of education. The knowledge translation and acquisition, mobilization of talent in support of global research and enrichment of the curriculum with international content are considered to be the benefits of internationalization of higher education. Though, internationalization holds many positives to higher education, there are grave risks associated with this multifaceted and growing phenomenon. Negative aspects include commercial profit, academic colonization and difficulty in ensuring quality education. The current review has implications for educational policy makers to ensure positive and reciprocal benefits to the higher education institutions and the countries concerned.

**WEB URL:** <http://www.iaesjournal.com/online/index.php/IJERE/article/view/9250>

**16. Jibeen, T., & Khan, M. A. Development of an Academic Achievement Risk Assessment Scale for Undergraduates: Low, Medium and High Achievers. *REMIE Multidisciplinary Journal of Educational Research*,6(1), 23.**

*Abstract not found*

**17. Fatima, S. (2015). Nature of Zionism & Protocols of Learned Elders of Zion. *American Research Thoughts*,2(1). 3012-3033.**

**ABSTRACT:**

Formally, the movement of Zionism was initiated by Theodore Herzl as he laid the foundations of World Zionist Organization but history witnesses that the seed of Zionism and Jewish settlements in Palestine had been sown in the hearts of the Jews since ancient times; however, what is important is to examine that techniques and plan of action which actually gave to sculpture the spirit and to dream the direction and that was 'The Protocols of Learned Elders of Zion' prepared by grade 33 representatives to 'technically' control the gentiles (non-Jews). In the current world scenario, to understand the actual purpose and intention behind every global policy and initiative this executive formula is indispensable to be operated which also used to be called as 'the Jew World Order' rather than 'the New World Order' as it may lead towards those organizations, personalities, schemes, resolutions and even specific kinds of thoughts and doctrines which are actually the products of 'The Protocols of Learned Elders of Zion'

**WEB URL:** <http://researchthoughts.us/UploadedArticle/254.pdf>

**18. Fatima. S (2015). "Adolescent Aggression as Predicted from Parent-Child Relationships and Executive Functions. *American Journal of Psychology*.**

*Abstract not found.*

**19. Rabia Ashraf. (2015). History: Re-Written, Revised Or Revisited In Gunter Grass's Crabwalk. *European Academic Research* 3(9). 9756-9765.**

**ABSTRACT:**

The paper aims at exploring the German guilt to the acknowledgement of German war suffering in Gunter Grass Crabwalk who is Germany's greatest post war voice. Set within the context of miseries of East Prussian Germans by revisiting the tragedy and forming another collective consciousness of the German historical memory, from perpetrators to victims, Grass poses his nationalistic stance by re positioning the German's identity and re affirming that past has strong ties with the present. The study highlights Crabwalk as depicting the consequences of perpetual suppression where reality becomes a changing entity as discussed by Grass

**WEB URL:** <http://euacademic.org/UploadArticle/2161.pdf>

**20. Fatima, S. Siddique, M. S. (2015) اسلامیہ شریعت اور فکر مکاتب متخالف عالم، مذاہبِ رحم قتل** *Al-Adwa*, 30(44) 49-70. **جائز کا نظر ہائے نقطہ کے**

Abstract not found

**WEB URL:** [http://pu.edu.pk/images/journal/szic/pdf\\_files/3-Saleha%20Fatima%20Mercy\\_Dec15.pdf](http://pu.edu.pk/images/journal/szic/pdf_files/3-Saleha%20Fatima%20Mercy_Dec15.pdf)

**21. Fatima, S. Lakhvi, M. H. (2015) The Authenticity Of Women's Witness In Islam: A Study In The Light Of AL-QUR'AN. 20(2) 1-16.**

**ABSTRACT:**

By keeping in view the dignity, delicacy and natural shyness of womanhood, Islam designed such laws and regulations which widen the space and include women in every field of life and introduced that social structure by which women can play an active role in all institutions of Islamic civilization by remaining into the boundaries of their actual field of action which is the development of a progressive new generation for the glorious future of Islamic civilization, the important responsibility which men cannot perform due to their natural masculinity and no capricious state of mind. This is the reason that Islam prefers the man more than woman in assigning the financial

responsibility which is one of the two basic institutions of human life. Apparently In Al-Qur'an sūrah al-Baqara: 282 the witness of one man is regarded as equal to two women which is unfortunately the most misunderstood phenomenon about the gender related verses of the holy Qur'an and is still remains in orientalist's writings which is actually the result of miscomprehension.

**WEB URL:**

[http://pu.edu.pk/images/journal/alqalam/PDF/1.Saleha%20Fatima+Dr.%20M.%20Hamad%20Lakhvi\\_Dec2015.pdf](http://pu.edu.pk/images/journal/alqalam/PDF/1.Saleha%20Fatima+Dr.%20M.%20Hamad%20Lakhvi_Dec2015.pdf)

**22. Ahmad, M. M. (2015). Challenge or Opportunity-Exploring Emergence and Historical Development of Hyper textual Representations. *International Journal of Research*, 2(9), 144-151.**

**ABSTRACT:**

With the invention of digital technologies, the activity of reading has become highly dependent on the display of language in new contexts and new forms, and thus, new reading environments play their role in comprehension while enhancing the experience of the reader. Since new devices/machines are invented keeping in view their utility/productivity and the preferences of the users, so the application of digital hypertext using electronic medium might attribute quite new dimensions to studying language comprehensibility because of the change in language (re)presentation. Therefore, whether with the advent of digital texts the nature of comprehension in new language forms, gets modified or not is a researchable question to be explored and studied. The emergence of hypertext representation started an unending debate about the nature of hypertext per se and the way it enriches the interactive process of meaning making, and the phenomenon of comprehension of texts and their production. It is important to consider the nature of hypertext representation because it is concerned with its exclusive comprehension patterns unlike traditional book reading. The present review article is basically a critical study of literature regarding the emergence and historical development of hypertext.

**WEB URL:** <http://sureshotpost.com/journals/index.php/IJR/article/view/2729>

**23. Muddasir, M. A. (2015) Fixing the Text: Is it Time to Do away with Tradition?. *European Academic Research* 3(6) 6436-6446.**

**ABSTRACT:**

Human intellect and knowledge has enjoyed an intimate relationship with text in different form(ats). With the evolution of human civilization languages undergo certain change and same is the case with languaged texts. Present study critically reviews the defining characteristics of text and the compositionary nature what attributing languaged scripts as text. It further reviews the theorist stance regarding text which seems to evolve as a fluid term currently. Relationship of reading and writing is also explored and why traditional textuality is considered superior.

**WEB URL:** <http://euacademic.org/UploadArticle/1948.pdf>

**24. Baig, M. Z., Mudassar M., Fazli, S.K. (2015). *Erotic Bodies: Bildungsroman of Love in Love in the Time of Cholera, Scholar Critic, 2(3) 24-30.***

**ABSTRACT:**

‘Love’ in *Love in the Time of Cholera* is eponymous that grows, develops, matures and ages in the plot with the development of main characters, Fermina Daza, Florentino Ariza and Dr. Juvenal Urbino and their love-affairs. The narrative invokes eroticism while it gives description to the subdued bodies, unexplored sexualities and instable liaisons of Fermiza. Bildungsroman of love in Marquez makes this study interesting where patriarchal construct of ‘love’ is personified that remains predominantly assertive throughout the novel in its chameleon like fluid existence changing from first sight love to fixation, from staring gaze to marriage, from its macho character to aging love, and from widowhood to revival of love in old age. Keywords: Love, Eroticism, Feminism, Sexuality.

**WEB URL:** <http://www.scholarcritic.com/papers/SCJ-Dec-2015-3.pdf>

25. Waseem, F. (2015) The Hidden Curriculum of English Language Teaching in Elite Pakistani Schools. *Journal of English as an International Language(EILJ)*. 10(2). 66-85.

Abstract not found.

**WEB URL:** <https://www.elejournals.com/1297/2015/eilj-2015/eilj-volume-10-issue-2-december-2015/>

# DEPARTMENT OF IRCBM

## Journal Papers

1. Rahim, A., Ahmad, K., Ullah, F., Ullah, H., & Nishan, U. (2015). In vitro antibacterial activity of selected medicinal plants from lower Himalayas. *Pakistan journal of pharmaceutical sciences*, 28(2) 581-587.

### **ABSTRACT:**

The present studies cover antibacterial activity of the crude methanolic extracts of 11 medicinal plants viz. Adhatoda vasica, Bauhenia variegata, Bombax ceiba, Carrisa opaca, Caryopteris grata, Debregeasia salicifolia, Lantana camara, Melia azedarach, Phyllanthus emblica, Pinus roxburghii and Olea ferruginea collected from lower Himalayas against two Gram positive (Staphylococcus aureus, Micrococcus luteus) and two Gram negative (Escherichia coli, Pseudomonas aeruginosa) bacterial strains. The extracts were applied at four different concentrations (120 mg/mL, 90mg/mL, 60mg/mL and 30mg/mL) in dimethyl sulfoxide (DMSO) by using agar well diffusion method. Antibacterial activities against Staphylococcus aureus and Micrococcus luteus were observed from methanolic extracts of all the above mentioned plants. Greater antibacterial activity against Pseudomonas aeruginosa was only exhibited by Phyllanthus emblica, Pinus roxburghii, Debregeasia salicifolia and Lantana camara. Escherichia coli was highly resistant to all the plant extracts at all concentrations. It is inferred that methanolic crude extracts of the above mentioned plants exhibit antibacterial activities against pathogenic bacteria, which proved the ethnobotanical importance of the selected plants that indigenous people use for cure against various diseases.

### **WEB URL:**

<http://web.a.ebscohost.com/abstract?direct=true&profile=ehost&scope=site&authtype=crawler&jrnl=1011601X&AN=101551960&h=QsW1V%2bykzpmOEwHvJid877xQNvPIMc46Wfbo6L7LqeKrJ4x0FwoD3Z3b9kBhMyMUs7oc%2blbVYi4x%2bOIVOaDz8g%3d%3d&cr>

[l=c&resultNs=AdminWebAuth&resultLocal=ErrCrINotAuth&crlhashWebURL=login.aspx%3fdirect%3dtrue%26profile%3dehost%26scope%3dsite%26authtype%3dcrawler%26jrnl%3d1011601X%26AN%3d101551960](#)

**2. Dominguez, R. B., Alonso, G. A., Muñoz, R., Hayat, A., & Marty, J. L. (2015). Design of a novel magnetic particles based electrochemical biosensor for organophosphate insecticide detection in flow injection analysis. *Sensors and Actuators B: Chemical*, 208, 491-496.**

**ABSTRACT:**

The fabrication of transducer interfaces with improved electroanalytical performance is still a challenge in the field of advanced flow based electrochemical biosensors. The use of magnetic nanoparticles for such a purpose to replace the routinely used immobilization matrix including glass, membrane, polymer, gel beads, sol–gel supports, porous silicon matrix, and porous monolithic materials is well documented in the recent literature. However, the application of magneto-based methods is restricted due to lack of reproducibility and renewal of the sensor surface. To overcome these limitations, the present work described a novel configuration strategy to integrate magnetic nanobeads into the flow based system to achieve the reproducible and renewable sensing surface. The designed flow based sensor was demonstrated for the detection of organophosphate insecticides using acetylcholinesterase (AChE) enzyme. System parameters such as optimal bead injection and flow rate were studied prior to insecticides analysis. The system can be potentially applied for on-line assessment in a sensitive, automatic, inexpensive, continuous and simple way for any other analyte of interest.

**WEB URL:** <http://www.sciencedirect.com/science/article/pii/S092540051401449X>

**3. Ramakrishnaiah, R., Rehman, G. U., Basavarajappa, S., Al Khuraif, A. A., Durgesh, B. H., Khan, A. S., & Rehman, I. U. (2015). Applications of Raman Spectroscopy in Dentistry: Analysis of Tooth Structure. *Applied Spectroscopy Reviews*, 50(4), 332-350.**

**ABSTRACT:**

Tooth enamel is the most mineralized tissue in the human body, and in this article the use of Raman spectroscopy for the analysis of tooth structure, a comparison with synthetic apatites, and use in dentistry are described. Spectral peaks that are related to dental hard and soft tissues are discussed, which provide crucial data in understanding the chemical structural properties of dentin and enamel. The Raman spectrum of dentin confirms the presence of crystalline phosphate-based minerals in dentin. Both dentin and enamel consist of two primary components: an inorganic or mineral phase that closely resembles hydroxyapatite and the Raman spectrum of dentin that confirms the presence of crystalline phosphate-based minerals in dentin. Hence, the mineral phase in dentin and enamel may be characterized essentially as nonstoichiometric substituted apatite. The presence of carbonate (A and B type) incorporated in the hydroxyapatite lattice is also confirmed by the presence of spectral bands. The organic phase, which is mainly composed of type I collagen, is confirmed by the spectral bands of amide I and amide II bands, tryptophan, and phenylalanine. Furthermore, these spectral bands associated with organic and inorganic parts of the enamel and dentin are useful in predicting early formation of carries formation.

**WEB URL:** <http://www.tandfonline.com/doi/abs/10.1080/05704928.2014.986734>

**4. Shahzad, S., Yar, M., Siddiqi, S. A., Mahmood, N., Rauf, A., Anwar, M. S., & Afzaal, S. (2015). Chitosan-based electrospun nanofibrous mats, hydrogels and cast films: novel anti-bacterial wound dressing matrices. *Journal of Materials Science: Materials in Medicine*, 26(3), 1-12.**

**ABSTRACT:**

The development of highly efficient anti-bacterial wound dressings was carried out. For this purpose nanofibrous mats, hydrogels and films were synthesized from chitosan, poly(vinyl alcohol) and hydroxyapatite. The physical/chemical interactions of the synthesized materials were evaluated by FTIR. The morphology, structure; average

diameter and pore size of the materials were investigated by scanning electron microscopy. The hydrogels showed a greater degree of swelling as compared to nanofibrous mats and films in phosphate buffer saline solution of pH 7.4. The in vitro drug release studies showed a burst release during the initial period of 4 h and then a sustained release profile was observed in the next upcoming 20 h. The lyophilized hydrogels showed a more slow release as compared to nanofibrous mats and films. Antibacterial potential of drug released solutions collected after 24 h of time interval was determined and all composite matrices showed good to moderate activity against Gram-positive and Gram-negative bacterial strains respectively. To determine the cytotoxicity, cell culture was performed for various cefixime loaded substrates by using neutral red dye uptake assay and all the matrices were found to be non-toxic.

**WEB URL:** <http://link.springer.com/article/10.1007/s10856-015-5462-y>

**5. Özel, R. E., Hayat, A., & Andreescu, S. (2015). Recent Developments in Electrochemical Sensors for the Detection of Neurotransmitters for Applications in Biomedicine. *Analytical Letters*, 48(7), 1044-1069.**

**ABSTRACT:**

Neurotransmitters are important biological molecules that are essential to many neurophysiological processes including memory, cognition, and behavioral states. The development of analytical methodologies to accurately detect neurotransmitters is of great importance in neurological and biological research. Specifically designed microelectrodes or microbiosensors have demonstrated potential for rapid, real-time measurements with high spatial resolution. Such devices can facilitate study of the role and mechanism of action of neurotransmitters and can find potential uses in biomedicine. This paper reviews the current status and recent advances in the development and application of electrochemical sensors for the detection of neurotransmitters. Measurement challenges and opportunities of electroanalytical methods to advance study and understanding of neurotransmitters in various biological models and disease conditions are discussed.

**WEB URL:** <http://www.tandfonline.com/doi/abs/10.1080/00032719.2014.976867>

6. Shah, A. T., Ain, Q., Chaudhry, A. A., Khan, A. F., Iqbal, B., Ahmad, S., ... & ur Rehman, I. (2015). A study of the effect of precursors on physical and biological properties of mesoporous bioactive glass. *Journal of Materials Science*, 50(4), 1794-1804.

**ABSTRACT:**

A novel mesoporous bioactive glass (MBG) of composition 64SiO<sub>2</sub>-26CaO-10P<sub>2</sub>O<sub>5</sub> (mol %) was prepared by hydrothermal method using H<sub>3</sub>PO<sub>4</sub> as a precursor for P<sub>2</sub>O<sub>5</sub>. The effect of use of organic triethylphosphate (TEP) and inorganic H<sub>3</sub>PO<sub>4</sub> in MBG synthesis on glass transition temperature ( $T_g$ ), crystallinity, morphology and bioactivity of MBGs was studied. Phase purity determination and structural analysis were done using powder X-ray diffraction (XRD) and Fourier transform infrared (FTIR) spectroscopy, respectively. XRD revealed that MBG prepared from H<sub>3</sub>PO<sub>4</sub> (MBG-H<sub>3</sub>PO<sub>4</sub>) when sintered at 700 °C was partially glassy/amorphous in nature and contained a mixture of crystalline apatite, wollastonite, calcium phosphate and calcium silicate phases. Calcined MBG prepared from TEP (MBG-TEP) contained only wollastonite and calcium silicate phases. Particle size and surface area determined by BET surface area analysis showed higher surface area (310 m<sup>2</sup> g<sup>-1</sup>) for MBG-H<sub>3</sub>PO<sub>4</sub> as compared to MBG-TEP (86 m<sup>2</sup> g<sup>-1</sup>). It also had a smaller particle size (20 nm) and 70 % higher pore volume (0.88 cm<sup>3</sup> g<sup>-1</sup>) for MBG-H<sub>3</sub>PO<sub>4</sub> as compared to MBG-TEP (60 nm particle size and 0.23 cm<sup>3</sup> g<sup>-1</sup> pore volume). Thermal studies showed that use of H<sub>3</sub>PO<sub>4</sub> decreases  $T_g$  and increased  $\Delta T$  (difference between  $T_g$  and crystallization initiation temperature  $T_{c_0}$ ). Low  $T_g$  and high  $\Delta T$  also enhanced bioactivity of MBGs. Bioactivity was determined by immersion in a simulated body fluid for varying time intervals for a maximum period of 14 days. It revealed enhanced bioactivity, as evident by the formation of apatite layer on the surface, for MBG-H<sub>3</sub>PO<sub>4</sub> as compared to MBG-TEP. Scanning electron microscopy and FTIR spectroscopy also supported this observation. Antibacterial studies with *Escherichia Coli* bacteria, MBG-H<sub>3</sub>PO<sub>4</sub> showed better antibacterial behaviour than MBG-TEP.

**WEB URL:** <http://link.springer.com/article/10.1007/s10853-014-8742-x>

**7. Khan, A. S., Azam, M. T., Khan, M., Mian, S. A., & Rehman, I. U. (2015). An update on glass fiber dental restorative composites: A systematic review. *Materials Science and Engineering: C*, 47, 26-39.**

**ABSTRACT:**

Dentistry is a much developed field in the last few decades. New techniques have changed the conventional treatment methods as applications of new dental materials give better outcomes. The current century has suddenly forced on dentistry, a new paradigm regarding expected standards for state-of-the-art patient care. Within the field of restorative dentistry, the incredible advances in dental materials research have led to the current availability of esthetic adhesive restorations. The chemistry and structure of the resins and the nature of the glass fiber reinforced systems in dental composites are reviewed in relation to their influence and properties including mechanical, physical, thermal, biocompatibility, technique sensitivity, mode and rate of failure of restorations on clinical application. It is clear that a deeper understanding of the structure of the polymeric matrix and resin-based dental composite is required. As a result of ongoing research in the area of glass fiber reinforced composites and with the development and advancement of these composites, the future prospects of resin-based composite are encouraging.

**WEB URL:** <http://www.sciencedirect.com/science/article/pii/S0928493114007164>

**8. Muhammad, N., Elsheikh, Y. A., Mutalib, M. I. A., Bazmi, A. A., Khan, R. A., Khan, H., ... & Man, Z. (2015). An overview of the role of ionic liquids in biodiesel reactions. *Journal of Industrial and Engineering Chemistry*, 21, 1-10.**

**ABSTRACT:**

The concerns on the depleting petroleum resources and increasing environmental problems have driven the scientific community worldwide to develop large-scale non-

petroleum-based alternative fuels, such as bioethanol and biodiesel. Biodiesel produced through the transesterification of vegetable oils or animal fats are highly attractive. On the other hand, ionic liquids which possess properties that are more environmental friendly have found significant applications as solvents and catalysts for reaction and separation. It is also beginning to find its way in many of the chemical process applications and has attracted significant attention including biodiesel production. This paper provides a brief overview on the feasibility of applying ionic liquids in biodiesel production for the purpose of powering diesel engines for transportation and utility generation. The potential of applying ionic liquids as catalyst and solvent for enzymatic production of biodiesel from feedstock is particularly highlighted.

**WEB URL:** <http://www.sciencedirect.com/science/article/pii/S1226086X14000859>

**9. Khan, U. S., Khattak, N. S., Manan, A., Rahman, A., Khan, F., & Rahim, A. (2015). Some Properties of Magnetite Nanoparticles Produced Under Different Conditions. *Journal of Electronic Materials*, 44(1), 303-312.**

**ABSTRACT:**

Temperature, stirring rate, stirring time, reaction pH, and concentration of precursors during synthesis were found to be crucial in determining the size of the magnetite nanoparticles (NPs) obtained. The relationship between synthetic conditions and the crystal structure, particle size, and size distribution of the NPs was studied. Surface coating of iron oxide NPs was performed in two steps. Magnetite NPs were prepared by coprecipitation then coated with silica by use of a sol-gel process. Saturation magnetization of the magnetite NPs increased from 47.23 to 49.12 emu/g when their size was increased from 8.89 to 9.39 nm. Magnetite NPs in the size range 11–12 nm, coated with silica, are monodispersed and their corresponding saturation magnetization is 40.67 emu/g (11 nm) and 34.65 emu/g (12 nm). The decrease in the saturation magnetization of the coated samples is attributed to the increase in the amount of tetraethyl orthosilicate.

**WEB URL:** <http://link.springer.com/article/10.1007/s11664-014-3467-9>

10. Khan, A. F., Afzal, A., Chaudhary, A. A., Saleem, M., Shahzadi, L., Jamal, A., ... & Habib, A. (2015). (Hydroxypropyl) methylcellulose Mediated Synthesis of Highly Porous Composite Scaffolds for Trabecular Bone Repair Applications. *Science of Advanced Materials*, 7(6), 1177-1186.

**ABSTRACT:**

This article presents an (hydroxypropyl)methylcellulose (HPMC) mediated synthesis of highly porous scaffolds containing nanocrystalline hydroxyapatite (*n*-HAp) and chitosan (CS) as major inorganic and organic phases, respectively. A mixture of *n*-HAp, CS, and HPMC is homogenized and freeze-dried to yield *n*-HAp/CS/HPMC composite scaffolds closely emulating trabecular bone in density ( $0.02 \text{ g} \cdot \text{cm}^{-3}$ ) and porosity (89%). SEM images substantiate the porous structure of the scaffolds (pore size: 100–300  $\mu\text{m}$ ). The mechanical analysis reveal excellent compressive strength of the porous *n*-HAp/CS/HPMC scaffold (9.65 MPa) that is also comparable with human trabecular bone. The *in vitro* bioactivity and degradability of the porous scaffolds are investigated in tris-HCl-buffered synthetic body fluid (SBF) and phosphate buffer solution (PBS), respectively. The results indicate a rapid increase in scaffold mass due to apatite-like deposition and good resorbability. The SEM images of SBF soaked samples demonstrate apatite-like deposition on the surface of scaffolds with Ca/P ratio of 1.63 after 7 days of soaking in SBF. These results suggest that porous *n*-HAp/CS/HPMC scaffolds, due to their structural similarity, mechanical and *in vitro* biological properties, can become useful alternatives for trabecular bone regeneration and repair.

**WEB URL:**

<http://www.ingentaconnect.com/content/asp/sam/2015/00000007/00000006/art00022>

11. Mujahid, A., Khan, A. I., Afzal, A., Hussain, T., Raza, M. H., Shah, A. T., & uz Zaman, W. (2015). Molecularly imprinted titania nanoparticles for selective recognition and assay of uric acid. *Applied Nanoscience*, 5(5), 527-534.

**ABSTRACT:**

Molecularly imprinted titania nanoparticles are successfully synthesized by sol-gel method for the selective recognition of uric acid. Atomic force microscopy is used to study the morphology of uric acid imprinted titania nanoparticles with diameter in the range of 100–150 nm. Scanning electron microscopy images of thick titania layer indicate the formation of fine network of titania nanoparticles with uniform distribution. Molecular imprinting of uric acid as well as its subsequent washing is confirmed by Fourier transformation infrared spectroscopy measurements. Uric acid rebinding studies reveal the recognition capability of imprinted particles in the range of 0.01–0.095 mmol, which is applicable in monitoring normal to elevated levels of uric acid in human blood. The optical shift (signal) of imprinted particles is six times higher in comparison with non-imprinted particles for the same concentration of uric acid. Imprinted titania particles have shown substantially reduced binding affinity toward interfering and structurally related substances, e.g. ascorbic acid and guanine. These results suggest the possible application of titania nanoparticles in uric acid recognition and quantification in blood serum.

**WEB URL:** <http://link.springer.com/article/10.1007/s13204-014-0346-x>

**12. Kaleem, M., Khan, A. S., Rehman, I. U., & Wong, F. S. (2015). Effect of Beverages on Viscoelastic Properties of Resin-Based Dental Composites *Materials*, 8(6), 2863-2872.**

Abstract:

The viscoelastic properties of three commercially available resin-based composites (Filtek™ P60, Filtek™ Supreme, and Filtek™ Z250; 3M ESPE, Bracknell, UK) were measured to determine the effect of beverages on their storage moduli and damping ratios. Rectangular samples of the three hybrid composites were immersed in three beverages at 37 °C for 1, 7, 30, and 60 days. At each time interval, these samples were subjected to three-point bend tests in temperature mode using a Perkin Elmer DMA7 Dynamic Mechanical Analyzer (Perkin Elmer Corp., Waltham, MA, USA) to measure the storage modulus and damping ratio. The immersion time had significant

influence on the viscoelastic property of composites and it was found that generally for all samples the storage modulus was reduced, whereas damping values increased with immersion time. The viscoelastic behavior of tested materials seems to be related to the pH environment, hydrophilicity and the chemical composition of composites

**WEB URL:** <http://www.mdpi.com/1996-1944/8/6/2863/htm>

**13. Azam, M. T., Khan, A. S., Muzzafar, D., Faryal, R., Siddiqi, S. A., Ahmad, R., ... Rehman, I. U. (2015). Structural, Surface, in vitro Bacterial Adhesion and Biofilm Formation Analysis of Three Dental Restorative Composites. *Materials*, 8(6), 3221-3237.**

**ABSTRACT:**

This study was conducted to investigate the relationship between dental materials and bacterial adhesion on the grounds of their chemical composition and physical properties. Three commercially available dental restorative materials (Filtek™Z350, Filtek™P90 and Spectrum®TPH®) were structurally analyzed and their wettability and surface roughness were evaluated by using Fourier Transform Infrared Spectroscopy, Contact Angle Measurement and Atomic Force Microscopy, respectively. These materials were molded into discs and tested with three bacterial strains (*Staphylococcus aureus*, *Pseudomonas aeruginosa* and *Escherichia*) for microbial attachment. The bacterial adhesion was observed at different time intervals, *i.e.*, 0 h, 8 h, 24 h, 48 h and 72 h, along with Colony Forming Unit Count and Optical Density measurement of the media. It was found that all materials showed a degree of conversion with time intervals, *i.e.*, 0 h, 8 h, 24 h, 48 h and 72 h, which led to the availability of functional groups (N–H and C–H) that might promote adhesion. The trend in difference in the extent of bacterial adhesion can be related to particle size, chemical composition and surface wettability of the dental materials.

**WEB URL:** <http://www.mdpi.com/1996-1944/8/6/3221?trendmd-shared=0>

14. Farooq, A., M Yar, A.S. Khan, L. Shahzadi, S.A. Siddiqi, N. Mahmood, A. Rauf, Z. A. Qureshi, A.A. Chaudhry, I. Rehma (2015) *Synthesis of Novel Electrospun Biodegradable Nanocomposite Scaffolds for Periodontal Regeneration. Materials Science and Engineering C*, 56. 104-113.

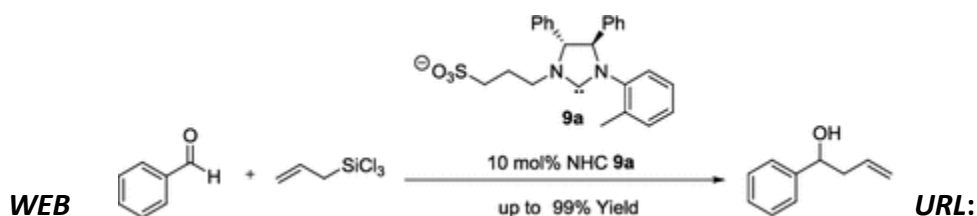
*Abstract not found*

15. Tabassum, S., Gilani, M. A., Ayub, K., & Wilhelm, R. (2015). First examples of carbene-catalyzed allylation of benzaldehyde with allyltrichlorosilane. *Journal of the Iranian Chemical Society*, 12(7), 1199-1205.

**ABSTRACT:**

We report here first examples of carbene-catalyzed allylation of benzaldehyde. *N*-Heterocyclic carbenes applied here, **9a** and **10a**, were derived from imidazolium zwitterions, and contained sulfonate and sulfamate substituents, respectively. Different reaction conditions such as temperature, organic solvents, additive and bases were used to optimize the reaction. Sulfonate substituted NHC **9a** is found more efficient organocatalyst for the allylation of benzaldehyde (greater than 99 % yield at lower temperature) than sulfamate-based NHC **10a** (a yield of no more than 15 %). These results are justified on the basis of philicity descriptors of the NHCs and their corresponding allyldichlorosilane complexes.

Graphical abstract



<http://link.springer.com/article/10.1007/s13738-014-0582-8>

16. Shah, A. T., Din, M. I., Kanwal, F. N., & Mirza, M. L. (2015). Direct synthesis of mesoporous molecular sieves of Ni-SBA-16 by internal pH adjustment method and its

performance for adsorption of toxic Brilliant Green dye. *Arabian Journal of Chemistry*, 8(4), 579-586.

**ABSTRACT:**

An ordered mesoporous novel material Ni-SBA-16 has been synthesized by internal pH-adjustment method. The synthesized material has been characterized by small angle XRD (SAXRD), wide angle XRD (WAXRD), Scanning Electron Microscope (SEM), High-Resolution Transmission Electron Microscope (HRTEM), Fourier-transform Infra-red (FTIR) spectroscopy and Nitrogen Adsorption-desorption techniques. The characterization results have shown that material possesses highly ordered mesostructure with high surface area ( $736 \text{ m}^2/\text{g}$ ) and large pore diameter (3.8 nm). FTIR and WAXRD spectra revealed that nickel was uniformly dispersed on SBA-16 surface. The synthesized material has been used as adsorbent for removal of toxic Brilliant Green dye due to its large surface area and pore size. At optimized conditions, almost 100% of Brilliant Green dye was removed from aqueous solution by Ni-SBA-16. The isotherms analysis indicates that the Langmuir and Hill models provide the best correlation of the experimental data. The maximum adsorption capacity ( $q_{\text{max}}$ ) of Ni-SBA-16 for Brilliant Green dye was 322.58 mg/g.

**WEB URL:** <http://www.sciencedirect.com/science/article/pii/S1878535214003244>

17. Hayat, A., Cunningham, J., Bulbul, G., & Andreescu, S. (2015). Evaluation of the oxidase like activity of nanoceria and its application in colorimetric assays. *Analytica chimica acta*, 885, 140-147.

**ABSTRACT:**

Nanomaterial-based enzyme mimics have attracted considerable interest in chemical analysis as alternative catalysts to natural enzymes. However, the conditions in which such particles can replace biological catalysts and their selectivity and reactivity profiles are not well defined. This work explored the oxidase like properties of nanoceria particles in the development of colorimetric assays for the detection of dopamine and

catechol. Selectivity of the system with respect to several phenolic compounds, the effect of interferences and real sample analysis are discussed. The conditions of use such as buffer composition, selectivity, pH, reaction time and particle type are defined. Detection limits of 1.5 and 0.2  $\mu\text{M}$  were obtained with nanoceria for dopamine and catechol. The same assay could be used as a general sensing platform for the detection of other phenolics. However, the sensitivity of the method varies significantly with the particle type, buffer composition, pH and with the structure of the phenolic compound. The results demonstrate that nanoceria particles can be used for the development of cost effective and sensitive methods for the detection of these compounds. However, the selection of the particle system and experimental conditions is critical for achieving high sensitivity. Recommendations are provided on the selection of the particle system and reaction conditions to maximize the oxidase like activity of nanoceria.

**WEB URL:** <http://www.sciencedirect.com/science/article/pii/S0003267015005620>

**18. Sharif F., Steenbergen PJ, Metz JR, Champagne DL. (2015). Long-lasting effects of dexamethasone on immune cells and wound healing in the zebrafish. *Wound Repair Regen.* 23(6):855-65.**

**ABSTRACT:**

This study assessed the lasting impact of dexamethasone (DEX) exposure during early development on tissue repair capacity at later life stages (5, 14, and 24 days post fertilization [dpf]) in zebrafish larvae. Using the caudal fin amputation model, we show that prior exposure to DEX significantly delays but does not prevent wound healing at all life stages studied. DEX-induced impairments on wound healing were fully restored to normal levels with longer post amputation recovery time. Further analyses revealed that DEX mainly exerted its detrimental effects in the early phase (0-5 hours) of wound-healing process. Specifically, we observed the following events: (1) massive amount of cell death both by necrosis and apoptosis; (2) significant reduction in the number as well as misplacement of macrophages at the wound site; (3) aberrant migration and misplacement of neutrophils and macrophages at the wound site. These events were

accompanied by significant (likely compensatory) changes in the expression of genes involved in tissue patterning, including up-regulation of FKBP5 6 hours post DEX exposure and that of Wnt3a and RAR $\gamma$  at 24 hours post amputation. Taken together, this study provides evidence that DEX exposure during early sensitive periods of development appears to cause permanent alterations in the cellular/molecular immune processes that are involved in the early phase of wound healing in zebrafish. These findings are consistent with previous studies showing that antenatal course of DEX is associated with immediate and lasting alterations of the immune system in rodent models and humans. Therefore, the current findings support the use of the larval zebrafish model to study the impact of stress and stress hormone exposure in immature organisms on health risks in later life.

**WEB URL:** <http://www.ncbi.nlm.nih.gov/pubmed/26342183>

**19. Yar, M., Shahzad, S., Siddiqi, S. A., Mahmood, N., Rauf, A., Anwar, M. S., ... ur Rehman, I. (2015). Triethyl orthoformate mediated a novel crosslinking method for the preparation of hydrogels for tissue engineering applications: characterization and in vitro cytocompatibility analysis. *Materials Science and Engineering: C*, 56, 154-164.**

**ABSTRACT:**

This paper describes the development of a new crosslinking method for the synthesis of novel hydrogel films from chitosan and PVA for potential use in various biomedical applications. These hydrogel membranes were synthesized by blending different ratios of chitosan (CS) and poly(vinyl alcohol) (PVA) solutions and were crosslinked with 2.5% (w/v) triethyl orthoformate (TEOF) in the presence of 17% (w/v) sulfuric acid. The physical/chemical interactions and the presence of specific functional groups in the synthesized materials were evaluated by Fourier transform infrared (FT-IR) spectroscopy. The morphology, structure and pore size of the materials were investigated by scanning electron microscopy (SEM). Thermal gravimetric analysis (TGA) proved that these crosslinked hydrogel films have good thermal stability which was

decreased as the CS ratio was increased. Differential scanning calorimetry (DSC) exhibited that CS and PVA were present in the amorphous form. The solution absorption properties were performed in phosphate buffer saline (PBS) solution of pH 7.4. The 20% PVA–80% CS crosslinked hydrogel films showed a greater degree of solution absorption (183%) as compared to other compositions. The hydrogels with greater CS concentration (60% and 80%) demonstrated relatively more porous structure, better cell viability and proliferation and also revealed good blood clotting ability even after crosslinking. Based on the observed facts these hydrogels can be tailored for their potential utilization in wound healing and skin tissue engineering applications.

**WEB URL:** <http://www.sciencedirect.com/science/article/pii/S0928493115301545>

**20. Khan, N. I., Ijaz, K., Zahid, M., Khan, A. S., Kadir, M. R. A., Hussain, R., ... & Chaudhry, A. A. (2015). Microwave assisted synthesis and characterization of magnesium substituted calcium phosphate bioceramics. *Materials Science and Engineering: C*, 56, 286-293.**

**ABSTRACT:**

Hydroxyapatite is used extensively in hard tissue repair due to its biocompatibility and similarity to biological apatite, the mineral component of bone. It differs subtly in composition from biological apatite which contains other ions such as magnesium, zinc, carbonate and silicon (believed to play biological roles). Traditional methods of hydroxyapatite synthesis are time consuming and require strict reaction parameter control. This paper outlines synthesis of magnesium substituted hydroxyapatite using simple microwave irradiation of precipitated suspensions. Microwave irradiation resulted in a drastic decrease in ageing times of amorphous apatitic phases. Time taken to synthesize hydroxyapatite (which remained stable upon heat treatment at 900 °C for 1 h) reduced twelve folds (to 2 h) as compared to traditionally required times. The effects of increasing magnesium concentration in the precursors on particle size, surface area, phase-purity, agglomeration and thermal stability, were observed using scanning electron microscopy, BET surface area analysis, X-ray diffraction and photo acoustic

Fourier transform infra-red spectroscopy. Porous agglomerates were obtained after a brief heat-treatment (1 h) at 900 °C.

**WEB URL:** <http://www.sciencedirect.com/science/article/pii/S0928493115300667>

**21. Gonfa, G., Bustam, M. A., Muhammad, N., & Ullah, S. (2015). Density and excess molar volume of binary mixture of thiocyanate-based ionic liquids and methanol at temperatures 293.15–323.15 K. *Journal of Molecular Liquids*, 211, 734-741.**

**ABSTRACT:**

Densities of binary mixture of three ionic liquids, 1-butyl-3-methylimidazolium thiocyanate ( $[C_4C_1im][SCN]$ ), 1-allyl-3-methylimidazolium thiocyanate ( $[C_1 = C_2]C_1im][SCN]$ ) and 3-(3-butyl-1H-imidazol-3-ium-1-yl)propanenitrile thiocyanate ( $[(NC)^2C_2C_4im][SCN]$ ), with methanol were measured over a temperature range of 293.15 to 323.15 K and at atmospheric pressure. Excess molar volumes ( $V_m^E$ ) were calculated from density values and correlated with Redlich–Kister polynomial equation. Partial molar volumes at infinite dilutions ( $V_{m,i}^\infty$ ) of the ILs and methanol were determined from the Redlich–Kister coefficients. For all the studied systems, the  $V_m^E$  is negative over the entire composition range. The  $V_m^E$  and  $V_{m,i}^\infty$  are interpreted in terms of intermolecular interactions in the binary mixture. Density functional theory has been used to investigate the interactions between methanol and the studied ILs.

**WEB URL:** <http://www.sciencedirect.com/science/article/pii/S0167732215302798>

**22. Farooq, A., Yar, M., Khan, A. S., Shahzadi, L., Siddiqi, S. A., Mahmood, N., ... & ur Rehman, I. (2015). Synthesis of piroxicam loaded novel electrospun biodegradable nanocomposite scaffolds for periodontal regeneration. *Materials Science and Engineering: C*, 56, 104-113.**

**ABSTRACT:**

Development of biodegradable composites having the ability to suppress or eliminate the pathogenic micro-biota or modulate the inflammatory response has attracted great

interest in order to limit/repair periodontal tissue destruction. The present report includes the development of non-steroidal anti-inflammatory drug encapsulated novel biodegradable chitosan (CS)/poly(vinyl alcohol) (PVA)/hydroxyapatite (HA) electro-spun (e-spun) composite nanofibrous mats and films and study of the effect of heat treatment on fibers and films morphology. It also describes comparative in-vitro drug release profiles from heat treated and control (non-heat treated) nanofibrous mats and films containing varying concentrations of piroxicam (PX). Electrospinning was used to obtain drug loaded ultrafine fibrous mats. The physical/chemical interactions were evaluated by Fourier Transform Infrared (FT-IR) spectroscopy. The morphology, structure and pore size of the materials were investigated by scanning electron microscopy (SEM). The thermal behavior of the materials was investigated by thermal gravimetric analysis (TGA) and differential scanning calorimetry (DSC). Control (not heat treated) and heat treated e-spun fibers mats and films were tested for in vitro drug release studies at physiological pH 7.4 and initially, as per requirement burst release patterns were observed from both fibers and films and later sustained release profiles were noted. In vitro cytocompatibility was performed using VERO cell line of epithelial cells and all the synthesized materials were found to be non-cytotoxic. The current observations suggested that these materials are potential candidates for periodontal regeneration.

**WEB URL:** <http://www.sciencedirect.com/science/article/pii/S0928493115301399>

**23. Nishan, U., Damas-Souza, D. M., Barbosa, G. O., Muhammad, N., Rahim, A., & Carvalho, H. F. (2015). New transcription factors involved with postnatal ventral prostate gland development in male Wistar rats during the first week. *Life sciences*, 143, 168-173.**

**ABSTRACT:**

The high incidence in men of prostatic diseases, including benign and malignant tumors, makes the understanding of prostate development and biology very important.

Understanding the organogenesis of the prostate gland has been a substantial challenge as “prostatic code” is not well defined at the present time. The novelty of this work lies in unveiling new transcription factors (TFs) during neonatal ventral prostate (VP) gland development in male Wistar rats.

### ***Main methods***

The techniques of qRT-PCR and immunohistochemistry have been employed to perform this work while the VP gland was obtained from neonatal rats at day zero (the day of birth) day 3 and 6.

### ***Key findings***

16 TFs were studied and we found an increased expression of *Eya2*, *Lhrh* and *Znf142*, invariable levels of *Znf703* and *Dbp*, and decreased expression of 11 others at postnatal development day 3 and 6 as compared to day zero. *ZNF703* was found by immunohistochemistry in epithelial cells at days 0, 3 and 6. qRT-PCR for *Eya2* and *Dmrt2* showed the highest and lowest fold change for them respectively, and immunohistochemistry showed that the former is being expressed at the three selected time points while the latter appears to be diminishing with very few cells expressing it until day 6.

### ***Significance***

Results from this work is reporting the role of these TFs for the first time and will significantly contribute to the current understanding of the development and branching morphogenesis of the neonatal VP gland during the first week of postnatal development.

**WEB URL:** <http://www.sciencedirect.com/science/article/pii/S002432051530062X>

**24. Hayat, A., Mishra, R. K., Catanante, G., & Marty, J. L. (2015). Development of an aptasensor based on a fluorescent particles-modified aptamer for ochratoxin A detection. *Analytical and bioanalytical chemistry*, 407(25), 7815-7822.**

**ABSTRACT:**

The presented work reports a generic fluorescent aptasensing design employing carboxy-modified fluorescent particles as a signal-generating probe and magnetic particles as a solid separation support. Carboxy-modified fluorescent particles were used to modify the aptamer and act as a signal-generating probe. Magnetic beads were used as an immobilization surface to perform the function of a solid separation support. As a proof of concept, the assay was used to detect ochratoxin A (OTA). Fluorescent detection based on the displacement and competition format was performed, and the obtained results were compared. The competition-based assays were characterized with improved analytical characteristics as compared to those based on the displacement principle. The competitive fluorescent assays showed a high sensitivity where the detection limit and IC<sub>50</sub> were 0.005 and 7.2 nM respectively. The aptasensing platform was finally demonstrated for the detection of OTA in a beer sample. However, this is a generic approach that can be very easily extended to other matrixes to determine OTA. Additionally, the proposed concept of fluorescent particles as a signal-generating probe in combination with magnetic particles can also be integrated to other fluorescent-based affinity assays.

**WEB URL:** <http://link.springer.com/article/10.1007/s00216-015-8952-3>

**25. Rahim, A., Muhammad, N., Nishan, U., Khan, U. S., Rehman, F., Kubota, L. T., & Gushikem, Y. (2015). Copper phthalocyanine modified SiO<sub>2</sub>/C electrode as a biomimetic electrocatalyst for 4-aminophenol in the development of an amperometric sensor. *RSC Advances*, 5(106), 87043-87050.**

**ABSTRACT:**

A selective, simple, and low cost method for 4-aminophenol (4-APh) determination was developed using the mesoporous carbon ceramic SiO<sub>2</sub>/50 wt% C ( $S_{\text{BET}} = 170 \text{ m}^2 \text{ g}^{-1}$ ), composite was prepared by the sol-gel method. The material was fabricated to use as matrix to support copper phthalocyanine (CuPc), prepared *in situ* on their surface, to

assure homogeneous dispersion of the electrocatalyst complex in the pores of the matrix. The pressed disk electrodes made of SiO<sub>2</sub>/C/CuPc was tested as amperometric sensors for 4-APh. Under the optimized conditions, at -75 mV vs. SCE in 0.06 mol dm<sup>-3</sup> Britton–Robinson buffer (BRB) solution (pH 7.0) containing 250 μmol dm<sup>-3</sup> of H<sub>2</sub>O<sub>2</sub>, a linear response range for 4APh from 5 up to 230 μmol dm<sup>-3</sup> was obtained with a sensitivity of 123 nA dm<sup>-3</sup> μmol<sup>-1</sup> cm<sup>-2</sup> and the limit of detection LOD was 2 (±0.002) nmol dm<sup>-3</sup>. The prepared sensors present a stable response during successive determinations. The repeatability, evaluated in terms of relative standard deviation of 3% for  $n = 10$  and μmol dm<sup>-3</sup> 4-APh. The response time was 1 s and life time 12 months. Finally, the sensor was tested to determine 4-APh in the sample, and gives very good results for its determination. The presence of other phenols like 2-aminophenol, hydroquinone, catechol, cysteine and resorcinol did not show any interference in the detection of 4-APh on this electrode, even in the same concentration with the 4-APh.

**WEB URL:**

<http://pubs.rsc.org/is/content/articlelanding/2015/ra/c5ra18617j/unauth#!divAbstract>

**26. Shahid, R., Muhammad, N., Gonfa, G., Toprak, M. S., & Muhammed, M. (2015). Synthesis, COSMO-RS analysis and optical properties of surface modified ZnS quantum dots using ionic liquids. *Journal of Physics and Chemistry of Solids*, 85, 34-38.**

**ABSTRACT:**

Zinc sulfide (ZnS) quantum dots (QDs) were synthesized using the microwave assisted ionic liquid (MAIL) route. Three ionic liquids (ILs), namely, 1-butyl-3-methylimidazolium tetrafluoroborate ([BMIM]BF<sub>4</sub>), trihexyl(tetradecyl) phosphonium bis(trifluoromethanesulfonyl) amide ([P<sub>6,6,6,14</sub>][TSFA]) and trihexyl(tetradecyl) phosphonium chloride ([P<sub>6,6,6,14</sub>][Cl]) were used in this study. The size and structure of the QDs were characterized by high-resolution transmission electron microscopy (HR-TEM) and selected area electron diffraction (SAED) pattern, respectively. The synthesized QDs were of wurtzite crystalline structure with size less than 5 nm. The QDs were more uniformly distributed while using the phosphonium based ILs as a reaction

medium during synthesis. The optical properties were investigated by UV–vis absorption and photoluminescence (PL) emission spectroscopy. The optical properties of QDs showed the quantum confinement effect in their absorption and the effect of cation and anion structural moiety was observed on their bandedge emission. The QDs emission intensity was measured higher for [P<sub>6,6,6,14</sub>][Cl] due to their better dispersion as well as high charge density of Cl anion. The capability of the ILs in stabilizing the QDs was interpreted by density functional theory (DFT) computations. The obtained results are in good agreement with the theoretical prediction.

**WEB URL:** <http://www.sciencedirect.com/science/article/pii/S0022369715001146>

**27. Rauf, A., Shahzad, S., Bajda, M., Yar, M., Ahmed, F., Hussain, N., ... & Jończyk, J. (2015). Design and synthesis of new barbituric-and thiobarbituric acid derivatives as potent urease inhibitors: Structure activity relationship and molecular modeling studies. *Bioorganic & medicinal chemistry*, 23(17), 6049-6058.**

**ABSTRACT:**

In this study 36 new compounds were synthesized by condensing barbituric acid or thiobarbituric acid and respective anilines (bearing different substituents) in the presence of triethyl orthoformate in good yields. In vitro urease inhibition studies against jack bean urease revealed that barbituric acid derived compounds (**1–9** and **19–27**) were found to exhibit low to moderate activity however thiobarbituric acid derived compounds (**10–18** and **28–36**) showed significant inhibition activity at low micro-molar concentrations. Among the synthesized compounds, compounds (**15**), (**12**), (**10**), (**36**), (**16**) and (**35**) showed excellent urease inhibition with IC<sub>50</sub> values 8.53 ± 0.027, 8.93 ± 0.027, 12.96 ± 0.13, 15 ± 0.098, 18.9 ± 0.027 and 19.7 ± 0.63 μM, respectively, even better than the reference compound thiourea (IC<sub>50</sub> = 21 ± 0.011). The compound (**11**) exhibited comparable activity to the standard with IC<sub>50</sub> value 21.83 ± 0.19 μM. In silico molecular docking studies for most active compounds (**10**), (**12**), (**15**), (**16**), (**35**) and (**36**) and two inactive compounds (**3**) and (**6**) were performed to predict the binding patterns.

**WEB URL:** <http://www.sciencedirect.com/science/article/pii/S0968089615004484>

**28. Bülbül, G., Hayat, A., & Andreescu, S. (2015). Portable Nanoparticle-Based Sensors for Food Safety Assessment. *Sensors*, 15(12), 30736-30758.**

**ABSTRACT:**

The use of nanotechnology-derived products in the development of sensors and analytical measurement methodologies has increased significantly over the past decade. Nano-based sensing approaches include the use of nanoparticles (NPs) and nanostructures to enhance sensitivity and selectivity, design new detection schemes, improve sample preparation and increase portability. This review summarizes recent advancements in the design and development of NP-based sensors for assessing food safety. The most common types of NPs used to fabricate sensors for detection of food contaminants are discussed. Selected examples of NP-based detection schemes with colorimetric and electrochemical detection are provided with focus on sensors for the detection of chemical and biological contaminants including pesticides, heavy metals, bacterial pathogens and natural toxins. Current trends in the development of low-cost portable NP-based technology for rapid assessment of food safety as well as challenges for practical implementation and future research directions are discussed.

**WEB URL:** <http://www.mdpi.com/1424-8220/15/12/29826>

**29. Khan, Z. U. H., Kong, D., Chen, Y., Muhammad, N., Khan, A. U., Khan, F. U., ... & Wan, P. (2015). Ionic liquids based fluorination of organic compounds using electrochemical method. *Journal of Industrial and Engineering Chemistry*, 31, 26-38.**

**ABSTRACT:**

Ionic liquids due to their advantageous properties gain importance in many fields. This study aims to overview the use of ionic liquids in the selective partial fluorination of organic compounds through electrochemical method. In addition to ionic liquid based fluorination, the earlier approaches of fluorination through an electrochemical process

have also been highlighted. The factors such as electrode materials (Pt, Ni, and C), types of solvents (CH<sub>3</sub>CN, DMC, THF, DME, Sulfone, etc.) and type of electrolytes (Et<sub>3</sub>N·3HF, Et<sub>3</sub>NF·3HF, py·HF, etc.) which affect the electrochemical fluorination of organic compounds have been reviewed. For electrode preparation, the carbon, platinum and nickel were considered suitable materials to be used as an electrode. In CH<sub>3</sub>CN media, Et<sub>3</sub>N·3HF and Et<sub>4</sub>NF·3HF showed better efficiency during fluorination of organic compounds. Solvent play an important role in electrochemical fluorination of organic compounds, with the change of solvent the percentage yield is highly affected. Py·HF is a convenient solvent-supporting electrolyte medium with a reasonably good conductivity. The electrolyte containing solvents have some side effects on electrochemical fluorination of organic compounds as observed in cyclic voltammetric analysis. Therefore electrochemical fluorination to organic compounds without the use of solvent gained more importance. The ionic liquids have been reported for its dual properties, as solvent as well as a fluorinating agent for organic compounds in electrochemical processes. It has been concluded that solvents free electrochemical fluorination of organic compounds gives good results as compare to solvent based. Ionic liquids due to more oxidative stability were noted to have considerable effect on the yield and selectivity of organic compound fluorination.

**WEB URL:** <http://www.sciencedirect.com/science/article/pii/S1226086X15002865>

**30. Gonfa, G., Bustam, M. A., Sharif, A. M., Mohamad, N., & Ullah, S. (2015). Tuning ionic liquids for natural gas dehydration using COSMO-RS methodology. *Journal of Natural Gas Science and Engineering*, 27, 1141-1148.**

**ABSTRACT:**

The quantum chemical COSMO-RS (Conductor like Screening Model for Real Solvents) methodology was applied to evaluate the ability ionic liquids as alternative solvents for dehydration of natural gas. First, a general evaluation of COSMO-RS model to predict activity coefficients at infinite dilution of water in ionic liquids were performed by comparing the computed results with a set of experimentally measured activity

coefficient of water in different ionic liquids over various temperatures. The mean prediction error (MPE) and linear correlation coefficient ( $R^2$ ) between the experimental and predicted activity coefficients are 29.9% and 0.968, respectively. Then, a detailed analysis of water and ionic liquids behaviors and the effects of possible structural variation of ionic liquids on the water-ionic liquids interactions were performed using the sigma-profile and sigma-potential generated by COSMO-RS model. For which, a total of 31 cations and 43 anions resulting in 1333 possible combinations were screened via COSMO-RS model by calculating the activity coefficient of water in these ionic liquids at infinite dilution over temperature range of (298.15–368.15) K. It was found that ionic liquids the contain cations with longer alkyl chain show less affinity for water molecules. Moreover, ionic liquids with fluorinated and cyano anions shows lower affinity and selectivity for water molecules. However, ionic liquids containing carboxylate and amino acid based anions and cations with shorter alkyl side chain have strong affinity and more selectivity for water molecules.

**WEB URL:** <http://www.sciencedirect.com/science/article/pii/S1875510015301955>

**31. Ihsan, M., Niaz, A., Rahim, A., Zaman, M. I., Arain, M. B., Sharif, T., & Najeeb, M. (2015). Biologically synthesized silver nanoparticle-based colorimetric sensor for the selective detection of Zn<sup>2+</sup>. *RSC Advances*,5(111), 91158-91165.**

**ABSTRACT:**

A simple, selective and cost effective colorimetric sensor has been investigated for the detection of Zn<sup>2+</sup> using biologically synthesized silver nanoparticles (AgNPs). The AgNPs were prepared from the leaf extract of *Amomum subulatum* via two different procedures *i.e.*, at room temperature and by a heat treatment procedure. The AgNPs prepared through the heat treatment procedure exhibited efficient results. The as synthesized AgNPs were studied by simple UV-vis spectroscopy which showed an intense absorption band at 425 nm which was further confirmed by FT-IR and SEM analysis. The synthesized AgNPs exhibited a good colorimetric sensing property towards Zn<sup>2+</sup> by changing the color of the solution from yellowish-brown to colorless

accompanying a decrease in absorption intensity. The proposed detection mechanism of the sensor has been discussed. The sensor showed an excellent linear response towards  $Zn^{2+}$  in the concentration range from  $1 \times 10^{-5}$  to  $8 \times 10^{-5}$  M with a correlation coefficient ( $R^2$ ) of 0.996. The detection limit of the method was found to be  $3.5 \times 10^{-6}$  M. There was no interference effect observed for  $Zn^{2+}$  detection in the presence of other heavy metal ions. The proposed sensor was successfully applied for the detection of  $Zn^{2+}$  in drinking water samples.

**WEB URL:**

<http://pubs.rsc.org/is/content/articlelanding/2015/ra/c5ra17055a/unauth#!divAbstract>

**32. Sharma, A., Hayat, A., Mishra, R. K., Catanante, G., Bhand, S., & Marty, J. L. (2015). Titanium Dioxide Nanoparticles (TiO<sub>2</sub>) Quenching Based Aptasensing Platform: Application to Ochratoxin A Detection. *Toxins*, 7(9), 3771-3784.**

**ABSTRACT:**

We demonstrate for the first time, the development of titanium dioxide nanoparticles (TiO<sub>2</sub>) quenching based aptasensing platform for detection of target molecules. TiO<sub>2</sub> quench the fluorescence of FAM-labeled aptamer (fluorescein labeled aptamer) upon the non-covalent adsorption of fluorescent labeled aptamer on TiO<sub>2</sub> surface. When OTA interacts with the aptamer, it induced aptamer G-quadruplex complex formation, weakens the interaction between FAM-labeled aptamer and TiO<sub>2</sub>, resulting in fluorescence recovery. As a proof of concept, an assay was employed for detection of Ochratoxin A (OTA). At optimized experimental condition, the obtained limit of detection (LOD) was 1.5 nM with a good linearity in the range 1.5 nM to 1.0  $\mu$ M for OTA. The obtained results showed the high selectivity of assay towards OTA without interference to structurally similar analogue Ochratoxin B (OTB). The developed aptamer assay was evaluated for detection of OTA in beer sample and recoveries were recorded in the range from 94.30%–99.20%. Analytical figures of the merits of the developed aptasensing platform confirmed its applicability to real

samples analysis. However, this is a generic aptasensing platform and can be extended for detection of other toxins or target analyte.

**WEB URL:** <http://www.mdpi.com/2072-6651/7/9/3771/htm>

**33. Mishra, R. K., Hayat, A., Catanante, G., Ocaña, C., & Marty, J. L. (2015). A label free aptasensor for Ochratoxin A detection in cocoa beans: An application to chocolate industries. *Analytica chimica acta*, 889, 106-112.**

**ABSTRACT:**

Contamination of food by mycotoxin occurs in minute/trace quantities. Nearly 92.5% of the cocoa samples present Ochratoxin A (OTA) levels at trace quantity. Hence, there is a necessity for a highly sensitive and selective device that can detect and quantify these organic toxins in various matrices such as cocoa beans. This work reports for the first time, a facile and label-free electrochemical impedimetric aptasensor for rapid detection and quantitation of OTA in cocoa beans. The developed aptasensor was constructed based on the diazonium-coupling reaction mechanism for the immobilization of anti-OTA-aptamer on screen printed carbon electrodes (SPCEs). The aptasensor exhibited a very good limit of detection (LOD) as low as 0.15 ng/mL, with added advantages of good selectivity and reproducibility. The increase in electron transfer resistance was linearly proportional to the OTA concentration in the range 0.15–2.5 ng/mL, with an acceptable recovery percentage (91–95%, RSD = 4.8%) obtained in cocoa samples. This work can facilitate a general model for the detection of OTA in cocoa beans based on the impedimetric aptasensor. The analysis can be performed onsite with pre-constructed and aptamer modified electrodes employing a portable EIS set up.

**WEB URL:** <http://www.sciencedirect.com/science/article/pii/S0003267015008727>

**34. Razaq, A., Asif, M. H., Kalsoom, R., Khan, A. F., Awan, M. S., Ishrat, S., & Ramay, S. M. (2015). Conductive and electroactive composite paper reinforced by coating of polyaniline on lignocelluloses fibers. *Journal of Applied Polymer Science*, 132(29).**

**ABSTRACT:**

Direct use of lignocelluloses fibers as substrate for fabrication of conductive, electroactive, biodegradable, and low-cost electrode materials are in demand for high-tech applications of ion-exchange and energy storage devices. This article presents the preparation and characterizations of conductive and electroactive lignocelluloses-polyaniline (cellulose/PANI) composite paper. Lignocelluloses fibers were directly collected from the stem of self-growing plant, *Typha Angustifolia*, and subsequently coated with the conductive and electroactive layer of PANI through chemical synthesis. Individual PANI-coated lignocelluloses fibers were converted into sheet and further characterized with Scanning Electron Microscopy, Fourier Transform Infrared, Thermogravimetric Analysis, electronic conductivity, and Cyclic Voltammetry. Cellulose/PANI composite paper revealed superior thermal characteristics and used as a working electrode in three different electrolytes for ion-exchange properties. Conductive composite paper (CCP) showed the charge storage capacity of ~52 C/g at scan rate of 5 mV/s in 2M HCl solution. © 2015 Wiley Periodicals, Inc. *J. Appl. Polym. Sci.* **2015**, *132*, 42293.

**WEB URL:** <http://onlinelibrary.wiley.com/doi/10.1002/app.42293/full>

**35. Ahmad, P., Khandaker, M. U., Amin, Y. M., Muhammad, N., Usman, A. R., & Amin, M. (2015). The effect of reaction atmosphere and growth duration on the size and morphology of boron nitride nanotubes. *New Journal of Chemistry*, *39*(10), 7912-7915.**

**ABSTRACT:**

The effect of different reaction atmospheres is analyzed on the size and morphology of boron nitride nanotubes within a single and continuous growth duration of 180 min at 1200 °C. Field emission scanning electron microscopy micrographs show smaller and larger diameter boron nitride nanotubes in the range of 70–700 nm, with straight and curve parts. Some of the larger diameter boron nitride nanotubes have pipe-like morphologies at their top with the diameter in the range of 270–380 nm. High

resolution transmission electron microscopy shows the tubular structure of the synthesized nanotubes with a non-uniform diameter. X-ray photoelectron spectroscopy shows B1s and N1s peaks at 190.3 eV and 398 eV for hexagonal boron nitride nature of the synthesized nanotubes. The Raman spectrum reports a higher intensity peak at 1370 ( $\text{cm}^{-1}$ ) that corresponds to  $E_{2g}$  mode of vibration in hexagonal boron nitride.

**WEB URL:**

<http://pubs.rsc.org/is/content/articlelanding/2015/nj/c5nj01466b/unauth#!divAbstract>

**36. Ullah, Z., Bustam, M. A., Man, Z., Muhammad, N., & Khan, A. S. (2015). Synthesis, characterization and the effect of temperature on different physicochemical properties of protic ionic liquids. *RSC Advances*, 5(87), 71449-71461.**

**ABSTRACT:**

In this work, eleven protic ionic liquids (PILs) containing different cations and anions were prepared and their physicochemical properties were measured. The structures of all the PILs were confirmed using NMR, and elemental analysis (CHNS) was carried out. The physicochemical properties such as density, surface tension, viscosity and thermal degradation behaviour were measured, and the effect of the cations/anions was investigated. The density and viscosity were measured within the temperature range of 293.15–373.15 K at atmospheric pressure. The thermal expansion coefficient values were calculated from the density data. Surface tension was measured in the temperature range of 293.15 to 353.15 K and the values were used to estimate the surface entropy and enthalpy of the ionic liquids at 303.15 K. The boiling and critical temperature are also estimated according to the Eötvös and Rebelo methods. The refractive indices were measured within the temperature range of 293.15 to 323.15 K. The thermal gravimetric analysis was performed in the temperature range of 373.15–773.15 K.

**WEB URL:**

<http://pubs.rsc.org/en/content/articlelanding/2015/ra/c5ra07656k/unauth#!divAbstract>

t

**37. Mutahir, S., Yar, M., Khan, M. A., Ullah, N., Shahzad, S. A., Khan, I. U., ... & Pontiki, E. (2015). Synthesis, characterization, lipoxygenase inhibitory activity and in silico molecular docking of biaryl bis (benzenesulfonamide) and indol-3-yl-hydrazide derivatives. *Journal of the Iranian Chemical Society*,12(6), 1123-1130.**

**ABSTRACT:**

In this paper, we have screened a library of two different series of compounds to identify potent lipoxygenase (LOX) inhibitors. A number of new biphenyl bis(benzenesulfonamides) **2–3**, indol-3-yl-benzenesulfonyl and acetohydrazides **4–5** and indol-3-yl-hydrazinecarboxylate **6** were synthesized and evaluated in vitro for LOX inhibitory activity. Compounds biphenyl bis(benzenesulfonamide) **2a** and indol-3-yl-benzenesulfonylhydrazide **4e** presented the best anti-LOX activity within these series with IC<sub>50</sub> values  $96.31 \pm 0.18$  and  $81.21 \pm 2.14$   $\mu$ M, respectively. The results were confirmed with docking studies.

**WEB URL:** <http://link.springer.com/article/10.1007/s13738-014-0573-9>

**38. Khan, U. S., Manan, A., Khan, N., Mahmood, A., & Rahim, A. (2015). Transformation mechanism of magnetite nanoparticles. *Materials Science-Poland*, 33(2), 278-285.**

**ABSTRACT:**

A simple oxidation synthesis route was developed for producing magnetite nanoparticles with controlled size and morphology. Investigation of oxidation process of the produced magnetite nanoparticles (NP) was performed after synthesis under different temperatures. The phase transformation of synthetic magnetite nanoparticles into maghemite and, henceforth, to hematite nanoparticles at different temperatures under dry oxidation has been studied. The natural magnetite particles were directly transformed to hematite particles at comparatively lower temperature, thus, maghemite phase was bypassed. The phase structures, morphologies and particle sizes of the produced magnetic nanoparticles have been investigated by X-ray diffraction

(XRD), transmission electron microscopy (TEM), energy dispersive X-ray spectrometry (EDX) and BET surface area analysis.

**WEB URL:** <http://www.degruyter.com/view/j/msp.2015.33.issue-2/msp-2015-0037/msp-2015-0037.xml>

**39. Ahmad, P., Khandaker, M. U., Amin, Y. M., & Muhammad, N. (2015). Synthesis and characterization of boron nitride microtubes. *Materials Express*, 5(3), 249-254.**

**ABSTRACT:**

Boron nitride microtubes (BNMTs) are successfully synthesized via a simple technique at 1200 °C. The method and logics used in the present study are relatively different and easy in comparison to previously synthesized boron nitride nanotubes, boron nitride microtubes and boron-carbon-nitride microtubes regarding the choice of precursors, experimental set up and reaction atmosphere. Field emission scanning electron microscopy (FESEM) shows a unique pipe-like morphology of the as-synthesized BNMTs with thin wall structure and larger internal space. X-ray photoelectron spectroscopy (XPS) survey shows B 1s and N 1s peaks at 190.8 eV and 398.5 eV that represent hexagonal boron nitride (h-BN) composition of synthesized microtubes. Raman spectroscopy demonstrates a peak at 1372.53 (cm<sup>-1</sup>) that corresponds to  $E_{2g}$  mode of h-BN.

**WEB URL:**

<http://www.ingentaconnect.com/content/asp/me/2015/00000005/00000003/art00010>

**40. Bashir, M., Mehmood, M. S., Choudary, M. A., Yasin, T., Ahmad, I., Tariq, M., ... & Ikram, M. (2015). Analysis of Pulse-Laser-Induced Modifications on High-Density Polyethylene for Laser Processing of Polyethylene. *Journal of Russian Laser Research*, 36(3), 258-268.**

**ABSTRACT:**

We study the effects of the energetic pulsed laser on the surface of high-density polyethylene (HDPE). The modifications were induced on HDPE using short laser pulses (pulse duration 5 ns, repetition rate 10 Hz, and pulse energy 150 mJ) in air. Experiments were carried out using a Q-switched Nd:YAG laser (E08BR, Brilliant) operating at 532 and 1,064 nm. The visual inspection in lateral and vertical directions of modifications, which were stimulated by laser irradiation, were performed using optical and scanning electron microscopy. The structural changes induced in the vicinity of the modified area were evaluated by FT-IR spectroscopy. The systematic microscopic analysis of modified areas revealed that the values of modification and ablation threshold fluence were 16 and 20 J/cm<sup>2</sup> for 532 nm and 44 and 38 J/cm<sup>2</sup> for 1,064 nm laser wavelength, respectively. The spectroscopic analysis of the vicinity of the illuminated area (when illuminated with 50 and 100 pulses) showed a significant increase in the IR absorption bands, which belong to hydroperoxide or alcohols, i.e., from 3300 to 3500 cm<sup>-1</sup> for 1,064 nm laser wavelength; however, an opposite situation was observed for 532 nm laser wavelength.

**WEB URL:** <http://link.springer.com/article/10.1007/s10946-015-9498-8>

**41. Hayat, A., Haider, W., Raza, Y., & Marty, J. L. (2015). Colorimetric cholesterol sensor based on peroxidase like activity of zinc oxide nanoparticles incorporated carbon nanotubes. *Talanta*, 143, 157-161.**

**ABSTRACT:**

A sensitive and selective colorimetric method based on the incorporation of zinc oxide nanoparticles (ZnO NPs) on the surface of carbon nanotubes (CNTs) was shown to possess synergistic peroxidase like activity for the detection of cholesterol. The proposed nanocomposite catalyzed the oxidation of 2,2'-azino-bis(3-ethylbenzthiazoline-6-sulfonic acid (ABTS) in the presence of hydrogen peroxide (H<sub>2</sub>O<sub>2</sub>) to produce a green colored product which can be monitored at 405 nm. H<sub>2</sub>O<sub>2</sub> is the oxidative product of

cholesterol in the presence of cholesterol oxidase. Therefore, the oxidation of cholesterol can be quantitatively related to the colorimetric response by combining these two reactions. Under the optimal experimental conditions, the colorimetric response was proportional to the concentration of cholesterol in the range of 0.5–500 nmol/L, with a detection limit of 0.2 nmol/L. The applicability of the proposed assays was demonstrated for the determination of cholesterol in milk powder samples with good recovery results.

**WEB URL:** <http://www.sciencedirect.com/science/article/pii/S0039914015300084>

**42. Ocaña, C., Hayat, A., Mishra, R. K., Vasilescu, A., Del Valle, M., & Marty, J. L. (2015). Label free aptasensor for Lysozyme detection: A comparison of the analytical performance of two aptamers. *Bioelectrochemistry*, 105, 72-77.**

**ABSTRACT:**

This work presents a comparison of two different aptamers (Apts) (COX and TRAN) for the detection of a ubiquitous protein Lysozyme (Lys) using Apt-based biosensors. The detection is based on the specific recognition by the Apt immobilized on screen printed carbon electrodes (SPCEs) via diazonium coupling reaction. The quantitative detection of Lys protein was achieved by electrochemical impedance spectroscopy (EIS). A very good linearity and detection limits for the quantitation of Lys were obtained from 0.1 to 0.8  $\mu\text{M}$  and 100 nM using Apt COX and from 0.025 to 0.8  $\mu\text{M}$  and 25 nM using Apt TRAN respectively. The obtained results showed that the developed aptasensors exhibit good specificity, stability and reproducibility for Lys detection. For real application, the aptasensors were tested in wine samples and good recovery rates were recorded in the range from 94.2 to 102% for Lys detection. The obtained recovery rates confirm the reliability and suitability of the developed method in wine matrix. The developed method could be a useful and promising platform for detection of Lys in different applications.

**WEB URL:** <http://www.sciencedirect.com/science/article/pii/S1567539415000675>

**43. Ghafoor, I., Siddiqi, S. A., Atiq, S., Riaz, S., & Naseem, S. (2015). Sol–gel synthesis and investigation of structural, electrical and magnetic properties of Pb doped La<sub>0.1</sub>Bi<sub>0.9</sub>FeO<sub>3</sub> multiferroics. *Journal of Sol-Gel Science and Technology*, 74(2), 352-356.**

**ABSTRACT:**

A sol–gel based auto-combustion technique has been employed to synthesize polycrystalline La<sub>0.1</sub>Bi<sub>0.9-x</sub>Pb<sub>x</sub>FeO<sub>3</sub> (x = 0.0, 0.05, 0.10, 0.20, 0.30) ceramics. The samples have been characterized by X-ray diffraction, scanning electron microscopy, an LCR-meter and a vibrating sample magnetometer for their structural and morphological features, as well as electrical and magnetic properties, respectively. The structural analysis revealed that when Pb was doped at Bi-sites in La<sub>0.1</sub>Bi<sub>0.90</sub>FeO<sub>3</sub>, the host retained the rhombohedrally distorted perovskite structure, attributed to the non centrosymmetric space group R3c. The surface morphological studies revealed that the grain size was increased and formed agglomerates at high concentrations of Pb contents. The dielectric parameters displayed conventional ferrite behavior depicting high values at low frequencies and decreasing with rise in frequencies, leading to constant values at still higher frequencies. The magnetic properties were changed non-monotonically with increasing Pb concentration. This non-monotonical behavior with increasing Pb could be attributed to the canting of the antiferromagnetic spins in BiFeO<sub>3</sub> based multiferroics.

**WEB URL:** <http://link.springer.com/article/10.1007/s10971-014-3517-z>

**44. Muhammad, N., Gao, Y., Khan, M. I., Khan, Z., Rahim, A., Iqbal, F., & Iqbal, J. (2015). Effect of ionic liquid on thermo-physical properties of bamboo biomass. *Wood Science and Technology*, 49(5), 897-913.**

**ABSTRACT:**

In this work, [Emim]Gly ionic liquid was used for the pretreatment of bamboo biomass followed by regeneration of cellulose-rich material. Thermal degradation study of untreated bamboo and cellulose-rich material was carried out under dynamic condition

using thermogravimetric analysis. Free kinetics models of Kissinger, Ozawa, Flynn–Wall–Ozawa, and Kissinger–Akahira–Sunose were used to determine the kinetic parameters of thermal degradation process. The pattern of activation energy ( $E_a$ ) values with respect to % conversion values was noted different for the aforementioned models. The  $E_a$  calculated using the Kissinger method were 184 and 156 kJ mol<sup>-1</sup>, and Ozawa method were 185 and 157 kJ mol<sup>-1</sup> of untreated and treated sample of bamboo, respectively, while the values of  $E_a$  calculated by Flynn–Wall–Ozawa and Kissinger–Akahira–Sunose were 71.7–203.4 kJ mol<sup>-1</sup> and 281.7–230.7 kJ mol<sup>-1</sup> for untreated and treated sample of bamboo, respectively. Calorific and CHNS values of both untreated and regenerated cellulose-rich material were measured by bomb calorimeter and elemental analyzer (CHNS), respectively. Both the calorific value and carbon content of the regenerated cellulose-rich material (15.62 J/kg, 37.86 %, respectively) were found to be less than those of untreated bamboo (17.40 J/kg and 43.14 %, respectively). The bamboo and regenerated cellulose-rich material were investigated by X-ray diffraction and X-ray Photoelectron Spectroscopy, and changes in the cellulose crystalline structure were correlated with thermal degradation behavior and kinetics parameters.

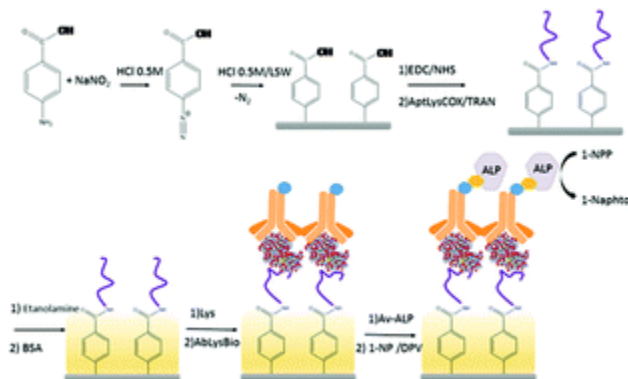
**WEB URL:** <http://link.springer.com/article/10.1007/s00226-015-0736-6>

**45. Ocaña, C., Hayat, A., Mishra, R., Vasilescu, A., Del Valle, M., & Marty, J. L. (2015). A novel electrochemical aptamer–antibody sandwich assay for lysozyme detection. *Analyst*, 140(12), 4148-4153.**

**ABSTRACT:**

In this paper, we have reported a novel electrochemical aptamer–antibody based sandwich biosensor for the detection of lysozyme. In the sensing strategy, an anti-lysozyme aptamer was immobilized onto the carbon electrode surface by covalent binding *via* diazonium salt chemistry. After incubating with a target protein (lysozyme), a biotinylated antibody was used to complete the sandwich format. The subsequent additions of avidin-alkaline phosphatase as an enzyme label, and a 1-naphthyl phosphate substrate (1-NPP) allowed us to determine the concentration of lysozyme

(Lys) *via* Differential Pulse Voltammetry (DPV) of the generated enzyme reaction product, 1-naphthol. Using this strategy, a wide detection range from 5 fM to 5 nM was obtained for a target lysozyme, with a detection limit of 4.3 fM. The control experiments were carried out by using bovine serum albumin (BSA), cytochrome *c* and casein. The results showed that the proposed biosensor had good specificity, stability and reproducibility for lysozyme analysis. In addition, the biosensor was applied for detecting lysozyme in spiked wine samples, and very good recovery rates were obtained in the range from 95.2 to 102.0% for lysozyme detection. This implies that the proposed sandwich biosensor is a promising analytical tool for the analysis of lysozyme in real samples.



**WEB URL:**

<http://pubs.rsc.org/en/content/articlelanding/2015/an/c5an00243e/unauth#!divAbstract>

**46. Ullah, Z., Bustam, M. A., Muhammad, N., Man, Z., & Khan, A. S. (2015). Synthesis and thermophysical properties of hydrogen sulfate based acidic ionic liquids. *Journal of Solution Chemistry*, 44(3-4), 875-889.**

**ABSTRACT:**

Three ionic liquids (ILs): 1-butyl-3-methyl-imidazolium hydrogen sulfate  $[C_4C_1Im][HSO_4]$ , 1-butyl-imidazolium hydrogen sulfate  $[C_4C_0Im][HSO_4]$ , and 1-methyl-imidazolium hydrogen sulfate  $[C_1C_0Im][HSO_4]$ , were synthesized and characterized. The effect of alky

group incorporation into the imidazolium cation was evaluated in terms of changes in density, surface tension, viscosity, and thermal degradation of the ILs. The viscosity and density were measured within the temperature range of 293.15–373.15 K, and experimental values of density were used to calculate molar volume, standard molar entropy, lattice energy, and thermal expansion coefficients. Glasser's approach was used to calculate the lattice energies of the ILs. Surface tensions in the temperature range of 293.15–353.15 K were also measured and surface tension values were used to estimate the surface entropy and enthalpy of the ILs. Refractive indices were measured with an ATAGO refractometer (RX-5000α) within the temperature range of 293.15–323.15 K. Thermal gravimetric analysis was performed in the temperature range of 323.15–773.15 K.

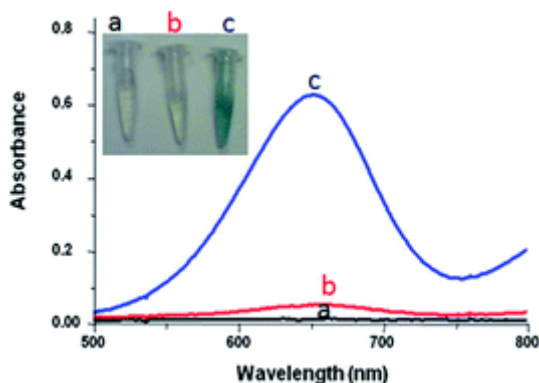
**WEB URL:** <http://link.springer.com/article/10.1007/s10953-015-0329-x>

**47. Haider, W., Hayat, A., Raza, Y., Chaudhry, A. A., & Marty, J. L. (2015). Gold nanoparticle decorated single walled carbon nanotube nanocomposite with synergistic peroxidase like activity for d-alanine detection. *RSC Advances*,5(32), 24853-24858.**

**ABSTRACT:**

In this report, a gold nanoparticle decorated single walled carbon nanotube (SWCNTs) nanocomposite was shown to possess synergistic intrinsic peroxidase like activity and enhanced affinity towards H<sub>2</sub>O<sub>2</sub> oxidation. The gold nanoparticle decorated SWCNTs nanocomposite was characterized by high catalytic activity, enhanced stability from the gold nanoparticles and improved dispersion from the SWCNTs. Subsequently, this nanocomposite was proved to be a novel peroxidase mimetic with great potential to catalyze the oxidation of 3,3',5,5'-tetramethylbenzidine (TMB) in the presence of H<sub>2</sub>O<sub>2</sub> to yield a blue colored product. As a proof of concept, the gold nanoparticle decorated SWCNTs composite was used as a robust nanoprobe for the detection of D-alanine with improved analytical characteristics. Taking into account the valuable

intrinsic peroxidase activity of the nanohybrid, the present work may find widespread applications in the field of sensors and biosensors for diverse applications.



**WEB URL:**

<http://pubs.rsc.org/en/content/articlelanding/2015/ra/c5ra01258a/unauth#!divAbstract>

**48. Shah, A. T., Din, M. I., Bashir, S., Qadir, M. A., & Rashid, F. (2015). Green Synthesis and Characterization of Silver Nanoparticles Using Ferocactus echidne Extract as a Reducing Agent. *Analytical Letters*, 48(7), 1180-1189.**

**ABSTRACT:**

The green synthesis of silver nanoparticles using an aqueous extract of *Ferocactus echidne* (a member of the cactus family) as a reducing agent is reported. It is simple, efficient, rapid, and ecologically friendly compared to chemical-mediated methods. *Ferocactus echidne* is a plant of high medicinal value and rich in polyphenolic antioxidants. The extraction is simple and the product rapidly reduces silver ions without involvement of any external chemical agent. The reduction of silver nanoparticles was characterized by ultraviolet-visible spectrometry as a function of time and concentration. The results show that *Ferocactus echidne* reduces silver ions within 6 h depending upon the concentration. Further increases in reaction time may result in

a blue shift, indicating an increase in particle size, whereas concentration had a minor effect on the particle size. The structure of synthesized nanoparticles was investigated by infrared spectroscopy, scanning electron microscopy, and *X-ray diffraction*. The infrared spectra indicated the association of organic materials with silver nanoparticles to serve as capping agents. Scanning electron micrographs showed that synthesized silver nanoparticles were nearly uniform and elliptical in shape with diameters of 20 to 60 nm. *X-ray diffraction* confirmed the formation of silver nanoparticles with an approximate 20 nm particle size calculated using the Debye-Scherrer equation. Biological tests revealed that the silver nanoparticles were active against gram positive and negative bacteria (*Escherichia coli* and *Staphylococcus aureus*) and fungi (*Candida albicans*), indicating their broad spectrum antibiotic and antifungal abilities.

**WEB URL:** <http://www.tandfonline.com/doi/abs/10.1080/00032719.2014.974057>

**49. Yar, M., Bajda, M., Shahzad, S., Ullah, N., Gilani, M. A., Ashraf, M., ... & Shaukat, A. (2015). Organocatalyzed solvent free an efficient novel synthesis of 2, 4, 5-trisubstituted imidazoles for  $\alpha$ -glucosidase inhibition to treat diabetes. *Bio-organic chemistry*, 58, 65-71.**

**ABSTRACT:**

A new and efficient solvent free synthesis of 2,4,5-trisubstituted imidazoles (**3a–3j**) was achieved by N-acetyl glycine (NAG) catalyzed three components condensation of aldehydes, benzil and ammonium acetate. Our synthetic methodology accommodated a range of various substituted alkyl and aryl aldehydes. Evaluation of  $\alpha$ -glucosidase inhibitory activity of these imidazole derivatives revealed that most of them presented good  $\alpha$ -glucosidase inhibition at low micro-molar concentrations. Among the synthesized compounds, compound **3c**, bearing the *ortho*-hydroxy phenyl substituent at position 2 displayed the highest inhibitory activity with an  $IC_{50}$  value  $74.32 \pm 0.59 \mu\text{M}$ . *In silico* molecular docking for all compounds and computational studies of the most active compound **3c** were also performed.

**WEB URL:** <http://www.sciencedirect.com/science/article/pii/S0045206814001138>

**50. Koppenwallner, M., Rais, E., Uzarewicz-Baig, M., Tabassum, S., Gilani, M. A., & Wilhelm, R. (2015). Synthesis of New Camphor-Based Carbene Ligands and Their Application in a Copper-Catalyzed Michael Addition with B2Pin2. *Synthesis-Stuttgart*, 47(6), 789-800.**

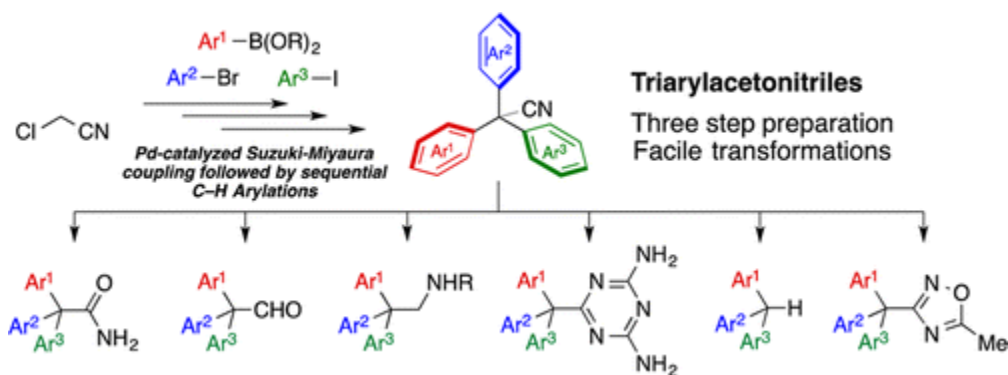
**ABSTRACT:**

In this work the synthesis of new asymmetric camphor-based carbene ligands from camphoric acid is described. The new carbenes can be prepared directly in high yields by the sequence: regioselective arylation of the less hindered primary amine group of (+)-cis-1,2,2-trimethylcyclopentane-1,3-diamine by Buchwald-Hartwig amination, treatment with trimethyl orthoformate, and finally treatment with a benzylic halide. The resulting carbenes, incorporating an aryl and a benzylic substituent, were successfully applied as ligands in a copper-catalyzed B2Pin2 [bis(pinacolato)diboron] addition to an unsaturated carbonyl compound. Depending on the substituents dual stereocontrol was observed and one enantiomer was obtained in up to 82% ee and the opposite enantiomer in up to 78% ee.

**WEB URL:**

[https://www.researchgate.net/publication/273692676\\_Synthesis\\_of\\_New\\_Camphor-Based\\_Carbene\\_Ligands\\_and\\_Their\\_Application\\_in\\_a\\_Copper-Catalyzed\\_Michael\\_Addition\\_with\\_B2Pin2](https://www.researchgate.net/publication/273692676_Synthesis_of_New_Camphor-Based_Carbene_Ligands_and_Their_Application_in_a_Copper-Catalyzed_Michael_Addition_with_B2Pin2)

**51. Nambo, M., Yar, M., Smith, J. D., & Crudden, C. M. (2015). The Concise Synthesis of Unsymmetric Triarylacetonitriles via Pd-Catalyzed Sequential Arylation: A New Synthetic Approach to Tri-and Tetraarylmethanes. *Organic letters*, 17(1), 50-53.**

**ABSTRACT:**

The selective synthesis of multiarylated acetonitriles via sequential palladium-catalyzed arylations of chloroacetonitrile is reported. The three aryl groups are installed via a Pd-catalyzed Suzuki–Miyaura cross coupling reaction followed by back-to-back C–H arylations to afford triarylacetonitriles in three steps with no over-arylation at any step. The triarylacetonitrile products can be converted into highly functionalized species including tetraarylmethanes. This new strategy provides rapid access to a variety of unsymmetrical tri- and tetraarylmethane derivatives from simple, readily available starting materials.

**WEB URL:** <http://pubs.acs.org/doi/ipdf/10.1021/ol503213z>

**52. Abbas, G., Hassan, A., Irfan, A., Mir, M., & Wu, G. (2015). A new pentacoordinate polymeric copper (II) complex with 2-amino-2-methyl-1, 3-propandiol: Structural investigations using XRD and DFT. *Journal of Structural Chemistry*, 56(1), 92-101.**

**ABSTRACT:**

A novel mononuclear copper complex [Cu(NH<sub>2</sub>mpdH)(NH<sub>2</sub>mpd)<sub>2</sub>Cl] (**1**) is synthesized from 2-amino-2-methyl-1,3-propandiol (ampdH<sub>4</sub>). The crystal structure of (**1**) is determined using X-ray diffraction studies. The copper complex crystallizes in the triclinic space group *P*-1(2) with *a* = 6.10.48(4) Å, *b* = 10.0915(7) Å, *c* = 10.9249(9) Å,  $\alpha$  = 95.925(6)°,  $\beta$  = 101.830(6)°,  $\gamma$  = 90.637(5)°, *V* = 649.53(95) Å<sup>3</sup> and *Z* = 2. The central

copper(II) atom in (**1**) is coordinated by three oxygen and two nitrogen atoms possessing a five-coordinate distorted square pyramidal geometry arranged in a one dimensional polymeric chain. The ground state geometry of the mononuclear copper complex is optimized using the DFT/B3LYP/6-31G\*\* (LANL2DZ) level of theory. Intra-molecular charge transfer is investigated based on the frontier molecular orbitals. The distribution pattern of the highest occupied molecular orbital and the lowest unoccupied molecular orbital is studied. Absorption spectra are computed using The time dependent density functional theory (TDDFT). The absorption wavelengths are calculated using different functionals, i.e., BHandHLYP, CAM-B3LYP, and LC-BLYP.

**WEB URL:** <http://link.springer.com/article/10.1134/S0022476615010138>

**53. Gonfa, G., Bustam, M. A., Muhammad, N., & Khan, A. S. (2015). Evaluation of Thermophysical Properties of Functionalized Imidazolium Thiocyanate Based Ionic Liquids. *Industrial & Engineering Chemistry Research*, 54(49), 12428-12437.**

**ABSTRACT:**

New cyano-based ionic liquids with thiocyanate anion and nitrile, ally, benzyl, and hydroxyl functionalized imidazolium cations were prepared, and some of their important thermophysical properties were measured. Properties such as density, viscosity, and refractive index were measured over various temperature ranges. From the experimental density values, the molecular volume, standard molar entropy, lattice energy, and thermal expansion coefficient of the ionic liquids were calculated. The thermal stabilities of the ionic liquids were investigated using thermogravimetric analysis. The effects of functionalized imidazolium side chains on the thermophysical properties of the ionic liquids were investigated. Density functional theory calculations were performed to study the effect of the structural variation of the imidazolium cation on properties of the ionic liquids.

**WEB URL:** <http://pubs.acs.org/doi/abs/10.1021/acs.iecr.5b03707>

54. Yar, M., Arshad, M., Farooq, A., Gilani, M. A., Ayub, K., Ejaz, A., ... & Ninomiya, I. (2015). Synthesis and DPPH scavenging assay of reserpine analogues, computational studies and in silico docking studies in AChE and BChE responsible for Alzheimer's disease. *Brazilian Journal of Pharmaceutical Sciences*, 51(1), 53-61.

**ABSTRACT:**

Alzheimer's disease (AD) is a fast growing neurodegenerative disorder of the central nervous system and anti-oxidants can be used to help suppress the oxidative stress caused by the free radicals that are responsible for AD. A series of selected synthetic indole derivatives were biologically evaluated to identify potent new antioxidants. Most of the evaluated compounds showed significant to modest antioxidant properties ( $IC_{50}$  value 399.07  $140.0 \pm 50 \mu M$ ). Density Functional Theory (DFT) studies were carried out on the compounds and their corresponding free radicals. Differences in the energy of the parent compounds and their corresponding free radicals provided a good justification for the trend found in their  $IC_{50}$  values. *In silico*, docking of compounds into the proteins acetylcholinesterase (AChE) and butyrylcholinesterase (BChE), which are well known for contributing in AD disease, was also performed to predict anti-AD potential.

**WEB URL:** [http://www.scielo.br/scielo.php?pid=S1984-82502015000100053&script=sci\\_arttext](http://www.scielo.br/scielo.php?pid=S1984-82502015000100053&script=sci_arttext)

55. Saleem, M., Anwar, M. S., Mahmood, A., Atiq, S., Ramay, S. M., & Siddiqi, S. A. (2015). Defects induced magnetization in B-doped ZnFeO dilute magnetic semiconductors. *Physica B: Condensed Matter*, 465, 16-20.

**ABSTRACT:**

Zn<sub>0.95-x</sub>Fe<sub>0.05</sub>BxO ( $x=0, 0.05$ ) nano-particles have been synthesized using a modified chemically derived citrate gel method. X-ray diffraction analysis demonstrates the wurtzite type hexagonal structure belonging to  $P6_3mc$  space group without the presence

of any secondary phase in both compositions. The Diffraction analysis shows that  $\text{Fe}^{2+}$  and  $\text{B}^{3+}$  ions have replaced some of the  $\text{Zn}^{2+}$  ions while some occupy un-detectable interstitial and inter-granular positions inside the structure. Scanning electron micrographs obtained using scanning electron microscopy show typical smaller size of particles in B-doped composition. Temperature dependent electrical resistivity analysis shows the semiconducting characteristics of the compositions and that doping of Fe and B up to 10 at% does not change the electrical behavior of the host material. Magnetic measurements display room temperature ferromagnetism in both compositions with enhanced magnetization in B-doped composition associated with defect induced magnetic mechanism belonging to intrinsically augmented interstitial and inter-granular effects.

**WEB URL:** <http://www.sciencedirect.com/science/article/pii/S0921452615001143>

**56. Piracha, A. H., Ramay, S. M., Atiq, S., Siddiqi, S. A., Saleem, M., & Anwar, M. S. (2015). Dielectric and magnetic investigations of mixed cubic spinel Co-ferrites with controlled Mg content. *Journal of Electroceramics*, 34(2-3), 122-129.**

**ABSTRACT:**

High temperature frequency dependent dielectric properties, and room temperature magnetic behavior of mixed ferrites with controlled content of Mg in  $\text{Co}_{1-x}\text{Mg}_x\text{Fe}_2\text{O}_4$  ( $x=0.0, 0.1, 0.3, 0.5, 0.7, 0.9$  and  $1.0$ ) compositions are studied. Single phase spinel structure with cubic symmetry, lattice parameters, crystallite size, magnetic and dielectric properties were substantiated with x-ray diffractometer, transmission electron microscope, vibrating sample magnetometer and impedance analysis, respectively. Due to interfacial polarization, dielectric behavior of all the compositions shows dispersion with increase in frequency. The dielectric data was investigated by comparing the tangent loss and electric modulus for assigning the type and mechanism of dielectric relaxation. Temperature dependent dielectric constant, tangent loss and AC conductivity increase due to thermal activation of charge carriers

and drift mobility. Furthermore, room temperature weak ferromagnetic behavior is observed due to the incorporation of non-magnetic Mg ions

**WEB URL:** <http://link.springer.com/article/10.1007/s10832-014-9960-y>

**57. Yaqoob, M. Z., Ghaffar, A., Alkanhal, M. A., Shakir, I., & Naqvi, Q. A. (2015). Scattering of electromagnetic waves from a chiral coated nihility cylinder hosted by isotropic plasma medium. *Optical Materials Express*,5(5), 1224-1229.**

**ABSTRACT:**

Theoretical analysis of the electromagnetic wave scattering of cylindrical waves from chiral coated nihility cylinder placed in isotropic plasma medium is carried out. The scattering problem is analytically formulated in the frame work of extended classical scattering theory. The cylindrical vector wave functions (CVWFs) are used for the expansion and representation of fields. The appropriate boundary conditions are applied on each interface i.e., Plasma/Chiral and chiral/nihility to get the unknown scattering coefficients. It is concluded that the scattering amplitude can be controlled and tuned by the plasma parameters (plasma density and effective collision frequency) as well as the chirality. Moreover, the present work has practical applications in target protection and microwave controlling devices. Under the special conditions, present work found good agreement with already published literature.

**WEB URL:** <https://www.osapublishing.org/ome/abstract.cfm?uri=ome-5-5-1224>

**58. Riaz, S., Khan, I. U., Bajda, M., Ashraf, M., Shaukat, A., Rehman, T. U., ... & Yar, M. (2015). Pyridine sulfonamide as a small key organic molecule for the potential treatment of type-II diabetes mellitus and Alzheimer's disease: In vitro studies against yeast  $\alpha$ -glucosidase, acetylcholinesterase and butyrylcholinesterase. *Bioorganic chemistry*, 63, 64-71.**

**ABSTRACT:**

This paper presents the efficient high yield synthesis of novel pyridine 2,4,6-tricarbohydrazide derivatives (**4a–4i**) along with their  $\alpha$ -glucosidase, acetylcholinesterase (AChE) and butyrylcholinesterase (BChE) inhibition activities. The enzymes inhibition results showed the potential of synthesized compounds in controlling both type-II diabetes mellitus and Alzheimer's disease. *In vitro* biological investigations revealed that most of compounds were more active against yeast  $\alpha$ -glucosidase than the reference compound acarbose ( $IC_{50} 38.25 \pm 0.12 \mu M$ ). Among the tested series the compound **4c** bearing 4-flouro benzyl group was noted to be the most active ( $IC_{50} 25.6 \pm 0.2 \mu M$ ) against  $\alpha$ -glucosidase, and it displayed weak inhibition activities against AChE and BChE. Compound **4a** exhibited the most desired results against all three enzymes, as it was significantly active against all the three enzymes;  $\alpha$ -glucosidase ( $IC_{50} 32.2 \pm 0.3 \mu M$ ), AChE ( $IC_{50} 50.2 \pm 0.8 \mu M$ ) and BChE ( $IC_{50} 43.8 \pm 0.8 \mu M$ ). Due to the most favorable activity of **4a** against the tested enzymes, for molecular modeling studies this compound was selected to investigate its pattern of interaction with  $\alpha$ -glucosidase and AChE targets.

**WEB URL:** <http://www.sciencedirect.com/science/article/pii/S0045206815300237>

**59. Razaq, A., Khan, A. A., Asif, M. H., Iqbal, S., Ali, J., Manzoor, F., & Awan, M. S. (2015). Dielectric studies of environmentally friendly and flexible lignocelluloses fibrils for miniaturization of patch antenna. *Modern Physics Letters B*, 29(30), 1550187.**

**ABSTRACT:**

Naturally, existing lignocelluloses fibers showed outstanding potential in paper industry and other conventional applications. On the other hand, lignocellulose fibers are suitable candidate for high-tech applications under the scope of abundance, flexibility, light-weight and environment friendliness. In this study, paper sheets were prepared from lignocelluloses fibers extracted from self-growing plant, *typha angustifolia*. Lignocelluloses paper sheets were characterized for scanning electron microscopy

(SEM), universal testing machine (UTM) and vector network analyzer (VNA). Flexible paper sheets displayed a tensile strength of 9.1 MPa and further used as a substrate in patch antenna to observe dielectric characteristics. The patch antenna is designed at 5.1 GHz which showed return loss less than -10 dB and dielectric constant 3.71. The use of lignocelluloses paper sheet as a substrate in patch antenna will provide the opportunity of miniaturization of size and weight in comparison of a jean substrate based antenna.

**WEB URL:** <http://www.worldscientific.com/doi/abs/10.1142/S0217984915501870>

**60. Sharif, F., Steenbergen, P. J., Metz, J. R., & Champagne, D. L. (2015). Long-lasting effects of dexamethasone on immune cells and wound healing in the zebrafish. *Wound Repair and Regeneration*, 23(6), 855-865.**

**ABSTRACT:**

This study assessed the lasting impact of dexamethasone (DEX) exposure during early development on tissue repair capacity at later life stages (5, 14, and 24 days post fertilization [dpf]) in zebrafish larvae. Using the caudal fin amputation model, we show that prior exposure to DEX significantly delays but does not prevent wound healing at all life stages studied. DEX-induced impairments on wound healing were fully restored to normal levels with longer post amputation recovery time. Further analyses revealed that DEX mainly exerted its detrimental effects in the early phase (0–5 hours) of wound-healing process. Specifically, we observed the following events: (1) massive amount of cell death both by necrosis and apoptosis; (2) significant reduction in the number as well as misplacement of macrophages at the wound site; (3) aberrant migration and misplacement of neutrophils and macrophages at the wound site. These events were accompanied by significant (likely compensatory) changes in the expression of genes involved in tissue patterning, including up-regulation of FKBP5 6 hours post DEX exposure and that of *Wnt3a* and *RAR $\gamma$*  at 24 hours post amputation. Taken together, this study provides evidence that DEX exposure during early sensitive periods of

development appears to cause permanent alterations in the cellular/molecular immune processes that are involved in the early phase of wound healing in zebrafish. These findings are consistent with previous studies showing that antenatal course of DEX is associated with immediate and lasting alterations of the immune system in rodent models and humans. Therefore, the current findings support the use of the larval zebrafish model to study the impact of stress and stress hormone exposure in immature organisms on health risks in later life.

**WEB URL:** <http://onlinelibrary.wiley.com/doi/10.1111/wrr.12366/full>

**61. Nasrullah, A., Khan, H., Khan, A. S., Man, Z., Muhammad, N., Khan, M. I., & Abd El-Salam, N. M. (2015). Potential biosorbent derived from *Calligonum polygonoides* for removal of methylene blue dye from aqueous solution. *The Scientific World Journal*.**

**ABSTRACT:**

The ash of *C. polygonoides* (locally called balanza) was collected from Lakki Marwat, Khyber Pakhtunkhwa, Pakistan, and was utilized as biosorbent for methylene blue (MB) removal from aqueous solution. The ash was used as biosorbent without any physical or chemical treatment. The biosorbent was characterized by using various techniques such as Fourier transform infrared spectroscopy (FTIR), thermogravimetric analysis (TGA), and scanning electron microscopy (SEM). The particle size and surface area were measured using particle size analyzer and Brunauer-Emmett-Teller equation (BET), respectively. The SEM and BET results expressed that the adsorbent has porous nature. Effects of various conditions such as initial concentration of methylene blue (MB), initial pH, contact time, dosage of biosorbent, and stirring rate were also investigated for the adsorption process. The rate of the adsorption of MB on biomass sample was fast, and equilibrium has been achieved within 1 hour. The kinetics of MB adsorption on biosorbent was studied by pseudo-first- and pseudo-second-order kinetic models and the pseudo-second-order has better mathematical fit with correlation coefficient value () of 0.999. The study revealed that *C. polygonoides* ash proved to be an effective,

alternative, inexpensive, and environmentally benign biosorbent for MB removal from aqueous solution.

**WEB URL:** <http://www.hindawi.com/journals/tswj/2015/562693/abs/>

**62. Khan, A. S. (2015). Finite element method analysis of a jaw structure upon surgically assisted rapid maxillary expansion with various surgical procedures. 24(02), 70.**

**ABSTRACT:**

The surgically assisted rapid maxillary expansion is a clinical surgical procedure which is used for the patients lacking in transverse match between upper and lower jaws and with malocclusions. Depending on the judgment of a clinician doing treatment, different kind of surgical procedures are adapted. In reality the best method chosen among the different procedure varies with the clinician's personal subjective experiences. The aim of this study was to analyze the displacement (strain) and stress distributions using Finite Element Method (FEM) following the applications of different surgical procedures during surgically assisted rapid maxillary expansion. Methods: There were two groups which were control and test group, subjects to which the FEM analysis was performed in this study. In control group non-surgical rapid maxillary expansion was applied while in test group surgically assisted rapid maxillary expansion was applied. Results: This analysis allowed the choice of location for the surgical operations and determination of the procedures for the surgically assisted rapid maxillary expansion. The maximum strain was substantially increased from Test 1 to Test 4 which was due to the application of pterygomaxillary separation and it is indicated that pterygomaxillary separation is the most effective surgical method for rapid maxillary expansion. Conclusion: This study predicted methodology of clinical treatments of patients with maximum efficiency in the shortest time on the basis of FEA.

**WEB URL:** <http://jpda.com.pk/volume-24-issue-2/finite-element-method-analysis-of-a-jaw-structure-upon-surgically-assisted-rapid-maxillary-expansion-with-various-surgical-procedures/download-article-03-volume-24-issue-2/>

**63. Muhammad, N., Man, Z., Mutalib, M. I., Bustam, M. A., Wilfred, C. D., Khan, A. S., ... & Nasrullah, A. (2015). Dissolution and Separation of Wood Biopolymers Using Ionic Liquids. *ChemBioEng Reviews*, 2(4), 257-278.**

**ABSTRACT:**

The majority of the world energy needs have been supplied from petroleum resources. While they are an efficient energy provider, their usage has caused pollution problems that warrant the need to search for efficient and cleaner energy sources. The ever growing global demand of energy and the concerns for the environment have prompted researchers to develop convenient and efficient ways to convert biomass into valuable chemicals, bio-fuels, and useful biomaterials. This review focuses on the application of ionic liquids for the dissolution of wood biomass and wood-derived compounds. The factors which affect the dissolution of cellulose and lignin in ionic liquids are described as well as the effects of ionic liquids on the physical properties of cellulose. The use of ionic liquids alone or in combination with other co-solvent systems which help in the fractionation of wood biomass are discussed. Additionally, the cost economic aspects of ionic liquid applications are highlighted.

**WEB URL:** <http://onlinelibrary.wiley.com/doi/10.1002/cben.201500003/abstract>

**64. Hussain, T., Shah, A. T., Shehzad, K., Mujahid, A., Farooqi, Z. H., Raza, M. H., ... & Nisa, Z. U. (2015). Formation of self-ordered porous anodized alumina template for growing tungsten trioxide nanowires. *International Nano Letters*, 5(1), 37-41.**

**ABSTRACT:**

Uniform porous anodized aluminum oxide (AAO) membrane has been synthesized by two-step anodization for fabricating tungsten trioxide (WO<sub>3</sub>) nanowires. Under assayed conditions, uniform porous structure of alumina (Al<sub>2</sub>O<sub>3</sub>) membrane with long range ordered hexagonal arrangements of nanopores was achieved. The self-assembled template possesses pores of internal diameter of 50 nm and interpore distance ( $d_{int}$ ) of 80 nm with a thickness of about 80  $\mu$ m, i.e., used for fabrication of

nanostructures.  $WO_3$  nanowires have been fabricated by simple electroless deposition method inside  $Al_2O_3$  nanopores. SEM images show tungsten trioxide nanowire with internal diameter of about 50 nm, similar to porous diameter of AAO template. XRD results showed that nanowires exist in cubic crystalline state with minor proportion of monoclinic phase.

**WEB URL:** <http://link.springer.com/article/10.1007/s40089-014-0134-3>

**65. Afzal, M., Zhang, L., Cox, R. J., Muhammad, N., & Khan, S. (2015). Isolation of Two New Mallotoates with Antifungal and Radical Scavenging Activities from *Mallotus philippensis* muell. *Asian Journal of Chemistry*,27(10), 3891.**

**ABSTRACT:**

Two new chalcone derivatives mallotoate A and mallotoate B were isolated from ethyl acetate fraction of *Mallotus philippensis* muell. Structure elucidation and the assignment of the isolates were achieved with the help of extensive 1D and 2D NMR studies. These compounds were identified using chemical and spectral data, as mallotoate A and mallotoate B, respectively. Both the compounds (mallotoate A and mallotoate B) showed significant fungicidal activity against *Cladosporium cladosporioides* in TLC bio-autography method. Using the same method, both mallotoate A and mallotoate B were tested for their antioxidant activities in DPPH radical scavenging activity in which, mallotoate B showed maximum and competitive activity ( $91.43 \pm 0.82$  %) against control drugs.

**WEB URL:**

<http://search.proquest.com/openview/7869454cfae63c5077d75bc7e5ddf49d/1?pq-origsite=gscholar>

# DEPARTMENT OF MANAGEMENT SCIENCE

## Journal Papers

1. Ali, A., Mujahid, N., Rashid, Y., & Shahbaz, M. (2015). Human capital outflow and economic misery: Fresh evidence for Pakistan. *Social Indicators Research*, 124(3), 747-764.

**ABSTRACT:**

This paper visits the impact of economic misery on human capital outflow using time series data over the period of 1975–2012. We have applied the combined cointegration tests and innovation accounting approach to examine long run and causal relationship between the variables. Our results affirm the presence of cointegration between the variables. We find that economic misery increases human capital outflow. Foreign remittances add in human capital outflow from Pakistan. The migration from Pakistan to rest of world is boosted by depreciation in local currency. Income inequality is also a major contributor to human capital outflow. The present study is comprehensive effort and may provide new insights to policy makers for handling the issue of human capital outflow by controlling economic misery in Pakistan.

**WEB URL:** <http://link.springer.com/article/10.1007/s11205-014-0821-5>

2. Faisal, A. & Naqvi, I. H. (2015). "Effect of rework on project success." *Science International* 27 (1)575-580.

**ABSTRACT:**

This paper provides an insight to project success (PS) factors & criteria. Software project teams focus on various factors to achieve the predetermined PS criteria based on the nature of the project. Achieving the project milestones in terms of the triple constraints of iron triangle did not guarantee the PS. PS could never be guaranteed by doing the right

work until & unless the stakeholder's perception & vision is not converted into reality. This study contributed in exploring the various rework types & their impact on PS. This study contributed that magnitude of rework is dependent on total project completion duration & rework can be avoided in SDLC. The study analyzed the association between rework & PS. Major causes of unsuccessful projects in view of project team members were explored through a survey conducted in the software industry of Lahore Pakistan.

**WEB URL:** <file:///C:/Users/sahmed/Downloads/ScienceInt.pdf>

**3. Shahbaz, M., Loganathan, N., Sbia, R., & Afza, T. (2015). The effect of urbanization, affluence and trade openness on energy consumption: A time series analysis in Malaysia. *Renewable and Sustainable Energy Reviews*,47, 683-693.**

**ABSTRACT:**

This paper investigates the impact of urbanization on energy consumption by applying the Stochastic Impacts by Regression on Population, Affluence and Technology (STIRPAT) in case of Malaysia. The study covers the time period of 1970Q1–2011Q4. The unit root test and the ARDL bounds testing approach have been applied to examine integrating properties and long run relationship in the presence of structural breaks. Our results validated the existence of cointegration and exposed that urbanization is a major contributor in energy consumption. Affluence raises energy demand. Capital stock boosts energy consumption. Trade openness leads to affluence and hence increases energy consumption. The causality analysis finds that urbanization Granger causes energy consumption. The feedback effect is found between energy consumption and affluence and, energy consumption and capital. The bidirectional causality exists between trade openness and energy consumption.

**WEB URL:** <http://www.sciencedirect.com/science/article/pii/S1364032115001975>

**4. Shuja, A., & Abassi, A. S. (2015). Effect of Ethics Training on Resilience of Non-Governmental Organizations. *Sci.Int.(Lahore)*, 27(3), 2381-2386.**

**ABSTRACT:**

Ethics training is an important factor that enables organizational members to sort out complex ethical dilemmas and prevent organizations from facing any criminal suit and involve in any unlawful activity and therefore, considered as vital component of organizations to ensure sustainable operational continuity and achieving high organizations' performance levels during external social crisis conditions through development of organizational resilience. The paper explores the effect of ethics training on organizational resilience. The underlying study is an empirical investigation involving collection of survey data from managerial level employees working in NGOs of Lahore, Pakistan. The results of the study opposed to the findings of the previous literature studies and led to conclude that ethics training in community development organizations has insignificant effect on development of organizational resilience. Therefore, during occurrence of critical environmental situations characterized by intense ethical dilemmas, ethics training does not play any contribution for enhancing the response and recovery efforts of the organizations in order to resolve complicated social or workplace decisional predicaments. NGOs need to emphasize and develop effective ethics training programs for ethical and moral development of individuals which ultimately leads to improved organizational performance reputation and sustainability

**5. Saleem, A. (2015). Impact Of Life And Job Domain Characteristics On Work Life Balance Of Textile Employees In Pakistan. *Sci.Int.(Lahore)*,27(3),2409-2416.**

**ABSTRACT:**

Now a day's work-life balance has become a common apprehension for both employees and employer due to demographic changes, women participation in work, increasing number of dual career families and change in work settings. Work life balance is the state of equilibrium where any person is able to get satisfies with personal and professional life. In literature, although the combination of some variables from job domain and life domain have been widely considered in determining the employee work life balance, no

investigation has indicated the combined influence employee work life balance. This study examines the impact of both job and life domain characteristics on employee work life balance. A total of 300 employees from different 31 textile companies participated in this study. Sample was selected using the probability sampling techniques. The results of this study confirmed that both life and job domain significantly affect the work life balance. Employees who have greater control over work schedule, supervisory, co worker and social support and have low level of work role expectations, family role expectations, numbers of kids, less working hours have positive perception about work life balance. It is recommended that textile companies revamp the negatively affected job characteristics, encourage positively affected job characteristics, offer various work life balance strategies; so employees can enjoy work life balance and show more positive work behaviors.

**WEB URL:**

[https://www.researchgate.net/profile/Abdus\\_Abbasi/publication/288828970\\_IMPACT\\_OF\\_LIFE\\_AND\\_JOB\\_DOMAIN\\_CHARACTERISTICS\\_ON\\_WORK\\_LIFE\\_BALANCE\\_OF\\_TEXTILE\\_EMPLOYEES\\_IN\\_PAKISTAN/links/5685004208aebccc4e1142c9.pdf](https://www.researchgate.net/profile/Abdus_Abbasi/publication/288828970_IMPACT_OF_LIFE_AND_JOB_DOMAIN_CHARACTERISTICS_ON_WORK_LIFE_BALANCE_OF_TEXTILE_EMPLOYEES_IN_PAKISTAN/links/5685004208aebccc4e1142c9.pdf)

**6. Shuja, A., & Abbasi, A. S. (2015)An Investigation Of The Impact Of Resource Mobilization On Business Continuity Management: A Study On Banking Sector Of Pakistan. *Sci.Int.(Lahore)*, 27(3). 2409-2416.**

**ABSTRACT:**

The purpose of the study is to examine and investigate the effect of resource mobilization on the business continuity management practices in banks. Data was collected from managers from a sample of 20 banks operating in Lahore, Pakistan. A seven point Likert scale based questionnaire was used in the intended study consisting of eight items for measuring resource mobilization and fifteen items for the measurement of business continuity management. A total of 274 responses were received with a response rate of 62.02%. The results and findings of the study suggest that resource mobilization is an effective tool used in implementing business continuity and disaster and crisis management

plans. Mobilizing organizational resources in an event of crisis, disaster or risk involves planning, attaining and arranging resources such as equipment, technical systems, workforces and their services required and needed for serving most affected or vulnerable location in order to manage a crisis or disaster and ensure smooth recovery and continuity of the business operations. Resource mobilization is an important function for ensuring prompt management with disasters, crises and disruptions in order to ensure well timed recovery, restoration and continuity of the business processes, and therefore has a positive impact on practices directed towards business continuity management.

**WEB URL:** <http://www.ciitlahore.edu.pk/Papers/Abstracts/539-8587523035731182058.pdf>

**7. Khan, M., & Damalas, C. A. (2015). Farmers' knowledge about common pests and pesticide safety in conventional cotton production in Pakistan. *Crop Protection*, 77, 45-51.**

**ABSTRACT:**

Innovations in cotton (*Gossypium hirsutum* L.) pest management should be initially based on the perspective of cotton farmers, recognizing farmers' constraints and their existing technical knowledge as the basis for an effective collaboration. A survey of 318 randomly selected farmers from two districts of the cotton belt of Punjab in Pakistan was conducted to study common crop protection problems and related behaviors in cotton production in the area. Data were collected through group discussions with farmers and individual interviews. Relative frequencies of distribution for the tested variables, weighted average scores based on the weight assigned to each answer for the rating scales, and the Borich Needs Assessment Model for the training needs were used for relevant comparisons. Most farmers considered pest damage to be important in cotton production causing significant yield losses. Farmers had awareness of some major insect pests, but the majority of them used descriptive than specific names when defining a pest. Among well-known insects whiteflies, aphids, leafhoppers, thrips, and bollworms were mentioned, but farmers had great difficulty in distinguishing the different species. Identification of cotton diseases was practically non-existent, except from cotton leaf cWeb URL. Farmers were aware of a

limited number of major weeds. Most of them stated purple nutsedge and bermudagrass as frequent weed problems in cotton production in the area. In general, weeds were perceived as a constant and unresolved problem in cotton production, but with less impact on yield than insects. The majority of the farmers relied on the chemical method for pest control, but knowledge on pesticide safety issues was below average. High needs for training were found on a) the proper period for pesticide application, b) the identification of natural enemies for cotton pests, and c) the discrimination of symptoms of various diseases. Understanding farmers' views of pests and their impact can be a first major step for more efficient pest management in cotton production.

**WEB URL:** <http://www.sciencedirect.com/science/article/pii/S0261219415300697>

**8. Bouoiyour, J., Selmi, R., Tiwari, A. K., & Shahbaz, M. (2015). The nexus between oil price and Russia's real exchange rate: Better paths via unconditional vs conditional analysis. *Energy Economics*, 51, 54-66.**

**ABSTRACT:**

Instead of analyzing the causality between two time series (unconditional analysis), as it is usually done, the present study deals with the nexus between oil price and Russia's real exchange rate conditioning upon potential control variables at well-specified horizons and on a frequency by frequency basis. This research accounts also for the possible transient linkages and signal discontinuities. A major finding of this paper is deeply suggestive of a sharp causality running from oil price to real exchange rate in lower frequencies. This implies that Russia should better tackle with turbulence triggered by oil price and continue to reduce its energy dependency via drastic and proactive measures. The economic and fiscal initiatives of Putin administration may help to cope with sudden shocks, to lessen the great oil dependence and to build confidence needed for economic recovery. While our research does not say much about the routes through which oil price may affect differently real exchange rate, it clearly indicates the presence of short-term relationship conditional to GDP, government expenditures, terms of trade and productivity differential. The conditional

analysis and signal detection appear as meaningful exercises to find new insights into the focal issue.

**WEB URL:** <http://www.sciencedirect.com/science/article/pii/S0140988315001747>

**9. Adnan, F., & Naqvi, I. H. (2015). Automated Software Requirements Management Tools: A Methodology For Project Success. Sci.Int.(Lahore),27(4),3179-3184.**

**ABSTRACT:**

This paper provides an insight of automated software requirements management and its role in project success (PS). Different features of automated software requirements management tools were critically reviewed. The underlying associations among software requirements management, software requirements traceability, changing requirements, using automated software requirements management tools and rework with PS were explored through a survey conducted among the software houses. This study found a lack of proficiency in automated SRM skills and practices among the software projects which caused rework in software development life cycle. This study is a novel contribution in exploring the role of automated software requirements management tools as an effective methodology for project success.

**WEB URL:** <http://www.ciitlahore.edu.pk/Papers/Abstracts/538-8587611055458994558.pdf>

**10. Shahbaz, M., Rehman, I. U., & Muzaffar, A. T. (2015). Re-Visiting Financial Development and Economic Growth Nexus: The Role of Capitalization in Bangladesh. South African Journal of Economics, 83(3), 452-471.**

**ABSTRACT:**

This paper revisits the relationship between financial development and economic growth in Bangladesh by incorporating trade openness in production function using quarter frequency data over the period of 1976-2012. We applied combined Bayer–Hanck cointegration approach to examine cointegration among the series. Our empirical evidence suggests that development of financial sector facilitates economic growth but capitalization impedes it. In

addition, trade openness stimulates economic growth. Labour is also positively linked to economic growth. The vector error correction model Granger causality results divulge that financial development causes real per capita gross domestic product (GDP) growth, and resultantly, real per capita GDP growth causes financial development in a Granger sense. The results also show that trade and labour Granger cause economic growth. The findings of the paper provide insights for policymakers to use financial development and trade openness as a tool for sustained economic growth in the long run. The paper also suggests policymakers to utilise capitalization in a way that is beneficial for economic growth of Bangladesh.

**WEB URL:** <http://onlinelibrary.wiley.com/doi/10.1111/saje.12063/full>

**11. Shahbaz, M., Solarin, S. A., Sbia, R., & Bibi, S. (2015). Does energy intensity contribute to CO<sub>2</sub> emissions? A trivariate analysis in selected African countries. *Ecological indicators, 50*, 215-224.**

**ABSTRACT:**

The present study investigates the dynamic relationship between energy intensity and CO<sub>2</sub> emissions by incorporating economic growth in environment CO<sub>2</sub> emissions function using data of Sub Saharan African countries. For this purpose, we applied panel cointegration to examine the long run relationship between the series. We employed the VECM Granger causality to test the direction of causality amid the variables.

At panel level, our results validate the existence of cointegration among the series. The long run panel results show that energy intensity has positive and statistically significant impact on CO<sub>2</sub> emissions. There is also positive and negative link of non-linear and linear terms of real GDP per capita with CO<sub>2</sub> emissions supporting the presence of environmental Kuznets curve (EKC). The causality analysis reveals the bidirectional causality between economic growth and CO<sub>2</sub> emissions while energy intensity Granger causes economic growth and hence CO<sub>2</sub> emissions, while across the individual countries, the results differ. This paper

opens up new insights for policy makers to design comprehensive economic, energy and environmental policy for sustainable long run economic growth.

**WEB URL:** <http://www.sciencedirect.com/science/article/pii/S1470160X14005305>

**12. Shuja, A., & Abassi, A. S. (2015). Effect Of Ethics Training On Resilience Of Non-Governmental Organizations.Sci.Int.(Lahore),27(3),2381-2386.**

**ABSTRACT:**

Ethics training is an important factor that enables organizational members to sort out complex ethical dilemmas and prevent organizations from facing any criminal suit and involve in any unlawful activity and therefore, considered as vital component of organizations to ensure sustainable operational continuity and achieving high organizations' performance levels during external social crisis conditions through development of organizational resilience. The paper explores the effect of ethics training on organizational resilience. The underlying study is an empirical investigation involving collection of survey data from managerial level employees working in NGOs of Lahore, Pakistan. The results of the study opposed to the findings of the previous literature studies and led to conclude that ethics training in community development organizations has insignificant effect on development of organizational resilience. Therefore, during occurrence of critical environmental situations characterized by intense ethical dilemmas, ethics training does not play any contribution for enhancing the response and recovery efforts of the organizations in order to resolve complicated social or workplace decisional predicaments. NGOs need to emphasize and develop effective ethics training programs for ethical and moral development of individuals which ultimately leads to improved organizational performance reputation and sustainability.

**WEB URL:** <http://www.ciitlahore.edu.pk/Papers/Abstracts/539-8587523033677119558.pdf>

**13. Khan, M., & Damalas, C. A. (2015). Farmers' willingness to pay for less health risks by pesticide use: A case study from the cotton belt of Punjab, Pakistan. *Science of the Total Environment*, 530, 297-303.**

**ABSTRACT:**

The amount of pesticides used in crop production in Pakistan has increased rapidly in the last decades, whereas farmers in many areas of the country show little knowledge of safe and efficient use of pesticides. The level of willingness to pay (WTP) for avoiding health risks by pesticides was studied among 318 randomly selected cotton farmers from two districts of the area of Punjab (i.e., Vehari and Lodhran) in Pakistan, using the contingent valuation method. Most farmers felt that pesticide use is a prerequisite for successful cotton production, whereas at the same time they were well aware of pesticide health risks, which they considered minor. The majority of the farmers (77%) showed varying levels of WTP some fee up to 20% of the current pesticide expenditures for avoiding pesticide health risks, but few were willing to pay a fee over 20%. The mean WTP per farmer was low, reaching 5.8 \$US on an annual basis. By contrast, a considerable proportion of the farmers (23%) were not willing to pay any fee for avoiding pesticide health risks. These individuals were mostly poor small-scale farmers with limited or no education. High levels of risk perception about pesticides, past experience of pesticide intoxication, high levels of education, and high income were associated with high farmers' WTP for less health risks by pesticides. Farmers who perceived major health risks by pesticides appeared to be highly willing to pay a premium for safe pesticides. Elderly farmers appeared more likely to pay some premium for safe pesticides as a result of higher farming experience and higher income than young farmers. Well-educated farmers were more likely to pay a high premium for safe pesticides. Large farm size was a significant predictor of positive WTP, which was interpreted as an indicator of farmers' wealth.

**WEB URL:** <http://www.sciencedirect.com/science/article/pii/S0048969715301686>

**14. Rasool, G., Ehsan, F., & Shahbaz, M. (2015). A systematic literature review on electricity management systems. *Renewable and Sustainable Energy Reviews, 49*, 975-989.**

**ABSTRACT:**

Many countries in the world and most importantly Pakistan is suffering from severe electricity crisis. Information Technology (IT) is being used in every field of the life and we may apply IT to overcome electricity crisis. A large number of papers are presented by different researchers on electricity management. The key motivation of this systematic literature review is to study, analyze and explore the status of different solutions presented for management of electricity throughout the world and determine requirements for the development of a new electricity management system. We apply standard systematic review method with the manual search of three digital libraries. Out of 74 primary studies, 27 studies are software contributions, 13 studies are hardware solutions, 18 studies represent the theoretical work and 16 studies contribute proposed ideas. The quality of the contributions is fair as 74 articles out of 209 were selected as candidate studies after manual peer review. Currently, the solutions presented by different researchers are limited in scope. Many researchers are working on tool contributions, but most of them are only providing solutions for specific regions and communities. There is a need to develop a generic Electricity Management System (EMS) that should be customizable and can be used as generic solution.

**WEB URL:** <http://www.sciencedirect.com/science/article/pii/S136403211500324X>

**15. Shahbaz, M., Tiwari, A. K., & Tahir, M. I. (2015). Analyzing time–frequency relationship between oil price and exchange rate in Pakistan through wavelets. *Journal of Applied Statistics, 42(4)*, 690-704.**

**ABSTRACT:**

This study analyzed the time–frequency relationship between oil price and exchange rate for Pakistan by using measures of continuous wavelet such as wavelet power, cross-wavelet power, and cross-wavelet coherency (WTC). The results of cross-wavelet analysis indicated that covariance between oil price and exchange rate is unable to give clear-cut results, but both variables have been in phase and out phase (i.e. they are anti-cyclical and cyclical in nature) in some or other durations. However, results of squared wavelet coherence disclose that both variables are out of phase and real exchange rate was leading during the entire period studied, corresponding to the 10–15 months’ scale. These results are the unique contribution of the present study, which would have not been drawn if one would have utilized any other time series or frequency domain-based approach. This finding provides evidence of anti-cyclical relationship between oil price and real effective exchange rate; however, in most of the period studied, real exchange rate was leading and passing anti-cycle effects on oil price shocks which is the major contribution of the study.

**WEB URL:** <http://www.tandfonline.com/doi/abs/10.1080/02664763.2014.980784>

**16. Shahbaz, M., Khraief, N., & Jemaa, M. M. B. (2015). On the causal nexus of road transport CO 2 emissions and macroeconomic variables in Tunisia: Evidence from combined cointegration tests. *Renewable and Sustainable Energy Reviews, 51*, 89-100.**

**ABSTRACT:**

This paper investigates the causal relationship between road transportation energy consumption, fuel prices, transport sector value added and CO<sub>2</sub> emissions in Tunisia for the period of 1980–2012. We apply the newly developed combined cointegration test proposed by Bayer, C, Hanck, C. Combining non-cointegration tests. *J Time Ser Anal* 2013; 34(1): 83–95 and the ARDL bounds testing approach to cointegration for establishing the existence of long-run relationship in presence of structural breaks. The direction of causality between these variables is determined *via* vector error correction model (VECM).

Our empirical exercise reveals that cointegration is present. Energy consumption adds in CO<sub>2</sub> emissions. Fuel prices decline CO<sub>2</sub> emissions. Road infrastructure boosts CO<sub>2</sub> emissions. Transport value-added also increases CO<sub>2</sub> emissions. The causality analysis indicates the bidirectional casual relationship between energy consumption and CO<sub>2</sub> emissions. Road infrastructure causes CO<sub>2</sub> emissions and similar is true from opposite side in Granger sense. The bidirectional causality is also found between transport value-added and CO<sub>2</sub> emissions. Fuel prices cause CO<sub>2</sub> emissions, energy consumption, road infrastructure and transport value-added in Granger sense. This paper provides new insights to policy makers for designing a comprehensive energy, transport and environment policies for sustainable economic growth in long run.

**WEB URL:** <http://www.sciencedirect.com/science/article/pii/S1364032115005845>

**17. Shahbaz, M., Khraief, N., & Jemaa, M. M. B. (2015). On the causal nexus of road transport CO<sub>2</sub> emissions and macroeconomic variables in Tunisia: Evidence from combined cointegration tests. *Renewable and Sustainable Energy Reviews, 51*, 89-100.**

**ABSTRACT:**

This paper investigates the causal relationship between road transportation energy consumption, fuel prices, transport sector value added and CO<sub>2</sub> emissions in Tunisia for the period of 1980–2012. We apply the newly developed combined cointegration test proposed by Bayer, C, Hanck, C. Combining non-cointegration tests. *J Time Ser Anal* 2013; 34(1): 83–95 and the ARDL bounds testing approach to cointegration for establishing the existence of long-run relationship in presence of structural breaks. The direction of causality between these variables is determined *via* vector error correction model (VECM).

Our empirical exercise reveals that cointegration is present. Energy consumption adds in CO<sub>2</sub> emissions. Fuel prices decline CO<sub>2</sub> emissions. Road infrastructure boosts CO<sub>2</sub> emissions. Transport value-added also increases CO<sub>2</sub> emissions. The causality analysis indicates the bidirectional casual relationship between energy consumption and CO<sub>2</sub> emissions. Road infrastructure causes CO<sub>2</sub> emissions and similar is true from opposite side in Granger sense.

The bidirectional causality is also found between transport value-added and CO<sub>2</sub> emissions. Fuel prices cause CO<sub>2</sub> emissions, energy consumption, road infrastructure and transport value-added in Granger sense. This paper provides new insights to policy makers for designing a comprehensive energy, transport and environment policies for sustainable economic growth in long run.

**WEB URL:** <http://www.sciencedirect.com/science/article/pii/S1364032115005845>

**18. Shahbaz, M., Nasreen, S., Abbas, F., & Anis, O. (2015). Does foreign direct investment impede environmental quality in high-, middle-, and low-income countries?. *Energy Economics*, 51, 275-287.**

**ABSTRACT:**

Under a multivariate framework, this paper aims to investigate the nonlinear correlation between foreign direct investment and environmental degradation for high-, middle-, and low-income countries with economic growth and energy consumption as additional determinants of environmental degradation. All variables were found to be nonstationary and cointegrated based on recent panel data unit-root tests and cointegration techniques. On applying fully modified ordinary least squares (FMOLS), the long-run results suggest the presence of an environmental Kuznets curve. In turn, foreign direct investment increases environmental degradation, thus confirming the pollution haven hypothesis (PHH). Moreover, the bidirectional causality between CO<sub>2</sub> emissions and foreign direct investment is observed globally. The findings are sensitive to different income groups and regional analyses. In particular, these empirical findings aid sound economic policymaking for improving environmental quality and sustainable economic development.

**WEB URL:** <http://www.sciencedirect.com/science/article/pii/S0140988315001905>

**19. Shahbaz, M., Mallick, H., Mahalik, M. K., & Loganathan, N. (2015). Does globalization impede environmental quality in India?. *Ecological Indicators*, 52, 379-393.**

**ABSTRACT:**

Using annual data for the period 1970–2012, the study explores the relationship between globalization and CO<sub>2</sub> emissions by incorporating energy consumption, financial development and economic growth in CO<sub>2</sub> emission function for India. It applies Lee and Strazicich (2013) unit root test for examining the stationary properties of variables in presence of structural breaks and employs the cointegration method proposed by Bayer and Hanck (2013) to test the long-run relationships in the model. The robustness of cointegration result from the latter model was further verified with the application of the ARDL bounds testing approach to cointegration proposed by Pesaran et al. (2001). After confirming the existence of cointegration, the overall long run estimates of the estimation of carbon emission model points out that acceleration in the process of globalization (measured in its three dimensions – economic, social and political globalizations) and energy consumption result in increasing CO<sub>2</sub> emissions, along with the contribution of economic development and financial development toward the deterioration of the environmental quality by raising CO<sub>2</sub> emissions over the long-run. This finding validates the holding of environmental Kuznets curve (EKC) hypothesis for the Indian context.

**WEB URL:** <http://www.sciencedirect.com/science/article/pii/S1470160X14006013>

**20. Raza, S. A., Shahbaz, M., & Nguyen, D. K. (2015). Energy conservation policies, growth and trade performance: evidence of feedback hypothesis in Pakistan. *Energy Policy*, 80, 1-10.**

**ABSTRACT:**

This study investigates the energy–growth–trade nexus in Pakistan by using the annual time series data for the period of 1973–2013. Our main results show: (i) the presence of long-run link between energy consumption and trade performance; (ii) positive impact of gross domestic product, exports, and imports on energy consumption; (iii) bidirectional causal relationship between exports and energy consumption, and also between imports and energy demand; and (iv) bidirectional causality between gross domestic product and energy

consumption points to the presence of feedback hypothesis in Pakistan. We therefore note that energy conservation policies will reduce the trade performance which in turn leads to decline in economic growth in Pakistan. The present study may guide policymakers in formulating a conclusive energy and trade policies for sustainable growth for long span of time.

**WEB URL:** <http://www.sciencedirect.com/science/article/pii/S0301421515000129>

**21. Shahbaz, M., Loganathan, N., Tiwari, A. K., & Sherafatian-Jahromi, R. (2015). Financial Development and Income Inequality: Is There Any Financial Kuznets Curve in Iran?. *Social Indicators Research*, 124(2), 357-382.**

**ABSTRACT:**

This paper deals with the investigation of the relationship between financial development and income inequality in case of Iran. In doing so, we have applied the ARDL bounds testing approach to examine the long-run relationship in the presence of structural break in the series. The unit root properties have been tested by applying Zivot and Andrews (in *J Bus Econ Stat* 10:251–270, 1992) and Clemente et al. (in *Econ Lett* 59, 175–182, 1998) structural break tests. The VECM Granger causality approach is used to detect the direction of the causal relationship between financial development and income inequality. Moreover, Greenwood–Jovanovich (GJ) hypothesis has also been tested for Iranian economy. Our results confirm the long run relationship between the variables. Furthermore, financial development reduces income inequality. Economic growth worsens income inequality, but inflation and globalization improve income distribution. Finally, GJ hypothesis is found as well as U-shaped relationship between globalization and income inequality in case of Iran. This study might provide new insights for policy makers to reduce income inequality by making economic growth more fruitful for poor segment of population and directing financial sector to provide access to financial resources of poor individuals at cheaper cost.

**WEB URL:** <http://link.springer.com/article/10.1007/s11205-014-0801-9>

**22. Polat, A., Shahbaz, M., Rehman, I. U., & Satti, S. L. (2015). Revisiting linkages between financial development, trade openness and economic growth in South Africa: Fresh evidence from combined cointegration test. *Quality & Quantity*, 49(2), 785-803.**

**ABSTRACT:**

This study revisits the impact of financial development on economic growth in South Africa by incorporating trade openness in the production function. The paper covers the period of 1970–2011. We apply the Bayer–Hanck combined cointegration approach to examine the long run relationship between the variables. Our results indicate that financial development stimulates economic growth. Capital use adds in economic growth but trade openness impedes economic growth. The demand-side hypothesis is validated in South Africa. This paper suggests that government should redirect trade policies to reap optimal fruits of financial development for long run economic growth.

**WEB URL:** <http://link.springer.com/article/10.1007/s11135-014-0023-x>

**23. Ahmed, K., Shahbaz, M., Qasim, A., & Long, W. (2015). The linkages between deforestation, energy and growth for environmental degradation in Pakistan. *Ecological Indicators*, 49, 95-103.**

**ABSTRACT:**

This study explores the validation of the Environmental Kuznets Curve (EKC) hypothesis for Pakistan using time series data from 1980–2013 with deforestation as an indicator (dependent variable) for environmental degradation, and four independent variables (economic growth, energy consumption, trade openness, and population) were also examined. The Autoregressive Distributed Lag (ARDL) bounds testing approach to cointegration and the VECM–Granger causality test were applied. The results confirmed the existence of cointegration among the variables both in long- and short-run paths. However, the diminishing negative impact of economic growth on deforestation in the long-run confirms the EKC hypothesis for deforestation in Pakistan. Moreover, economic growth and

energy consumption Granger cause deforestation. A bidirectional causal effect is detected between economic growth and energy consumption, however, in the long-run, economic growth and trade openness Granger cause energy consumption. This study was designed with several significant tests to ensure the reliability of results for policy use and to contribute to future studies on the environment-growth-energy nexus.

**WEB URL:** <http://www.sciencedirect.com/science/article/pii/S1470160X14004725>

**24. Solarin, S. A., & Shahbaz, M. (2015). Natural gas consumption and economic growth: The role of foreign direct investment, capital formation and trade openness in Malaysia. *Renewable and Sustainable Energy Reviews*,42, 835-845.**

**ABSTRACT:**

The objective of this paper is to reinvestigate the relationship between natural gas consumption and economic growth by including foreign direct investment, capital and trade openness in Malaysia for the period of 1971–2012. The structural break unit root test is employed to investigate the stationary properties of the series. We have applied combined cointegration test to examine the relationship between the variables in the long run. For robustness sake, the ARDL bounds testing method is also employed to test for a possible long run relationship in the presence of structural breaks. We note the validity of cointegration between the variables. Natural gas consumption, foreign direct investment, capital formation and trade openness have positive influence on economic growth in Malaysia. The results support the presence of feedback hypothesis between natural gas consumption and economic growth, foreign direct investment and economic growth, and natural gas consumption and foreign direct investment. The policy implications of these results are provided.

**WEB URL:** <http://www.sciencedirect.com/science/article/pii/S1364032114009009>

**25. Nasir, M., & Shahbaz, M. (2015). War on terror: Do military measures matter? Empirical analysis of post 9/11 period in Pakistan. *Quality & Quantity*, 49(5), 1969-1984.**

**ABSTRACT:**

This paper is the first attempt to investigate the causal relationship between military spending, terrorist attacks and intensity of terrorism in case of Pakistan, by applying the ARDL approach to cointegration and innovation accounting approach for causality analysis. The results indicate that war on terror is the major determinant of military spending followed by terrorism intensity and the number of terrorist attacks respectively. The study further finds that terrorism intensity and terrorist attacks Granger-cause military spending but the reverse is not present. The failure of military measures to curtail terrorism and its intensity induces one to suggest greater involvement of civil intelligence agencies by raising their budgets instead of pure military budget.

**WEB URL:** <http://link.springer.com/article/10.1007/s11135-014-0084-x>

**26. Al Mamun, M., Sohag, K., Uddin, G. S., & Shahbaz, M. (2015). Remittance and domestic labor productivity: evidence from remittance recipient countries. *Economic Modelling*, 47, 207-218.**

**ABSTRACT:**

For countries with significant labor force like China, India, Bangladesh, Pakistan etc. any long-run growth strategy should focus on augmenting the domestic labor productivity. The advents of globalization and factor mobility have given a recipe to reap up gains from labor abundance for most of the labor abundant countries by strategically converting abundant labor into capital. However, remittance inflow may become counterproductive strategy for growth, if it is viewed within the work–leisure framework. Using heterogeneous non-stationary panel data with cross-sectional bias this empirical study explores the best-fitted estimator to explain remittance and labor productivity dynamics for 61 top remittance recipient countries of the world. Our results suggest that though remittance has a positive impact on domestic labor productivity for countries with higher size of remittance inflow and abundant labor force; however, there is new evidence that such impact diminishes

after certain level. Moreover, such result does not hold for countries with higher remittance-share of GDP.

**WEB URL:** <http://www.sciencedirect.com/science/article/pii/S0264999315000413>

**27. Shahbaz, M., Farhani, S., & Ozturk, I. (2015). Do coal consumption and industrial development increase environmental degradation in China and India?. *Environmental Science and Pollution Research*, 22(5), 3895-3907.**

**ABSTRACT:**

The present study is aimed to explore the relationship between coal consumption, industrial production, and CO<sub>2</sub> emissions in China and India for the period of 1971–2011. The structural break unit root test and cointegrating approach have been applied. The direction of causal relationship between the variables is investigated by applying the VECM Granger causality test. Our results validate the presence of cointegration among the series in both countries. Our results also validate the existence of inverted U-shaped curve between industrial production and CO<sub>2</sub> emissions for India, but for China, it is a U-shaped relationship. Coal consumption adds in CO<sub>2</sub> emissions. The causality analysis reveals that industrial production and coal consumption Granger cause CO<sub>2</sub> emissions in India. In the case of China, the feedback effect exists between coal consumption and CO<sub>2</sub> emissions. Due to the importance of coal in China and India, any reduction in coal consumption will negatively affect their industrial value added as well as economic growth.

**WEB URL:** <http://link.springer.com/article/10.1007/s11356-014-3613-1>

**28. Kyophilavong, P., Shahbaz, M., Anwar, S., & Masood, S. (2015). The energy-growth nexus in Thailand: Does trade openness boost up energy consumption?. *Renewable and Sustainable Energy Reviews*, 46, 265-274.**

**ABSTRACT:**

The nexus between trade openness and energy demand is hot topic of discussion among academicians and researchers, and numerous studies are available in existing literature

while investigating the nexus between trade openness and energy demand. This paper explores the relationship between energy consumption, trade openness and economic growth in case of Thailand. In doing so, we have applied Bayer and Hanck cointegration approach to test whether the long run relationship exists between the variables. Our results confirm the presence of cointegration between the variables. Energy consumption stimulates economic growth. Trade openness adds in economic growth. The causality analysis reveals that energy consumption Granger causes economic growth and in resulting, economic growth Granger causes energy consumption. Trade openness and energy consumption are interdependent i.e. trade openness Granger causes energy consumption and in return, energy consumption Granger causes trade openness. This paper openness up new directions for policy making authorities in Thailand to design a comprehensive energy and trade policies to sustain economic growth for long run.

**WEB URL:** <http://www.sciencedirect.com/science/article/pii/S1364032115000921>

**29. Kandil, M., Shahbaz, M., & Nasreen, S. (2015). The interaction between globalization and financial development: new evidence from panel cointegration and causality analysis. *Empirical Economics*, 49(4), 1317-1339.**

**ABSTRACT:**

The paper studies the impact of globalization on financial development in a sample of 32 developed and developing economies over the period 1989–2012. Indicators of financial development include three banking indicators (private sector credit, domestic credit, and liquid liabilities) and three indicators of stock market development (value traded, turnover ratio, and stock market capitalization), all relevant to GDP. Two panel estimation methodologies are under consideration: panel cointegration and panel VAR. The findings reveal that financial development affects economic growth and globalization positively. Globalization helps mobilize economic growth, but does not help financial development as it helps increase access to external financing. Quality institutions do not impact financial

development although the latter increases incentives for better quality institutions in support of sustainable growth.

**WEB URL:** <http://link.springer.com/article/10.1007/s00181-015-0922-2>

**30. Khan, M., & Damalas, C. A. (2015). Factors preventing the adoption of alternatives to chemical pest control among Pakistani cotton farmers. *International Journal of Pest Management*, 61(1), 9-16.**

**ABSTRACT:**

Providing pest control solutions that are less harmful to the farmers and the environment, while maintaining effectiveness on pests is a major goal in modern crop protection. A survey of randomly selected cotton farmers from two districts of Punjab in Pakistan was conducted to study common crop protection practices and related behaviors of farmers in an attempt to identify factors preventing the adoption of alternatives to chemical pest control in the area. Almost all farmers reported using pesticides extensively as the only way of controlling pests and often by mixing two or more different pesticide products. Most farmers felt that spraying with chemicals is not only highly effective, but it is also the only viable option available at the moment. Thus, despite significant health concerns, they felt forced to use pesticides. Almost half (49%) of the farmers, irrespective of age, showed a tendency toward pesticide overuse by spraying higher quantities of pesticides than those required. To model farmers' behavior toward environmentally sound alternatives of pest control, a binary probit regression model was used expressing behavior as a function of age, education, farm size, income, risk perception levels, adverse health effects by pesticides, and training. Education and training were the main determinants of environmentally sound behavior in pest control, in the sense that high levels of education and training appeared to discourage pesticide use in the study area. In contrast, experience of health problems was not associated with behaviors toward pesticide reduction or adoption of alternative pest control practices. Additionally, governmental policies, such as the outdated extension system and the easy availability of pesticides under a non-existing or poor regulation

system, which encourage farmers to utilize pesticides, should be considered as extra major barriers in the adoption of alternative pest control practices.

**WEB URL:** <http://www.tandfonline.com/doi/abs/10.1080/09670874.2014.984257>

**31. Khan, M., Mahmood, H. Z., & Damalas, C. A. (2015). Pesticide use and risk perceptions among farmers in the cotton belt of Punjab, Pakistan. *Crop Protection*, 67, 184-190.**

**ABSTRACT:**

The need to evaluate pesticide use in rural populations, particularly in developing countries, is urgent. Pesticide use and related risk perceptions were studied among 318 randomly selected farmers from two areas of the cotton belt of Punjab, Pakistan. A total amount of 4875 kg of pesticide active ingredients was reported to be applied by the farmers per annum and most of these active ingredients were classified as moderately hazardous (55%) or highly hazardous (23%) according to WHO classification. The number of pesticide applications per growing season ranged from 6 to 16, with an average of 10 or 11 applications, depending on district. Better-educated farmers were found to spray less. Most farmers (52%) considered the risk from pesticide use to be low, whereas a solid fraction (12%) considered there was no risk at all. To model farmers' behavior on pesticide overuse, a binary probit regression model was used expressing behavior as a function of age, education, level of risk perception, health effects, pesticide toxicity class, and Integrated Pest Management (IPM) training. Irrespective of age, there was a clear tendency towards pesticide overuse, but the probability decreased with IPM training, a high level of education, and use of highly toxic pesticides. Awareness of the high toxicity of a pesticide product tended to discourage overuse. On the contrary, neither the experience of health effects nor the levels of risk perception affected overuse. Farmers were not well informed about correct application practices and safe handling of pesticides. Overall, findings affirm an urgent need for training programs on pesticide use in the study area with the aim of conveying more specific information on health hazards from pesticides that will avert hazardous behaviors of farmers derived from misleading beliefs about pesticide use.

**WEB URL:** <http://www.sciencedirect.com/science/article/pii/S0261219414003251>

**32. Khan, M., & Damalas, C. A. (2015). Occupational exposure to pesticides and resultant health problems among cotton farmers of Punjab, Pakistan. *International journal of environmental health research*, 25(5), 508-521.**

**ABSTRACT:**

Occupational exposure to pesticides and resultant health problems were assessed among 318 randomly selected cotton farmers from the two districts of Punjab, Pakistan. Heavy dependence of farmers on pesticides for pest control was reported. A large part (23.3 %) of the pesticides belonged to the category highly hazardous, whereas the largest part (54.7 %) belonged to the category moderately hazardous. Some of them (8 %) were reported to be used on vegetables. Common working practices of high exposure risk were: the confrontation of pesticide spills in the stage of spray solution preparation (76.4 %), the use of low-technology and faulty sprayers (67.9 %), and spraying under inappropriate weather (46.5 %). A large proportion (34 %) of the farmers reported multiple intoxication symptoms by pesticide use; the most common were irritation of skin and eyes, headache, and dizziness. Nevertheless, most farmers thought these symptoms were usual; only few reported visiting the doctor. Findings clearly indicated a high level of risk exposure to pesticides among farmers of the study area, calling upon immediate interventions toward increasing awareness about alternative pest control practices with less pesticide use.

**WEB URL:** <http://www.tandfonline.com/doi/abs/10.1080/09603123.2014.980781>

**33. Ling, C. H., Ahmed, K., Muhamad, R. B., & Shahbaz, M. (2015). Decomposing the trade-environment nexus for Malaysia: what do the technique, scale, composition, and comparative advantage effect indicate?. *Environmental Science and Pollution Research*, 22(24), 20131-20142.**

**ABSTRACT:**

This paper investigates the impact of trade openness on CO<sub>2</sub> emissions using time series data over the period of 1970Q1-2011Q4 for Malaysia. We disintegrate the trade effect into scale, technique, composition, and comparative advantage effects to check the environmental consequence of trade at four different transition points. To achieve the purpose, we have employed augmented Dickey-Fuller (ADF) and Phillips-Perron (PP) unit root tests in order to examine the stationary properties of the variables. Later, the long-run association among the variables is examined by applying autoregressive distributed lag (ARDL) bounds testing approach to cointegration. Our results confirm the presence of cointegration. Further, we find that scale effect has positive and technique effect has negative impact on CO<sub>2</sub> emissions after threshold income level and form inverted U-shaped relationship—hence validates the environmental Kuznets curve hypothesis. Energy consumption adds in CO<sub>2</sub> emissions. Trade openness and composite effect improve environmental quality by lowering CO<sub>2</sub> emissions. The comparative advantage effect increases CO<sub>2</sub> emissions and impairs environmental quality. The results provide the innovative approach to see the impact of trade openness in four sub-dimensions of trade liberalization. Hence, this study attributes more comprehensive policy tool for trade economists to better design environmentally sustainable trade rules and agreements.

**WEB URL:** <http://link.springer.com/article/10.1007/s11356-015-5217-9>

**34. Idrees, F., Hassan, H., & Ghauri, T. K. (2015). Study on Brand Relevance: Cross Category and Cross Gender Comparison, the Case of Pakistan. *International Journal of Economics and Empirical*. 3(5), 211-223.**

**ABSTRACT:**

Purpose: This study is done in an effort to dissect new dimensions of brand relevance with core focus on determining as to how important are brands in shaping consumer purchase behavior and influencing their decision process. Though brand relevance studies plays very considerable role in determining potential success of new product in unfavorable conditions

but still there are many areas to be unfolded yet. This study accounts for BRiC with gender perspective as its base. Methodology: Moreover it will also compares cross-category with six product categories under study in case of Pakistan. Findings: Results provide sufficient evidence in support of BRiC measures chosen for this study to do cross-category and cross gender comparisons. It is also deduced from results that gender differences, do impact on brand relevance in some categories while it might have similar impact in other. However cross categories comparison also provide evidence that in some case two independent categories might have similar impact on brand relevance however in other it can vary. Recommendations: Findings from this study will not only help managers in minimizing risk associated with brand investments but it will also help them in understanding true dynamics of market.

**WEB URL:** [http://www.tesdo.org/shared/upload/pdf/papers/IJEER,%203\\_5,%20211-223%20.pdf](http://www.tesdo.org/shared/upload/pdf/papers/IJEER,%203_5,%20211-223%20.pdf)

**35. Usman, M., Akhter, W., & Akhtar, A. (2015). Role of Board and Firm Performance in Determination of CEO Compensation: Evidence from Islamic Republic of Pakistan. *Pakistan Journal of Commerce and Social Sciences*,9(2), 641-657.**

**ABSTRACT:**

The current research aims to investigate the influence of board effectiveness and firm performance on CEO compensation within the context of developing economy of Islamic Republic of Pakistan. The study uses Partial Least Square (PLS) based Structural Equation Modeling (SEM) Technique to draw the inference using PLS Graph Version 3.0. It uses Karachi Stock Exchange (KSE)-100 index companies as a sample for the period of five years 2007-2011. Before analyzing the structural model the validity and reliability of the model is confirmed through bootstrapping technique and variance inflationary factor respectively. The structural model results reveal that board effectiveness has negative influence on CEO compensation. Opposite to agency theory and current studies from developed countries, we have found a negative association between the firm performance (firm value and firm profitability) and CEO compensation. These results are due to different business

environment of Pakistan and poor corporate governance structure. So, it is concluded that board of directors of Pakistani companies are not that much effective to facilitate the objective determination of CEO compensation and failed to design such contracts which can link the CEO pay with firm performance. Our results also support the international literature that firm size is the major determinant of CEO compensation. Most of the previous studies have been conducted with reference to developed economies so we need to know the procedure through which the corporate managers in developing economies are compensated. The unique characteristics of Pakistani business environment like concentrated ownership, family owned businesses and poor governance structure make it interesting to study this issue. Moreover, unlike developed economies the CEO compensation does not include stock options as a part of the total compensation representing the difference in CEO compensation contracts with respect to developed economies and developing economies. So, current study makes a valuable addition to the Board and Firm Performance in Determination of CEO Compensation 642 available literature by investigating the issue within the context of unique business environment of Pakistan.

**WEB URL:** <http://www.jespk.net/publications/255.pdf>

**36. Amir, H. (2015). Impact of trade liberalization on Government Revenue. *International Journal in Commerce, IT & Social Sciences*. 2(5).**

*Abstract not found*

**37. Mahmood, H. Z., Fatima, M., Khan, M., & Qamar, M. A. (2015). Islamic Microfinance and Poverty Alleviation: An Empirical Ascertainment from Pakistan. *Journal of Islamic Economics, Banking and Finance*. 11(2), 85-103.**

**ABSTRACT:**

Islamic Microfinance (IMF) is an emerging mode for empowering the poor. The current study has been devised to observe the implications of IMF on the assets and poverty status of the households who borrowed from three pioneering organizations i.e. Akhuwat

Foundation, Farz Foundation and NAYMAT based in Lahore, Punjab, Pakistan. Pre and post project approach was rendered to observe the impacts of microfinance on the targeted respondents. In this regard, purposive sampling was employed for data collection to avoid randomized error where self-administered structured questionnaires were used for data collection. Foster, Greer and Thorbecke measures of poverty assessment were used to achieve the objectives of the study. Results exhibited positive impacts of Islamic microfinance on the lives of the poor. This study is a contribution in the literature as there is no empirical study about the impact casted by the Islamic microfinance in Pakistan.

**WEB URL:** [http://ibtra.com/pdf/journal/v11\\_n2\\_article6.pdf](http://ibtra.com/pdf/journal/v11_n2_article6.pdf)

**38. Khurram, N., & Saeed, U. (2015). Factors Influencing the Intention of People to Use Islamic Banking: An Evidence from Lahore, Pakistan. *International Journal of Economics*. 3(8), 411-418.**

**ABSTRACT:**

Purpose: The purpose of this paper is to find the factors which influence the intention of Muslims of Lahore to use Islamic banking. Methodology: Therefore data was collected through distributing questionnaires. In total 220 questionnaires were distributed and 154 were collected and analysis was performed on 150 questionnaires because 4 of them were not fully filled (Return rate was around 69%). Analysis was performed by using hierarchical regression technique. Findings: Both attitude and social influence were proven significant in the initial stages of the technique but attitude proved insignificant in the later stages. Knowledge also proved significant in influencing the intention of the people. In the final stage the effect of price as a moderator is also observed. Recommendations: Policy recommendations are made on the basis of empirical results.

**WEB URL:** [http://www.tesdo.org/shared/upload/pdf/papers/IJEER,%203\\_8,%20411-418%20.pdf](http://www.tesdo.org/shared/upload/pdf/papers/IJEER,%203_8,%20411-418%20.pdf)

**39. Malik, M. E., Naeem, B., & Bano, N. (2015). Linking Workplace Spirituality to Intrinsic Work Motivation. *AL-ADWA*, 29(42).**

**ABSTRACT:**

There has been a growing interest among organizational researchers in workplace spirituality area for the last few years (1, 2, 3, 4, 5, 6). Major research work on workplace spirituality has been addressed in Western context, and little attention was devoted to study it in Eastern context (7). Organizations are now recognizing spiritual dimension at workplace which is characterized by meaningfulness in work and sense of community (8). Theoretical and empirical support is emerging, though with slow pace, on how workplace spirituality could affect positive work outcomes such as creativity, effort, job satisfaction and job performance (3, 9, 10, 11, 12, 13). However, there is dearth of literature viewing the link of workplace spirituality dimensions such as meaning at work and conditions for community to intrinsic motivation through the lens of self-determination theory in banking context of Eastern country (Pakistan). Practitioners and academics view a motivated work force as a sustainable source of competitive advantage in highly complex, competitive and dynamic work environment. Today, work motivation is considered as fundamental building block for effective management of workforce as popular motivational mantra (14). Such intrinsic work motivation stems from the work itself and positive engagement in tasks (15). Ryan and Deci define intrinsic motivation as “[A] natural inclination toward assimilation, mastery, spontaneous interest, and exploration that is so essential to cognitive and social development and that represents a principal source of enjoyment and vitality throughout life” (16). In this study, intrinsic work motivation is contended as state which can be developed and enhanced by workplace spirituality aspects such as meaning at work and conditions for community. The findings are of practical and theoretical relevance to improve not only understanding of how and to what extent workplace spirituality is related to intrinsic motivation which is critical for satisfied, committed, creative and high performing work force but also make workplace spirituality more legitimate and mainstream research area to organizational studies. Therefore, the following research question was addressed in the present study: What relationship does workplace spirituality have with banking employees’ intrinsic work motivation?

**WEB URL:** [http://pu.edu.pk/images/journal/szic/pdf\\_files/7-%20Basharat%20Naeem%20Linking%20Workplace%20Spirituality%20to%20Intrinsic%20Work%20Motivation\\_Dec%2014.pdf](http://pu.edu.pk/images/journal/szic/pdf_files/7-%20Basharat%20Naeem%20Linking%20Workplace%20Spirituality%20to%20Intrinsic%20Work%20Motivation_Dec%2014.pdf)

**40. Khan, M., Akram, N., Mahmood, H. Z., & Shaheen, F. (2015). Public Expenditure, Taxes and Economic Development: An Empirical Analysis for Pakistan. *Middle-East Journal of Scientific Research*, 23(11), 2756-2762.**

**ABSTRACT:**

The relationship between public expenditure, taxes and economic development has been extensively analyzed in literature with no consensus. This study adds to the literature as it divides public expenditure and taxes into different components to see their individual impact on economic development in case of Pakistan. Two types of regression models were estimated; in the first regression total public expenditure and taxes were used as fiscal tools while in the second model public expenditure and taxes were divided into different categories. The results show that taxes have negative effect while public expenditures have insignificant effect on development when considered in totality. However, current expenditures stimulate growth while capital expenditure has insignificant effect on growth. Indirect taxes impede development while direct taxes have insignificant effect. This suggests that development expenditures are not sufficient to put a significant impact on economic growth. Hence, there is dire need to increase developmental expenditures in Pakistan. Furthermore direct taxes should be focused more to increase revenue instead of indirect taxes.

**WEB URL:** [http://idosi.org/mejsr/mejsr23\(11\)15/21.pdf](http://idosi.org/mejsr/mejsr23(11)15/21.pdf)

**41. Rana, M. E., & Akhter, W. (2015). Performance of Islamic and conventional stock indices: empirical evidence from an emerging economy. *Financial Innovation*, 1(1), 1.**

**ABSTRACT:**

This study aims to investigate the extent to which the conditional volatilities of both Shari'ah compliant stock and conventional stock are related to those of interest rate and exchange rate in the emerging economy of Pakistan.

**Methods**

We used KMI 30 and KSE 100 indices for Islamic and conventional stock for the period of July 2008 to November 2013. We employed Generalized Autoregressive Conditional Heteroskedastic in the mean (GARCH-M) model. This framework relaxes constancy assumption of classical linear regression (CLRM) model and allows exchange rate and interest rate volatility to evolve over time. The GARCH-M framework also reveals results about risk-return trade-off in the context of both Islamic and conventional stock indices.

**Results**

The findings show positive and statistically significant effect of interest rate volatility on KSE-100, whereas KMI-30 remains unaffected by the same. Exchange rate volatility is found to be significant for both conventional and Islamic indices. The relationship of risk coefficient ( $\gamma$ ) and stocks returns, as expected, is positive and statistically significant for both KMI-30 and KSE-100. This result is consistent with the theory of risk-return trade-off. The results of parametric t-test show significant difference between returns of both indices. This implies that Shari'ah compliant stock index (KMI-30) of Pakistan underperforms its conventional counterpart.

**Conclusion**

By using different performance measures (Sharp ratio, Jensen alpha, Treynor ratio), this study also investigates the hypothesis that Islamic stock index has inferior performance compared with unscreened conventional counterparts due to availability of a smaller investment universe, increased monitoring costs, and limited diversification.

**WEB URL:** <http://jfin-swufe.springeropen.com/articles/10.1186/s40854-015-0016-3>

**42. Saeed, U., Khurram, N. (2015). Factors Influencing the Financial Performance of Non-life Insurance Companies of Pakistan. *International Journal of Empirical Finance*.4(6)354-361.**

*Abstract not found*

**43. Husnain, M. I. U., Haider, A., Salman, A., Zahid, H. M., Khan, M., & Shaheen, F. An Econometric Analysis of the Statistical Relationship between Carbon Dioxide Emissions and Infant Mortality in South Asia.**

**ABSTRACT:**

This study provides an econometric analysis of the link between infant mortality and carbon dioxide emissions in four south Asian countries-Pakistan, India, Sri Lanka and Bangladesh for the period 1978-2010 while controlling other variables, inflation, trade, remittance and rural population growth, socioeconomic characteristics of the household, that can potentially impact the number of infant deaths. Panel data technique Fixed Effect was preferred to Random Effect on the basis of Hausman test. The results show that high carbon emissions lead to higher rate of infant mortality and the link is indirect instead of direct. The different intercept show that the impact of carbon emission is higher in Bangladesh followed by India, Pakistan and Sri Lanka. Trade and remittances reduce mortality rates while rural population growth works in opposite direction. Inflation has a negative sign yet statistically not significant. The results suggest that carbon dioxide emissions must be reduced to improve infant health at least in the long run. Measures to check population growth are mandatory to overcome infant deaths. Trade and remittance increase should be ensured to improve health index of infants. However our results are suggestive and be taken with care as different other channels can reverse the results which require further research on this front

**WEB URL:**

[https://www.researchgate.net/profile/Muhammad\\_Husnain2/publication/282853235\\_An](https://www.researchgate.net/profile/Muhammad_Husnain2/publication/282853235_An)

Econometric Analysis of the Statistical Relationship between Carbon Dioxide Emissions and Infant Mortality in South Asia/links/561ebd2d08ae50795aff482c.pdf

**44. Mahmood, Z., & Mehmood, I. (2015). Economics Of Peri-Urban Radish Production And Marketing In Faisalabad. *Pakistan J. Agric. Res. Vol, 28(2)* 159-168.**

**ABSTRACT:**

This study uses primary data collected from 70 radish growing farmers selected randomly from peri-urban area of district Faisalabad, Pakistan. It was found that majority of farmers were not following recommendations of the agriculture department regarding seed rate, fertilizers, and irrigations. Majority of respondents (94.2%) reported the local Meno as the best yielding variety. Imported and 40 day varieties were not popular as only 5.8% farmers were cultivating these varieties in the study area. On the basis of survey data, benefit cost and total factor productivity analyses depict that radish cultivation is a profitable enterprise in the study area. Productivity gap between current and potential yield of radish can be minimized by the adoption of recommended production and marketing practices.

**WEB URL:** [http://www.pjar.org.pk/Issues/Vol28\\_2015No\\_2/j\\_88.pdf](http://www.pjar.org.pk/Issues/Vol28_2015No_2/j_88.pdf)

**45. Qasim, M., Hassan, S., Bashir, A., & Zahid, H. (2015). Analyzing Production Potential Of Selected Food And Legume Crops For Food Security In Punjab, Pakistan. *Pakistan Journal of Agricultural Research, 28(3)* 255-262.**

**ABSTRACT:**

The present study was designed to assess growth rate in area, yield and production of selected major food commodities and to project these parameters on the basis of estimated growth co-efficient. Time-series data for area, yield and production were collected for wheat, sugarcane, rice, mung and gram since 1980-81. The semi-log trend function was employed to find out the growth rate of selected commodities. The findings of the study showed the positive growth rates of area, production and yield of all selected food grain and legume crops. The estimated co-efficient for all growth models (area, production and

yield) of selected commodities were statistically highly significant at 1% level except yield of gram which was significant at 10% level. The estimated annual growth rate of area for wheat, rice and sugarcane was 0.9%, 2.1% and 0.8%, respectively with the production growth of 3.0%, 3.8% and 2.2%, respectively and yield growth of 2.1%, 1.6% and 1.5%, respectively. The results highlighted that the major contribution for expansion in production for rice and sugarcane was area while it was yield for wheat. In this scenario the wheat production can be enhanced by increasing its area than that of rice and sugarcane. The annual growth rate for gram and mung area was estimated about 1.0% and 4.9%, respectively, with the production growth rate of 2.3% and 6.4% while yield growth rate of 2.9% and 1.4%, respectively. Keeping in view the higher growth of gram yield the increase in its area may enhance its production more than that of mung. The proportionate higher increase in the area of wheat and gram may enhance the welfare of producers in particular and provide food security to masses in general.

**WEB URL:** [http://www.pjar.org.pk/Issues/Vol28\\_2015No\\_3/j\\_1.pdf](http://www.pjar.org.pk/Issues/Vol28_2015No_3/j_1.pdf)

**46. Kyophilavong, P., Shahbaz, M., & Uddin, G. S. (2015). A Note on Nominal and Real Devaluation in Laos. *Global Business Review*, 16(2), 236-243.**

**ABSTRACT:**

In this article, we investigate whether or not nominal devaluation leads to real devaluation in Laos by using autoregressive-distributed lag (ARDL) bounds testing and the Granger causality test in a vector error correction model (VECM) framework. Our empirical evidence shows that nominal devaluation Granger causes real devaluation in the short run and the long run. This finding implies that nominal devaluation leads to real devaluation.

**WEB URL:** <http://gbr.sagepub.com/content/16/2/236.short>

**47. Rahman, M. M., Shahbaz, M., & Farooq, A. (2015). Financial development, international trade, and economic growth in Australia: new evidence from multivariate framework analysis. *Journal of Asia-Pacific Business*, 16(1), 21-43.**

**ABSTRACT:**

This study investigates the relationship between financial development, international trade and economic growth for Australia over the period of 1965 to 2010. The autoregressive distributed lag (ARDL) bounds testing approach to cointegration is applied to examine the long-run relationship among the series, whereas stationarity properties of the variables are tested by applying two structural break tests. Results confirm the long-run relationship among the variables. Financial development, international trade, and capital appear as the drivers of economic growth in short and long runs. The feedback effect exists between international trade and economic growth. Financial development Granger causes economic growth validating supply-side hypothesis.

**WEB URL:** <http://www.tandfonline.com/doi/abs/10.1080/10599231.2015.997625>

**48. Shahbaz, M., Dube, S., Ozturk, I., & Jalil, A. (2015). Testing the environmental Kuznets curve hypothesis in Portugal. *International Journal of Energy Economics and Policy*, 5(2) 475-481.**

**ABSTRACT:**

This paper provides empirical evidence of an environmental Kuznets curve (EKC) hypothesis for Portugal by applying autoregressive distributed lag bounds testing approach from 1971 to 2008. In order to capture Portugal's historical experience, demographic changes and international trade on carbon emissions, we augment the traditional income-emissions model with variables such as energy consumption, urbanization, and trade openness in time series framework. Empirical results confirm the evidence of EKC hypothesis in both the short-run and long-run. All variables carry the expected signs except trade openness. Despite the success of Portugal in containing CO<sub>2</sub> emissions so far, it is important to note that in recent years, carbon emissions have risen. In order to comply with the 1992 Kyoto Protocol on CO<sub>2</sub> emissions, there is need for policies that focus on the sectors responsible for CO<sub>2</sub> emissions

**WEB URL:**

<http://search.proquest.com/openview/0c28739f46e22d3eb220971a2a24851a/1?pq-origsite=gscholar>

**49. Shahbaz, M., Dube, S., Ozturk, I., & Jalil, A. (2015). Testing the environmental Kuznets curve hypothesis in Portugal. *International Journal of Energy Economics and Policy*, 5(2) 475-481.**

**ABSTRACT:**

This paper provides empirical evidence of an environmental Kuznets curve (EKC) hypothesis for Portugal by applying autoregressive distributed lag bounds testing approach from 1971 to 2008. In order to capture Portugal's historical experience, demographic changes and international trade on carbon emissions, we augment the traditional income-emissions model with variables such as energy consumption, urbanization, and trade openness in time series framework. Empirical results confirm the evidence of EKC hypothesis in both the short-run and long-run. All variables carry the expected signs except trade openness. Despite the success of Portugal in containing CO<sub>2</sub> emissions so far, it is important to note that in recent years, carbon emissions have risen. In order to comply with the 1992 Kyoto Protocol on CO<sub>2</sub> emissions, there is need for policies that focus on the sectors responsible for CO<sub>2</sub> emissions

**WEB URL:**

<http://search.proquest.com/openview/0c28739f46e22d3eb220971a2a24851a/1?pq-origsite=gscholar>

**50. Naqvi, I. H., & Naveed, Z. (2015). Islamic Formula of Future Value of Asset. *European Journal of Islamic Finance*, (3). 1-9**

**ABSTRACT:**

Increasing price of an asset being sold on credit is a common practice of Islamic Financial Institutions (IFIs) and certain retailers using formulas of compound interest (*Riba*) and

speculation (*Maysir*). As Islam prohibits both these both concepts, relevant literature was qualitatively probed to find *Shariah* compliant mechanism for setting future value of an asset being sold on credit negating *Riba* and *Maysir*. The study thus extracted a formula from authentic *Shariah* sources and presented it quantitatively as an alternate to abandon the conventional formulas of interest and speculation. It further contributed recommendations for credit sellers and buyers in the light of *Shariah* principles and possible future research.

**WEB URL:** <http://www.ojs.unito.it/index.php/EJIF/article/view/1075>

**51. Amir-ud-Din, R., & Zaman, A. (2015). Failures of the “Invisible Hand”. In *Forum for Social Economics* 45(1)1-20.**

**ABSTRACT:**

Despite many failures of the invisible hand both empirically and theoretically, it continues to be vigorously asserted and widely believed. We document the failures and explain why it continues to be asserted despite these failures.

**WEB URL:** <http://www.tandfonline.com/doi/abs/10.1080/07360932.2015.1019536>

**52. Masood, S. Qamar, M. A , Aisha, A. Q. (2015). Microfinance and Disasters: Islamic Microfinance a New Paradigm to Serve the Unserved. *J. Appl. Environ. Biol. Sci.*, 5(8)7-16.**

**ABSTRACT:**

To mitigate the adverse consequences of disasters, the poor employ various formal and informal strategies. One such source is microfinance that can help the poor in early recovery from the aftermaths of covariates shocks. Study results have revealed formal financial services if available are more effective than informal financial services as their costs outweigh their benefits. Like commercial finance institutions, microfinance institutions are not willing to serve the poor during emergencies due increased default risk. In such cases, Islamic Financial services based on *Shariah* principles such as Islamic microfinance can

serve the economically active and destitute as well. For this purpose, the study also proposed model to serve the economically active and inactive people.

**WEB URL:**

[http://www.textroad.com/pdf/JAEBS/J.%20Appl.%20Environ.%20Biol.%20Sci.,%205\(8\)7-16,%202015.pdf](http://www.textroad.com/pdf/JAEBS/J.%20Appl.%20Environ.%20Biol.%20Sci.,%205(8)7-16,%202015.pdf)

**53. Amir, H., Khan, M., & Bilal, K. (2015) Impact of educated labor force on Economic growth of Pakistan: A human capital perspective. *European Online Journal of Natural and Social Sciences*, 4(4), 814-831.**

**ABSTRACT:**

A considerable body of research has concentrated on the role of human capital investment in explaining the level and variation in production and growth and it has been shown that long-term sustainable growth and development across countries is driven to a large extent by productivity growth. Most of the studies in Pakistan measure human capital by using its proxy as enrollment rate of primary, secondary and tertiary level or expenditure on education. This widespread practice has coexisted with longstanding doubts about using school enrollments as a measure of human capital since there exists a gap between school attendance and entrance into the Labor Market. Further, public expenditure on education is not enough proxy in case of Pakistan because of the fact that there is a large private education sector in the country. Taking cognizance of it, instead of using the school enrollments and public expenditure on education as a measure of human capital, this research examines the role of human capital formation described by education levels of labor force in Pakistan which is more direct measure of human capital than school enrollments and public expenditure on education. Data of educated labor force at primary secondary, tertiary and higher level is collected from Pakistan. Time series data is used from the period 1973 to 2013. The data is taken from various issues of Pakistan Economic Survey, Pakistan Labor Force Survey, Federal bureau of statistics, State Bank of Pakistan Annual reports and 50 Years statistics of Pakistan. Johnson's Cointegration, Error Correction model (ECM) and vector error correction method (VECM) Granger Causality statistical tools are

used to measure the impact of human capital on economic growth in the long run and short run. Finding shows that all proxy variables of human capital in this study have significant impact on economic growth in the long run; however, some variables are found insignificant in short run. This study concludes that education is a key determinant of Economic growth.

**WEB URL:**

[https://www.researchgate.net/profile/Hina\\_Amir/publication/287208205\\_Impact\\_of\\_educated\\_labor\\_force\\_on\\_Economic\\_growth\\_of\\_Pakistan\\_A\\_human\\_capital\\_perspective/links/5673c1e408ae04d9b09bdb66.pdf](https://www.researchgate.net/profile/Hina_Amir/publication/287208205_Impact_of_educated_labor_force_on_Economic_growth_of_Pakistan_A_human_capital_perspective/links/5673c1e408ae04d9b09bdb66.pdf)

**54. Luqman K. M., Javaid F., Umair, T. (2015). Combined Effects of Perceived Organizational Politics and Emotional Intelligence on Job Satisfaction and Counterproductive Work Behaviors. 4(4) 891-811.**

**ABSTRACT:**

With a sample of 190 employees from telecom sector of Pakistan, the authors intended to test the main effects of three dimensions of perceived organizational politics (General Political Behavior, Go Along to Get Ahead and Pay and Promotion Policies) on Employees' job satisfaction and counterproductive work behaviors. Moderating role of emotional intelligence was also examined on the politics-outcomes relationship. General Political behavior and Go along to get ahead were found to have significant negative relationship with job satisfaction and positive with counterproductive work behaviors. Pay and promotion policies and outcomes relationship could not reach statistical significance. Emotional Intelligence was positively related to job satisfaction and negatively related to counterproductive work behaviors. As hypothesized, emotional intelligence moderated the relationship between general political behavior, go along to get ahead and outcomes. Contrary to expectations, interaction for pay and promotion policies and emotional intelligence was negatively related to job satisfaction and positively related to counterproductive work behaviors.

**WEB URL:** [file:///C:/Users/sahmed/Downloads/2968-8641-1-PB%20\(1\).pdf](file:///C:/Users/sahmed/Downloads/2968-8641-1-PB%20(1).pdf)

55. Javaid, M. F., Luqman, K., Amir, H., & Umair, T. (2015). Authentic leadership affects employee's attitudes (Affective Commitment) through the mediation role of Personal Identification and Organizational Identification. *International Journal of Academic Research in Business and Social Sciences*, 5(12), 215-231.

**ABSTRACT:**

In Current study author has examined the influence of authentic leadership on organizational affective commitment and to explore that to what extent the followers' social identification with work unit and personal identification with leaders mediate this relationship. However these hypothesized outcomes gained very little attention in empirical studies. The quantitative methodology used in this study incorporates cross sectional survey method with sample size is (N=250). Sample was selected from Pakistani local and foreign banks' employees who work under the branch manager. Author found a positive relationship between authentic leadership and organizational affective commitment and both personal identification with leader and social identification with work unit significantly mediate the afore-mentioned relationship. Structural equation model was used for data analysis and hypothesis testing. Keywords: Authentic Leadership, Employee's Attitudes, Personal Identification and Organizational Identification.

**WEB URL:**

[http://hrmars.com/hrmars\\_papers/Authentic\\_leadership\\_affects\\_employee%E2%80%99s\\_attitudes\\_\(Affective\\_Commitment\)\\_through\\_the\\_mediation\\_role\\_of\\_Personal\\_Identification\\_and\\_Organizational\\_Identification.pdf](http://hrmars.com/hrmars_papers/Authentic_leadership_affects_employee%E2%80%99s_attitudes_(Affective_Commitment)_through_the_mediation_role_of_Personal_Identification_and_Organizational_Identification.pdf)

56. Khan, A. M., Sadiq, M. W., & Naqvi, S. M. I. H. (2015). Effect of Ostracism and General Education on Career Development under Mediation of Personality: A Study of Religious Schools in Pakistan. *European Online Journal of Natural and Social Sciences*, 4(3), 582.

**ABSTRACT:**

How ostracism affects personality and career development of the students in recognized religious schools (Madrassas) in Pakistan? How general education averts ostracism and

improves personality and career development in Madrassas? How all these variables are associated? It was significant finding answers to these questions as yet in literature the mentioned variables are considered separate constructs whereas this study observed them interplaying in 4 recognized Madrassas. The study collected data from a simple random sample of size 280 protégés using reliable and valid instrument. Data analyses were conducted using Pearson's correlation, regression and mediation test. Ostracism played positive role both on personality and career development while general education was lagging behind against expectation. Study recommended rational improvements, direction for future research expressing its limitations.

**WEB URL:**

<http://search.proquest.com/openview/3a930a0a4efd9acff2a7e7745ae938a4/1?pq-origsite=gscholar>

**57. Bodla, M. A., Afza, T., Ali, H., & Naeem, B. (2015). Role of Psychological Sense of Community in Enhancing Employee's Well-Being. *European Online Journal of Natural and Social Sciences*, 4(2), 256.**

**ABSTRACT:**

Yearning for sense of community is in part fostered by decline of traditional place of community due to which people feel less satisfied at workplace. Thus drawing on psychological sense of community theory, this paper is going to focus on relationship between employee's sense of community and life satisfaction; a critical, yet under research relationship. Using regression analysis, it was found that if employees are provided with sense of community at workplace, then they are satisfied with their life.

**WEB URL:**

<http://search.proquest.com/openview/08f5ecfd4eaaa9dc9f65d38d8f92bcdd/1?pq-origsite=gscholar>

**58. Khan, A. M., Nazeer, S. U., & Naqvi, S. M. I. H. (2015). Personality Mediated Career Development under Islamic Work Ethics in Pakistani Religious Schools. *European Online Journal of Natural and Social Sciences*, 4(4), 691.**

**ABSTRACT:**

Religious schools known as Madrassas in Pakistan contribute significant human resource development (HRD) to the society enabling career development (CD) of protégés under Islamic work ethics (IWE). Yet the impact of IWE on CD and protégés' personalities in recognized and well reputed Madrassas need elaboration. This study hypothesized that personality mediates the relationship between IWE and CD. It collected data employing stratified random sampling for 280 final year protégés in the Madrassas from Lahore, Pakistan. Data was analyzed using Pearson's correlation, linear regression and Baron and Kenny test. Results confirmed full mediation of personality among IWE and CD and also the direct correlation of IWE as a significant determinant of CD in the selected context. While results of this study remained akin to various studies describing CD for business organizations it contributed value adding role of IWE in CD of religious human resource.

**WEB URL:**

<http://search.proquest.com/openview/540a2ed42b6729ef9f9cfde41126bde9/1?pq-origsite=gscholar&cbl=2029677>

**59. Afza, T., Ehsan, S., & Nazir, S. (2015). Whether Companies Need to be Concerned about Corporate Social Responsibility for their Financial Performance or Not? A Perspective of Agency and Stakeholder Theories. *European Online Journal of Natural and Social Sciences*, 4(4), 664-682.**

**ABSTRACT:**

Present study used the theoretical framework of both the Agency and Stakeholder theories in order to empirically investigate the importance of Corporate Social Responsibility (CSR) for the financial performance (FP) of firm both in the short and long run. According to the agency theory approach core motive of the company's existence is to maximize their

owner's wealth and therefore spending on other stakeholders in the form of CSR is an additional cost that leads to decrease in the FP. Contrary to this, Stakeholder theory argues that firms should satisfy the social needs of various stakeholders and perform CSR as it protects the firm from negative confrontations and boycotts of their stakeholders that reduces the operating cost and boosts the financial performance. A sample of 76 Pakistani manufacturing firms listed at Karachi Stock Exchange has been used for the time period ranged from 2009-2012. A series of tests like F-test, LM-test and Hausman-test have been applied to identify optimum panel data model and Random model found to be the appropriate one. Results of Generalized Least Square Regression results revealed that CSR has a positive impact not only on the short term financial performance of Pakistani manufacturing firms but also helped them to maintain the sustainable long term financial performance.

**WEB URL:**

<http://search.proquest.com/openview/f9b7817805143bc99c44bce2cf4b6d81/1?pq-origsite=gscholar&cbl=2029677>

**60. Afza, T., & Nazir, M. S. (2015). Role of Institutional Shareholders' Activism in Enhancing Firm Performance: The Case of Pakistan. *Global Business Review*, 16(4), 557-570.**

**ABSTRACT:**

Globalization and financial breakdown of many corporate conglomerates in the developed world engrossed the attention of researchers and policy makers towards the need and importance of an effective corporate governance system for resolving the agency conflict between the stakeholders and managers, and hence a firms' success. Among corporate governance mechanisms, how ownership is structured between all the shareholders of a firm is considered to be of much importance. The purpose of this article is two-fold: first, to analyze the impact of institutional ownership on firm performance and, second, to throw some light on the two scenarios of institutional ownership prevailing in Pakistan's capital market. In the first scenario, financial institutions have a board representation (active

financial institutions), while in the second scenario, financial institutions do not have board representation (passive financial institutions). Using the data of 200 non-financial Pakistani firms listed at the Karachi Stock Exchange (KSE) from 2005 to 2011, the results revealed that institutional ownership significantly impacts a firms' performance. It is also found that the firm performance can be enhanced through effective monitoring by active financial institutions that have long-term stakes in firms through board nomination.

**WEB URL:** <http://gbr.sagepub.com/content/16/4/557.short>

**61. Usman, M., Malik, S., & Imran, A. (2015). How has Outsourcing Human Resource (HR) Services within National Health Services (NHS) Impacted upon Staff Turnover and Wider Local Economy in UK?. *European Online Journal of Natural and Social Sciences*, 4(3), 438-443.**

**ABSTRACT:**

This paper critically investigates how outsourcing human resource (HR) services within National Health Services (NHS) have affected staff turnover and wider local economy of UK. Interviews were structured with the view to investigate this issue. The research shows that despite the pressure of outsourcing by Department of Health (DoH), NHS acute trusts are reluctant to outsource their HR functions. Those who outsourced have done this with some strategic planning. Reverse trend of outsourcing has also been observed. Outsourcing HR functions have not lost as many jobs as it was expected. No direct relationship was observed in the wider local economy and outsourcing in NHS trusts. According to findings of the research HR outsourcing has not drastic effects on wider local economy if observed on small scale.

**WEB URL:**

<http://search.proquest.com/openview/d3c61e0a2e12bcb99f7d93a75926a173/1?pq-origsite=gscholar>

**62. Basharat, B., Hudon, M., & Nawaz, A. (2015). Does efficiency lead to lower prices? A new perspective from microfinance interest rates. *Strategic Change*, 24(1), 49-66.**

**ABSTRACT:**

Pricing is a central strategic decision for all companies, and is particularly sensitive for social enterprises with both financial and social objectives. High interest rates in microfinance are a topic of intense debate. Using an original database of 291 MFIs, this paper provides empirical evidence of the impact the efficiency of an MFI has on its microcredit interest rate. We use the non-parametric Data Envelopment Analysis (DEA) framework to calculate efficiency and differentiate financial and social efficiency. The results show that financial efficiency has a positive impact on interest rates, with more financially efficient MFIs having lower interest rates, while social efficiency has no impact on microcredit interest rates.

**WEB URL:** <http://onlinelibrary.wiley.com/doi/10.1002/jsc.1997/abstract>

**63. Bodla, M. A., Afza, T., & Danish, R. Q. (2015). Perceived Organizational Politics and Employee Morale: Mediating Role of Social Exchange Perceptions in Pakistani Organizations. *European Online Journal of Natural and Social Sciences*, 4(1), 66-75.**

**ABSTRACT:**

Politics in organizations is an important aspect of organizational life which has been an interesting research area since last four decades. However, it is still deprived of practical approach due to its inconclusive studies and fragmented arguments. In politicized organizations, morale and motivation of employees depend mostly on their type of exchange relationships. The study in hand is another effort to view these exchange perceptions as intervening between the relationship of perceptions of organizational politics and morale of employees. As a part of larger study, data was collected through self administered questionnaire distributed among master of business administration students who were completing their management degree as part time along with their jobs during day time. All the Pakistani business schools were included in this study and surveys were distributed to 2000 employees during their classes and participation was voluntary ensuring anonymity and compliance with ethical considerations. Overall, 2000 questionnaires were distributed among which 1163 useable surveys were returned after screening and cleaning

for unengaged response, left over pages and missing critical information. Thus response rate was 58%. Results of regression analysis indicated that social exchange perceptions was partial mediators in the relationship between perceptions of organizational politics and employee morale and about 70% of the total effect was mediated by these perceptions which was an important indicator for understanding organizational life. Practical policy implications have also been discussed in discussion sections along with limitation of the study and guidelines for future research.

**WEB URL:**

<http://search.proquest.com/openview/e9d4a4d065b470d54269530cc6b1fe5b/1?pq-origsite=gscholar>

**64. Mirza, H. H., Afza, T., & Shahbaz, M. Q.(2015). Ownership Structure And Dividend Policy: Evidence From South Asia. *Vidyabharati International Interdisciplinary Research Journal* 3(2) 13-23.**

**ABSTRACT:**

Cash dividend is among the most important sources of cash flow for the shareholders through which they gauge firm's performance. Corporate managers also use dividends to signal company's financial strength to attract potential investors. Empirical findings on determinants of dividend policy provide mixed and inconclusive results which has made the whole issue a "puzzle" as described by Black (1976), whose pieces do not fit together. Allen et. al. (2000) argued the dividend problem as one of the thorniest puzzles in corporate finance. The present study investigates the relationship between managers' ownership and dividend policy in emerging economies of South Asia. The data of listed non-financial companies is collected from Bangladesh, India, Pakistan and Sri Lanka and analyzed with least square and Tobit regression models during the period 2006-2010. It is found that managers' ownership is significantly and positively related with dividend payout in Bangladesh and India but negatively related in Pakistan and Sri Lanka.

**WEB URL:** <http://viirj.org/vol3issue2/3.pdf>

**65. Afza, T., & Alam, A.(2015) Foreign currency derivatives: hedging or speculation. Vidyabharati International Interdisciplinary Research Journal 3(2) 24-34.**

***ABSTRACT:***

Asian financial Crises, at one end, if increase the usage of Foreign Currency Derivative (FCD) instruments to hedge exchange rate (ER) exposure, then on the other end, extensive usage of derivative instruments exposes firms to more financial risk, due to speculation. This highlights the academicians concern regarding the relationship between FCD usage and firm's risk in both developed and developing countries. Current study contributes in existing literature, by examining the effect of FCD usage on firm's risk, controlling firm-specific factors, by employing sample data of Malaysian non-financial firms. Empirical findings report that Malaysian firms are using FCD instruments for hedging purposes as its usage minimizes variability in the firm's operating cash flows. While, detailed analysis illustrates that firm's having no Foreign exchange (FX) exposure are using financial hedging instruments along with operational hedging in order to reduce firm's risk in contrast to firms having FX exposure. The findings are robust to alternative specifications like endogeneity and self-selection problem. JEL Classification: F3, G1, G150c.

***WEB URL:*** <http://viirj.org/vol3issue2/4.pdf>

# DEPARTMENT OF MATHEMATICS

## Journal Papers

1. Akram, M., Farooq, A., Saeid, A. B., & Shum, K. P. (2015). Certain types of vague cycles and vague trees. *Journal of Intelligent & Fuzzy Systems*, 28(2), 621-631.

**ABSTRACT:**

Fuzzy models are becoming useful because of their aim of reducing the differences between the traditional numerical models used in engineering and sciences and the symbolic models used in expert systems. A vague graph is a generalized structure of a fuzzy graph that gives more precision, flexibility, and compatibility to a system when compared with systems that are designed using fuzzy graphs. In this paper, we introduce various types of vague bridges, vague cut-vertices, vague cycles and vague trees in vague graphs, and investigate some of their interesting properties. Most of these various types are defined in terms of levels. We also describe comparison of these types.

**WEB URL:** <http://content.iospress.com/articles/journal-of-intelligent-and-fuzzy-systems/ifs1344>

2. Kerre, E., & Ashraf, S. (2015). Group Decision Making by Using Incomplete Fuzzy Preference Relations Based on T-Consistency and the Order Consistency. *International Journal of Intelligent Systems*, 30(2), 120-143.

**ABSTRACT:**

The existing group decision making techniques may not satisfy the order consistency for aggregation in some cases. The algorithm proposed in this paper overcomes the weaknesses of the existing techniques. The method determines the unknown preferences for group decision making in such a manner that the resulting matrix is T-consistent and order consistent simultaneously.

**WEB URL:** <http://onlinelibrary.wiley.com/doi/10.1002/int.21691/pdf>

**3. Noureen, I., & Zubair, M. (2015). On dynamical instability of spherical star in  $f(R, T)$  gravity. *Astrophysics and Space Science*, 356(1), 103-110.**

**ABSTRACT:**

This work is based on stability analysis of spherically symmetric collapsing star surrounding in locally anisotropic environment in  $f(R, T)$  gravity, where  $R$  is Ricci scalar and  $T$  corresponds to the trace of energy momentum tensor. Field equations and dynamical equations are presented in the context of  $f(R, T)$  gravity. Perturbation scheme is employed on dynamical equations to find the collapse equation. Furthermore, condition on adiabatic index  $\Gamma$  is constructed for Newtonian and post-Newtonian eras to address instability problem. Some constraints on physical quantities are imposed to maintain stable stellar configuration. The results in this work are in accordance with  $f(R)$  gravity for specific case.

**WEB URL:** <http://link.springer.com/article/10.1007/s10509-014-2202-6>

**4. Zubair, M., & Waheed, S. (2015). Energy conditions in  $f(T)$  gravity with non-minimal torsion-matter coupling. *Astrophysics and Space Science*, 355(2), 361-369.**

**ABSTRACT:**

The present paper examines the validity of energy bounds in a modified theory of gravity involving non-minimal coupling of torsion scalar and perfect fluid matter. In this respect, we formulate the general inequalities of energy conditions by assuming the flat FRW universe. For the application of these bounds, we particularly focus on two specific models that are recently proposed in literature and also choose the power law cosmology. We find the feasible constraints on the involved free parameters and evaluate their possible ranges graphically for the consistency of these energy bounds.

**WEB URL:** <http://link.springer.com/article/10.1007/s10509-014-2181-7>

5. Jawad, A. (2015). Cosmological reconstruction of pilgrim dark energy model in  $f(T, T_G)$  gravity. *Astrophysics and Space Science*, 356(1), 119-127.

**ABSTRACT:**

In this paper, we study  $f(T, T_G)$  gravity in FRW spacetime taking into account correspondence scheme. For this purpose, we assume pilgrim dark energy model with event horizon as infrared cutoff. We construct  $f(T, T_G)$  model to analyze the behavior of the model as well as evolution trajectories of some cosmological parameters. That is, we study equation of state parameter, squared speed of sound and  $w_{PDE} - w'_{PDE}$  analysis taking into account two cases of model parameter. The equation of state parameter in this scenario shows consistency with pilgrim dark energy phenomenon with quintom behavior. The squared speed of sound exhibits stability and instability of the model corresponding to model parameter. We also attain the thawing and freezing regions as well as  $\Lambda$ CDM limits through  $w_{PDE} - w'_{PDE}$  plane. Also, we construct a solution by taking  $\Lambda$ CDM model in underlying gravity.

**WEB URL:** <http://link.springer.com/article/10.1007/s10509-014-2191-5>

6. Arshad, S., Sohail, A., & Javed, S. (2015). Dynamical Study of Fractional Order Tumor Model. *International Journal of Computational Methods*, 12(05), 1550032.

**ABSTRACT:**

In this paper, we have studied the fractional order model of tumor cells growth and their interactions with general immune effector cells, by using multi-step generalized differential transform method (MSGDTM). We discussed this nonlinear model because it differs from most others in the literature. It takes into account (i) the infiltration of the tumor by CTLs (cytotoxic T lymphocytes) and (ii) the possible effects of effector cell inactivation. The approximate solutions obtained by MSGDTM are highly accurate and valid for a longer period of time.

**WEB URL:** <http://www.worldscientific.com/doi/abs/10.1142/S0219876215500322>

7. Tomescu, I., & Javed, S. (2015). Extremal bicyclic 3-chromatic graphs. *Graphs and Combinatorics*, 31(4), 1043-1052.

**ABSTRACT:**

A partial order relation in the set  $G(n,k)$  of graphs of order  $n$  and chromatic number  $k$  can be defined as follows: Let  $G$  and  $H$  be two graphs in  $G(n,k)$ .  $G$  is said to be less than  $H$  if  $c_i(G) \leq c_i(H)$  holds for every  $i$ ,  $k \leq i \leq n$  and at least one inequality is strict, where  $c_i(G)$  denotes the number of  $i$ -color partitions of  $G$ . These numbers are the coefficients of the chromatic polynomial in factorial form. In (J Graph Theory 43:210–222, 2003) the first  $\lfloor n/2 \rfloor$  levels of the diagram of the partially ordered set of connected 3-chromatic graphs of order  $n$  were described. In this paper the previous work is continued and a description of the  $(\lfloor n/2 \rfloor + 1)$ -st level is given; it contains  $n/2 + 1$  bicyclic graphs for even  $n$  and  $(n-1)/2$  bicyclic graphs for odd  $n$ . Some consequences concerning ordering chromatic polynomials of these graphs are deduced.

**WEB URL:** <http://link.springer.com/article/10.1007/s00373-014-1421-5>

8. Rizvi, S. T. R., Khalid, M., Ali, K., Miller, M., & Ryan, J. (2015). On cycle-supermagicness of subdivided graphs. *Bulletin of the Australian Mathematical Society*, 92(01), 11-18.

**ABSTRACT:**

Lladó and Moragas ['Cycle-magic graphs', *Discrete Math.* 307 (2007), 2925–2933] showed the cyclic-magic and cyclic-supermagic behaviour of several classes of connected graphs. They discussed cycle-magic labellings of subdivided wheels and friendship graphs, but there are no further results on cycle-magic labellings of other families of subdivided graphs. In this paper, we find cycle-magic labellings for subdivided graphs. We show that if a graph has a cycle-(super)magic labelling, then its uniform subdivided graph also has a cycle-(super)magic labelling. We also discuss some cycle-supermagic labellings for nonuniform subdivided fans and triangular ladders.

**WEB URL:**

<http://journals.cambridge.org/action/displayAbstract?fromPage=online&aid=9821100&fileId=S0004972715000325>

9. Anwar, I., & Raza, Z. (2015). Quasi-linear Quotients and Shellability of Pure Simplicial Complexes. *Communications in Algebra*, 43(11), 4698-4704.

**ABSTRACT:**

For a square-free monomial ideal  $I \subset S = k[x_1, x_2, \dots, x_n]$ , we introduce the notion of *quasi-linear quotients*. By using the *quasi-linear quotients*, we give a new algebraic criterion for the *shellability* of a pure simplicial complex  $\Delta$  over  $[n]$ . Also, we provide a new criterion for the Cohen–Macaulayness of the face ring of a pure simplicial complex  $\Delta$ . Moreover, we show that the face ring of the spanning simplicial complex (defined in [2]) of an  $r$ -cyclic graph is Cohen–Macaulay.

**WEB URL:** <http://www.tandfonline.com/doi/abs/10.1080/00927872.2014.937952>

10. Anwar, I., Raza, Z., & Kashif, A. (2015, December). Spanning simplicial complexes of uni-cyclic graphs. In *Algebra Colloquium* 22(04)707-710.

**ABSTRACT:**

In this paper, we introduce the concept of the spanning simplicial complex  $\Delta_s(G)$  associated to a simple finite connected graph  $G$ . We characterize all spanning trees of the uni-cyclic graph  $U_{n,m}$ . In particular, we give a formula for computing the Hilbert series and  $h$ -vector of the Stanley-Reisner ring  $k[\Delta_s(U_{n,m})]$ . Finally, we prove that the spanning simplicial complex  $\Delta_s(U_{n,m})$  is shifted and hence is shellable.

**WEB URL:** <http://www.worldscientific.com/doi/abs/10.1142/S1005386715000590>

11. Ali, K., Hussain, M., Shaker, H., & Javaid, M. (2015). Super edge-magic total labeling of subdivided stars. *Ars Combin*, 120, 161-167.

**ABSTRACT:**

An edge-magic total labeling of a graph  $G$  is a one-to-one map  $\lambda$  from  $V(G) \cup E(G)$  onto the integers  $\{1, 2, \dots, |V(G) \cup E(G)|\}$  with the property that, there is an integer

constant  $c$  such that  $\lambda(x) + \lambda(x, y) + \lambda(y) = c$  for any  $(x, y) \in E(G)$ . If  $\lambda(V(G)) = \{1, 2, \dots, |V(G)|\}$  then edge-magic total labeling is called super edgemagic total labeling. In this paper, we formulate super edge-magic total labeling on subdivision of stars  $K_{1,p}$ , for  $p \geq 5$ .

**WEB URL:** <http://www.ciitlahore.edu.pk/Papers/64-8589042556987588308.pdf>

**12. Nadeem, M. F., Zafar, S., & Zahid, Z. (2015). On certain topological indices of the line graph of subdivision graphs. *Applied Mathematics and Computation*, 271, 790-794.**

**ABSTRACT:**

In QSAR/QSPR study, topological indices such as Shultz index, generalized Randic index, Zagreb index, general sum-connectivity index, atom-bond connectivity (ABC) index and geometric-arithmetic (GA) index are utilized to guess the bioactivity of chemical compounds. A topological index in fact relates a chemical structure with a numeric number. Graph theory has established a significant use in this area of research. In this paper we computed  $ABC_4$  and  $GA_5$  indices of the line graph of tadpole, wheel and ladder graphs using the notion of subdivision.

**WEB URL:** <http://www.sciencedirect.com/science/article/pii/S0096300315012990>

**13. Butt, S. I., & Khan, K. A.(2015) Popoviciu Type Inequalities Via Green Function And Generalized Montgomery Identity. *Mathematical Inequalities & Applications*.18(4), 1519-1538.**

**ABSTRACT:**

We obtained useful identities via generalized Montgomery identity, by which the inequality of Popoviciu for convex functions is generalized for higher order convex functions. We investigate the bounds for the identities related to the generalization of the Popoviciu inequality using inequalities for the Cebysev functional. Some results relating to the Grüss and Ostrowski type inequalities are constructed. Further, we also construct new families of exponentially convex functions and Cauchy-type means by looking at linear functionals associated with the obtained inequalities.

**WEB URL:** <http://files.ele-math.com/abstracts/mia-18-118-abs.pdf>

**14. Ali, K., Tomescu, I., & Javaid, I. (2015) On path-sunflower Ramsey numbers. *Mathematical Reports. 17(67)/4. 385-390.***

**ABSTRACT:**

For given graphs  $G$  and  $H$ , the Ramsey number  $R(G, H)$  is the least natural number  $n$  such that for every graph  $F$  of order  $n$  the following condition holds: either  $F$  contains  $G$  or the complement of  $F$  contains  $H$ . In this paper, we determine the Ramsey number of path  $P_n$  versus sunflower graph  $SF_m$  when  $n$  grows at least as a quadratic function of  $m$ . In this case  $R(P_n, SF_m) = 3n-2$  if  $m$  is odd and  $2n + m - 2$  otherwise.

**WEB URL:**

[https://www.researchgate.net/profile/Imran\\_Javid/publication/264553547\\_On\\_path-sunflower\\_Ramsey\\_numbers/links/53e5f7470cf25d674e9c496a.pdf](https://www.researchgate.net/profile/Imran_Javid/publication/264553547_On_path-sunflower_Ramsey_numbers/links/53e5f7470cf25d674e9c496a.pdf).

**15. Sohail, A., Uddin, M. J., & Rashidi, M. M. (2015). Numerical Study of Free Convective Flow of a Nanofluid over a Chemically Reactive Porous Flat Vertical Plate with a Second-Order Slip Model. *Journal of Aerospace Engineering, 04015047.***

**ABSTRACT:**

Mathematical model for free convective boundary-layer flow of a nanofluid with second-order velocity slip over a permeable vertical flat plate has been presented. The system of governing equations is first nondimensionalized, and then similarity transformations are used to convert the governing partial differential equations into a set of coupled ordinary differential equations. A numerical algorithm is applied to this boundary value problem (BVP) of coupled ordinary differential equations. Collocation method is used for the solution of the nonlinear ordinary BVP. The dimensionless analysis revealed that the dimensionless field variables (velocity, temperature, and nanoparticle volume fraction), and the flow characteristics (skin friction factor, heat transfer, and nanoparticle volume fraction transfer) in the respective boundary layers depend on the Prandtl number ( $Pr$ ), the Lewis numbers ( $Le$ ), the thermophoresis parameter ( $N_t$ ), the Brownian motion parameter ( $N_b$ ), the buoyancy ratio parameter

(Nr), the convective parameter ( $\gamma\gamma$ ), the reaction parameter (KK), first-order velocity slip parameter (aa), and second-order velocity slip parameter (bb). Flow field and physical quantities strongly depend on the governing parameters. The present problem has applications in nanofluid synthesis for medicine. A tabular validation of the present numerical approach with the existing results in the literature is provided as a limiting case.

**WEB URL:** <http://ascelibrary.org/doi/abs/10.1061/%28ASCE%29AS.1943-5525.0000544>

**16. Younis, M., Rizvi, S. T. R., Mahmood, S. A., Guzman, J. V., Zhou, Q., Biswas, A., & Belic, M. (2015). Optical solitons in dual-core fibers with inter-modal dispersion. *Optoelectronics And Advanced Materials-Rapid Communications*, 9(9-10), 1126-1134.**

**ABSTRACT:**

This paper obtains optical 1-soliton solutions in dual-core fibers with inter modal dispersion. These solitons are constructed with two types of nonlinearities namely, Kerr law and power law by the aid of ansatz approach. Additionally, the constraint conditions, for the existence of the soliton solutions are listed.

**WEB URL:**

[https://www.researchgate.net/profile/Milivoj\\_Belic/publication/283053789\\_Optical\\_solitons\\_in\\_dual-core\\_fibers\\_with\\_inter-modal\\_dispersion/links/564acf7508ae295f644ffc45.pdf](https://www.researchgate.net/profile/Milivoj_Belic/publication/283053789_Optical_solitons_in_dual-core_fibers_with_inter-modal_dispersion/links/564acf7508ae295f644ffc45.pdf)

**17. Jawad, A. (2015). Analysis of dark energy models in DGP braneworld. *Astrophysics and Space Science*, 360(2), 1-11.**

**ABSTRACT:**

In this paper, we reconsider the accelerated expansion phenomenon in the DGP braneworld scenario which leads to an accelerated universe without cosmological constant or other form of dark energy for the positive branch ( $\epsilon=+1$ ) which is not more attractive model. Thus, we assume the DGP braneworld scenario with ( $\epsilon=-1$ ) and also interacting Hubble and event horizons pilgrim dark energy models. We extract

various cosmological parameters in this scenario and displayed our results with respect to redshift parameter. It is found that the ranges of Hubble parameter are coincided with observational results. The equation of state parameter lies within the suggested ranges of different observational schemes. The squared speed of sound shows stability for all present models in DGP braneworld scenario. The  $\omega_{\vartheta}-\omega'_{\vartheta}$  planes lie in the range ( $\omega_{\vartheta}=-1.13+0.24-0.25, \omega'_{\vartheta}<1.32$ ) which has been obtained through different observational schemes. It is remarked that our results of various cosmological parameters shows consistency with different observational data like Planck, WP, BAO, H0H0 and SNLS.

**WEB URL:** <http://link.springer.com/article/10.1007/s10509-015-2569-z>

**18. Jawad, A., Rani, S., & Chattopadhyay, S. (2015). Modified QCD ghost f (T, T G) gravity. *Astrophysics and Space Science*, 360(2), 1-7.**

**ABSTRACT:**

In this paper, we explore the reconstruction scenario of modified QCD ghost dark energy model and newly proposed  $f(T,TG)f(T,TG)$  gravity in flat FRW universe. We consider the well-known assumption of scale factor, i.e., power law form. We construct the  $f(T,TG)f(T,TG)$  model and discuss its cosmological consequences through various cosmological parameters such as equation of state parameter, squared speed of sound and  $\omega_{DE}-\omega'_{DE}$ . The equation of state parameter provides the quintom-like behavior of the universe. The squared speed of sound exhibits the stability of model in the later time. Also,  $\omega_{DE}-\omega'_{DE}$  corresponds to freezing as well as thawing regions. It is also interesting to remark here that the results of equation of state parameter and  $\omega_{DE}-\omega'_{DE}$  coincide with the observational data.

**WEB URL:** <http://link.springer.com/article/10.1007/s10509-015-2548-4>

**19. Jawad, A., & Rani, S. (2015). Dynamical instability of shear-free collapsing star in extended teleparallel gravity. *The European Physical Journal C*, 75(11), 1-9.**

**ABSTRACT:**

We study the spherically symmetric collapsing star in terms of dynamical instability. We take the framework of extended teleparallel gravity with a non-diagonal tetrad, a power-law form of the model presenting torsion and a matter distribution as a non-dissipative anisotropic fluid. The vanishing shear scalar condition is adopted to gain insight in a collapsing star. We apply a first order linear perturbation scheme to the metric, the matter, and  $f(T)$  functions. The dynamical equations are formulated under this perturbation scheme to develop collapsing equation for finding dynamical instability limits in two regimes, such as the Newtonian and the post-Newtonian regime. We obtain a constraint-free solution of a perturbed time dependent part with the help of a vanishing shear scalar. The adiabatic index exhibits the instability ranges through the second dynamical equation which depend on physical quantities such as the density, the pressure components, the perturbed parts of the symmetry of the star, etc. We also develop some constraints on the positivity of these quantities and obtain instability ranges to satisfy the dynamical instability condition.

**WEB URL:** <http://link.springer.com/article/10.1140/epjc/s10052-015-3748-3>

**20. Chattopadhyay, S., Jawad, A., Rani, S. (2015) Holographic Polytopic  $f(T)$ -Gravity Models. *Advances in High Energy Physics*.798902.**

*Abstract not found*

**21. Jawad, A., Debnath, U., & Batool, F. (2015). Generalized Ghost Pilgrim Scalar Field Models of Dark Energy. *Communications in Theoretical Physics*, 64(5), 590.**

**ABSTRACT:**

We assume generalized ghost Pilgrim dark energy (GGPDE) model in the presence of cold dark matter in flat FRW universe. With suitable choice of interaction term between GGPDE and cold dark matter, we investigate the nature of equation of state parameter for GGPDE. Also, we investigate the natures of dynamical scalar field models (such as quintessence, tachyon, k-essence, and dilaton dark energy) and concerned potentials through the correspondence phenomenon between GGPDE and these models.

**WEB URL:** <http://iopscience.iop.org/article/10.1088/0253-6102/64/5/590/meta>

**22. Jawad, A., & Rani, S. (2015). Reconstruction of generalized ghost pilgrim dark energy in  $F(\tilde{R})$  gravity. *Astrophysics and Space Science*, 359(1), 1-11.**

**ABSTRACT:**

In this paper, we study the reconstruction scenario of a dark energy model in the framework of modified Horava-Lifshitz  $F(R)F(R)$  gravity or  $F(\tilde{R})F(\tilde{R})$  gravity. We assume generalized ghost pilgrim dark energy model in flat universe. We consider three well-known scale factors to analyze the behavior of reconstructed  $F(\tilde{R})F(\tilde{R})$  model. These scale factors include bouncing and intermediate scale factors as well as scale factor representing the unification of matter and accelerated phases. The graphical representation is adopted to analyze the behavior of reconstructed model and equation of state parameter for different values of model parameter. The reconstructed model represents increasing and decreasing behavior with respect to time in all cases. The equation of state parameter represents phantom-like universe after transition for intermediate scale factor while quintessence behavior for bouncing and unified scale factors. We also found that the squared speed of sound exhibits the stability of all reconstructed models.

**WEB URL:** <http://link.springer.com/article/10.1007/s10509-015-2477-2>

**23. Sharif, M., & Jawad, A. (2015). Thermodynamics with Entropy Corrections in a Kaluza-Klein Universe. *Chinese Journal of Physics*, 53(6), 110112-1.**

Abstract: not found

**24. Zubair, M., & Waheed, S. (2015). Thermodynamic study in modified  $f(T)$  gravity with cosmological constant regime. *Astrophysics and Space Science*, 360(2), 1-9.**

**ABSTRACT:**

This study is conducted to examine the validity of thermodynamical laws in a modified  $f(T)f(T)$  gravity involving a direct coupling of torsion scalar with matter contents. For this purpose, we consider spatially flat FRW geometry with matter

contents as perfect fluid and formulate the first thermodynamical law in this gravity at apparent horizon. It is found that equilibrium description of thermodynamics exists in this modified gravity in a similar way to Einstein and other gravities. Further we discuss generalized second law of thermodynamics at apparent horizon of FRW universe for three different  $f(T)$  models using Gibbs law as well as the assumption that temperature of matter within apparent horizon is similar to that of horizon. It is found that for some particular cosmologically consistent values of coupling parameters, GSLT remains valid in observationally consistent cosmic eras.

**WEB URL:** <http://link.springer.com/article/10.1007/s10509-015-2586-y>

**25. Hussain, M., & Tabraiz, A. (2015). Super d-anti-magic labeling of subdivided  $K_5$ . *Turkish Journal of Mathematics*, 39(5), 773-783.**

**ABSTRACT:**

A graph  $(G=(V,E,F))$  admits labeling of type  $(1,1,1)$  if we assign labels from the set  $\{1,2,3,\dots,|V(G)|+|E(G)|+|F(G)|\}$  to the vertices, edges, and faces of a planar graph  $G$  in such a way that each vertex, edge, and face receives exactly one label and each number is used exactly once as a label and the weight of each face under the mapping is the same. Super d-antimagic labeling of type  $(1,1,1)$  on snake  $K_5$ , subdivided  $K_5$  as well as isomorphic copies of  $K_5$  for string  $(1,1,\dots,1)$  and string  $(2,2,\dots,2)$  is discussed in this paper.

**WEB URL:** <http://journals.tubitak.gov.tr/math/abstract.htm?id=16954>

**26. Javaid, M. A. A. Bhatti, M. Hussain (2015) On  $(a,d)$  edge-antimagic total labeling of subdivided caterpillar. *Utilitas Mathematica*.98, 227-241.**

*Abstract not found*

**27. Jawad, A., & Majeed, A. (2015). Correspondence of pilgrim dark energy with scalar field models. *Astrophysics and Space Science*, 356(2), 375-381.**

**ABSTRACT:**

In this paper, we consider interacting pilgrim dark energy (Hubble horizon as an infrared cutoff) with cold dark matter in flat universe. We develop the equation of state parameter in this scenario which shows the consistency with pilgrim dark energy phenomenon. In this framework, we analyze the behavior of scalar field and corresponding scalar potentials (which describe the dynamics of the scalar fields) of various scalar field models, graphically. The dynamics of scalar fields and potentials indicate accelerated expansion of the universe which is consistent with the current observations.

**WEB URL:** <http://link.springer.com/article/10.1007/s10509-014-2206-2>

**28. Younis, M., RIZVI, S. T. R., Zhou, Q., BISWAS, A., & Belic, M. (2015). Optical solitons in dual-core fibers with G'/G-expansion scheme. *Journal Of Optoelectronics And Advanced Materials*, 17(3-4), 505-510.**

**ABSTRACT:**

This paper obtains dark and singular 1-soliton solutions in dual-core fibers by the aid of G'/G-expansion scheme. The constraint conditions, for the existence of the soliton solutions, are listed. Additionally, a couple of other solutions known as singular periodic solutions, fall out as a by-product of this scheme. This scheme however fails to retrieve bright soliton solutions.

**WEB URL:**

[https://www.researchgate.net/publication/280580790\\_Optical\\_solitons\\_in\\_dual-core\\_fibers\\_with\\_G%27G-expansion\\_scheme](https://www.researchgate.net/publication/280580790_Optical_solitons_in_dual-core_fibers_with_G%27G-expansion_scheme)

**29. Noureen, I., & Zubair, M. (2015). Dynamical instability and expansion-free condition in f (R, T) gravity. *The European Physical Journal C*, 75(2), 1-10.**

**ABSTRACT:**

A dynamical analysis of a spherically symmetric collapsing star surrounded by a locally anisotropic environment under an expansion-free condition is presented

in  $f(R,T)$  gravity, where  $R$  corresponds to the Ricci scalar and  $T$  stands for the trace of the energy momentum tensor. The modified field equations and evolution equations are reconstructed in the framework of  $f(R,T)$  gravity. In order to acquire the collapse equation we implement the perturbation on all matter variables and dark source components comprising the viable  $f(R,T)$  model. The instability range is described in the Newtonian and post-Newtonian approximation. It is observed that the unequal stresses and density profile define the instability range rather than the adiabatic index. However, the physical quantities are constrained to maintain positivity of the energy density and a stable stellar configuration.

**WEB URL:** <http://link.springer.com/article/10.1140/epjc/s10052-015-3289-9>

**30. Noureen, I., Bhatti, A. A., & Zubair, M. (2015). Impact of extended Starobinsky model on evolution of anisotropic, vorticity-free axially symmetric sources. *Journal of Cosmology and Astroparticle Physics*, 2015(02), 033.**

**ABSTRACT:**

We study the implications of  $Rn$  extension of Starobinsky model on dynamical instability of Vorticity-free axially symmetric gravitating body. The matter distribution is considered to be anisotropic for which modified field equations are formed in context of  $f(R)$  gravity. In order to achieve the collapse equation, we make use of the dynamical equations, extracted from linearly perturbed contracted Bianchi identities. The collapse equation carries adiabatic index  $\Gamma$  in terms of usual and dark source components, defining the range of stability/instability in Newtonian (N) and post-Newtonian (pN) eras. It is found that supersymmetric supergravity  $f(R)$  model represents the more practical substitute of higher order curvature corrections.

**WEB URL:** <http://iopscience.iop.org/article/10.1088/1475-7516/2015/02/033/meta>

**31. Jawad, A., & Rani, S. (2015). Cosmological Analysis of Dynamical Chern-Simons Modified Gravity via Dark Energy Scenario. *Advances in High Energy Physics*, 2015.**

**ABSTRACT:**

The purpose of this paper is to study the cosmological evolution of the universe in the framework of dynamical Chern-Simons modified gravity. We take pilgrim dark energy model with Hubble and event horizons in interacting scenario with cold dark matter. For this scenario, we discuss cosmological parameters such as Hubble and equation of state and cosmological plane like and squared speed of sound. It is found that Hubble parameter approaches the ranges (for ) and (74, 74.30) (for ) for Hubble horizon pilgrim dark energy. It implies the ranges (for ) and (73.4, 74) (for ) for event horizon pilgrim dark energy. The equation of state parameter provides consistent ranges with different observational schemes. Also, planes lie in the range (). The squared speed of sound shows stability for all present models in the present scenario. We would like to mention here that our results of various cosmological parameters show consistency with different observational data like Planck, WP, BAO, , SNLS, and WMAP.

**WEB URL:** <http://www.hindawi.com/journals/ahep/2015/259578/abs/>

**32. Zubair, M. (2015). Quintessence and Holographic Dark Energy in Gravity. *Advances in High Energy Physics*, 292767.**

**ABSTRACT:**

We regard theory as an efficient tool to explain the current cosmic acceleration and associate its evolution with the known dark energy models. The numerical scheme is applied to reconstruct theory from dark energy model with constant equation of state parameter and holographic dark energy model. We set the model parameters and as describing the different evolution eras and show the distinctive behavior of each case realized in theory. We also present the future evolution of reconstructed and find that it is consistent with the recent observations.

**WEB URL:** <http://www.hindawi.com/journals/ahep/2015/292767/abs/>

**33. Jawad, A., & Sohail, A. (2015). Cosmological evolution of modified QCD ghost dark energy in dynamical Chern-Simons gravity. *Astrophysics and Space Science*, 359(2), 1-9.**

**ABSTRACT:**

In this paper, we discuss the dark energy phenomenon by considering the modified QCD ghost dark energy in the framework of dynamical Chern-Simons modified gravity. We find analytical solution of scale factor and explore different cosmological parameters in this scenario. We observe that the deceleration parameter characterizes different phases of the universe under certain conditions of constant parameters. It is pointed out that equation of state parameter as well as cosmological planes ( $\omega_D - \omega'_D \omega_D - \omega'_D$  and  $r - sr - s$ ) provides the consistent results with the present day observations. Also, the squared speed of sound predicts the stability of the present dark energy model for all the time. We also discuss the dynamics of scalar field and potentials of various scalar field models and found interesting results in this framework.

**WEB URL:** <http://link.springer.com/article/10.1007/s10509-015-2506-1>

**34. Salako, I. G., & Jawad, A. (2015). Bianchi type-III models with anisotropic dark energy in Brans–Dicke–Rastall theory. *Astrophysics and Space Science*, 359(2), 1-15.**

**ABSTRACT:**

In this paper, we consider the Bianchi type-III metric (which is a spatially homogeneous and anisotropic) in the framework of a newly proposed Brans–Dicke–Rastall theory of gravitation by Caramês et al. (Eur. Phys. J. C 74:3145, 2014). In this scenario, we obtain the generalized form of the anisotropy parameter of the expansion, the dynamically anisotropic equation of state parameter, and a dynamical energy density in the presence of a single diagonal imperfect fluid. By assuming the anisotropy of the fluid, and exponential and power-law volumetric expansions, we find the exact solutions of the Brans–Dicke–Rastall field equations. We examine the isotropy of the fluid, of space, and of the expansion of the universe. It is observed that the universe can approach the isotropy monotonically even in the presence of an anisotropic fluid. We also note that

the strong anisotropy observed in RG, respectively, is diminished considerably in the Rastall theory and Brans–Dicke–Rastall theory because of the influence of the parameters  $\lambda_{Ras}$  and  $\omega_{BD}$ .

**WEB URL:** <http://link.springer.com/article/10.1007/s10509-015-2494-1>

**35. Waheed, S., & Zubair, M. (2015). Energy constraints and  $F(T, T, G)$  cosmology. *Astrophysics and Space Science*, 359(2), 1-12.**

**ABSTRACT:**

The present paper is elaborated to discuss the energy condition bounds in a modified teleparallel gravity namely  $F(T, TG)$ , involving torsion invariant  $TT$  and contribution from a term  $TGTG$ , the teleparallel equivalent of the Gauss-Bonnet term. For this purpose, we consider flat FRW universe with matter contents as perfect fluid. We formulate the SEC, NEC, WEC and DEC in terms of some cosmic parameters including Hubble, deceleration, jerk and snap parameters. By taking two interesting models for  $F(T, TG)$  and some recent limits of these cosmic parameters, we explore the constraints on the free parameters present in both assumed models. We also discuss these constraints graphically in terms of cosmic time by taking power law cosmology into account.

**WEB URL:** <http://link.springer.com/article/10.1007/s10509-015-2438-9>

**36. Ashraf, S. (2015). Fuzzy dissimilarity and generalization of Valverde's theorem on T-indistinguishability relations. *Fuzzy Sets and Systems*, 275, 144-154.**

**ABSTRACT:**

Similarity and dissimilarity between fuzzy sets are popular notions in decision making problems. This paper studies the representations of  $\epsilon$ -fuzzy dissimilarity relations as the counter part of  $\epsilon$ -fuzzy equivalence relations. It is proved that these newly defined  $\epsilon$ -fuzzy dissimilarity relations satisfy the axioms of self dissimilarity and symmetry along with certain inequalities which transform into Valverde's representation theorem in the particular case when the given relation is 1-fuzzy transitive.

**WEB URL:** <http://www.sciencedirect.com/science/article/pii/S0165011414004540>

**37. Sohail, A., Arshad, S., Javed, S., & Maqbool, K. (2015). Numerical analysis of fractional-order tumor model. *International Journal of Biomathematics*, 8(05), 1550069.**

**ABSTRACT:**

In this paper, the tumor-immune dynamics are simulated by solving a nonlinear system of differential equations. The fractional-order mathematical model incorporated with three Michaelis–Menten terms to indicate the saturated effect of immune response, the limited immune response to the tumor and to account the self-limiting production of cytokine interleukin-2. Two types of treatments were considered in the mathematical model to demonstrate the importance of immunotherapy. The limiting values of these treatments were considered, satisfying the stability criteria for fractional differential system. A graphical analysis is made to highlight the effects of antigenicity of the tumor and the fractional-order derivative on the tumor mass.

**WEB URL:** <http://www.worldscientific.com/doi/abs/10.1142/S1793524515500692>

**38. Younis, M., Rizvi, S. T. R., & Ali, S. (2015). Analytical and soliton solutions: nonlinear model of nanobioelectronics transmission lines. *Applied Mathematics and Computation*, 265, 994-1002.**

**ABSTRACT:**

In this article, analytical solutions and different types of soliton envelopes: bright, dark and singular for the nonlinear model, namely, nanobioelectronics transmission lines have been constructed along with constrained conditions. The modified extended tanh-function method and exp-function method have been used to find analytical solutions, and while solitary wave ansatz is used to construct these soliton solutions. Additionally, the constraint conditions, for the existence of the soliton solutions are also listed.

**WEB URL:** <http://www.sciencedirect.com/science/article/pii/S0096300315007523>

**39. Jawad, A., & Debnath, U. (2015). New Agegraphic Pilgrim Dark Energy in f (T, TG) Gravity. *Communications in Theoretical Physics*, 64(2), 145.**

**ABSTRACT:**

In this work, we briefly discuss a novel class of modified gravity like  $f(T, T_G)$  gravity. In this background, we assume the new agegraphic version of pilgrim dark energy and reconstruct  $f(T, T_G)$  models for two specific values of  $s$ . We also discuss the equation of state parameter, squared speed of sound and  $w_{DE}-w'_{DE}$  plane for these reconstructed  $f(T, T_G)$  models. The equation of state parameter provides phantom-like behavior of the universe. The  $w_{DE}-w'_{DE}$  plane also corresponds to  $\Lambda$ CDM limit, thawing and freezing regions for both models.

**WEB URL:** <http://iopscience.iop.org/article/10.1088/0253-6102/64/2/145/meta>

**40. Jawad, A., & Abbas, G. (2015). Interacting new agegraphic version of pilgrim dark energy. *International Journal of Modern Physics D*, 24(08), 1550061.**

**ABSTRACT:**

We discuss the cosmological evolution of the interacting pilgrim dark energy (DE) with conformal age of the universe in flat FRW universe. We evaluate the equation of state (EoS) parameter for three different values of interacting parameter which evolves the universe from matter dominated to phantom-like eras by evolving quintessence as well as vacuum DE eras. We also give the correspondence of the present DE model with quintessence, tachyon, k-essence, dilaton and DBI-essence scalar field models. We discuss the dynamics of scalar field and corresponding potentials. We find that the behavior of scalar field, corresponding potentials and kinetic energy terms (in k-essence and dilaton field) consistent with the present day observations. Also, cosmological planes such as  $\omega_g - \omega'_g$  and  $r - s$  planes corresponds to  $\Lambda$ CDM limit.

**WEB URL:** <http://www.worldscientific.com/doi/abs/10.1142/S0218271815500613>

**41. Salako, I. G., Jawad, A., & Chattopadhyay, S. (2015). Holographic dark energy reconstruction in  $f(T, T)$  gravity. *Astrophysics and Space Science*, 358(1), 1-9.**

**ABSTRACT:**

The present paper reports a holographic reconstruction scheme for  $f(T,T)f(T,T)$  gravity proposed in Harko et al. (J. Cosmol. Astropart. Phys. 12:021, 2014), where  $T$  is the torsion scalar and  $T$  is the trace of the energy-momentum tensor considering future event horizon as the enveloping horizon of the universe. We consider  $f(T,T)=T+\gamma g(T)$  and  $f(T,T)=\beta T+g(T)$  for reconstruction. We also extract the equation of state parameter for these models. We also give the comparison of the results with observational data and found the consistency of our results.

**WEB URL:** <http://link.springer.com/article/10.1007/s10509-015-2406-4>

**42. Zubair, M., & Noureen, I. (2015). Evolution of axially symmetric anisotropic sources in  $f(R, T)$  gravity. *The European Physical Journal C*, 75(6), 1-9.**

**ABSTRACT:**

We discuss the dynamical analysis in  $f(R, T)$  gravity (where  $R$  is the Ricci scalar and  $T$  is the trace of the energy momentum tensor) for gravitating sources carrying axial symmetry. The self-gravitating system is taken to be anisotropic and the line element describes an axially symmetric geometry avoiding rotation about the symmetry axis and meridional motions (zero vorticity case). The modified field equations for axial symmetry in  $f(R, T)$  theory are formulated, together with the dynamical equations. Linearly perturbed dynamical equations lead to the evolution equation carrying the adiabatic index  $\Gamma$ , which defines the impact of a non-minimal matter to geometry coupling on the range of instability for Newtonian and post-Newtonian approximations.

**WEB URL:** <http://link.springer.com/article/10.1140%2Fepjc%2Fs10052-015-3496-4>

<http://download.springer.com/static/pdf/782/art%253A10.1007%252Fs10509-015-2337-0.pdf?originWeb>

[URL=http%3A%2F%2Flink.springer.com%2Farticle%2F10.1007%2Fs10509-015-2337-0&token2=exp=1465451217~acl=%2Fstatic%2Fpdf%2F782%2Fart%25253A10.1007%252Fs10509-015-2337-0.pdf](http://download.springer.com/static/pdf/782/art%253A10.1007%252Fs10509-015-2337-0.pdf?originWeb&token2=exp=1465451217~acl=%2Fstatic%2Fpdf%2F782%2Fart%25253A10.1007%252Fs10509-015-2337-0.pdf)

[5252Fs10509-015-2337-0.pdf%3ForiginWeb](https://www.scribd.com/document/5252Fs10509-015-2337-0)  
[URL%3Dhttp%253A%252F%252Flink.springer.com%252Farticle%252F10.1007%252Fs10509-015-2337-0\\*~hmac=2d81abac59245999f039a307481b2f26a77ae19d94f44bf1fba45c2e20d08028](http://www.springer.com/article/10.1007/s10509-015-2337-0)

**43. Jawad, A (2015). Energy conditions in  $f(T, T_G)$  gravity. Eur. Phys. J. Plus (2015) 130: 94**

**ABSTRACT:**

This paper is devoted to study the energy conditions in  $f(T, T_G)$  gravity for the FRW universe with perfect fluid, where  $T$  is the torsion scalar and  $T_G$  is the quartic torsion scalar. We construct the energy conditions in this theory and discuss them for two specific  $f(T, T_G)$  models. These models are  $f(T, T_G) = T + \alpha_1 \sqrt{T^2 + \alpha_2 T_G}$  and  $f(T, T_G) = \beta_1 \left( -\frac{\beta_3 T_G}{\sqrt{T}} \right)^{\beta_2}$ , which represent viability through some cosmological scenarios. We consider cosmographic parameters to simplify the energy condition expressions. The present-day values of these parameters are assumed to check the constraints on model parameters through energy condition inequalities.

**WEB URL:**

[http://epjplus.epj.org/articles/epjplus/abs/2015/05/13360\\_2015\\_Article\\_824/13360\\_2015\\_Article\\_824.html](http://epjplus.epj.org/articles/epjplus/abs/2015/05/13360_2015_Article_824/13360_2015_Article_824.html)

**44. Jawad, A. (2015). Cosmological analysis of pilgrim dark energy in loop quantum cosmology. *The European Physical Journal C*, 75(5), 1-9.**

**ABSTRACT:**

The proposal of pilgrim dark energy is based on the speculation that phantom-like dark energy (with strong enough resistive force) can prevent black hole formation in the universe. We explore this phenomenon in the loop quantum cosmology framework by taking pilgrim dark energy with a Hubble horizon. We evaluate the

cosmological parameters such as the Hubble parameter, the equation of state parameter, the squared speed of sound, and also cosmological planes like  $\omega\theta\omega\theta - \omega'\theta\omega\theta'$  and  $rr - ss$  on the basis of the pilgrim dark energy parameter ( $uu$ ) and the interacting parameter ( $d_2d_2$ ). It is found that the values of the Hubble parameter lie in the range  $74+0.005-0.00574-0.005+0.005$ . It is mentioned here that the equation of state parameter lies within the ranges  $-1\mp 0.00005-1\mp 0.00005$  for  $u=2, 1u=2, 1$  and  $(-1.12,-1), (-5,-1)(-1.12,-1), (-5,-1)$  for  $u=-1, -2u=-1,-2$ , respectively. Also, the  $\omega\theta\omega\theta - \omega'\theta\omega\theta'$  planes provide a  $\Lambda$ CDM limit, and freezing and thawing regions for all cases of  $uu$ . It is also interesting to mention here that the  $\omega\theta\omega\theta - \omega'\theta\omega\theta'$  planes lie in the range ( $\omega\theta=-1.13+0.24-0.25, \omega'\theta < 1.32\omega\theta=-1.13-0.25+0.24, \omega'\theta < 1.32$ ). In addition, the  $rr - ss$  planes also correspond to  $\Lambda$ CDM for all cases of  $uu$ . Finally, it is remarked that all the above constraints of the cosmological parameters (corresponding to  $u=\pm 2, \pm 1u=\pm 2, \pm 1$  and  $d_2=0.2+1-1d_2=0.2-1+1$ ) show consistency with different observational data like Planck, WP, BAO, H0H0, SNLS, and nine-year WMAP.

**WEB URL:** <http://link.springer.com/article/10.1140/epjc/s10052-015-3430-9>

**45. Jawad, A. (2015). Cosmological analysis of pilgrim dark energy in loop quantum cosmology. *The European Physical Journal C, 75(5), 1-9.***

**ABSTRACT:**

The proposal of pilgrim dark energy is based on the speculation that phantom-like dark energy (with strong enough resistive force) can prevent black hole formation in the universe. We explore this phenomenon in the loop quantum cosmology framework by taking pilgrim dark energy with a Hubble horizon. We evaluate the cosmological parameters such as the Hubble parameter, the equation of state parameter, the squared speed of sound, and also cosmological planes like  $\omega\theta\omega\theta - \omega'\theta\omega\theta'$  and  $rr - ss$  on the basis of the pilgrim dark energy parameter ( $uu$ ) and the interacting parameter ( $d_2d_2$ ). It is found that the values of the Hubble parameter lie in the range  $74+0.005-0.00574-0.005+0.005$ . It is mentioned here that the equation of

state parameter lies within the ranges  $-1 \mp 0.00005$  for  $u=2$ ,  $1u=2$ ,  $1$  and  $(-1.12, -1), (-5, -1), (-1.12, -1), (-5, -1)$  for  $u=-1, -2u=-1, -2$ , respectively. Also, the  $\omega\vartheta\omega\vartheta-\omega'\vartheta\omega\vartheta'$  planes provide a  $\Lambda$ CDM limit, and freezing and thawing regions for all cases of  $uu$ . It is also interesting to mention here that the  $\omega\vartheta\omega\vartheta-\omega'\vartheta\omega\vartheta'$  planes lie in the range  $(\omega\vartheta=-1.13+0.24-0.25, \omega'\vartheta<1.32\omega\vartheta=-1.13-0.25+0.24, \omega'\vartheta<1.32)$ . In addition, the  $rr$ - $ss$  planes also correspond to  $\Lambda$ CDM for all cases of  $uu$ . Finally, it is remarked that all the above constraints of the cosmological parameters (corresponding to  $u=\pm 2, \pm 1u=\pm 2, \pm 1$  and  $d^2=0.2+1-1d^2=0.2-1+1$ ) show consistency with different observational data like Planck, WP, BAO,  $H_0H_0$ , SNLS, and nine-year WMAP.

**WEB URL:** <http://link.springer.com/article/10.1140/epjc/s10052-015-3430-9>

**46. Jawad, A. (2015). Interacting modified QCD ghost scalar field models of dark energy. *Astrophysics and Space Science*, 357(1), 1-7.**

**ABSTRACT:**

The interacting framework of modified QCD ghost dark energy with cold dark matter is being considered for illustrating the accelerated expansion of the universe. We develop the Hubble parameter numerically and find that it shows increasing behavior which is consistent with the present observations. Also, the equation state parameter shows evolution of the universe from matter dominated universe towards phantom era by evolving the quintessence as well as vacuum eras of the universe. The dynamics of scalar field and corresponding potential of various scalar field models shows consistence behavior with the accelerated expansion phenomenon. Also, the kinetic energy term of  $k$ -essence and dilaton models lies within the range where equation of state parameter represents the accelerated expansion of the universe.

**WEB URL:** <http://link.springer.com/article/10.1007/s10509-015-2299-2>

**47. Jawad, A., Chattopadhyay. (2015) Cosmological analysis of  $F(R)$  models via pilgrim dark energy. *Astrophysics and Space Science*. 357(37). 1-10**

**ABSTRACT:**

In this work, we elaborate the correspondence phenomenon in the scenario of modified Horava-Lifshitz  $F(R)$  gravity and pilgrim dark energy. We assume Hubble as well as event horizons of pilgrim dark energy and reconstruct the  $F(R) \sim$  models in the present context which satisfy the realistic condition of modified gravities. The equation of state parameter shows quintom-like behavior for most of cases of  $m$  in both Hubble as well as event horizons cases. The squared speed of sound provides stability of  $F(R) \sim$  models for all cases of  $m$  and  $u$ . The  $\omega_{DE} - \omega_{DE}$  analysis in this scenario corresponds to freezing as well as thawing regions which is consistent with accelerated expansion of the universe. It is also interesting to mention here that the statefinders approaches to  $\Lambda$ CDM limit for all cases of  $m$  and  $u$ . It is concluded that all the cosmological parameters corresponding to reconstructed  $F(R) \sim$  models consistent with present day observations.

**WEB URL:**

[http://download.springer.com/static/pdf/302/art%253A10.1007%252Fs10509-015-2285-8.pdf?originWebURL=http%3A%2F%2Flink.springer.com%2Farticle%2F10.1007%2Fs10509-015-2285-8&token2=exp=1465453856~acl=%2Fstatic%2Fpdf%2F302%2Fart%25253A10.1007%25252Fs10509-015-2285-8.pdf%3ForiginWebURL%3Dhttp%253A%252F%252Flink.springer.com%252Farticle%252F10.1007%252Fs10509-015-2285-8\\*~hmac=eb6344bf20479f3a4720b8c91de5070e4c4a2a5fd375eec3145e365142d49995](http://download.springer.com/static/pdf/302/art%253A10.1007%252Fs10509-015-2285-8.pdf?originWebURL=http%3A%2F%2Flink.springer.com%2Farticle%2F10.1007%2Fs10509-015-2285-8&token2=exp=1465453856~acl=%2Fstatic%2Fpdf%2F302%2Fart%25253A10.1007%25252Fs10509-015-2285-8.pdf%3ForiginWebURL%3Dhttp%253A%252F%252Flink.springer.com%252Farticle%252F10.1007%252Fs10509-015-2285-8*~hmac=eb6344bf20479f3a4720b8c91de5070e4c4a2a5fd375eec3145e365142d49995)

**48. Jawad, A., & Rani, S. (2015). Lorentz distributed noncommutative wormhole solutions in extended teleparallel gravity. *The European Physical Journal C*,75(4), 1-12.**

**ABSTRACT:**

In this paper, we study static spherically symmetric wormhole solutions in extended teleparallel gravity with the inclusion of noncommutative geometry under a Lorentzian distribution. We obtain expressions of matter components for a non-diagonal tetrad. The effective energy-momentum tensor leads to the violation of

energy conditions which impose a condition on the normal matter to satisfy these conditions. We explore the noncommutative wormhole solutions by assuming a viable power-law  $f(T)f(T)$  and shape function models. For the first model, we discuss two cases in which one leads to teleparallel gravity and the other is for  $f(T)f(T)$  gravity. The normal matter violates the weak energy condition for the first case, while there exists a possibility for micro physically acceptable wormhole solution. There exists a physically acceptable wormhole solution for the power-law  $b(r)b(r)$  model. Also, we check the equilibrium condition for these solutions, which is only satisfied for the teleparallel case, while for the  $f(T)f(T)$  case, these solutions are less stable.

**WEB URL:** <http://link.springer.com/article/10.1140/epjc/s10052-015-3386-9>

**49. Younis, M., & Rizvi, S. T. R. (2015). Optical solitons for ultrashort pulses in nano fibers. *Journal of Nanoelectronics and Optoelectronics*, 10(2), 179-182.**

**ABSTRACT:**

The nonlinear Schrödinger equation (NLSE) is the governing equation for ultrashort pulse transmission in a nonlinear nano optical fibers. In this paper, the NLSE equation has been solved by the ansatz to celebrate the bright and dark optical solitons. Since the soliton, in which the shape and speed can remain constant during propagation, is expected that transmission of nonlinear ultrashort pulses in optical fibers can effectively control the dispersion. So the bright and dark optical solitons in the proper dispersion management systems are discussed, along with their constraint conditions.

**WEB URL:**

<http://www.ingentaconnect.com/content/asp/jno/2015/00000010/00000002/art00003>

**50. Jawad, A., Chattopadhyay, S., Bhattacharya, S., & Pasqua, A. (2015). Modified Holographic Ricci Dark Energy in Chameleon Brans–Dicke Cosmology and Its Thermodynamic Consequence. The financial Supported from Department of Science and Technology, Govt. of India under Project Grant No. SR/FTP/PS-167/2011 is thankfully acknowledged by SC. *Communications in Theoretical Physics*, 63(4), 453.**

**ABSTRACT:**

The objective of this paper is to discuss the Chameleon Brans–Dicke gravity with non-minimally matter coupling of scalar field. We take modified Holographic Ricci dark energy model in this gravity with its energy density in interaction with energy density of cold dark matter. We assume power-law ansatz for scale factor and scalar field to discuss potential as well as coupling functions in the evolving universe. These reconstructed functions are plotted versus scalar field and time for different values of power component of scale factor  $n$ . We observe that potential and coupling functions represent increasing behavior, in particular, consistent results for a specific value of  $n$ . Finally, we have examined validity of the generalized second law of thermodynamics and we have observed its validity for all values of  $n$ .

**WEB URL:** <http://iopscience.iop.org/article/10.1088/0253-6102/63/4/453/meta>

**51. Ali, S., Rizvi, S. T. R., & Younis, M. (2015). Traveling wave solutions for nonlinear dispersive water-wave systems with time-dependent coefficients. *Nonlinear Dynamics*, 82(4), 1755-1762.**

**ABSTRACT:**

In this article, the solitary wave and topological soliton solutions in the models that describe the propagation of surface water waves in a uniform channel are successfully constructed. The solitary wave ansatz is used to carry out these distinct solutions. The corresponding integrability criteria, also known as constraint conditions, naturally emerge from the analysis of these models.

**WEB URL :**<http://link.springer.com/article/10.1007/s11071-015-2274-z>

**52. Ahmad, S., & Anwar, I. (2015, December). On Characteristic Poset and Stanley Decomposition of  $S/I$ . In *Algebra Colloquium* 22(01), 739-744.**

**ABSTRACT:**

Let  $K$  be a field and  $S = K[x_1, \dots, x_n]$  be the polynomial ring in  $n$  variables. Let  $I \subset S$  be a monomial ideal such that  $S/I$  is Cohen-Macaulay. By associating a finite poset  $\tilde{T}_{S/I}$  to  $S/I$ , we show that if  $S/I$  is a Stanley ideal then  $T/\tilde{T}$  is also a Stanley ideal, where  $T = K[x_{11}, \dots, x_{1a1}, \dots, x_{n1}, \dots, x_{nan}]$  and  $\tilde{T}$  is the polarization of  $I$ .

**WEB URL:** <http://www.worldscientific.com/doi/abs/10.1142/S1005386715000644>

**53. Ashraf, S., ur Rehman, A., & Kerre, E. E. (2015). Group Decision Making with Incomplete Interval-valued Fuzzy Preference Relations Based on the Minimum Operator. *International Journal of Computers Communications & Control*, 10(6), 29-42.**

**ABSTRACT:**

This paper presents a new method to estimate the unknown values in incomplete interval-valued fuzzy preference relations (IVFPRs). The method is based on the min-consistency and is used to develop the algorithm for group decision making (GDM) dealing with incomplete IVFPRs.

**WEB URL:** <http://univagora.ro/jour/index.php/ijccc/article/view/2070>

**54. Bhar, P., Rahaman, F., Jawad, A., & Islam, S. (2015). Anisotropic charged fluids with Chaplygin equation of state in (2+ 1) dimension. *Astrophysics and Space Science*, 360(1), 1-7.**

**ABSTRACT:**

Present paper provides a new non-singular model for anisotropic charged fluid sphere in (2+12+1)-dimensional anti de-Sitter spacetime corresponding to the exterior BTZ spacetime (Banados et al., Phys. Rev. Lett. 69:1849, 1992). The model is obtained by assuming Krori and Barua (KB) ansatz (Krori and Barua, J. Phys. A, Math. Gen., 8:508, 1975). To solve the Einstein-Maxwell field equations we choose modified Chaplygin gas. Various physical quantities have been discussed and from our analysis we show that our model satisfies all required physical conditions for representing compact stars.

**WEB URL:** <http://link.springer.com/article/10.1007/s10509-015-2543-9>

**55. Zubair, M., & Jawad, A. (2015). Generalized second law of thermodynamics in  $f(T, T G)$  gravity. *Astrophysics and Space Science*, 360(1), 1-12.**

**ABSTRACT:**

We discuss the equilibrium picture of thermodynamic at the apparent horizon of FRW universe in  $f(T, TG)f(T, TG)$  gravity, where  $TT$  represents the torsion invariant and  $TGTG$  is the teleparallel equivalent of the Gauss-Bonnet term. It is found that one can translate the Friedmann equations to the standard form of first law of thermodynamics. We discuss GSLT in the locality of assumption that temperature of matter inside the horizon is similar to that of apparent horizon. Furthermore, we consider particular models in this theory and generate constraints on the coupling parameters for the validity of GSLT. For this purpose we set the present day values of cosmic parameters and find the possible constraints on  $f(T, TG)f(T, TG)$  models. We also choose the power law cosmology and found that GSLT can be met in accelerated cosmic expansion. We have also presented the cosmological reconstruction of some viable  $f(T, TG)f(T, TG)$  models and discussed the cosmic evolution and validity of GSLT.

**WEB URL:** <http://link.springer.com/article/10.1007/s10509-015-2527-9>

**56. Javed, S., Riasat, A., & Kanwal, S. (2015) On super edge-magincness and deficiencies of forests. *Utilitas Mathematica*, 98. 149-169.**

**ABSTRACT:**

For a  $(p, q)$ -graph  $G = (V, E)$ , a bijection  $f : V(G) \cup E(G) \rightarrow \{1, 2, \dots, p + q\}$  is called an edge-magic total labeling of  $G$  if there exists a constant  $k$  such that  $f(x) + f(xy) + f(y) = k$ , for every edge  $xy \in E(G)$ . An edge-magic total labeling  $f$  is called super if  $f(V(G)) = \{1, 2, \dots, p\}$ . The super edge-magic deficiency of a graph  $G$ , denoted by  $\mu_s(G)$ , is the minimum nonnegative integer  $n$  such that  $G \cup nK_1$  has a super edge-magic total labeling or  $+\infty$  if there exists no such  $n$ . In this paper we study the super edge-magic total labeling and deficiency of forests consisting of combs, generalized combs and stars. These facts

provide the evidence to support the conjecture proposed by Figueroa-Centeno, Ichishima and Muntaner-Bartle [7].

**WEB URL:** [http://http.sms.edu.pk/journals/preprint/pre\\_450.pdf](http://http.sms.edu.pk/journals/preprint/pre_450.pdf)

**57. Sardar, A., Husnine, S. M., Rizvi, S. T. R., Younis, M., & Ali, K. (2015). Multiple travelling wave solutions for electrical transmission line model. *Nonlinear Dynamics*, 82(3), 1317-1324.**

**ABSTRACT:**

In this paper, we find multiple travelling wave solutions using three integration schemes to integrate the model of electrical transmission line. These schemes are  $(G'/G)(G'/G)$ -expansion method, extended tanh method and sine–cosine method, which are applied with computerized symbolic computation. The different kinds of solutions: solitary, shock, singular, periodic, rational and kink-shaped, are obtained. The corresponding integrability criteria, also known as constraint conditions, naturally emerge from the analysis of the transmission line equation.

**WEB URL:** <http://link.springer.com/article/10.1007/s11071-015-2240-9>

**58. Sardar, A., Husnine, S. M., Rizvi, S. T. R., Younis, M., & Ali, K. (2015). Multiple travelling wave solutions for electrical transmission line model. *Nonlinear Dynamics*, 82(3), 1317-1324.**

**ABSTRACT:**

In this paper, we find multiple travelling wave solutions using three integration schemes to integrate the model of electrical transmission line. These schemes are  $(G'/G)(G'/G)$ -expansion method, extended tanh method and sine–cosine method, which are applied with computerized symbolic computation. The different kinds of solutions: solitary, shock, singular, periodic, rational and kink-shaped, are obtained. The corresponding integrability criteria, also known as constraint conditions, naturally emerge from the analysis of the transmission line equation.

**WEB URL:** <http://link.springer.com/article/10.1007/s11071-015-2240-9>

**59. Zubair, M., & Abbas, G. (2015). Reconstructing QCD ghost  $f(R, T)$  models. *Astrophysics and Space Science*, 357(2), 1-10.**

**ABSTRACT:**

We reconstruct  $f(R, T)$  theory (where  $R$  is the scalar curvature and  $T$  is the trace of energy-momentum tensor) in the framework of QCD ghost dark energy models. In this study, we concentrate on particular models of  $f(R, T)$  gravity which permits the standard continuity equation in this theory. It is found that reconstructed function can represent phantom and quintessence regimes of the universe in the background of flat FRW universe. In addition, we explore the stability of ghost  $f(R, T)$  models.

**WEB URL:** <http://link.springer.com/article/10.1007/s10509-015-2387-3>

**60. Younis, M., & Rizvi, S. T. R. (2015). Dispersive dark optical soliton in (2+ 1)-dimensions by  $G'/G$ -expansion with dual-power law nonlinearity. *Optik-International Journal for Light and Electron Optics*, 126(24), 5812-5814.**

**ABSTRACT:**

The article proposes the dispersive dark optical solitons with dual-power law nonlinearity, that are governed by (2+1)-dimensions nonlinear Schrödinger equation. The  $G'/G$ -expansion method is being utilized to celebrate soliton solution, to this equation, that reveals dark 1-soliton.

**WEB URL:** <http://www.sciencedirect.com/science/article/pii/S0030402615010025>

**61. Younis, M., Sardar, A., Rizvi, S. T. R., & Zhou, Q. (2015). Exact solitons in a medium with competing weakly nonlocal nonlinearity and parabolic law nonlinearity. *Journal of Nonlinear Optical Physics & Materials*, 24(04), 1550049.**

**ABSTRACT:**

This work studies the optical solitons in the physical model that describes the propagation of optical solitons in a medium with competing weakly nonlocal nonlinearity and parabolic law nonlinearity via the  $(G'/G)(G'/G)$ -expansion scheme,

exact dark and singular one-soliton solutions, along with the constraint conditions, are reported.

**WEB URL:**

<http://www.worldscientific.com/doi/abs/10.1142/S0218863515500496?journalCode=jnopm>

**62. Chighoub, F., Sohail, A., & Alia, I. (2015). Near-optimality conditions in mean-field control models involving continuous and impulse controls. *Nonlinear Studies*, 22(4).719-738.**

**ABSTRACT:**

In this paper we discuss stochastic control models which are described by a stochastic differential equation of mean-field type, in the sense that the coefficients are permitted to depend on the state process as well as of its expected value. The control variable has two components, the first being absolutely continuous and the second is a piecewise impulse process which is not necessarily increasing. Necessary and sufficient conditions for a control to be near optimal are studied in the form of stochastic maximum principle by using Ekeland's variational principle, which allows to produce two approximate variational inequalities in integral form. The first inequality is constructed by the spike variation technique in terms of the  $\eta$ -function employed for absolutely continuous part of all near optimal control. The second one is defined in term of the first order adjoint process by using a convex perturbation technique for all near optimal impulse controls.

**WEB URL:**

<http://web.a.ebscohost.com/abstract?direct=true&profile=ehost&scope=site&authtype=crawler&jrnl=13598678&AN=111832524&h=vGU1OzAVYkfE1yXkuARanPWX%2f%2fbDy7FxfvbcndHatRKYft3Glm%2fN24LJQs5WGbSd7OV05ved9Cfi7ZWsmZoc2A%3d%3d&crl=c&resultNs=AdminWebAuth&resultLocal=ErrCrlNotAuth&crlhashWebURL=login.aspx%3fdirect%3dtrue%26profile%3dehost%26scope%3dsite%26authtype%3dcrawler%26jrnl%3d13598678%26AN%3d111832524>

**63. Agarwal, R. P., Arshad, S., Lupulescu, V., & O'regan, D. O. N. A. L. (2015) Evolution equations with causal operators. *Differential Equations & Applications*, 7(1), 15-26.**

**ABSTRACT:**

In this paper we present an existence result for causal functional evolution equations. The result is obtained under a condition with respect to the Hausdorff measure of noncompactness. An application with partial differential equations is given to illustrate our main result.

**WEB URL:**

[https://www.researchgate.net/profile/Vasile\\_Lupulescu/publication/282516760\\_Evolution\\_equations\\_with\\_causal\\_operators/links/5630249708aefac54d8f1492.pdf](https://www.researchgate.net/profile/Vasile_Lupulescu/publication/282516760_Evolution_equations_with_causal_operators/links/5630249708aefac54d8f1492.pdf)

**64. Sohail, A., Maqbool, K., Asif, A., & Ahmad, H. (2015). Numerical Modelling of Effective Diffusivity in Bone Tissue Engineering. *World Academy of Science, Engineering and Technology, International Journal of Medical, Health, Biomedical, Bioengineering and Pharmaceutical Engineering*, 9(1), 82-86.**

**ABSTRACT:**

These days, the field of tissue engineering is getting serious attention due to its usefulness. Bone tissue engineering helps to address and sort-out the critical sized and non-healing orthopedic problems by the creation of manmade bone tissue. We will design and validate an efficient numerical model, which will simulate the effective diffusivity in bone tissue engineering. Our numerical model will be based on the finite element analysis of the diffusion-reaction equations. It will have the ability to optimize the diffusivity, even at multi-scale, with the variation of time. It will also have a special feature "parametric sweep", with which we will be able to predict the oxygen, glucose and cell density dynamics, more accurately. We will fix these problems by modifying the governing equations, by selecting appropriate spatio-temporal finite element schemes and by transient analysis.

**WEB URL:** <http://www.waset.org/publications/10000617>

65. Agarwal, R. P., Arshad, S., Lupulescu, V., & O'REGAN, D. O. N. A. L. (2015). Evolution equations with causal operators. *Applied Mathematics and Information science* 7(1), 15-26.

**ABSTRACT:**

In this paper we present an existence result for causal functional evolution equations. The result is obtained under a condition with respect to the Hausdorff measure of noncompactness. An application with partial differential equations is given to illustrate our main result.

**WEB URL:**

[https://www.researchgate.net/profile/Vasile\\_Lupulescu/publication/282516760\\_Evolution\\_equations\\_with\\_causal\\_operators/links/5630249708aefac54d8f1492.pdf](https://www.researchgate.net/profile/Vasile_Lupulescu/publication/282516760_Evolution_equations_with_causal_operators/links/5630249708aefac54d8f1492.pdf)

66. Riasat, A., Javed, S. (2015). Odd Graceful Labeling of Acyclic Graphs. *American Journal of Applied Mathematics*. 3(3-1) 14-18.

**ABSTRACT:**

Let  $G = (V, E)$  be a finite, simple and undirected graph. A graph  $G$  with  $q$  edges is said to be odd-graceful if there is an injection  $f : V(G) \rightarrow \{0, 1, 2, \dots, 2q-1\}$  such that, when each edge  $xy$  is assigned the label  $|f(x) - f(y)|$ , the resulting edge labels are  $\{1, 3, 5, \dots, 2q-1\}$  and  $f$  is called an odd graceful labeling of  $G$ . Motivated by the work of Z. Gao [6] in which he studied the odd graceful labeling of union of any number of paths and union of any number of stars, we have determined odd graceful labeling for some other union of graphs. In this paper we formulate odd-graceful labeling for disjoint unions of graphs consisting of generalized combs, stars, bistars and paths.

**WEB URL:**

<http://article.sciencepublishinggroup.com/html/10.11648.j.ajam.s.2015030301.13.html>

67. Abid1, M., Shahid, M. Khalil & Wajid, H. A, (2015). *IIUM Engineering Journal*, 16(1) 43-52.

**ABSTRACT:**

Loss of pre-load with time, commonly known as 'relaxation' is an established phenomena. Behaviour of a bolted joint depends upon the pre-load in the bolts in use, not the pre-load introduced by the mechanic. Loss of pre-load is expected due to many factors such as embedment relaxation, gasket creep, elastic interactions, and vibration loosening or stress relaxation. In a gasketed joint, due to the gasket flexibility, relaxation in almost all bolts is always substantial during preliminary bolt tightening passes, as 80 to 100% loss is common hence resulting in a dynamic behaviour. It is observed that pre-load in a gasketed joint is controlled to a certain extent only in the final bolt-tightening passes. Experimental study presented in this paper highlights the factors affecting the amount of bolt preload relaxation with time. Important considerations are recommended to reduce bolt relaxation. Both the short and long term relaxations are recorded and a 'best fit' model for relaxation behaviour is derived.

**WEB URL:** <file:///C:/Users/sahmed/Downloads/539-2277-1-PB.pdf>

**68. Hussain,. M. Tabraiz,. A.(2015). Face Antimagic Labeling Of Generalized Kcn Snake Graph, Sci.Int.(Lahore),27(3),1715-1718.**

**ABSTRACT:**

This paper deal with the labeling of type  $(1, 1, 1)$ . If we assign labels from the set  $\{1,2,3, \Lambda, V(G) + E(G) + F(G)\}$  to the vertices, edges and faces of plane graph  $G$  in such a way that each vertex, edge and face receives exactly one label and each number is used exactly once as a label such a labeling is called magic labeling of type  $(1, 1, 1)$ . In this paper super 1-antimagic labeling of type  $(1, 1, 1)$  on  $KC_n$  snake graph and subdivision of  $KC_n$  snake graph for string  $(1, 1, \dots, 1)$  and string  $(2, 2, \dots, 2)$  are discussed.

**WEB URL:** <http://www.sci-int.com/pdf/19524998801%20a%201715-1718-%20SIJ-00035%20Final%20form%20co%20IMRAN%20COMPOSED.pdf>

**69. Cheema, I. Z., Hussain, M., & Shaker, H. (2015). On Cycle Anti-Supermagic Labelling Of Isomorphic Copies Of Ladder And Triangular Ladder. Science International, 27(3) ) 1719-1722.**

**ABSTRACT:**

A graph  $G = (V, E)$  has an  $H$ -covering if every edge in  $E$  belongs to a subgraph of  $G$  isomorphic to  $H$ . Suppose  $G$  admits an  $H$ -covering. An  $H$ -magic labeling is a total labeling  $\lambda$  from  $V \cup E$  onto the integers  $\{1, 2, \dots, |V| + |E|\}$  with the property that, for every subgraph  $A$  of  $G$  isomorphic to  $H$  there is a positive integer  $c$  such that  $\sum_{v \in V \cap A} \lambda(v) + \sum_{e \in E \cap A} \lambda(e) = c$ . A graph that admits such a labeling is called  $H$ -magic. In addition, if  $\{\lambda(v) - \lambda(v')\}_{v, v' \in V, \varepsilon = \pm 1}$ , then the graph is called  $H$ -supermagic. Moreover a graph is said to be  $H$ - $(a, d)$ -antimagic if the magic constant for an arithmetic progression with initial value  $a$  and common difference  $d$ . In this paper we formulate cycle anti-supermagic labeling for the disjoint union of isomorphic copies of ladder and triangular ladder graphs.

**WEB URL:** <http://www.sci-int.com/pdf/17884028701%20a%201719-1722-%20SIJ-00040%20++Final%20Form-CO--IMRAN-COMPOSED.pdf>

**70. Abid, M. K. S. Karimov, H. A. Wajid, F. Farooq, H. Ahmed, O. H. Khan.(2015). *Iranica Journal of Energy and Environment* 6(1): 1-4.**

**ABSTRACT:**

With a growing focus on renewable energy, interest in design of wind turbines has also been expanding. In today's market, the horizontal axis (windmill) turbine is the most common type in use; but, vertical axis (Darrieus) turbines have certain advantages. Darrieus turbines, which are lift-driven, have a higher power potential than the horizontal, or drag-driven turbines. The main flaw with their design is their inability to self-start. Darrieus turbines require an external energy source to bring the device to a minimum rotational speed. This paper presents design, construction and testing of a vertical axis (Darrieus) wind turbine with 3 blades, starting solely from the low energy of the wind. A separate drag device (Savonius type turbine) on the top of an existing Darrieus turbine was mounted to make the turbine self start at low wind speed. The cut-in speed of the turbine was 3 m/s, cut-off speed was 20 m/s and power obtained was 50

Watts at wind velocity of 6 m/s. The testing with primarily available permanent magnetic generator sponsored by industry resulted in 35 Watts at 9m/s.

**WEB URL:** <http://www.ijee.net/Journal/ijee/vol6/no1/1.pdf>

**71. Zada, A., Arshad, S., Rahmat, G., & Khan, A. (2015). On the dichotomy of non-autonomous systems over finite dimensional spaces. *Appl. Math*, 9(4), 1941-1946.**

**ABSTRACT:**

In this article we study the dichotomy of the  $q$  periodic system  $X'(t) = A(t)X(t)$  in terms of the boundedness of the solutions of the following Cauchy problems  $X'(t) = A(t)X(t) + e^{i\mu t}Pb$ ,  $t \geq 0$ ,  $X(0) = 0$ , and  $X'(t) = -X(t)A(t) + e^{i\mu t}(I - P)b$ ,  $t \geq 0$ ,  $X(0) = 0$ , where  $A(t)$  is a square size matrix of order  $m$ ,  $\mu$  is any real number,  $b$  is a non zero vector in  $C^m$  and  $P$  is an orthogonal projection.

**WEB URL:**

[https://www.researchgate.net/profile/Akbar\\_Zada/publication/275715136\\_On\\_the\\_Dichotomy\\_of\\_Non-Autonomous\\_Systems\\_Over\\_Finite\\_Dimensional\\_Spaces/links/5544ef440cf24107d397ad7e.pdf](https://www.researchgate.net/profile/Akbar_Zada/publication/275715136_On_the_Dichotomy_of_Non-Autonomous_Systems_Over_Finite_Dimensional_Spaces/links/5544ef440cf24107d397ad7e.pdf)

**72. Arshad, S., Sohail, A., & Maqbool, K. (2015). Nonlinear shallow water waves: A fractional order approach. *Alexandria Engineering Journal*. 55(1), 525-532**

**ABSTRACT:**

Nonlinear partial differential equations governing the obscure phenomena of shallow water waves are discussed in this article. Time fractional model is considered to understand the upcoming solutions on the basis of all historical states of the solution. A semi-analytic technique, Homotopy Perturbation Transform Method (HPTM) is used in conjunction with a numerical technique to validate the approximate solutions. With the aid of graphical interpretation, the favorable wave parameters, to avoid wave breaking are estimated.

**WEB URL:** <http://www.sciencedirect.com/science/article/pii/S1110016815001696>

# DEPARTMENT OF PHYSICS

## Journal Papers

1. Saleem, M., Fang, L., Shaukat, S. F., Ahmad, M. A., Raza, R., Akhtar, M. N., ... & Abbas, G. (2015). Structural and photovoltaic characteristics of hierarchical ZnO nanostructures electrodes. *Applied Surface Science*, 334, 145-150.

**ABSTRACT:**

Structural and photovoltaic characteristics of hierarchical ZnO nanostructures solar cell have been studied in relation to growth reaction temperature. It is found that the hierarchical ZnO nanostructures network to act not only as large surface area substrates but also as a transport medium for electrons injected from the dye molecules. The incident photon-to-current conversion efficiency is decreased by increasing the growth reaction temperature of ZnO electrodes. The best conversion efficiency of a 0.25 cm<sup>2</sup> cell is measured to be 1.24% under 100 mW cm<sup>-2</sup> irradiation.

**WEB URL:** <http://www.sciencedirect.com/science/article/pii/S0169433214019345>

2. Amjad, R. J., Dousti, M. R., & Sahar, M. R. (2015). Spectroscopic investigation and Judd–Ofelt analysis of silver nanoparticles embedded Er<sup>3+</sup>-doped tellurite glass. *Current Applied Physics*, 15(1), 1-7.

**ABSTRACT:**

A series of silver nanoparticles (NPs) embedded zinc-tellurite glass is prepared by melt-quenching technique. The transmission electron microscopic images reveal spherical as well as anisotropic silver NPs having average diameter in the range of 14–48 nm. The Er<sup>3+</sup>-free glass sample containing AgCl exhibits surface plasmon resonance (SPR) band of Ag NPs centered at ~ 501 nm. From Judd–Ofelt analysis, it is found that by increasing the concentration of NPs, the value of  $\Omega_2$  is enhanced suggesting increased covalency and decreased symmetry around the Er<sup>3+</sup> ions. Integrated emission cross-section (IEC) is

enhanced as the concentration of silver NPs is increased up to 0.5 mol% AgCl. Fourier infrared spectra show that the intensity of the vibrational band of the water molecule and fundamental stretching band of OH group are suppressed. Furthermore, under an excitation wavelength of 786 nm, three prominent upconversion emissions are observed at 520 nm, 550 nm and 650 nm which are attributed to  ${}^2H_{11/2} \rightarrow {}^4I_{15/2}$ ,  ${}^4S_{3/2} \rightarrow {}^4I_{15/2}$ , and  ${}^4F_{9/2} \rightarrow {}^4I_{15/2}$  transitions, respectively. The upconversion emissions are enhanced significantly by introduction of silver NPs. The enhancement is mainly attributed to the local field effect of silver NPs. Studied nanocomposites are potential candidates for the development of solid state lasers.

**WEB URL:** <http://www.sciencedirect.com/science/article/pii/S156717391400337X>

**3. Dousti, M. R., Amjad, R. J., Salehi, M., & Sahar, M. R. (2015). Photoluminescence study of Sm<sup>3+</sup>–Yb<sup>3+</sup> co-doped tellurite glass embedding silver nanoparticles. *Journal of Luminescence*, 159, 100-104.**

**ABSTRACT:**

We report on the upconversion emission of Sm<sup>3+</sup> ions doped tellurite glass in the presence of Yb<sup>3+</sup> ions and silver nanoparticles. The enhancement of infrared-to-visible upconversion emissions is achieved under 980 nm excitation wavelength and attributed to the high absorption cross section of Yb<sup>3+</sup> ions and an efficient energy transfer to Sm<sup>3+</sup> ions. Further enhancements are attributed to the plasmonic effect via metallic nanoparticles resulting in the large localized field around rare earth ions. However, under excitation at 406 nm, the addition of Yb<sup>3+</sup> content and heat-treated silver nanoparticles quench the luminescence of Sm<sup>3+</sup> ions likely due to quantum cutting and plasmonic diluent effects, respectively.

**WEB URL:** <http://www.sciencedirect.com/science/article/pii/S0022231314006310>

**4. Zhu, B., Lund, P. D., Raza, R., Ma, Y., Fan, L., Afzal, M., ... & Huang, Q. A. (2015). Schottky junction effect on high performance fuel cells based on nanocomposite materials. *Advanced Energy Materials*, 5(8).**

**ABSTRACT:**

A novel fuel cell device based on integrating the Schottky junction effect with the electrochemical principle is designed, constructed, and verified through experiments. It is found that the Schottky junction has a significant effect on the greatly enhanced device performance, and the fuel cell device incorporating the Schottky junction effect reaches a power output of  $1000 \text{ mW cm}^{-2}$  at  $550 \text{ }^\circ\text{C}$ .

**WEB URL:** <http://onlinelibrary.wiley.com/doi/10.1002/aenm.201401895/full>

**5. S. Nisar et al (BES-III collaboration). (2015). Study of  $J/\psi \rightarrow \eta \phi \pi^+ \pi^-$  at BESIII. *Physical Review D*, 91 (5),**

**ABSTRACT:**

invariant mass spectrum of  $\phi f_0(980)$  with a statistical significance of greater than  $10 \sigma$ . The corresponding mass and width are determined to be  $M = 2200 \pm 6(\text{stat}) \pm 5(\text{syst}) \text{ MeV}/c^2$  and  $\Gamma = 104 \pm 15(\text{stat}) \pm 15(\text{syst}) \text{ MeV}$ , respectively, and the product branching fraction is measured to be  $B(J/\psi \rightarrow \eta Y(2175), Y(2175) \rightarrow \phi f_0(980), f_0(980) \rightarrow \pi^+ \pi^-) = (1.20 \pm 0.14(\text{stat}) \pm 0.37(\text{syst})) \times 10^{-4}$ . The results are consistent within errors with those of previous experiments. We also measure the branching fraction of  $J/\psi \rightarrow \phi f_1(1285)$  with  $f_1(1285) \rightarrow \eta \pi^+ \pi^-$  and set upper limits on the branching fractions for  $J/\psi \rightarrow \phi \eta(1405)/\phi X(1835)/\phi X(1870)$  with  $\eta(1405)/X(1835)/X(1870) \rightarrow \eta \pi^+ \pi^-$  at the 90% confidence level.

**WEB URL:** <http://openaccess.dogus.edu.tr/handle/11376/1990>

**6. S. Nisar et al (BES-III collaboration) (2015). Precision measurement of the  $D^* 0$  decay branching fractions. *Physical Review D*, 91(3), 031101.**

**ABSTRACT:**

Using  $482 \text{ pb}^{-1}$  of data taken at  $\sqrt{s} = 4.009 \text{ GeV}$ , we measure the branching fractions of the  $D^* 0$  decays  $D^* 0 \rightarrow D 0 \pi 0$  and  $D^* 0 \rightarrow D 0 \gamma$  to be  $B(D^* 0 \rightarrow D 0 \pi 0) = (65.5 \pm 0.8 \pm 0.5)\%$  and  $B(D^* 0 \rightarrow D 0 \gamma) = (34.5 \pm 0.8 \pm 0.5)\%$ , respectively, by

assuming that the  $D^{*0}$  decays only into these two modes. The ratio of the two branching fractions is  $B(D^{*0} \rightarrow D^0 \pi^0)/B(D^{*0} \rightarrow D^0 \gamma) = 1.90 \pm 0.07 \pm 0.05$ , which is independent of the assumption made above. The first uncertainties are statistical and the second ones systematic. The precision is improved by a factor of 3 compared to the present world average values.

**WEB URL:** <http://journals.aps.org/prd/abstract/10.1103/PhysRevD.91.031101>

**7. S. Nisar et al (BES-III collaboration). (2015). Search for the  $\Upsilon(4140)$  via  $e^+ e^- \rightarrow \gamma \phi J/\psi$  at  $s = 4.23, 4.26$  and  $4.36$  GeV. *Physical Review D*, 91(3), 032002.**

**ABSTRACT:**

Using data samples collected at center-of-mass energies  $\sqrt{s} = 4.23, 4.26,$  and  $4.36$  GeV with the BESIII detector operating at the BEPCII storage ring, we search for the production of the charmoniumlike state  $\Upsilon(4140)$  through a radiative transition followed by its decay to  $\phi J/\psi$ . No significant signal is observed and upper limits on  $\sigma[e^+ e^- \rightarrow \gamma \Upsilon(4140)] \cdot B(\Upsilon(4140) \rightarrow \phi J/\psi)$  at the 90% confidence level are estimated as 0.35, 0.28, and 0.33 pb at  $\sqrt{s} = 4.23, 4.26,$  and  $4.36$  GeV, respectively.

**WEB URL:** <http://journals.aps.org/prd/abstract/10.1103/PhysRevD.91.032002>

**8. Ablikim, M., Achasov, M. N., Ai, X. C., Albayrak, O., Albrecht, M., Ambrose, D. J., ... & Ferroli, R. B. (2015). Study of  $e^+ e^- \rightarrow \omega \chi_{cJ}$  at Center of Mass Energies from 4.21 to 4.42 GeV. *Physical review letters*, 114(9), 092003.**

**ABSTRACT:**

Based on data samples collected with the BESIII detector at the BEPCII collider at nine center of mass energies from 4.21 to 4.42 GeV, we search for the production of  $e^+ e^- \rightarrow \omega \chi_{cJ}$  ( $J=0, 1, 2$ ). The process  $e^+ e^- \rightarrow \omega \chi_{c0}$  is observed for the first time, and the Born cross sections at  $\sqrt{s} = 4.23$  and  $4.26$  GeV are measured to be  $(55.4 \pm 6.0 \pm 5.9)$  and  $(23.7 \pm 5.3 \pm 3.5)$  pb, respectively, where the first uncertainties are

statistical and the second are systematic. The  $\omega\chi_0$  signals at the other seven energies and the  $e+e\rightarrow\omega\chi_1$  and  $\omega\chi_2$  signals are not significant, and the upper limits on the cross sections are determined. By examining the  $\omega\chi_0$  cross section as a function of center of mass energy, we find that it is inconsistent with the line shape of the  $Y(4260)$  observed in  $e+e\rightarrow\pi+\pi-J/\psi$ . Assuming the  $\omega\chi_0$  signals come from a single resonance, we extract the mass and width of the resonance to be  $(4230\pm 8\pm 6)$  MeV/c<sup>2</sup> and  $(38\pm 12\pm 2)$  MeV, respectively, and the statistical significance is more than  $9\sigma$ .

**WEB URL:** <http://journals.aps.org/prl/abstract/10.1103/PhysRevLett.114.092003>

**9. Jamil, M., Ali, M., Rasheed, A., Zubia, K., & Salimullah, M. (2015). Dust-lower-hybrid instability with fluctuating charge in quantum plasmas. *Physics of Plasmas (1994-present)*, 22(3), 032107.**

**ABSTRACT:**

The instability of Dust-Lower-Hybrid (DLH) wave is examined in detail in the uniform dusty magnetoplasmas. The time dependent charging effects on dust particles around its equilibrium charge  $Q_{d0}$  are taken into account based on Orbit-Limited Probe theory. The quantum characteristics of the system like Bohm potential and Fermi degenerate pressure are dealt using the quantum hydrodynamic model of plasmas. The external magnetic field and size of the dust particles have new physical effects over the dissipative instability of DLH wave in the quantum plasma regime.

**WEB URL:** <http://scitation.aip.org/content/aip/journal/pop/22/3/10.1063/1.4914167>

**10. Bashir, M. F., & Vranjes, J. (2015). Drift wave stabilized by an additional streaming ion or plasma population. *Physical Review E*, 91(3), 033113.**

**ABSTRACT:**

It is shown that the universally unstable kinetic drift wave in an electron-ion plasma can very effectively be suppressed by adding an extra flowing ion (or plasma) population.

The effect of the flow of the added ions is essential, their response is of the type  $(v_{ph}-v_{f0})\exp[-(v_{ph}-v_{f0})^2]$ , where  $v_{f0}$  is the flow speed and  $v_{ph}$  is the phase speed parallel to the magnetic field vector. The damping is strong and it is mainly due to this ion exponential term, and this remains so for  $v_{f0} < v_{ph}$ .

**WEB URL:** <http://journals.aps.org/pre/abstract/10.1103/PhysRevE.91.033113>

**11. Javed, M. S., Dai, S., Wang, M., Guo, D., Chen, L., Wang, X., ... & Xi, Y. (2015). High performance solid state flexible supercapacitor based on molybdenum sulfide hierarchical nanospheres. *Journal of Power Sources*, 285, 63-69.**

**ABSTRACT:**

Molybdenum sulfide ( $\text{MoS}_2$ ) hierarchical nanospheres are synthesized using a hydrothermal method and characterized by X-ray powder diffraction, Brunauer–Emmett–Teller, scanning electron microscopy and transmission electron microscopy. The prepared  $\text{MoS}_2$  is used to fabricate solid state flexible supercapacitors which show excellent electrochemical performance such as high capacitance  $368 \text{ F g}^{-1}$  at a scan rate of  $5 \text{ mV s}^{-1}$  and high power density of  $128 \text{ W kg}^{-1}$  at energy density of  $5.42 \text{ Wh kg}^{-1}$ . The fabricated supercapacitor presents good characteristics such as lightweight, low cost, portability, high flexibility, and long term cycling stability by retaining 96.5% after 5000 cycles at constant discharge current of 0.8 mA. Electrochemical impedance spectroscopy (EIS) results reveal low resistance and suggest that  $\text{MoS}_2$  nanospheres would be a promising candidate for supercapacitors. Three charged supercapacitors connected in series can light 8 red color commercial light emitting diodes (LEDs) for 2 min, demonstrating its capability as a good storage device.

**WEB URL:** <http://www.sciencedirect.com/science/article/pii/S0378775315004954>

**12. De Sao Carlos, F. (2015). Enhanced Near-Infrared Emission Of Er 3-Doped Tellurite Glass Containing Silver Nanoparticles. *Chalcogenide Letters*, 12(3), 123-128.**

**ABSTRACT:**

The broadband luminescence of the Er<sup>3+</sup> -doped glasses is an excellent optical feature to develop the telecommunication devices. In this report, the effect of silver nanoparticles (NPs) on the near-infrared luminescence properties of Er<sup>3+</sup> -doped tellurite glasses is studied. The growth of NPs is attained by heat-treatment above the glass transition temperature. Transmission electron microscopic technique revealed the presence of NPs with average size of 14 nm. Under 980 nm excitation wavelength, the broadband of Er<sup>3+</sup> ions is enhanced by increasing the heat-treatment duration up to 10 h. The involved mechanisms are described to discuss the observed enhancement.

**WEB URL:** [http://chalcogen.ro/123\\_Dousti.pdf](http://chalcogen.ro/123_Dousti.pdf)

**13. Razaq, A., Asif, M. H., Kalsoom, R., Khan, A. F., Awan, M. S., Ishrat, S., & Ramay, S. M. (2015). Conductive and electroactive composite paper reinforced by coating of polyaniline on lignocelluloses fibers. *Journal of Applied Polymer Science*, 132(29).**

**ABSTRACT:**

Direct use of lignocelluloses fibers as substrate for fabrication of conductive, electroactive, biodegradable, and low-cost electrode materials are in demand for high-tech applications of ion-exchange and energy storage devices. This article presents the preparation and characterizations of conductive and electroactive lignocelluloses-polyaniline (cellulose/PANI) composite paper. Lignocelluloses fibers were directly collected from the stem of self-growing plant, *Typha Angustifolia*, and subsequently coated with the conductive and electroactive layer of PANI through chemical synthesis. Individual PANI-coated lignocelluloses fibers were converted into sheet and further characterized with Scanning Electron Microscopy, Fourier Transform Infrared, Thermogravimetric Analysis, electronic conductivity, and Cyclic Voltammetry. Cellulose/PANI composite paper revealed superior thermal characteristics and used as a working electrode in three different electrolytes for ion-exchange properties. Conductive composite paper (CCP) showed the charge storage capacity of ~52 C/g at

scan rate of 5 mV/s in 2M HCl solution. © 2015 Wiley Periodicals, Inc. J. Appl. Polym. Sci. 2015, 132, 42293.

**WEB URL:** <http://onlinelibrary.wiley.com/doi/10.1002/app.42293/full>

**14. Razaq, A., Idrees, M., Malik, A., Mushtaq, N., Nadeem, M., Hussain, I., & Yar, M. (2015). Dielectric studies of composite paper reinforced with polypyrrole coated pulp fibers from wasted egg holders. *Journal of Applied Polymer Science*, 132(33).**

**ABSTRACT:**

Development of thin, flexible, light-weight, renewable, low-cost, and environmentally friendly electrode materials are highly feasible in era of modern disposable electronic technology. This article presents the synthesis and dielectric studies of polypyrrole (PPy) coated pulp fibers, directly collected from wasted egg holder's tray. PPy coated pulp fibers converted into compact sheet for the development of potential renewable and low-cost electrode materials. The morphology, chemical structure, and thermal stability of naked and PPy coated pulp fibril sheets were investigated by scanning electron microscopy (SEM), Fourier transform infrared (FTIR) and thermogravimetric analysis (TGA), respectively. PPy coated pulp fibers revealed better thermal stability and compactness of sheet morphology. Impedance measurements showed a high value of dielectric constant of  $1.15 \times 10^6$  at 0.5 Hz and conductivity of  $7.45 \times 10^{-4}$  S/cm at room temperature for PPy coated pulp fibril sheet.

**WEB URL:** <http://onlinelibrary.wiley.com/doi/10.1002/app.42422/full>

**15. S., Nisar (BESS Collaboration). (2015). Precision Measurement of  $B(\psi(3770) \rightarrow \gamma \chi_{c1})$  and Search for  $B(\psi(3770) \rightarrow \gamma \chi_{c2})$  with  $\chi_{c1, 2} \rightarrow \gamma J/\psi \rightarrow \gamma \ell^+ \ell^-$ . *arXiv preprint arXiv:1504.07450*.**

**ABSTRACT:**

We report a measurement of the branching fraction of  $\psi(3770) \rightarrow \gamma \chi_{c1}$  and search for the transition  $\psi(3770) \rightarrow \gamma \chi_{c2}$  based on  $2.92 \times 10^7$  of  $e^+e^-$  data accumulated

at  $\sqrt{s}=3.773\sim\text{GeV}$  with the BESIII detector at the BEPCII collider. The measured branching fraction of  $\psi(3770)\rightarrow\gamma\chi_{c1}$  is  $B(\psi(3770)\rightarrow\gamma\chi_{c1})=(2.48\pm 0.15\pm 0.23)\times 10^{-3}$ , which is the most precise measurement to date. The upper limit on the branching fraction of  $\psi(3770)\rightarrow\gamma\chi_{c2}$  at a 90% confidence level is  $B(\psi(3770)\rightarrow\gamma\chi_{c2})<0.64\times 10^{-3}$ . The corresponding partial widths are  $\Gamma(\psi(3770)\rightarrow\gamma\chi_{c1})=(67.5\pm 4.1\pm 6.7)\sim\text{keV}$  and  $\Gamma(\psi(3770)\rightarrow\gamma\chi_{c2})<17.4\sim\text{keV}$ .

**WEB URL:** <http://arxiv.org/abs/1504.07450>

**16. S., Nisar (BESS Collaboration) (2015). Observation of the Dalitz Decay  $\eta' \rightarrow \gamma e^+e^-$ . *Phys.Rev. D.91*.**

Abstract not found

**17. Ablikim, M., Achasov, M. N., Ai, X. C., Albayrak, O., Albrecht, M., Ambrose, D. J., ... & Ferroli, R. B. (2015). Observation of the electromagnetic doubly OZI-suppressed decay  $J/\psi \rightarrow \phi \pi^0$ . *arXiv preprint arXiv:1504.03194*.**

**ABSTRACT:**

Using a sample of 1.31 billion  $J/\psi$  events accumulated with the BESIII detector at the BEPCII collider, we report the observation of the decay  $J/\psi \rightarrow \phi \pi^0$ , which is the first evidence for a doubly Okubo-Zweig-Iizuka suppressed electromagnetic  $J/\psi$  decay. A clear structure is observed in the  $K+K^-$  mass spectrum around 1.02 GeV/c<sup>2</sup>, which can be attributed to interference between  $J/\psi \rightarrow \phi \pi^0$  and  $J/\psi \rightarrow K+K-\pi^0$  decays. Due to this interference, two possible solutions are found. The corresponding measured values of the branching fraction of  $J/\psi \rightarrow \phi \pi^0$  are  $[2.94\pm 0.16(\text{stat.})\pm 0.16(\text{syst.})]\times 10^{-6}$  and  $[1.24\pm 0.33(\text{stat.})\pm 0.30(\text{syst.})]\times 10^{-7}$ .

**WEB URL:** <http://arxiv.org/abs/1504.03194>

18. Ablikim, M., Achasov, M. N., Ai, X. C., Albayrak, O., Albrecht, M., Ambrose, D. J., ... & Ferroli, R. B. (2015). Measurement of the proton form factor by studying  $e^+e^- \rightarrow p\bar{p}$ . *arXiv preprint arXiv:1504.02680*.

**ABSTRACT:**

Using data samples collected with the BESIII detector at the BEPCII collider, we measure the Born cross section of  $e^+e^- \rightarrow p\bar{p}$  at 12 center-of-mass energies from 2232.4 to 3671.0 MeV. The corresponding effective electromagnetic form factor of the proton is deduced under the assumption that the electric and magnetic form factors are equal ( $|G_E|=|G_M|$ ). In addition, the ratio of electric to magnetic form factors,  $|G_E/G_M|$ , and  $|G_M|$  are extracted by fitting the polar angle distribution of the proton for the data samples with larger statistics, namely at  $\sqrt{s} = 2232.4$  and 2400.0 MeV and a combined sample at  $\sqrt{s} = 3050.0, 3060.0$  and 3080.0 MeV, respectively. The measured cross sections are in agreement with recent results from BaBar, improving the overall uncertainty by about 30%. The  $|G_E/G_M|$  ratios are close to unity and consistent with BaBar results in the same  $q^2$  region, which indicates the data are consistent with the assumption that  $|G_E|=|G_M|$  within uncertainties.

**WEB URL:** <http://arxiv.org/abs/1504.02680>

19. Ablikim, M., Achasov, M. N., Ai, X. C., Albayrak, O., Albrecht, M., Ambrose, D. J., ... & Ferroli, R. B. (2015). Measurements of  $\psi(3686)$  to  $K^-\Lambda\bar{\Xi}^+$  and  $\psi(3686)$  to  $\gamma K^-\Lambda\bar{\Xi}^+$ . *arXiv preprint arXiv:1504.02025*.

**ABSTRACT:**

Using a sample of  $1.06 \times 10^8$   $\psi$  events produced in  $e^+e^-$  collisions at  $\sqrt{s} = 3.686$  GeV and collected with the BESIII detector at the BEPCII collider, we present studies of the decays  $\psi \rightarrow K^+K^-c.c.$  and  $\psi \rightarrow \gamma K^+K^-c.c.$ . We observe two hyperons,  $\Xi(1690)^-$  and  $\Xi(1820)^-$ , in the  $K-\Lambda$  invariant mass distribution in the decay  $\psi \rightarrow K^+K^-c.c.$  with significances of  $4.9\sigma$  and  $6.2\sigma$ , respectively. The branching

fractions of  $\psi_{kx+c.c.}$ ,  $\psi_{ksx+c.c.}$ ,  $\psi_{\text{psip}\to\gamma \chi_{cJ}\to \gamma K^- \Lambda} \bar{\chi}^+ +c.c.$  ( $J=0, 1, 2$ ), and  $\psi_{\text{psip}\to \chi(1690/1820)^{-} \bar{\chi}^+ +c.c.}$  with subsequent decay  $\Xi(1690/1820) \rightarrow K^- \Lambda$  are measured for the first time.

**WEB URL:** <http://arxiv.org/abs/1504.02025>

**20. Azmat, I., & Afaq, A. (2015). Photodetachment of H<sup>-</sup> near a hard wall with arbitrary laser polarization direction. *Chinese Physics B*, 24(8), 083201.**

**ABSTRACT:**

The photodetachment of H<sup>-</sup> near a hard wall is investigated with linear polarized laser light travelling in arbitrary direction  $\vartheta_L$  with respect to the z axis. An analytical formula for the total cross section is derived using semi-classical closed orbit theory, which consists of two terms, i.e., the smooth background term and the oscillatory term with an extra factor  $2(\vartheta_L)$ . This factor controls oscillations in the total photodetachment cross section. The amplitude of oscillation is maximum at  $\vartheta_L = 0$  when the laser polarization direction is perpendicular to the wall and it approaches zero at  $\vartheta_L = \pi/2$  when the laser polarization direction is parallel to the wall. It is also observed that the total cross section depends on the source-wall distance and it reduces to a free space case when the wall is at infinite distance from the source.

**WEB URL:** <http://iopscience.iop.org/article/10.1088/1674-1056/24/8/083201/meta>

**21. Dousti, M. R., & Amjad, R. J. (2015). Spectroscopic properties of Tb<sup>3+</sup>-doped lead zinc phosphate glass for green solid state laser. *Journal of Non-Crystalline Solids*, 420, 21-25.**

**ABSTRACT:**

This work reports the spectroscopic properties of a new Tb<sup>3+</sup>-doped zinc lead phosphate glass, prepared by a conventional melt-quenching technique. Glasses show good rare earth solubility and high thermal stability. Optical properties of the glasses are studied by absorption, photoluminescence excitation and emission spectroscopy and lifetime

measurement. Several luminescence bands of Tb<sup>3+</sup> ions are observed under 376 nm excitation wavelength in 400–650 nm spectral region. The green to blue intensity ratio increases by concentration of terbium ions up to 5 mol%. The lifetime of the <sup>5</sup>D<sub>4</sub> excited state was found to be 2.70 to 2.54 ms for low and high concentration of dopant ions, respectively. The strong green emission of the studied glasses with large experimental branching ratio highlights their capability as solid state green lasers.

**WEB URL:** <http://www.sciencedirect.com/science/article/pii/S0022309315001568>

**22. Amin, N., Afzal, M., Yousaf, M., & Javid, M. A. (2015). Choice of the pulse sequence and parameters for improved signal-to-noise ratio in T1-weighted study of MRI. *JPMA. The Journal of the Pakistan Medical Association*,65(5), 512-518.**

**ABSTRACT:**

Objective: To investigate the practical impact of alteration of imaging parameters on signal-to-noise ratio for the most commonly used T1-weighted magnetic resonance sequences. Methods: The study was conducted in the Department of Medical Physics, Ninewells Hospital and Medical School, Dundee, UK, in 2007. Magnetic resonance images of a tissue-equivalent material were generated with a set of T1 and T2 values. Experimental variations in the imaging parameters were performed in echo time and repetition time. Quantitative analysis consisted of signal-to-noise ratio. Results: Percentage inaccuracy in signal-to-noise ratio was the result of inappropriate choice of parameters. We have investigated conventional spin echo, fast spin echo and fast fluid attenuated inversion recovery with one of corresponding percentage errors 28.68%, -36.65% and -40.34%, respectively. Conventional spin echo presented moderately low percentage error with the choice of repetition time and echo time. Factual error in fast spin echo was slightly higher than conventional spin echo. Fast fluid attenuated inversion recovery could create outstanding signal-to-noise ratio of high T1/T2 value phantoms in T1-weighted images. Conclusion: The role of repetition time and echo time in T1-weighted images was crucial to sustain the image quality.

**WEB URL:** <http://www.jpma.org.pk/PdfDownload/7348.pdf>

**23. Hong, W. P., Jamil, M., Rasheed, A., & Jung, Y. D. (2015). Quantum Electron-Exchange Effects on the Buneman Instability in Quantum Plasmas. *Zeitschrift für Naturforschung A*, 70(6), 413-418.**

**ABSTRACT:**

The quantum-mechanical electron-exchange effects on the Buneman instability are investigated in quantum plasmas. The growth rate and wave frequency of the Buneman instability for the quantum plasma system composed of the moving electron fluid relative to the ion fluid are obtained as functions of the electron-exchange parameter, de Broglie's wave length, Debye's length, and wave number. The result shows that the electron-exchange effect suppresses the growth rate of the quantum Buneman instability in quantum plasmas. It is also shown that the influence of electron exchange reduces the instability domain of the wave number in quantum plasmas. However, the instability domain enlarges with an increase in the ratio of the Debye length to the de Broglie wave length. In addition, the electron-exchange effect on the growth rate of the Buneman instability increases with an increase in the ratio of the Debye length to the de Broglie wave length. The variation in the growth rate of the Buneman instability due to the change in the electron-exchange effect and plasma parameters is also discussed.

**WEB URL:** <http://www.degruyter.com/view/j/zna.2015.70.issue-6/zna-2015-0080/zna-2015-0080.xml>

**24. Akram, M., Bashir, S., Rafique, M. S., Hayat, A., Mahmood, K., Dawood, A., & Bashir, M. F. (2015). Morphological and spectroscopic characterization of laser-ablated tungsten at various laser irradiances. *Applied Physics A*, 119(3), 859-870.**

**ABSTRACT:**

The variation in surface morphology and plasma parameters of laser irradiated tungsten has been investigated as a function of irradiance. For this purpose, Nd:YAG laser (1064 nm, 10 ns, 10 Hz) is employed. Tungsten targets were exposed to various laser irradiances ranging from 6 to 50 GW/cm<sup>2</sup> under ambient environment of argon at a

pressure of 20 Torr. Scanning electron microscope analysis has been performed to analyze the surface modification of irradiated tungsten. It revealed the formation of micro- and nanoscale surface structures. In central ablated area, distinct grains and crack formation are observed, whereas peripheral ablated areas are dominated by cones and pinhole formation. It was observed that at irradiances exceeding a value of 13 GW/cm<sup>2</sup>, the morphological trend of the observed structures has been changed from erosion to melting and re-deposition dominant phase. Ablation efficiency as a function of laser irradiance has also been investigated by measuring the crater depth using surface profilometry analysis. It is found to be maximum at an irradiance of 13 GW/cm<sup>2</sup> and decreases at high laser irradiances. In order to correlate the accumulated effects of plasma parameters with the surface modification, laser-induced breakdown spectroscopy analysis has been performed. The electron temperature and number density of tungsten plasma have been evaluated at various laser irradiances. Initially with the increase of the laser irradiance up to 13 GW/cm<sup>2</sup>, an increasing trend is observed for both plasma parameters due to enhanced energy deposition. Afterward, a decreasing trend is achieved which is attributed to the shielding effect. With further increase in irradiance, a saturation stage comes and insignificant changes are observed in plasma parameters. This saturation is explainable on the basis of the formation of a self-regulating regime near the target surface. Surface modifications of laser irradiated tungsten have been correlated with plasma parameters.

**WEB URL:** <http://link.springer.com/article/10.1007/s00339-015-9052-0>

**25. Bashir, M. F., Behery, E. E., & El-Taibany, W. F. (2015). Effect of anisotropic dust pressure and superthermal electrons on propagation and stability of dust acoustic solitary waves. *Physics of Plasmas (1994-present)*, 22(6), 062112.**

**ABSTRACT:**

Employing the reductive perturbation technique, Zakharov–Kuznetsov (ZK) equation is derived for dust acoustic (DA) solitary waves in a magnetized plasma which consists the

effects of dust anisotropic pressure, arbitrary charged dust particles, Boltzmann distributed ions, and Kappa distributed superthermal electrons. The ZK solitary wave solution is obtained. Using the small- $k$  expansion method, the stability analysis for DA solitary waves is also discussed. The effects of the dust pressure anisotropy and the electron superthermality on the basic characteristics of DA waves as well as on the three-dimensional instability criterion are highlighted. It is found that the DA solitary wave is rarefactive (compressive) for negative (positive) dust. In addition, the growth rate of instability increases rapidly as the superthermal spectral index of electrons increases with either positive or negative dust grains. A brief discussion for possible applications is included.

**WEB URL:** <http://scitation.aip.org/content/aip/journal/pop/22/6/10.1063/1.4922750>

**26. Naim, H., Bashir, M. F., Vranjes, J., & Murtaza, G. (2015). Kinetic instability of drift magnetosonic wave in anisotropic low beta plasmas. *Physics of Plasmas (1994-present)*, 22(6), 062117.**

**ABSTRACT:**

The kinetic instability of the obliquely propagating drift magnetosonic wave for temperature anisotropic low beta plasmas is studied by using the gyro-kinetic model. The interplay between the temperature anisotropy and the density inhomogeneity free energy sources is discussed in order to provide stabilization of drift instability by the temperature anisotropy effect. It is shown that the anisotropy suppresses the growth rate when the anisotropy ratio  $A_{e,i} (=T_{\perp}(e,i)/T_{\parallel}(e,i))$  is greater than unity, whereas it enhances the growth rate for  $A_{e,i} < 1$ . Comparison of kinetic instability with reactive instability [Naim *et al.*, Phys. Plasmas 21, 102112 (2014)] and the scaling of growth time with the diffusion and the anisotropy relaxation times are presented. Additionally, the stability analysis applicable to a wide range of plasma parameters is also performed.

**WEB URL:** <http://scitation.aip.org/content/aip/journal/pop/22/6/10.1063/1.4923297>

**27. Dousti, M. R., & Amjad, R. J. (2015). Enhanced green emission of terbium-ions-doped phosphate glass embedding metallic nanoparticles. *Journal of Nanophotonics*, 9(1), 093068-093068.**

**ABSTRACT:**

Tb<sup>3+</sup>-doped glasses are promising materials for green lasers working at a UV-excitation light. It is essential to find a commercially low-cost host with high quantum efficiency in the visible region. We report the preparation and optical characterization of a thermally stable and optically transparent phosphate glass containing silver nanoparticles with nominal composition 57P2O5-40(ZnO-PbO)-2Tb2O3-1AgNO3 (mol%) obtained by a melt-quenching technique and subsequent heat-treatments. The glasses are transparent in UV to near-infrared region and are not hygroscopic at ambient environment. The optical absorption and luminescence excitation spectra of the samples with and without silver nanoparticles are identical, and no sign of any silver species is revealed, while the luminescence spectrum is enhanced up to 1.7 times after heat-treating the samples for 15 h. The transmission electron microscopy and selected area diffraction pattern of glasses show the presence of silver nanoparticles with an average size of ~15 nm and growth at [200] crystallographic direction. The lifetime of the <sup>5</sup>D<sub>4,5</sub> state of Tb<sup>3+</sup> ions decreases from 3.06 to 2.85 ms by increasing the heat-treatment duration, which is indicative of the plasmonic effect of nanoparticles on the radiative rates of Tb<sup>3+</sup>-doped glasses.

**WEB URL:** <http://nanophotonics.spiedigitallibrary.org/article.aspx?articleid=2375474>

**28. Javed, Q. U. A., Abbas, H., Mahmood, H., Sattar, A., Wang, F. P., Kamran, M. A., ... & Toufiq, A. M. (2015, July). Morphology-Controlled Synthesis of Single Crystalline  $\alpha$ -Mn<sub>2</sub>O<sub>3</sub> Sea-Urchins Assembled with Pen-Type Nanoneedles and Broad Absorption Spectrum. In *Journal of Nano Research*(Vol. 33, pp. 38-48).**

**ABSTRACT:**

Single crystalline high quality  $\alpha$ -Mn<sub>2</sub>O<sub>3</sub> nanorods and sea-urchins assembled with pen-type nanoneedles have been successfully synthesized by template-free hydrothermal route. The variation in hydrothermal temperature has affected the morphology of the  $\alpha$ -Mn<sub>2</sub>O<sub>3</sub> sea-urchin assembled with the nanoneedles noticeably. The influence of temperature change on the thickness, crystallinity, surface morphology and optical properties of  $\alpha$ -Mn<sub>2</sub>O<sub>3</sub> has been characterized by X-ray Diffraction (XRD), Scanning Electron Microscopy (SEM), Energy Dispersive X-ray (EDX) analysis, Transmission Electron Microscopy (TEM), High Resolution Transmission Electron Microscopy (HRTEM), Raman Spectroscopy (RS) and UV-visible Spectroscopy. The results showed that in our experimental conditions, single crystalline nanorods of the  $\alpha$ -Mn<sub>2</sub>O<sub>3</sub> were obtained at a low temperature of 180 °C, while single crystalline sea-urchin assembled with pen-type nanoneedles were obtained by increasing the temperature to 280 °C. Nanorods and sea-urchin assembled with pen-type nanoneedles obtained had the well-defined morphology and crystalline quality. The sea-urchin synthesized at 280 °C exhibited more than 90% absorption in UV-visible spectrum.

**WEB URL:** <http://www.scientific.net/JNanoR.33.38>

**29. Ul Hasan, K., Asif, M. H., Hassan, M. U., Sandberg, M. O., Nur, O., Willander, M., ... & Strålfors, P. (2015). A miniature graphene-based biosensor for intracellular glucose measurements. *Electrochimica Acta*, 174, 574-580.**

**ABSTRACT:**

We report on a small and simple graphene-based potentiometric sensor for the measurement of intracellular glucose concentration. A fine borosilicate glass capillary coated with graphene and subsequently immobilized with glucose oxidase (GOD) enzyme is inserted into the intracellular environment of a single human cell. The functional groups on the edge plane of graphene assist the attachment with the free amine terminals of GOD enzyme, resulting in a better immobilization. The sensor

exhibits a glucose-dependent electrochemical potential against an Ag/AgCl reference microelectrode which is linear across the whole concentration range of interest (10 – 1000  $\mu$ M). Glucose concentration in human fat cell measured by our graphene-based sensor is in good agreement with nuclear magnetic resonance (NMR) spectroscopy.

**WEB URL:** <http://www.sciencedirect.com/science/article/pii/S0013468615014061>

**30. Akhtar, N. M., Yahya, N., Sattar, A., Ahmad, M., Idrees, M., Hasan Asif, M., & Azhar Khan, M. (2015). Investigations of Structural and Magnetic Properties of Nanostructured Ni<sub>0.5+x</sub>Zn<sub>0.5-x</sub>Fe<sub>2</sub>O<sub>4</sub> Magnetic Feeders for CSEM Application. *International Journal of Applied Ceramic Technology*, 12(3), 625-637.**

**ABSTRACT:**

Marine CSEM is a new technique for detection of deep target hydrocarbons. Aluminum EM antenna was developed, and nanostructured NiZn magnetic feeders were used to increase the field strength from EM antenna for deep hydrocarbons. The doping of Ni<sup>2+</sup> was aimed at the optimization of initial permeability and magnetic losses. Ni<sub>0.5+x</sub>Zn<sub>0.5-x</sub>Fe<sub>2</sub>O<sub>4</sub> ( $x = 0.3$ ) samples sintered at 950°C presented highest initial permeability (106.23) and low magnetic loss (0.0002) as compared to other samples. Due to better magnetic properties, Ni<sub>0.5+x</sub>Zn<sub>0.5-x</sub>Fe<sub>2</sub>O<sub>4</sub> ( $x = 0.3$ ) samples were used as magnetic feeders for EM antenna. Magnitude of EM waves from the antenna increased up to 186%.

**WEB URL:** <http://onlinelibrary.wiley.com/doi/10.1111/ijac.12222/full>

**31. Hussain, S. Q., Yen, C., Khan, S., Kwon, G. D., Kim, S., Ahn, S., ... & Yi, J. (2015). Uniform 3D hydrothermally deposited zinc oxide nanorods with high haze ratio. *Materials Science in Semiconductor Processing*, 37, 99-104.**

**ABSTRACT:**

We present low cost hydrothermally deposited uniform zinc oxide (ZnO) nanorods with high haze ratios for the a-Si thin film solar cells. The problem of low transmittance and

conductivity of hydrothermally deposited ZnO nanorods was overcome by using RF magnetron sputtered aluminum doped zinc oxide (ZnO:Al ~300 nm) films as a seed layer. The length and diameters of the ZnO nanorods were controlled by varying growth times from 1 to 4 h. The length of the ZnO nanorods was varied from 1 to 1.5  $\mu\text{m}$ , while the diameter was kept larger than 300 nm to obtain various aspect ratios. The uniform ZnO nanorods showed higher transmittance (~89.07%) and haze ratio in the visible wavelength region. We also observed that the large diameters (>300 nm) and average aspect ratio (3–4) of ZnO nanorods favored the light scattering in the longer wavelength region. Therefore, we proposed uniformly deposited ZnO nanorods with high haze ratio for the future low cost and large area amorphous silicon thin film solar cells.

**WEB URL:** <http://www.sciencedirect.com/science/article/pii/S1369800115001043>

**32. Hussain, S. Q., Kwon, G. D., Ahn, S., Kim, S., Park, H., Le, A. H. T., ... & Balaji, N. (2015). SF<sub>6</sub>/Ar plasma textured periodic glass surface morphologies with high transmittance and haze ratio of ITO: Zr films for amorphous silicon thin film solar cells. *Vacuum*, 117, 91-97.**

**ABSTRACT:**

We report various SF<sub>6</sub>/Ar plasma textured periodic glass surface morphologies with high transmittance, haze ratio, and root mean square (rms) roughness of ITO:Zr films for amorphous silicon thin film solar cells (a-Si TFSCs). SF<sub>6</sub>/Ar plasma textured glass surface morphologies contain micro- and nano-textured features that help to scatter the light in visible and near infra-red (NIR) wavelength regions. We designed the textured glass surface morphologies with big square craters to smaller pyramids for various glass etching times from 30 to 75 min. Magnetron sputtered ITO:Zr (~210 nm) films were deposited on textured glass surface morphologies and showed higher transmittance and haze ratio of 88.48% and 77.61%, respectively, in the visible-NIR (400–1100 nm) wavelength region. The sheet resistance and resistivity of ITO:Zr films decreased with the increase of etching time, due to high rms roughness and better step coverage. A passivation AZO (30 nm) layer was added to the ITO:Zr films, due to its better stability

against hydrogen plasma exposure. The ITO:Zr/AZO films were employed as a front TCO layer and the current density–voltage (J–V) characteristics of a-Si TFSCs increased by light scattering effect, without any reduction in either the open circuit voltage ( $V_{oc}$ ) or the fill factor (FF). Relative to flat glass substrate,  $J_{sc}$  and the efficiency of a-Si TFSCs were enhanced by 7.51% and 19.39%, respectively, for textured glass surface morphology.

**WEB URL:** <http://www.sciencedirect.com/science/article/pii/S0042207X15001396>

**33. Çetin, S. A., & BESIII Collaboration. (2015). Search for  $D^0 \rightarrow \gamma \gamma$  and improved measurement of the branching fraction for  $D^0 \rightarrow \pi^0 \pi^0$ .**

**ABSTRACT:**

Using 2.92 fb<sup>-1</sup> of electron-positron annihilation data collected at root  $s = 3.773$  GeV with the BESIII detector, we report the results of a search for the flavor-changing neutral current process  $D^0 \rightarrow \gamma \gamma$  using a double-tag technique. We find no signal and set an upper limit at 90% confidence level for the branching fraction of  $B(D^0 \rightarrow \gamma \gamma) < 3.8 \times 10^{-6}$ . We also investigate  $D^0$ -meson decay into two neutral pions, obtaining a branching fraction of  $B(D^0 \rightarrow \pi^0 \pi^0) = (8.24 \pm 0.21(\text{stat}) \pm 0.30(\text{syst})) \times 10^{-4}$ , the most precise measurement to date and consistent with the current world average.

**WEB URL:** <http://openaccess.dogus.edu.tr/handle/11376/1865>

**34. Usman, A., Rafique, M. S., Shaukat, S. F., Anjum, S., Latif, H., & Sattar, A. (2015). Morphology, Structural And Electrical Transport Properties Of Graphite Based Multilayer Thin Films. *Digest Journal Of Nanomaterials And Biostructures*, 10(3), 915-925**

**ABSTRACT:**

Silver doped graphite multilayer films were grown on silicon substrate by employing a modified pulsed laser ablation (PLA) process. Excimer laser ( $\lambda=248\text{nm}$ ) was used for the deposition of these films. The effects of Ag incorporation on the micro structure as well

as on surface morphologies were investigated using Raman Spectroscopy, XRD and AFM. The structural investigation reveals that diamond phase reduces gradually by the incorporation of silver content. It was also observed that Ag doping enhanced the  $sp^2$  fraction in films which is a clear indication of graphitization. The surface analysis revealed that some clustering was observed on the surface which is due to encapsulation of silver nano particles within carbon network. Some elevated textures were also found on surface. A small change in surface roughness was also observed which is ranging from 2.41 nm to 10.1 nm. The optical band gap ( $E_g$ ) has been reduced exponentially from 2.11 eV to 1.55 eV. Electrical measurement illustrated that the resistivity also decrease exponentially with an increase in Ag content

**WEB URL:** [http://www.chalcogen.ro/915\\_Usman.pdf](http://www.chalcogen.ro/915_Usman.pdf)

**35. Idrees, M., Nadeem, M., Siddiqi, S. A., Ahmad, R., Hussnain, A., & Mehmood, M. (2015). The organic residue and synthesis of  $LaFeO_3$  by combustion of citrate and nitrate precursors. *Materials Chemistry and Physics*, 162, 652-658.**

**ABSTRACT:**

Perovskite type  $LaFeO_3$  has been synthesized by autocombustion of the gel complex obtained from citrate and metal nitrate precursors. The crystallinity in the as-combusted powder and effects of heat treatment temperature up to 800 °C have been investigated by XRD. Thermal stability of the organic residue obtained after combustion has been studied by TGA of as-combusted powder and FTIR analysis after heat treatment at different temperatures. In addition to the crystalline  $LaFeO_3$ , amorphous organic residue was found in the as-combusted powder that gradually decomposed upon heat treatment. Effects of the amorphous organic residue on the dielectric properties of  $LaFeO_3$  has been explored and discussed in details by collecting the room temperature ac impedance data in a wide frequency range for the synthesized samples. The amorphous organic residue strongly alter the resistive and dielectric properties of  $LaFeO_3$ . The frequency response of the dielectric polarization is associated with the

dielectric relaxations from the amorphous residual carbonates, crystalline LaFeO<sub>3</sub> grain interiors and the grain boundaries.

**WEB URL:** <http://www.sciencedirect.com/science/article/pii/S0254058415301814>

**36. S., Nisar (BESS Collaboration). (2015). Observation of  $\eta' \rightarrow \omega e^+ e^-$  Phys.Rev. D. 92. 5, 051101.**

**ABSTRACT:**

Based on a sample of  $\eta'$  mesons produced in the radiative decay  $J/\psi \rightarrow \gamma \eta'$  in  $1.31 \times 10^9$   $J/\psi$  events collected with the BESIII detector, the decay  $\eta' \rightarrow \omega e^+ e^-$  is observed for the first time, with a statistical significance of  $8\sigma$ . The branching fraction is measured to be  $B(\eta' \rightarrow \omega e^+ e^-) = (1.97 \pm 0.34(\text{stat}) \pm 0.17(\text{syst})) \times 10^{-4}$ , which is in agreement with theoretical predictions. The branching fraction of  $\eta' \rightarrow \omega \gamma$  is also measured to be  $(2.55 \pm 0.03(\text{stat}) \pm 0.16(\text{syst})) \times 10^{-2}$ , which is the most precise measurement to date, and the relative branching fraction  $B(\eta' \rightarrow \omega e^+ e^-) B(\eta' \rightarrow \omega \gamma)$  is determined to be  $(7.71 \pm 1.34(\text{stat}) \pm 0.54(\text{syst})) \times 10^{-3}$ .

**WEB URL:** <http://inspirehep.net/record/1384776>

**37. S., Nisar (BESS Collaboration). (2015). Search for  $Z_c(3900)^\pm \rightarrow \omega \pi^\pm$  Phys.Rev. D.92. no.3, 032009.**

**ABSTRACT:**

The decay  $Z_c(3900)^\pm \rightarrow \omega \pi^\pm$  is searched for using data samples collected with the BESIII detector operating at the BEPCII storage ring at center-of-mass energies  $\sqrt{s} = 4.23$  and 4.26 GeV. No significant signal for the  $Z_c(3900)^\pm$  is found, and upper limits at the 90% confidence level on the Born cross section for the process  $e^+ e^- \rightarrow Z_c(3900)^\pm \pi^\mp \rightarrow \omega \pi^+ \pi^-$  are determined to be 0.26 and 0.18 pb at  $\sqrt{s} = 4.23$  and 4.26 GeV, respectively.

**WEB URL:** <http://inspirehep.net/record/1381936>

**38. Ellahi, M., Rafique, M. Y., Gao, Y., Ali, M. F., Cao, H., & Yang, H. (2015). Study on the effects of isotropic cross-linked pristine morphology and electro-optical properties of PDLC films. *Polymer Bulletin*, 72(11), 2917-2930.**

**ABSTRACT:**

PDLC films were prepared by polymerization-induced phase separation (PIPS) method along with varying composition ratio between curable epoxy monomers/poly-oxypropylene-di-amine (POPDA) cross-linking agent/Class  $\alpha$ , longitudinal nematic liquid crystal (LC) linear chain polymer mixtures and their optical and pristine morphological properties have been analyzed to investigate their suitability as aligned nematic phase of LC. The refractive index of isotropic cross-linked polymer network could be influenced by the relative content of curable monomers structure PPGDE ~380 and PPGDE ~640 which increased the LC droplet size with POPDA. Meanwhile, it is examined that the decreasing of peel strength and transmittance of all the samples decrease of wavelength in the wavelength range of 300–800 nm due to the lower cross-linking density of the polymer network with effect of strongly influenced by the alkoxy (R-O) and flexible chain length of curable monomers, which also affect the electro-optical properties and droplet size of LC in PDLC films. Our results demonstrate that the LC droplet size of the isotropic cross-linked polymer network could be regulated by adjusting the monomers structure, composition ratio, relative wt% of POPDA, PPGDE ~380 and PPGDE ~640; then aligned nematic phase of LC have the optical properties of uniaxial crystals and their potential applications for PDLC smart glass market and display fields.

**WEB URL:** <http://link.springer.com/article/10.1007/s00289-015-1444-y>

**39. Hong, W. P., Jamil, M., Rasheed, A., & Jung, Y. D. (2015). Karpman-Washimi magnetization with electron-exchange effects in quantum plasmas. *Physics of Plasmas* (1994-present), 22(7), 073302.**

**ABSTRACT:**

The influence of quantum electron-exchange on the Karpman-Washimi ponderomotive magnetization is investigated in quantum plasmas. The ponderomotive magnetization and the total radiation power due to the non-stationary Karpman-Washimi interaction related to the time-varying field intensity are obtained as functions of the de Broglie wave length, Debye length, and electron-exchange parameter. The result shows that the electron-exchange effect enhances the cyclotron frequency due to the ponderomotive interactions in quantum plasmas. It is also shown that the electron-exchange effect on the Karpman-Washimi magnetization increases with increasing wave number. In addition, the Karpman-Washimi magnetization and the total radiation power increase with an increase in the ratio of the Debye length to the de Broglie wave length. In streaming quantum plasmas, it is shown that the electron-exchange effect enhances the ponderomotive magnetization below the resonant wave number and, however, suppresses the ponderomotive magnetization above the resonant wave number. The variation of the Karpman-Washimi magnetization and the radiation power due to the variation of the electron-exchange effect and plasma parameters is also discussed.

**WEB URL:** <http://scitation.aip.org/content/aip/journal/pop/22/7/10.1063/1.4927134>

**40. Jamil, M., Rasheed, A., Rozina, C., Jung, Y. D., & Salimullah, M. (2015). Jeans instability with exchange effects in quantum dusty magnetoplasmas. *Physics of Plasmas (1994-present)*, 22(8), 082113.**

**ABSTRACT:**

Jeans instability is examined in magnetized quantum dusty plasmas using the quantum hydrodynamic model. The quantum effects are considered via exchange-correlation potential, recoil effect, and Fermi degenerate pressure, in addition to thermal effects of plasma species. It is found that the electron exchange and correlation potential have significant effects over the threshold value of wave vector and Jeans instability. The presence of electron exchange and correlation effect shortens the time of dust sound

that comparatively stabilizes the self gravitational collapse. The results at quantum scale are helpful in understanding the collapse of the self-gravitating dusty plasma systems.

**WEB URL:** <http://scitation.aip.org/content/aip/journal/pop/22/8/10.1063/1.4928437>

**41. Khan, A. A., Jamil, M., & Hussain, A. (2015). Wake potential with exchange-correlation effects in semiconductor quantum plasmas. *Physics of Plasmas (1994-present)*, 22(9), 092103.**

**ABSTRACT:**

Using the non-relativistic quantum hydrodynamic model, wake potential has been studied in a magnetized semiconductor quantum plasma in the presence of upper hybrid wave which is excited via externally injected electron beam. The quantum effect contains electron exchange and correlation potential, Fermi degenerate pressure, and Bohm potential. It is found that the contribution of quantum mechanical electron exchange and correlation potential significantly modifies the amplitude and the effective length of the oscillatory wake potential. In the electron-hole plasma systems, electron exchange-correlation effects tend to increase the magnitude of the wake potential and are much effective at the distances of the order of Debye-length. The application of the work in context of the semiconductor plasmas have also been analyzed graphically.

**WEB URL:** <http://scitation.aip.org/content/aip/journal/pop/22/9/10.1063/1.4929862>

**42. Ahmad, M., Ahmad, M., Ali, I., Ahmad, W., Mustafa, G., Akhtar, M. N., ... & Abbas, G. (2015). Temperature dependent structural and magnetic behavior of Y-type hexagonal ferrites synthesized by sol-gel autocombustion. *Journal of Alloys and Compounds*, 651, 749-755.**

**ABSTRACT:**

A Y-type hexaferrite ( $\text{Sr}_2\text{Ni}_2\text{Fe}_{12}\text{O}_{22}$ ) sample was synthesized using the sol-gel autocombustion and heat treated at different temperatures (800–1200 °C). Different experimental techniques such as differential thermal and thermo-gravimetric analyses,

X-ray diffraction, Fourier transform infrared spectroscopy, scanning electron microscopy, energy dispersive X-ray spectroscopy and vibrating sample magnetometry were used to investigate the sample. The X-ray diffraction analysis shows that Y-type hexaferrite begins to appear at 1000 °C and the formation of pure Y-type hexaferrite phase gets completed at 1200 °C. IR spectrum for sample heat treated at 1200 °C further confirms that single phase sample of Y-type hexagonal ferrite can be prepared at this temperature. The highest values of coercivity and saturation magnetization were achieved at a temperature of 1000 °C due to the presence of M-type hexaferrite. Moreover single phase Y-type hexaferrite sample has a coercivity of a few hundred oersteds which is suitable for security, switching, sensing and high frequency applications.

**WEB URL:** <http://www.sciencedirect.com/science/article/pii/S0925838815308409>

**43. Amjad, R. J., Dousti, M. R., Iqbal, A., Hussain, S. Z., Sahar, M. R., & Shaukat, S. F. (2015). Influence of silver nanoparticles on the luminescence dynamics of Dy 3+ doped amorphous matrix. *Measurement*, 74, 87-91.**

**ABSTRACT:**

In this work, we report on the deactivation of Dy<sup>3+</sup> ions by increase in concentration of silver nanoparticles (NPs) in a silicate glassy system. The quench in luminescence of Dy<sup>3+</sup> ions is consistent with increase in the long and short lifetime of <sup>4</sup>F<sub>9/2</sub> excited state which develops as the concentration of silver NPs increases by heat-treatment duration.

**WEB URL:** <http://www.sciencedirect.com/science/article/pii/S0263224115003371>

**44. Khan, M. A., Riaz, S., Ali, I., Akhtar, M. N., Murtaza, G., Ahmad, M., ... & Warsi, M. F. (2015). Structural and magnetic behavior evaluation of Mg–Tb ferrite/polypyrrole nanocomposites. *Ceramics International*, 41(1), 651-656.**

**ABSTRACT:**

Nanocrystalline  $Mg_{0.96}Tb_{0.04}Fe_2O_4$  spinel ferrite was prepared by the co-precipitation technique. The polypyrrole was synthesized by in situ polymerization method. The nanocomposites were fabricated by mixing the  $Mg_{0.96}Tb_{0.04}Fe_2O_4$  ferrite nanomaterials with polypyrrole polymer. The structural, morphological and magnetic properties of nanoferrite powder and nanocomposites were characterized by X-ray diffraction (XRD), Fourier transform infrared spectroscopy (FTIR), scanning electron microscopy (SEM) and vibrating sample magnetometer (VSM). The results of XRD revealed that the small concentrations of terbium ions are successfully incorporated into the spinel lattice. The intensity of the most intense peak increases with the increase of ferrite contents while its broadening is decreased. FTIR spectra demonstrated that there are interactions between ferrite particles and polypyrrole. SEM showed that the nanocomposites have core shell structure and inhomogeneous grain size distribution. Under the influence of applied magnetic field these nanocomposites displayed hysteresis loops which unfold the ferromagnetic behavior. The magnetic parameters such as saturation magnetization and coercivity of nanocomposites are affected by the increased concentration of ferrite particles. The magnetic parameters of nanocomposites are tailored by controlling the ferrite contents. Super paramagnetic behavior of two compositions (FP1=25% ferrite and FP2=50%) suggested that these ferrite/polymer composites may be recommended for the hyperthermia applications.

**WEB URL:** <http://www.sciencedirect.com/science/article/pii/S0272884214013546>

**45. Khan, M. A., ur Rehman, M. J., Mahmood, K., Ali, I., Akhtar, M. N., Murtaza, G., ... & Warsi, M. F. (2015). Impacts of Tb substitution at cobalt site on structural, morphological and magnetic properties of cobalt ferrites synthesized via double sintering method. *Ceramics International*, 41(2), 2286-2293.**

**ABSTRACT:**

Cobalt ferrites substituted with terbium (Tb) at cobalt (Co) and iron sites were fabricated by double sintering method and were characterized by the XRD, fourier transform infrared (FTIR) spectroscopy, scanning electron microscope and hysteresis loops measurements. The XRD analyses confirm the formation of single spinel phase for  $x=0.0$  and thereafter a small peak of secondary phase occurred. The lattice parameter was found to increase by increasing Tb contents and this was attributed to the larger ionic radius of Tb ions as compared to Co ions. FTIR revealed two absorption bands which are characteristic feature of spinel ferrites. The morphology studies exhibit the inhomogeneous grain size distribution. The saturation magnetization was found to exist in the range of 63–67 emu/g and coercivity in the range of 405–435 Oe. The observed variation in saturation magnetization was attributed to the redistribution of cations due to the substitution of terbium at cobalt sites. The incorporation of terbium in cobalt ferrites substantially decreased the coercivity and remanence. The smaller values of coercive field suggest that these materials are potential candidates to be useful in high density data storage devices.

**WEB URL:** <http://www.sciencedirect.com/science/article/pii/S0272884214015582>

**46. Ali, I., Islam, M. U., Ashiq, M. N., Shakir, I., Karamat, N., Ishaque, M., ... & Khan, M. A. (2015). Investigation of the magnetic properties of nanometric SrSmCoNi ferrite/PST matrix. *Ceramics International*, 41(7), 8748-8754.**

**ABSTRACT:**

Y-type hexa-ferrite  $Sr_{1.8}Sm_{0.2}Co_2Ni_{1.50}Fe_{10.50}O_{22}$  was synthesized via micro-emulsion route. Ferrite/PST composites were obtained by mixing the different ferrite ratio in the pure PST matrix. The microstructure was examined by scanning electron microscopy (SEM) and exhibited heterogonous distribution of grains. A keen observation of these SEM images revealed that the grain morphology changes noticeably with increasing ferrite filler contents. The electrical modulus, Cole–Cole plots and quality factor of ferrite polymer composites have been investigated in the frequency range (1 MHz to

3 GHz). The field dependent magnetic properties of the prepared samples were investigated at room temperature by using vibrating sample magnetometer (VSM). The shape of hysteresis loops and linearity of  $M_s$ ,  $M_r$ ,  $H_c$  values vs. ferrite contents unfold that the ferrite nanoparticles are evenly dispersed within the composite. The occurrence of resonance at high frequency suggests that the present investigated composite samples are best candidate for multilayer chip inductors.

**WEB URL:** <http://www.sciencedirect.com/science/article/pii/S0272884215005027>

**47. Raza, M. R., Sulong, A. B., Akhtar, M. N., & Rajabi, J. (2015). Effects of binder system and processing parameters on formability of porous Ti/HA composite through powder injection molding. *Materials & Design*, 87, 386-392.**

**ABSTRACT:**

Porous titanium-hydroxyapatite (Ti/HA) composite is a developed composite material suitable for bio-medical applications. Powder injection molding (PIM) with space holder method is used to produce porous Ti/HA with mechanical properties, similar to human bone, and pores helps to initiate tissue growth. However, the differences in physical and mechanical properties of these composites are the main challenges during debinding and sintering. Therefore, the main objective is to determine effects of binder systems and processing parameters on formability of Ti/HA composite. In PIM, a binder system is necessary to produce green and ultimately sintered part. There are two binder systems and variation of sintering temperature has been used. Results revealed that Polyethylene glycol (PEG)-based binder system is applicable with NaCl space holder and optimum sintering parameters, including temperature, heating rate, and holding time of 1300 °C, 10 °C/min, and 5 h, respectively. The fabricated porous Ti/HA exhibits average porosity, pore size distribution, compressive strength, and roughness values of 55%, 60 µm to 170 µm, 370 MPa, and 0.323 µm, respectively. FESEM results showed that the pores are interconnected. It may be an appropriate material for future bio-medical applications.

**WEB URL:** <http://www.sciencedirect.com/science/article/pii/S0264127515302793>

**48. Razaq, A., Khan, A. A., Asif, M. H., Iqbal, S., Ali, J., Manzoor, F., ... & Pakistan, I. (2015). Environmentally Friendly and Flexible Lignocelluloses Fibrils Sheet for Substrate of Patch Antenna. *Modern Physics Letter B.8. 1550187.***

**ABSTRACT:**

Natural lignocelluloses fibers showed outstanding potential in paper industry and other conventional applications. Lignocelluloses fibers can reveal as suitable candidate for high-tech applications under the scope of abundance, flexibility, light-weight and environment friendliness. In this study, paper sheets were prepared from the lignocelluloses fibers extracted from self-growing plant, *Typha Angustifolia*. Lignocelluloses paper sheets were characterized for Scanning Electron Microscopy (SEM), Universal Testing Machine (UTM) and Vector Network Analyzer (VNA). Flexible paper sheets displayed a tensile strength of 9.1 MPa and further used as a substrate of patch antenna. The patch antenna is designed at 5.1 GHz which showed return loss less than -10 dB and dielectric constant 3.71. The use of lignocelluloses paper sheet as a substrate in patch antenna will provide the opportunity of miniaturization of size and weight in comparison of a jean substrate based antenna.

**WEB URL:**

[https://www.researchgate.net/profile/MS\\_Awan/publication/267027097\\_Environmentally\\_Friendly\\_and\\_Flexible\\_Lignocelluloses\\_Fibrils\\_Sheet\\_for\\_Substrate\\_of\\_Patch\\_Antenna/links/544158780cf2e6f0c0f613ee.pdf](https://www.researchgate.net/profile/MS_Awan/publication/267027097_Environmentally_Friendly_and_Flexible_Lignocelluloses_Fibrils_Sheet_for_Substrate_of_Patch_Antenna/links/544158780cf2e6f0c0f613ee.pdf)

**49. Rafique, A., Raza, R., Akram, N., Ullah, M. K., Ali, A., Irshad, M., ... & Dawson, R. (2015). Significance enhancement in the conductivity of core shell nanocomposite electrolytes. *RSC Advances, 5(105), 86322-86329.***

**ABSTRACT:**

Today, there is great demand of electrolytes with high ionic conductivities at low operating temperatures for solid-oxide fuel cells. Therefore, a co-doped technique was

used to synthesize a highly ionically conductive two phase nanocomposite electrolyte Sr/Sm–ceria–carbonate by a co-precipitation method. A significant increase in conductivity was measured in this co-doped Sr/Sm–ceria–carbonate electrolyte at 550 °C as compared to the more commonly studied samarium doped ceria. The fuel cell power density was 900 mW cm<sup>-2</sup> at low temperature (400–580 °C). The composite electrolyte was found to have homogenous morphology with a core–shell structure using SEM and TEM. The two phase core–shell structure was confirmed using XRD analysis. The crystallite size was found to be 30–60 nm and is in good agreement with the SEM analysis. The thermal analysis was determined with DSC. The enhancement in conductivity is due to two effects; co-doping of Sr in samarium doped ceria and it's composite with carbonate which is responsible for the core–shell structure. This co-doped approach with the second phase gives promise in addressing the challenge to lower the operating temperature of solid oxide fuel cells (SOFC).

**WEB URL:**

<http://pubs.rsc.org/en/content/articlelanding/2015/ra/c5ra16763a/unauth#!divAbstract>

**50. Raza, R., Ahmed, A., Akram, N., Saleem, M., Akhtar, M. N., Sherazi, T. A., ... & Alvi, F. (2015). Composite electrolyte with proton conductivity for low-temperature solid oxide fuel cell. *Applied Physics Letters*, 107(18), 183903.**

**ABSTRACT:**

In the present work, cost-effective nanocomposite electrolyte (Ba-SDC) oxide is developed for efficient low-temperature solid oxide fuel cells (LTSOFCs). Analysis has shown that dual phase conduction of O<sup>-2</sup>(oxygen ions) and H<sup>+</sup> (protons) plays a significant role in the development of advanced LTSOFCs. Comparatively high proton ion conductivity (0.19 s/cm) for LTSOFCs was achieved at low temperature (460 °C). In this article, the ionic conduction behaviour of LTSOFCs is explained by carrying out electrochemical impedance spectroscopy measurements. Further, the phase and

structure analysis are investigated by X-ray diffraction and scanning electron microscopy techniques. Finally, we achieved an ionic transport number of the composite electrolyte for LT-SOFCs as high as 0.95 and energy and power density of 90% and 550 mW/cm<sup>2</sup>, respectively, after sintering the composite electrolyte at 800 °C for 4 h, which is promising. Our current effort toward the development of an efficient, green, low-temperature solid oxide fuel cell with the incorporation of high proton conductivity composite electrolyte may open frontiers in the fields of energy and fuel cell technology.

**WEB URL:**

[http://scitation.aip.org/content/aip/journal/apl/107/18/10.1063/1.4934940\](http://scitation.aip.org/content/aip/journal/apl/107/18/10.1063/1.4934940)

**51. Janjua, N. K., Jabeen, M., Islam, M., Yaqub, A., Sabahat, S., Mehmood, S., ... & Abbas, G. (2015). Electrochemical Properties of Barium Cerate Doped with Zinc for Methanol Oxidation. *Journal of the Chemical Society of Pakistan*, 37(5).850-857.**

**ABSTRACT:**

Barium cerate and its zinc doped series, BaCe<sub>1-x</sub>Zn<sub>x</sub>O<sub>3</sub> with 0.02 ≤ x ≤ 0.16, were synthesized using ammonia as a co-precipitant. The influence of zinc on phase and morphology was characterized using XRD and SEM, respectively. XRD revealed orthorhombic crystallinity for x = 0 to 14 mol% but distorted hexagonal phase for x = 16 mol%. SEM images revealed homogeneity of synthesized powders. The synthesized materials were then tested for their function as electrocatalyst for model analyte, methanol. Methanol electro-oxidation in acidic media was studied by modifying platinum electrode with BaCeO<sub>3</sub> materials using cyclic voltammetry. Kinetic ( $k_{s,h}$ ,  $D_o$ ) and thermodynamic parameters ( $E_a$ ,  $\Delta G$ ,  $\Delta H$ ,  $\Delta S$ ) were estimated for methanol electrooxidation. The deduced value of diffusion coefficient of order of 10<sup>-10</sup> cm<sup>2</sup>s<sup>-1</sup> indicated faster kinetics of methanol oxidation using BaCeO<sub>3</sub> than zinc doped sample in

H<sub>2</sub>SO<sub>4</sub> medium. The increasing temperature and methanol concentration enhanced the peak currents which pointed to the suitability of these materials as electrocatalysts. The stability and catalytic activity of these materials at various temperatures also aided to their potentiality in PEMFC application.

**WEB URL:**

<http://web.b.ebscohost.com/abstract?direct=true&profile=ehost&scope=site&authtype=crawler&jrnl=02535106&AN=110819398&h=PDIRcJ2A%2bps9DBNp98bWEwOIWwkfEkUKcB%2fClqNwqL5MUaAOoA3ZWYCVHeXuoDdDmy4%2btPrZ6AXWRI4FcRO3CA%3d%3d&crl=c&resultNs=AdminWebAuth&resultLocal=ErrCrlNotAuth&crlhashWebURL=login.aspx%3fdirect%3dtrue%26profile%3dehost%26scope%3dsite%26authtype%3dcrawler%26jrnl%3d02535106%26AN%3d110819398>

**52. Afzal, M., Raza, R., Du, S., Lima, R. B., & Zhu, B. (2015). Synthesis of Ba<sub>0.3</sub>Ca<sub>0.7</sub>Co<sub>0.8</sub>Fe<sub>0.2</sub>O<sub>3-δ</sub> composite material as novel catalytic cathode for ceria-carbonate electrolyte fuel cells. *Electrochimica Acta*, 178, 385-391.**

**ABSTRACT:**

This work reports a new composite Ba<sub>x</sub>Ca<sub>1-x</sub>Co<sub>y</sub>Fe<sub>1-y</sub>O<sub>3-δ</sub> (BCCF) cathode material for advanced and low temperature solid oxide fuel cells (SOFCs). The BCCF-based composite material was synthesized by sol gel method and investigated as a catalytic cathode for low temperature (LT) SOFCs. XRD analysis of the as-prepared material revealed the dominating BCCF perovskite structure as the main phase accompanied with cobalt and calcium oxides as the secondary phases resulting into an overall composite structure. Structure and morphology of the sample was observed by Field Emission Scanning Electron Microscope (FE-SEM). In particular, the Ba<sub>0.3</sub>Ca<sub>0.7</sub>Co<sub>0.8</sub>Fe<sub>0.2</sub>O<sub>3-δ</sub> (BCCF37) showed a maximum conductivity of 143 S cm<sup>-1</sup> in air at 550 °C measured by DC 4 probe method. The BCCF at the optimized composition exhibited much higher electrical conductivities than the commercial Ba<sub>0.5</sub>Sr<sub>0.5</sub>Co<sub>0.8</sub>Fe<sub>0.2</sub>O<sub>3-δ</sub> (BSCF) perovskite cathode

material. A maximum power density of  $325 \text{ mW cm}^{-2}$  at  $550 \text{ }^\circ\text{C}$  is achieved for the ceria-carbonate electrolyte fuel cell with BCCF37 as the cathode material.

**WEB URL:** <http://www.sciencedirect.com/science/article/pii/S0013468615302498>

**53. Ullah, M., Ahmed, E., Hussain, F., Rana, A. M., Raza, R., & Ullah, H. (2015). Electronic structure calculations of oxygen-doped diamond using DFT technique. *Microelectronic Engineering*, 146, 26-31.**

**ABSTRACT:**

In this study, equilibrium geometry and band structure of oxygen-doped diamond have been investigated based on density function theory (DFT) using VASP code. These calculations have shown that the highest occupied molecular orbital is localized at the oxygen atom. Moreover,  $C_4\text{—O}$  bond lengths are equivalent to those of  $C\text{—}C$  bonds leading to no lattice distortions. Doping of oxygen into diamond seems to be thermodynamically favorable due to negative formation energy. Band structure calculations lead to the semiconducting behavior of oxygen-doped diamonds due to the creation of defects states inside the band gap extending to conduction band minimum. The spin projected density of states calculations illustrates significant contributions of  $O2p$  states at the Fermi level without the appearance of appreciable magnetic moments on oxygen or on carbon atoms (for all  $C_1\text{—}C_4$ ) leading to its non-magnetic semiconducting behavior with zero density of carriers at the Fermi level for both spin projections;  $O\downarrow\uparrow(E_F) = 0$ . Present DFT results verify our experimental findings that addition of oxygen into diamond lattice increases its conductivity so that oxygen-doped diamond films behave like a good semiconductor.

**WEB URL:** <http://www.sciencedirect.com/science/article/pii/S0167931715000994?np=y>

**54. Alla, A., Ahmad, M., Abbas, G., Akhtar, M. N., & Atif, M. (2015). UREA biosensor based on magnetic nano particles (Co3O4, Fe3O4) for the estimation of urea**

concentration in blood and urine samples. *Journal Of Optoelectronics And Advanced Materials*, 17(9-10), 1515-1521.

**ABSTRACT:**

In this study, a potentiometric urea biosensor through the immobilization of urease enzyme onto chitosan (CH)/Co<sub>3</sub>O<sub>4</sub> and CH/Fe<sub>3</sub>O<sub>4</sub> hybrid nano-biocomposites have been fabricated on glass filter paper. A copper wire of diameter 250 μm has been attached with nanoparticles in order to extract the voltage output signal. A physical absorption method has been adopted to immobilize the surface of CH/Co<sub>3</sub>O<sub>4</sub> and CH/Fe<sub>3</sub>O<sub>4</sub> hybrid nano-biocomposites. Urea biosensor based on magnetic nanoparticles (MNPs) was utilized for the estimation of urea concentration in blood and urine. Blood and urine samples of 25 healthy and 25 sick volunteers were collected and after that urease/ Fe<sub>3</sub>O<sub>4</sub>-CH/Cu biosensor electrode or urease/Co<sub>3</sub>O<sub>4</sub>-CH/Cu biosensor electrode with 20 L urease immobilization was used for estimation of blood and urine urea. The potentiometric sensitivity was measured over the concentration range 0.1 - 6.00 ppm; and the limit of detection is 0.073 ppm. The response time, efficiency and accuracy of this biosensor is 280 seconds, 50 samples and 94 - 99%, respectively. The concentration of urea in 100 times diluted blood and urine sample was found to be 4.1 10<sup>-4</sup> and 3.84 10<sup>-4</sup> M, respectively. The magnetic study shows that coercivity of both the samples is found to be a few oersteds which make them very promising candidates for a variety of applications in biomedical as well as recording technology.

**WEB URL:**

[https://www.researchgate.net/profile/Mukhtar\\_Ahmad8/publication/283354515\\_UREA\\_biosensor\\_based\\_on\\_magnetic\\_nano\\_particles\\_Co\\_3\\_O\\_4\\_Fe\\_3\\_O\\_4\\_for\\_the\\_estimation\\_of\\_urea\\_concentration\\_in\\_blood\\_and\\_urine\\_samples/links/5637309f08aebc004000de0c.pdf](https://www.researchgate.net/profile/Mukhtar_Ahmad8/publication/283354515_UREA_biosensor_based_on_magnetic_nano_particles_Co_3_O_4_Fe_3_O_4_for_the_estimation_of_urea_concentration_in_blood_and_urine_samples/links/5637309f08aebc004000de0c.pdf)

55. Gaaz, T. S., Sulong, A. B., Akhtar, M. N., Kadhun, A. A. H., Mohamad, A. B., & Al-Amiery, A. A. (2015). Properties and Applications of Polyvinyl Alcohol, Halloysite Nanotubes and Their Nanocomposites. *Molecules*,20(12), 22833-22847.

**ABSTRACT:**

The aim of this review was to analyze/investigate the synthesis, properties, and applications of polyvinyl alcohol–halloysite nanotubes (PVA–HNT), and their nanocomposites. Different polymers with versatile properties are attractive because of their introduction and potential uses in many fields. Synthetic polymers, such as PVA, natural polymers like alginate, starch, chitosan, or any material with these components have prominent status as important and degradable materials with biocompatibility properties. These materials have been developed in the 1980s and are remarkable because of their recyclability and consideration of the natural continuation of their physical and chemical properties. The fabrication of PVA–HNT nanocomposites can be a potential way to address some of PVA’s limitations. Such nanocomposites have excellent mechanical properties and thermal stability. PVA–HNT nanocomposites have been reported earlier, but without proper HNT individualization and PVA modifications. The properties of PVA–HNT for medicinal and biomedical use are attracting an increasing amount of attention for medical applications, such as wound dressings, drug delivery, targeted-tissue transportation systems, and soft biomaterial implants. The demand for alternative polymeric medical devices has also increased substantially around the world. This paper reviews individualized HNT addition along with crosslinking of PVA for various biomedical applications that have been previously reported in literature, thereby showing the attainability, modification of characteristics, and goals underlying the blending process with PVA.

**WEB URL:** <http://www.mdpi.com/1420-3049/20/12/19884/htm>

**56. Sattar, A., Amjad, R. J., Mahmood, H., Akhtar, M. N., Latif, H., Khalid, M., ... & Iqbal, A. (2015). Study Of Morphology Formation Of Near Threshold Percolating Metallic Nanoparticle Thin Films Showing Non-Ohmic Behavior. *Journal of Ovonic Research Vol, 11(3)*, 113-121.**

**ABSTRACT:**

Nanoparticles produced by inert gas aggregation system were deposited on the Silicon Nitride (Si<sub>3</sub>N<sub>4</sub>) substrates under good vacuum conditions. Nanoparticles coalesced and agglomerated rapidly as they were deposited on the substrate. A peculiar voltage dependent non-ohmic conductance behavior was observed for certain film morphologies, whereas the resultant morphology of these films was found to be dependent upon the initial size of particles, deposition rate and the ambient conditions of the films. The coalescence enhanced, due to large deposition rate or low oxidation rate, played a vital role in the formation of metallic films in large islands separated by cracks and voids suitable for conductance switching behavior. Simulations were performed to mimic and understand the morphology of these experimentally produced films. A new improved model is presented in which coalescence was restricted by deposition rate and maximum size limit of the particles formed by coalescence. Initial and cut-off sizes of particles along with a new parameter which is directly proportional to the deposition rate were used for our simulations. By varying these parameters, a range of simulated morphologies were generated for a successful comparison with experimental results and for the indirect calculation of the oxidation time after which the particles stop coalescing

**WEB URL:** [http://www.chalcogen.ro/113\\_Sattar.pdf](http://www.chalcogen.ro/113_Sattar.pdf)

**57. Akhtar, M. N., Sulong, A. B., Karim, S. A., Azhari, C. H., & Raza, M. R. (2015). Evaluation of thermal, morphological and mechanical properties of PMMA/NaCl/DMF electrospun nanofibers: an investigation through surface methodology approach. *Iranian Polymer Journal, 24(12)*, 1025-1038.**

**Abstract:**

Electrospinning is an efficient, flexible and versatile method of producing nanofibers. The aims of this study are to fabrication and characterize electrospun nanofibers and evaluation of the electrospinning parameters that influence on the nanofibers properties. In this work, polymethylmetacrylate (PMMA) and sodium chloride were dissolved in dimethylformamide for fabrication of PMMA nanofibers through electrospinning. Differential scanning calorimetry, thermogravimetric analysis, Fourier transform infrared spectroscopy, field emission scanning electron microscopy and mechanical testing were used to measure the structure, morphology, diameter, orientation and strength of the nanofibers, respectively. The effect of electrospinning parameters on diameter, morphology and mechanical properties of nanofibers was also investigated. Collector rotating speed and gap distance were also found to be the most important factors that affected diameter and orientation of the nanofibers. Response surface methodology L46 and Box–Behnken experimental design were used to analyze and optimize the results. The theoretical and experimental study revealed that increasing the gap between collector and needle resulted in reduction of the electrospun nanofibers. However, fiber diameter was significantly influenced by decreasing the solution concentration and pump rate. Moreover, fibers with ~720 nm diameter and ~90 % of orientation possessed an ultimate tensile strength of 1.4 MPa, which was exhibited at the following optimized parameters: distance, 10 cm; voltage, 10 kV; flow rate, 5 mL/h; collector rotating speed, 1800 rpm; and solution concentration, 10 wt%. Finally, these nanofibers with superior morphological properties may find application in biomedical, pharmaceutical, drug delivery and tissue scaffold for cell growth.

**WEB URL:** <http://link.springer.com/article/10.1007/s13726-015-0390-8>

**58. Amin, N., Afzal, M., Yousaf, M., & Javid, M. A. (2015). Choice of the pulse sequence and parameters for improved signal-to-noise ratio in T1-weighted study of MRI. *JPMA. The Journal of the Pakistan Medical Association*,65(5), 512-518.**

**ABSTRACT:**

Objective: To investigate the practical impact of alteration of imaging parameters on signal-to-noise ratio for the most commonly used T1-weighted magnetic resonance sequences. Methods: The study was conducted in the Department of Medical Physics, Ninewells Hospital and Medical School, Dundee, UK, in 2007. Magnetic resonance images of a tissue-equivalent material were generated with a set of T1 and T2 values. Experimental variations in the imaging parameters were performed in echo time and repetition time. Quantitative analysis consisted of signal-to-noise ratio. Results: Percentage inaccuracy in signal-to-noise ratio was the result of inappropriate choice of parameters. We have investigated conventional spin echo, fast spin echo and fast fluid attenuated inversion recovery with one of corresponding percentage errors 28.68%, -36.65% and -40.34%, respectively. Conventional spin echo presented moderately low percentage error with the choice of repetition time and echo time. Factual error in fast spin echo was slightly higher than conventional spin echo. Fast fluid attenuated inversion recovery could create outstanding signal-to-noise ratio of high T1/T2 value phantoms in T1-weighted images. Conclusion: The role of repetition time and echo time in T1-weighted images was crucial to sustain the image quality.

**WEB URL:** <http://www.jpma.org.pk/PdfDownload/7348.pdf>

**59. Hussain, S. Q., Kwon, G. D., Ahn, S., Kim, S., Balaji, N., Le, A. H. T., ... & Khan, S. (2015). Light scattering effect of ITO: Zr/AZO films deposited on periodic textured glass surface morphologies for silicon thin film solar cells. *Applied Physics A*, 120(3), 823-828.**

**ABSTRACT:**

Various SF<sub>6</sub>/Ar plasma-textured periodic glass surface morphologies for high transmittance, haze ratio and low sheet resistance of ITO:Zr films are reported. The SF<sub>6</sub>/Ar plasma-textured glass surface morphologies were changed from low aspect ratio

to high aspect ratio with the increase in RF power from 500 to 600 W. The micro- and nano-size features of textured glass surface morphologies enhanced the haze ratio in visible as well as NIR wavelength region. Micro-size textured features also influenced the sheet resistance and electrical characteristics of ITO:Zr films due to step coverage. The ITO:Zr/AZO bilayer was used as front TCO electrode for p-i-n amorphous silicon thin film solar cells with current density–voltage characteristics as:  $V_{oc} = 875$  mV,  $FF = 70.90$  %,  $J_{sc} = 11.31$  mA/cm<sup>2</sup>,  $\eta = 7.02$  %.

**WEB URL:** <http://link.springer.com/article/10.1007/s00339-015-9335-5>

**60. Lee, Y., Kim, H., Hussain, S. Q., Han, S., Balaji, N., Lee, Y. J., ... & Yi, J. (2015). Study of metal assisted anisotropic chemical etching of silicon for high aspect ratio in crystalline silicon solar cells. *Materials Science in Semiconductor Processing*, 40, 391-396.**

**ABSTRACT:**

Textured surface is commonly used to enhance the efficiency of silicon solar cells by reducing the overall reflectance and improving the light scattering. In this study, a comparison between isotropic and anisotropic etching methods was investigated. The deep funnel shaped structures with high aspect ratio are proposed for better light trapping with low reflectance in crystalline silicon solar cells. The anisotropic metal assisted chemical etching (MACE) was used to form the funnel shaped structures with various aspect ratios. The funnel shaped structures showed an average reflectance of 14.75% while it was 15.77% for the pillar shaped structures. The average reflectance was further reduced to 9.49% using deep funnel shaped structures with an aspect ratio of 1:1.18. The deep funnel shaped structures with high aspect ratios can be employed for high performance of crystalline silicon solar cells.

**WEB URL:** <http://www.sciencedirect.com/science/article/pii/S1369800115300470>

**61. Ablikim, M., Achasov, M. N., Ai, X. C., Albayrak, O., Albrecht, M., Ambrose, D. J., ... & Ferroli, R. B. (2015). Study of decay dynamics and C P asymmetry in  $D^+ \rightarrow K L 0 e^+ \nu e$  decay. *Physical Review D*, 92(11), 112008.**

**ABSTRACT:**

Using  $2.92 \text{ fb}^{-1}$  of electron-positron annihilation data collected at  $\sqrt{s}=3.773 \text{ GeV}$  with the BESIII detector, we obtain the first measurements of the absolute branching fraction  $B(D^+ \rightarrow K 0 L e^+ \nu e) = (4.481 \pm 0.027(\text{stat}) \pm 0.103(\text{sys}))\%$  and the CP asymmetry  $A_{D^+ \rightarrow K 0 L e^+ \nu e}^{\text{CP}} = (-0.59 \pm 0.60(\text{stat}) \pm 1.48(\text{sys}))\%$ . From the  $D^+ \rightarrow K 0 L e^+ \nu e$  differential decay rate distribution, the product of the hadronic form factor and the magnitude of the Cabibbo-Kobayashi-Maskawa matrix element,  $f_{K^+(0)} |V_{cs}|$ , is determined to be  $0.728 \pm 0.006(\text{stat}) \pm 0.011(\text{sys})$ . Using  $|V_{cs}|$  from the SM constrained fit with the measured  $f_{K^+(0)} |V_{cs}|$ ,  $f_{K^+(0)} = 0.748 \pm 0.007(\text{stat}) \pm 0.012(\text{sys})$  is obtained, and utilizing the unquenched Lattice QCD (LQCD) calculation for  $f_{K^+(0)}$ ,  $|V_{cs}| = 0.975 \pm 0.008(\text{stat}) \pm 0.015(\text{sys}) \pm 0.025(\text{LQCD})$ .

**WEB URL:** <http://journals.aps.org/prd/abstract/10.1103/PhysRevD.92.112008>

**62. Ablikim, M., Achasov, M. N., Ai, X. C., Albayrak, O., Albrecht, M., Ambrose, D. J., ... & Ferroli, R. B. (2015). Measurement of the Absolute Branching Fraction for  $\Lambda c^+ \rightarrow \Lambda e^+ \nu e$ . *Physical review letters*, 115(22), 221805.**

**ABSTRACT:**

We report the first measurement of the absolute branching fraction for  $\Lambda c^+ \rightarrow \Lambda e^+ \nu e$ . This measurement is based on  $567 \text{ pb}^{-1}$  of  $e^+e^-$  annihilation data produced at  $\sqrt{s}=4.599 \text{ GeV}$ , which is just above the  $\Lambda c^+ \Lambda^- c$  threshold. The data were collected with the BESIII detector at the BEPCII storage rings. The branching fraction is determined to be  $B(\Lambda c^+ \rightarrow \Lambda e^+ \nu e) = [3.63 \pm 0.38(\text{stat}) \pm 0.20(\text{syst})]\%$ , representing a significant improvement in precision over the current indirect determination. As the

branching fraction for  $\Lambda+c \rightarrow \Lambda e^+ e^-$  is the benchmark for those of other  $\Lambda+c$  semileptonic channels, our result provides a unique test of different theoretical models, which is the most stringent to date.

**WEB URL:** <http://journals.aps.org/prl/abstract/10.1103/PhysRevLett.115.221805>

**63. S., Nisar, BESIII Collaboration. (2016). Measurement of the  $e^+ e^- \rightarrow \pi^+ \pi^-$  cross section between 600 and 900 MeV using initial state radiation. *Physics Letters B*, 753, 629-638.**

**ABSTRACT:**

We extract the  $e^+ e^- \rightarrow \pi^+ \pi^-$  cross section in the energy range between 600 and 900 MeV, exploiting the method of initial state radiation. A data set with an integrated luminosity of  $2.93 \text{ fb}^{-1}$  taken at a center-of-mass energy of 3.773 GeV with the BESIII detector at the BEPCII collider is used. The cross section is measured with a systematic uncertainty of 0.9%. We extract the pion form factor  $|F_\pi|^2$  as well as the contribution of the measured cross section to the leading-order hadronic vacuum polarization contribution to  $(g-2)_\mu$ . We find this value to be  $a_\mu^{\pi\pi, LO}(600-900 \text{ MeV}) = (368.2 \pm 2.5_{\text{stat}} \pm 3.3_{\text{sys}}) \cdot 10^{-10}$ , which is between the corresponding values using the BaBar or KLOE data

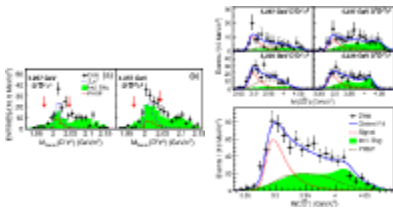
**WEB URL:** <http://www.sciencedirect.com/science/article/pii/S0370269315008990>

**64. Ablikim, M., Achasov, M. N., Ai, X. C., Albayrak, O., Albrecht, M., Ambrose, D. J., ... & Ferroli, R. B. (2015). Observation of a Neutral Structure near the  $D D^*$  Mass Threshold in  $e^+ e^- \rightarrow (D D^*)^0 \pi^0$  at  $s = 4.226$  and  $4.257$  GeV. *Physical review letters*, 115(22), 222002.**

**ABSTRACT:**

A neutral structure in the  $DD^*$  system around the  $DD^*$  mass threshold is observed with a statistical significance greater than  $10\sigma$  in the processes  $e^+ e^- \rightarrow D + D^* - \pi^0 + \text{c.c.}$  and  $e^+ e^- \rightarrow D^0 D^{*-} \pi^0 + \text{c.c.}$  at  $\sqrt{s} = 4.226$  and  $4.257$  GeV in

the BESIII experiment. The structure is denoted as  $Z_c(3885)0$ . Assuming the presence of a resonance, its pole mass and width are determined to be  $[3885.7+4.3-5.7(\text{stat})\pm 8.4(\text{syst})]$  MeV/c<sup>2</sup> and  $[35+11-12(\text{stat})\pm 15(\text{syst})]$  MeV, respectively. The Born cross sections are measured to be  $\sigma[e+e-\rightarrow Z_c(3885)0\pi^0, Z_c(3885)0\rightarrow DD^*]= [77\pm 13(\text{stat})\pm 17(\text{syst})]$  pb at 4.226 GeV and  $[47\pm 9(\text{stat})\pm 10(\text{syst})]$  pb at 4.257 GeV. The ratio of decay rates  $B[Z_c(3885)0\rightarrow D+D^*+c.c.]/B[Z_c(3885)0\rightarrow D^0D^{*-}+c.c.]$  is determined to be  $0.96\pm 0.18(\text{stat})\pm 0.12(\text{syst})$ , consistent with no isospin violation in the process,  $Z_c(3885)0\rightarrow DD^*$ .



**WEB URL:** <http://journals.aps.org/prl/abstract/10.1103/PhysRevLett.115.222002>

**65. Ablikim, M., Achasov, M. N., Ai, X. C., Albayrak, O., Albrecht, M., Ambrose, D. J., ... & Ferroli, R. B. (2015). Confirmation of a charged charmoniumlike state  $Z_c(3885)\bar{c}$  in  $e+e-\rightarrow \pi^\pm(D D^*)\bar{c}$  with double D tag. *Physical Review D*, 92(9), 092006.**

**ABSTRACT:**

We present a study of the process  $e+e-\rightarrow \pi^\pm(DD^*)\bar{c}$  using data samples of 1092 pb<sup>-1</sup> at  $\sqrt{s}=4.23$  GeV and 826 pb<sup>-1</sup> at  $\sqrt{s}=4.26$  GeV collected with the BESIII detector at the BEPCII storage ring. With full reconstruction of the D meson pair and the bachelor  $\pi^\pm$  in the final state, we confirm the existence of the charged structure  $Z_c(3885)\bar{c}$  in the  $(DD^*)\bar{c}$  system in the two isospin processes  $e+e-\rightarrow \pi^+D^0D^{*-}$  and  $e+e-\rightarrow \pi^+D^-D^{*0}$ . By performing a simultaneous fit, the statistical significance of  $Z_c(3885)\bar{c}$  signal is determined to be greater than  $10\sigma$ , and its pole mass and width are measured to be  $M_{\text{pole}}=(3881.7\pm 1.6(\text{stat})\pm 1.6(\text{syst}))$  MeV/c<sup>2</sup> and  $\Gamma_{\text{pole}}=(26.6\pm 2.0(\text{stat})\pm 2.1(\text{syst}))$  Me

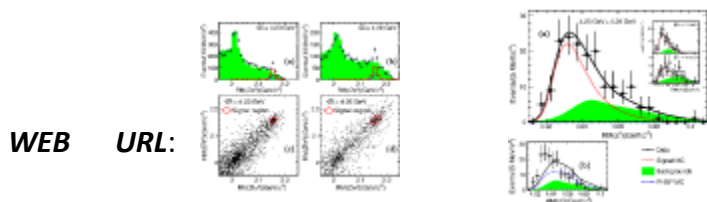
V, respectively. The Born cross section times the  $(DD^*)\bar{\pi}$  branching fraction  $(\sigma(e+e\rightarrow\pi^\pm Z_c(3885)\bar{\pi})\times Br(Z_c(3885)\bar{\pi}\rightarrow(DD^*)\bar{\pi}))$  is measured to be  $(141.6\pm 7.9(\text{stat})\pm 12.3(\text{syst}))$  pb at  $\sqrt{s}=4.23$  GeV and  $(108.4\pm 6.9(\text{stat})\pm 8.8(\text{syst}))$  pb at  $\sqrt{s}=4.26$  GeV. The polar angular distribution of the  $\pi^\pm-Z_c(3885)\bar{\pi}$  system is consistent with the expectation of a quantum number assignment of  $J^P=1^+$  for  $Z_c(3885)\bar{\pi}$ .

**WEB URL:** <http://journals.aps.org/prd/abstract/10.1103/PhysRevD.92.092006>

**66. Ablikim, M., Achasov, M. N., Ai, X. C., Albayrak, O., Albrecht, M., Ambrose, D. J., ... & Ferroli, R. B. (2015). Observation of a Neutral Charmoniumlike State  $Z_c(4025)0$  in  $e+e\rightarrow(D^*D^*)0\pi0$ . *Physical review letters*, 115(18), 182002.**

**ABSTRACT:**

We report a study of the process  $e+e\rightarrow(D^*D^*)0\pi0$  using  $e+e-$  collision data samples with integrated luminosities of  $1092\text{ pb}^{-1}$  at  $\sqrt{s}=4.23$  GeV and  $826\text{ pb}^{-1}$  at  $\sqrt{s}=4.26$  GeV collected with the BESIII detector at the BEPCII storage ring. We observe a new neutral structure near the  $(D^*D^*)0$  mass threshold in the  $\pi0$  recoil mass spectrum, which we denote as  $Z_c(4025)0$ . Assuming a Breit-Wigner line shape, its pole mass and pole width are determined to be  $(4025.5\pm 2.0-4.7\pm 3.1)$  MeV/c<sup>2</sup> and  $(23.0\pm 6.0\pm 1.0)$  MeV, respectively. The Born cross sections of  $e+e\rightarrow Z_c(4025)0\pi0\rightarrow(D^*D^*)0\pi0$  are measured to be  $(61.6\pm 8.2\pm 9.0)$  pb at  $\sqrt{s}=4.23$  GeV and  $(43.4\pm 8.0\pm 5.4)$  pb at  $\sqrt{s}=4.26$  GeV. The first uncertainties are statistical and the second are systematic.



<http://journals.aps.org/prl/abstract/10.1103/PhysRevLett.115.182002>

67. Ablikim, M., Yang, H. X., Zhang, Z. P., Ren, H. L., Hussain, T., Yu, H. W., ... & Gong, W. X. (2015). Measurement of the branching fractions of  $Ds^+ \rightarrow \eta' X$  and  $Ds^+ \rightarrow \eta' \rho^+$  in  $e^+ e^- \rightarrow Ds^+ Ds^-$ . *Physics letters B*.750.

**ABSTRACT:**

We study  $Ds^+$  decays to final states involving the  $\eta'$  with a  $482 \text{ pb}^{-1}$  data sample collected at  $\sqrt{s}=4.009 \text{ GeV}$  with the BESIII detector at the BEPCII collider. We measure the branching fractions  $B(Ds^+ \rightarrow \eta' X) = (8.8 \pm 1.8 \pm 0.5)\%$  and  $B(Ds^+ \rightarrow \eta' \rho^+) = (5.8 \pm 1.4 \pm 0.4)\%$  where the first uncertainty is statistical and the second is systematic. In addition, we estimate an upper limit on the non-resonant branching ratio  $B(Ds^+ \rightarrow \eta' \pi^+ \pi^0) < 5.1\%$  at the 90% confidence level. Our results are consistent with CLEO's recent measurements and help to resolve the disagreement between the theoretical prediction and CLEO's previous measurement of  $B(Ds^+ \rightarrow \eta' \rho^+)$ .

**WEB URL:** <http://repo.scoap3.org/record/12025>

68. Ablikim, M., Achasov, M. N., Ai, X. C., Albayrak, O., Albrecht, M., Ambrose, D. J., ... & Ferroli, R. B. (2015). Study of dynamics of  $D^0 \rightarrow K^- e^+ \nu_e$  and  $D^0 \rightarrow \pi^- e^+ \nu_e$  decays. *Physical Review D*, 92(7), 072012.

**ABSTRACT:**

In an analysis of a  $2.92 \text{ fb}^{-1}$  data sample taken at  $3.773 \text{ GeV}$  with the BESIII detector operated at the BEPCII collider, we measure the absolute decay branching fractions  $B(D^0 \rightarrow K^- e^+ \nu_e) = (3.505 \pm 0.014 \pm 0.033)\%$  and  $B(D^0 \rightarrow \pi^- e^+ \nu_e) = (0.295 \pm 0.004 \pm 0.003)\%$ . From a study of the differential decay rates we obtain the products of hadronic form factor and the magnitude of the Cabibbo-Kobayashi-Maskawa (CKM) matrix element  $f_{K^+(0)} |V_{cs}| = 0.7172 \pm 0.0025 \pm 0.0035$  and  $f_{\pi^+(0)} |V_{cd}| = 0.1435 \pm 0.0018 \pm 0.0009$ . Combining these products with the values of  $|V_{cs}(d)|$  from the SM constraint fit, we extract the hadronic form factors  $f_{K^+(0)} = 0.7368 \pm 0.0026 \pm 0.0036$  and  $f_{\pi^+(0)} = 0.6372 \pm 0.0080 \pm 0.0044$ , and their

ratio  $f_{\pi^+(0)}/f_{K^+(0)}=0.8649\pm 0.0112\pm 0.0073$ . These form factors and their ratio are used to test unquenched lattice QCD calculations of the form factors and a light cone sum rule (LCSR) calculation of their ratio. The measured value of  $f_{K(\pi)^+(0)}|V_{cs}(d)|$  and the lattice QCD value for  $f_{K(\pi)^+(0)}$  are used to extract values of the CKM matrix elements of  $|V_{cs}|=0.9601\pm 0.0033\pm 0.0047\pm 0.0239$  and  $|V_{cd}|=0.2155\pm 0.0027\pm 0.0014\pm 0.0094$ , where the third errors are due to the uncertainties in lattice QCD calculations of the form factors. Using the LCSR value for  $f_{\pi^+(0)}/f_{K^+(0)}$ , we determine the ratio  $|V_{cd}|/|V_{cs}|=0.238\pm 0.004\pm 0.002\pm 0.011$ , where the third error is from the uncertainty in the LCSR normalization. In addition, we measure form factor parameters for three different theoretical models that describe the weak hadronic charged currents for these two semileptonic decays. All of these measurements are the most precise to date.

**WEB URL:** <http://journals.aps.org/prd/abstract/10.1103/PhysRevD.92.072012>

**69. Ablikim, M., Achasov, M. N., Ai, X. C., Albayrak, O., Albrecht, M., Ambrose, D. J., ... & Ferroli, R. B. (2015). Measurement of the form factors in the decay  $D^+ \rightarrow \omega e^+ \nu_e$  and search for the decay  $D^+ \rightarrow \phi e^+ \nu_e$ . *Physical Review D*, 92(7), 071101.**

**ABSTRACT:**

Using  $2.92 \text{ fb}^{-1}$  of electron-positron annihilation data collected at a center-of-mass energy of  $\sqrt{s}=3.773 \text{ GeV}$  with the BESIII detector, we present an improved measurement of the branching fraction  $B(D^+ \rightarrow \omega e^+ \nu_e) = (1.63 \pm 0.11 \pm 0.08) \times 10^{-3}$ . The parameters defining the corresponding hadronic form factor ratios at zero momentum transfer are determined for the first time; we measure them to be  $r_V = 1.24 \pm 0.09 \pm 0.06$  and  $r_2 = 1.06 \pm 0.15 \pm 0.05$ . The first and second uncertainties are statistical and systematic, respectively. We also search for the decay  $D^+ \rightarrow \phi e^+ \nu_e$ . An improved upper limit  $B(D^+ \rightarrow \phi e^+ \nu_e) < 1.3 \times 10^{-5}$  is set at 90% confidence level.

**WEB URL:** <http://journals.aps.org/prd/abstract/10.1103/PhysRevD.92.071101>

70. Dousti, M. R., Amjad, R. J., Sahar, M. R., Zabidi, Z. M., Alias, A. N., & de Camargo, A. S. S. (2015). Er<sup>3+</sup>-doped zinc tellurite glasses revisited: Concentration dependent chemical durability, thermal stability and spectroscopic properties. *Journal of Non-Crystalline Solids*, 429, 70-78.

**ABSTRACT:**

Tellurite glasses are interesting materials with extensive infrared transmission window, relatively low phonon energy, high refractive indexes and the ability to incorporate reasonably high amount of rare earth ion dopants. These characteristics make them popular candidates for infrared and visible emissions. Particularly, Er<sup>3+</sup>-doped tellurite glass compositions have been actively studied for broadband near infrared applications where the requirement for low dimension needs to be compensated by higher doping ion concentration. In this work, we revisit Er<sup>3+</sup>-doped zinc tellurite glasses, which are among the most thermally and chemically stable tellurite compositions. The glasses were prepared by the melt-quenching technique and the favorable effects of increasing dopant concentration on chemical durability, water resistivity and thermal stability (up to 140 °C) are discussed. The photophysical properties of the glasses were studied by absorption and luminescence spectroscopic techniques. The Stokes and anti-Stokes emissions of erbium were analyzed and it was verified that the width of the emission band at 1532 nm strongly depends on Er<sup>3+</sup> concentration varying from 60 to 82 nm for 0.5 and 2.5 mol% of Er<sub>2</sub>O<sub>3</sub>, respectively. The intensity of green and red upconversion emissions was evaluated and the increased efficiency of red emission with increasing concentration is attributed to energy transfer mechanisms between infrared energy levels.

**WEB URL:** <http://www.sciencedirect.com/science/article/pii/S0022309315301290>

**71. Iqbal, A., Ahmad, A., & Amjad, R. J. (2015). Photodetachment of hydrogen negative ion near inelastic surfaces: Arbitrary laser polarization direction. *International Journal of Quantum Chemistry*, 115(21), 1526-1532.**

**ABSTRACT:**

The photodetachment of hydrogen negative ion  $H^-$  near different inelastic surfaces is investigated by the semiclassical closed orbit theory for arbitrary laser polarization direction  $\theta_L$ . A two-term formula of photodetachment cross section consisting of a smooth background term and an oscillatory term is derived. The oscillatory term contains an extra angular factor  $\cos^2(\theta_L)$  that describes the dependence of oscillations in total cross section on the laser polarization direction. It is observed that the amplitude of oscillations in cross section reaches maximum at  $\theta_L=0$  when laser polarization is parallel to the z-axis and it approaches zero as the laser polarization direction becomes perpendicular to the z-axis. It is also observed that as the reflection coefficient  $\alpha$ , which accounts for the inelastic behavior of the surfaces, increases the amplitude of oscillation also increases. © 2015 Wiley Periodicals, Inc.

**WEB URL:** <http://onlinelibrary.wiley.com/doi/10.1002/qua.24965/full>

**72. Aslam, M. N., Amjed, N., & Qaim, S. M. (2015). Evaluation of excitation functions of the  $^{68, 67, 66}Zn(p, xn)$ ,  $^{68, 67, 66}Ga$  and  $^{67}Zn(p, \alpha)^{64}Cu$  reactions: Validation of evaluated data through comparison with experimental excitation functions of the nat  $Zn(p, x)^{66, 67}Ga$  and nat  $Zn(p, x)^{64}Cu$  processes. *Applied Radiation and Isotopes*, 96, 102-113.**

**ABSTRACT:**

Experimentally available cross section data for formation of the radionuclides  $^{68}Ga$ ,  $^{67}Ga$ ,  $^{66}Ga$  and  $^{64}Cu$  in proton induced reactions on enriched  $^{68}Zn$ ,  $^{67}Zn$  and  $^{66}Zn$  were evaluated by comparison with the excitation functions calculated by the nuclear model codes, EMPIRE and TALYS, followed by statistical fitting

of the selected data. The recommended cross sections were used to obtain the integral yields. The validation of the recommended excitation functions was also attempted by normalization to  $^{nat}\text{Zn}$  and comparison with the experimental data for the  $^{nat}\text{Zn}(p,x)^{67}\text{Ga}$ ,  $^{nat}\text{Zn}(p,x)^{66}\text{Ga}$  and  $^{nat}\text{Zn}(p,x)^{64}\text{Cu}$  processes.

**WEB URL:** <http://www.sciencedirect.com/science/article/pii/S0969804314003832>

**73. BESIII Collaboration. (2015). An improved limit for  $\Gamma_{ee}$  of X (3872) and  $\Gamma_{ee}$  measurement of  $\psi$  (3686). *Physics Letters B*, 749, 414-420.**

**ABSTRACT:**

Using the data sets taken at center-of-mass energies above 4 GeV by the BESIII detector at the BEPCII storage ring, we search for the reaction  $e^+e^- \rightarrow \gamma_{\text{ISR}} X(3872) \rightarrow \gamma_{\text{ISR}} \pi^+\pi^- J/\psi$  via the Initial State Radiation technique. The production of a resonance with quantum numbers  $JPC=1^{++}$  such as the X(3872) via single photon  $e^+e^-$  annihilation is forbidden, but is allowed by a next-to-leading order box diagram. We do not observe a significant signal of X(3872), and therefore give an upper limit for the electronic width times the branching fraction  $\Gamma_{ee}^{X(3872)} \mathcal{B}(X(3872) \rightarrow \pi^+\pi^- J/\psi) < 0.13 \text{ eV}$  at the 90% confidence level. This measurement improves upon existing limits by a factor of 46. Using the same final state, we also measure the electronic width of the  $\psi(3686)$  to be  $\Gamma_{ee}^{\psi(3686)} = 2213 \pm 18_{\text{stat}} \pm 99_{\text{sys}} \text{ eV}$ .

**WEB URL:** <http://www.sciencedirect.com/science/article/pii/S0370269315006140>

**74. Çetin, S. A., & BESIII Collaboration. (2015). Measurement of  $b(\psi(3770) \rightarrow \gamma \chi(c1))$  and search for  $\psi(3770) \rightarrow \gamma \chi(c2)$ . 91/9. 092009.**

**ABSTRACT:**

We report a measurement of the branching fraction for  $\psi(3770) \rightarrow \gamma \chi(c1)$  and search for the transition  $\psi(3770) \rightarrow \gamma \chi(c2)$  based on  $2.92 \text{ fb}^{-1}$  of  $e^+e^-$  data accumulated at  $\sqrt{s} = 3.773 \text{ GeV}$  with the BESIII detector at the BEPCII collider. We measure  $B(\psi(3770) \rightarrow \gamma \chi(c1)) = (2.48 \pm 0.15 \pm 0.23) \times 10^{-3}$ , which is the most precise measurement to date. The upper limit on the branching fraction of  $\psi(3770) \rightarrow \gamma \chi(c2)$  at a 90% confidence level is  $B(\psi(3770) \rightarrow \gamma \chi(c2)) < 0.64 \times 10^{-3}$ . The corresponding partial widths are  $\Gamma(\psi(3770) \rightarrow \gamma \chi(c1)) = (67.5 \pm 4.1 \pm 6.7) \text{ keV}$  and  $\Gamma(\psi(3770) \rightarrow \gamma \chi(c2)) < 17.4 \text{ keV}$ .

**WEB URL:** <http://openaccess.dogus.edu.tr:8080/xmlui/handle/11376/1876>

**75. Çetin, S. A., & BESIII Collaboration. (2015). Measurement of  $\gamma$  (CP) in  $D^0$ -( $D$ ) over bar (0) oscillation using quantum correlations in  $e^+ e^- \rightarrow D^0$  ( $D$ ) over bar (0) at  $\sqrt{s} = 3.773 \text{ GeV}$ . 744,339-346.**

**ABSTRACT:**

We report a measurement of the parameter  $\gamma(\text{CP})$  in  $D^0$ -( $D$ ) over bar (0) oscillations performed by taking advantage of quantum coherence between pairs of  $D^0$ -( $D$ ) over bar (0) mesons produced in  $e^+e^-$  annihilations near threshold. In this work, doubly-tagged  $D^0$ -( $D$ ) over bar (0) events, where one  $D$  decays to a CP eigenstate and the other  $D$  decays in a semileptonic mode, are reconstructed using a data sample of  $2.92 \text{ fb}^{-1}$  collected with the BESIII detector at the center-of-mass energy of  $\sqrt{s} = 3.773 \text{ GeV}$ . We obtain  $\gamma(\text{CP}) = (-2.0 \pm 1.3 \pm 0.7)\%$ , where the first uncertainty is statistical and the second is systematic. This result is compatible with the current world average. (C) 2015 The Authors.

**WEB URL:** <http://openaccess.dogus.edu.tr/handle/11376/1896>

76. Çetin, S. A., & BESIII Collaboration. (2015). Measurement of the  $e^+ e^- \rightarrow \eta J/\psi$  cross section and search for  $e^+ e^- \rightarrow \pi^0 J/\psi$  at center-of-mass energies between 3.810 and 4.600 GeV. *Physical Review D*, 91(11), 112005.

**ABSTRACT:**

Using data samples collected with the BESIII detector operating at the BEPCII collider at 17 center-of-mass energies from 3.810 to 4.600 GeV, we perform a study of  $e^+e^- \rightarrow \eta J/\psi$  and  $\pi^0 J/\psi$ . The Born cross sections of these two processes are measured at each center-of-mass energy. The measured energy-dependent Born cross section for  $e^+e^- \rightarrow \eta J/\psi$  shows an enhancement around 4.2 GeV. The measurement is compatible with an earlier measurement by Belle.

**WEB URL:** <http://openaccess.dogus.edu.tr:8080/xmlui/handle/11376/1939>

77. Ablikim, M., Achasov, M. N., Ai, X. C., Albayrak, O., Albrecht, M., Ambrose, D. J., ... & Ferroli, R. B. (2015). Search for the isospin violating decay  $\Upsilon(4260) \rightarrow J/\psi \eta \pi^0$ . *Physical Review D*, 92(1), 012008.

**ABSTRACT:**

Using data samples collected at center-of-mass energies of  $\sqrt{s}=4.009, 4.226, 4.257, 4.358, 4.416,$  and  $4.599$  GeV with the BESIII detector operating at the BEPCII storage ring, we search for the isospin violating decay  $\Upsilon(4260) \rightarrow J/\psi \eta \pi^0$ . No signal is observed, and upper limits on the cross section  $\sigma(e^+e^- \rightarrow J/\psi \eta \pi^0)$  at the 90% confidence level are determined to be 3.6, 1.7, 2.4, 1.4, 0.9, and 1.9 pb, respectively.



**WEB URL:** <http://journals.aps.org/prd/abstract/10.1103/PhysRevD.92.012008>

**78. Ablikim, M., Achasov, M. N., Ai, X. C., Albayrak, O., Albrecht, M., Ambrose, D. J., ... & Ferroli, R. B. (2015). Observation and Spin-Parity Determination of the  $X(1835)$  in  $J/\psi \rightarrow \gamma K^0_S K^0_{S^*} \eta$ . *arXiv preprint arXiv:1506.04807*.**

**ABSTRACT:**

We report an observation of the process  $J/\psi \rightarrow \gamma X(1835) \rightarrow \gamma K^0_S K^0_{S^*} \eta$  at low  $K^0_S K^0_{S^*}$  mass with a statistical significance larger than  $12.9\sigma$  using a data sample of  $1.31 \times 10^9$   $J/\psi$  events collected with the BESIII detector. In this region of phase space the  $K^0_S K^0_{S^*}$  system is dominantly produced through the  $f_0(980)$ . By performing a partial wave analysis, we determine the spin-parity of the  $X(1835)$  to be  $J^{PC}=0^{-+}$ . The mass and width of the observed  $X(1835)$  are  $1844 \pm 9(\text{stat}) + 16 - 25(\text{syst}) \text{ MeV}$  and  $192 + 20 - 17(\text{stat}) + 62 - 43(\text{syst}) \text{ MeV}$ , respectively, which are consistent with the results obtained by BESIII in the channel  $J/\psi \rightarrow \gamma \pi^+ \pi^- \eta'$ .

**WEB URL:** <http://arxiv.org/abs/1506.04807>

**79. Ablikim, M., Achasov, M. N., Ai, X. C., Albayrak, O., Albrecht, M., Ambrose, D. J., ... & Ferroli, R. B. (2015). Measurement of the matrix elements for the decays  $\eta \rightarrow \pi^+ \pi^- \pi^0$  and  $\eta/\eta' \rightarrow \pi^0 \pi^0 \pi^0$ . *Physical Review D*, 92(1), 012014.**

**ABSTRACT:**

Based on a sample of  $1.31 \times 10^9$   $J/\psi$  events collected with the BESIII detector at the BEPCII collider, Dalitz plot analyses of selected 79,625  $\eta \rightarrow \pi^+ \pi^- \pi^0$  events, 33,908  $\eta \rightarrow \pi^0 \pi^0 \pi^0$  events, and 1,888  $\eta' \rightarrow \pi^0 \pi^0 \pi^0$  events are performed. The measured matrix elements of  $\eta \rightarrow \pi^+ \pi^- \pi^0$  are in reasonable agreement with previous measurements. The Dalitz plot slope parameters of  $\eta \rightarrow \pi^0 \pi^0 \pi^0$  and  $\eta' \rightarrow \pi^0 \pi^0 \pi^0$  are

determined to be  $-0.055 \pm 0.014 \pm 0.004$  and  $-0.640 \pm 0.046 \pm 0.047$ , respectively, where the first uncertainties are statistical and the second systematic. Both values are consistent with previous measurements, while the precision of the latter one is improved by a factor of 3. Final state interactions are found to have an important role in those decays.

**WEB URL:** <http://journals.aps.org/prd/abstract/10.1103/PhysRevD.92.012014>

**80. Ablikim, M., Achasov, M. N., Ai, X. C., Albayrak, O., Albrecht, M., Ambrose, D. J., ... & Ferroli, R. B. (2015). Precision measurement of the integrated luminosity of the data taken by BESIII at center-of-mass energies between 3.810 GeV and 4.600 GeV Supported by National Key Basic Research Program of China (2015CB856700), National Natural Science Foundation of China (NSFC)(11125525, 11235011, 11322544, 11335008, 11425524), Chinese Academy of Sciences (CAS) Large-Scale Scientific Facility Program, Joint Large-Scale Scientific Facility Funds of the NSFC and CAS (11179007, U1232201, U1332201) CAS (KJ CX2-YW-N29, KJ CX2 .... *Chinese physics C*, 39(9), 093001.**

**ABSTRACT:**

From December 2011 to May 2014, about  $5 \text{ fb}^{-1}$  of data were taken with the BESIII detector at center-of-mass energies between 3.810 GeV and 4.600 GeV to study the charmonium-like states and higher excited charmonium states. The time-integrated luminosity of the collected data sample is measured to a precision of 1% by analyzing events produced by the large-angle Bhabha scattering process.

**WEB URL:** <http://iopscience.iop.org/article/10.1088/1674-1137/39/9/093001/meta>

**81. BESIII Collaboration (2015). Observation of  $Z(c)(3900)(0)$  in  $e^+e^- \rightarrow \pi(0)\pi(0) J/\Psi$ . *Physical Review Letters*, 115(11), [112003].**

**ABSTRACT:**

Using a data sample collected with the BESIII detector operating at the BEPCII storage ring, we observe a new neutral state  $Z(c)(3900)(0)$  with a significance of 10.4 sigma. The mass and width are measured to be  $3894.8 \pm 2.3 \pm 3.2$  MeV/c<sup>2</sup> and  $29.6 \pm 8.2 \pm 8.2$  MeV, respectively, where the first error is statistical and the second systematic. The Born cross section for  $e^+e^- \rightarrow \pi^0\pi^0 J/\psi$  and the fraction of it attributable to  $\pi^0 Z(c)(3900)(0) \rightarrow \pi^0\pi^0 J/\psi$  in the range E-c.m. = 4.19-4.42 GeV are also determined. We interpret this state as the neutral partner of the four-quark candidate  $Z(c)(3900)(+/-)$ .

**WEB URL:** [http://www.rug.nl/research/portal/publications/observation-of-zc39000-in-ee--pi0pi0-jpsi\(f704dc89-1ccd-4e01-a8a3-837619d1f4e1\).html](http://www.rug.nl/research/portal/publications/observation-of-zc39000-in-ee--pi0pi0-jpsi(f704dc89-1ccd-4e01-a8a3-837619d1f4e1).html)

**82. Ablikim, M., Achasov, M. N., Ai, X. C., Albayrak, O., Albrecht, M., Ambrose, D. J., ... & Ferroli, R. B. (2015). Amplitude analysis of the  $\pi^0\pi^0$  system produced in radiative  $J/\psi$  decays. *Physical Review D*, 92(5), 052003.**

**ABSTRACT:**

An amplitude analysis of the  $\pi^0\pi^0$  system produced in radiative  $J/\psi$  decays is presented. In particular, a piecewise function that describes the dynamics of the  $\pi^0\pi^0$  system is determined as a function of  $M_{\pi^0\pi^0}$  from an analysis of the  $(1.311 \pm 0.011) \times 10^9$   $J/\psi$  decays collected by the BESIII detector. The goal of this analysis is to provide a description of the scalar and tensor components of the  $\pi^0\pi^0$  system while making minimal assumptions about the properties or number of poles in the amplitude. Such a model-independent description allows one to integrate these results with other related results from complementary reactions in the development of phenomenological models, which can then be used to directly fit experimental data to obtain parameters of interest. The branching fraction of  $J/\psi \rightarrow \gamma\pi^0\pi^0$  is determined to be  $(1.15 \pm 0.05) \times 10^{-3}$ , where the uncertainty is systematic only and the statistical uncertainty is negligible.

**WEB URL:** <http://journals.aps.org/prd/abstract/10.1103/PhysRevD.92.052003>

**83. Çetin, S. A., & BESIII Collaboration. (2015). Evidence for  $e^+ e^- \rightarrow \gamma \chi_{c1, 2}$  at center-of-mass energies from 4.009 to 4.360 GeV. *Phys. Rev. D*, **39/4**, 41001.**

**ABSTRACT:**

Using data samples collected at center-of-mass energies of  $\sqrt{s}=4.009, 4.230, 4.260,$  and  $4.360$  GeV with the BESIII detector operating at the BEPCII collider, we perform a search for the process  $e^+e^- \rightarrow \gamma \chi_{cJ}$  ( $J=0, 1, 2$ ) and find evidence for  $e^+e^- \rightarrow \gamma \chi_{c1}$  and  $e^+e^- \rightarrow \gamma \chi_{c2}$  with statistical significances of  $3.0 \sigma$  and  $3.4 \sigma$ , respectively. The Born cross sections  $\sigma_B(e^+e^- \rightarrow \gamma \chi_{cJ})$ , as well as their upper limits at the 90% confidence level (C.L.) are determined at each center-of-mass energy.

**WEB URL:** <http://openaccess.dogus.edu.tr/handle/11376/1986>

**84. Rufai, O. R., Bains, A. S., & Ehsan, Z. (2015). Arbitrary amplitude ion acoustic solitary waves and double layers in a magnetized auroral plasma with  $q$ -nonextensive electrons. *Astrophysics and Space Science*, **357(2)**, 1-7.**

**ABSTRACT:**

Using the Sagdeev pseudo-potential technique, further investigation on the effect of nonextensive hot electrons on finite amplitude nonlinear low-frequency electrostatic waves in a magnetized two-component plasma have been reported in detail. The plasma model consists of cold ions fluid and nonextensively distributed electrons. The existence domain for the nonlinear structures have been established analytically and numerically. Apart from the compressive and rarefactive soliton solutions that have been reported earlier, the present investigation shows that double layer structures can be obtained for certain values of nonextensive electrons in the supersonic Mach number regime. The present results may provide an explanation for the observed nonlinear structures in the auroral region of the Earth's magnetosphere.

**WEB URL:** <http://link.springer.com/article/10.1007/s10509-015-2329-0>

**85. Ullah, M., Ahmed, E., Hussain, F., Rana, A. M., & Raza, R. (2015). Electrical conductivity enhancement by boron-doping in diamond using first principle calculations. *Applied Surface Science*, 334, 40-44.**

**ABSTRACT:**

Boron doping in diamond plays a vital role in enhancing electrical conductivity of diamond by making it a semiconductor, a conductor or even a superconductor. To elucidate this fact, partial and total density of states has been determined as a function of B-content in diamond. Moreover, the orbital charge distributions, B–C bond lengths and their population have been studied for B-doping in pristine diamond thin films by applying density functional theory (DFT). These parameters have been found to be influenced by the addition of different percentages of boron atoms in diamond. The electronic density of states, B–C bond situations as well as variations in electrical conductivities of diamond films with different boron content and determination of some relationship between these parameters were the basic tasks of this study. Diamond with high boron concentration (~5.88% B-atoms) showed maximum splitting of energy bands (caused by acceptor impurity states) at the Fermi level which resulted in the enhancement of electron/ion conductivities. Because B atoms either substitute carbon atoms and/or assemble at grain boundaries (interstitial sites) inducing impurity levels close to the top of the valence band. At very high B-concentration, impurity states combine to form an impurity band which accesses the top of the valence band yielding metal like conductivity. Moreover, bond length and charge distributions are found to decrease with increase in boron percentage in diamond. It is noted that charge distribution decreased from +1.89 to –1.90 eV whereas bond length reduced by 0.04 Å with increasing boron content in diamond films. These theoretical results support our earlier experimental findings on B-doped diamond polycrystalline films which depict that the addition of boron atoms to diamond films gives a sudden fall in resistivity even up to  $10^5 \Omega \text{ cm}$  making it a good semiconductor for its applications in electrical devices.

**WEB URL:** <http://www.sciencedirect.com/science/article/pii/S0169433214016857>

**86. Asif, M. H., Danielsson, B., & Willander, M. (2015). ZnO Nanostructure-Based Intracellular Sensor. *Sensors*, 15(5), 11787-11804.**

**ABSTRACT:**

Recently ZnO has attracted much interest because of its usefulness for intracellular measurements of biochemical species by using its semiconducting, electrochemical, catalytic properties and for being biosafe and biocompatible. ZnO thus has a wide range of applications in optoelectronics, intracellular nanosensors, transducers, energy conversion and medical sciences. This review relates specifically to intracellular electrochemical (glucose and free metal ion) biosensors based on functionalized zinc oxide nanowires/nanorods. For intracellular measurements, the ZnO nanowires/nanorods were grown on the tip of a borosilicate glass capillary (0.7  $\mu\text{m}$  in diameter) and functionalized with membranes or enzymes to produce intracellular selective metal ion or glucose sensors. Successful intracellular measurements were carried out using ZnO nanowires/nanorods grown on small tips for glucose and free metal ions using two types of cells, human fat cells and frog oocytes. The sensors in this study were used to detect real-time changes of metal ions and glucose across human fat cells and frog cells using changes in the electrochemical potential at the interface of the intracellular micro-environment. Such devices are helpful in explaining various intracellular processes involving ions and glucose

**WEB URL:** <http://www.mdpi.com/1424-8220/15/5/11787/htm>

**87. Dildar, I. M., Rehman, S., Khaleeq-ur-Rahman, M., Bhatti, K. A., & Shuaib, A. (2015). Collective behavior of silver plasma during pulsed laser ablation. *Laser Physics*, 25(7), 076102.**

**ABSTRACT:**

The present work reports an electrical investigation of silver plasma using a self-fabricated Langmuir probe in air and under a low vacuum ( $\sim 10^{-3}$  torr). A silver target

was irradiated with a Q-switched Nd:YAG laser with the wavelength  $1.064\ \mu\text{m}$ , energy 10 mJ, pulse duration 9–14 ns and power 1.1 MW. The collective behavior of a silver plasma plume is studied using a Langmuir probe as an electrical diagnostic technique. By applying different positive and negative voltages to the probe, the respective signals are collected on a four channels digital storage oscilloscope having a frequency of 500 MHz. An I-V curve helps to measure electron temperature and electron density directly and plasma frequency, response time, Debye length and number of particles in 'Debye's sphere' indirectly using the theory of Langmuir probe and mathematical formulas. The floating potential is measured as negative for laser induced silver plasma in air and vacuum, following the theory of plasma.

**WEB URL:** <http://iopscience.iop.org/article/10.1088/1054-660X/25/7/076102/meta>

**88. Dousti, M. R., Amjad, R. J., & Mahraz, Z. A. S. (2015). Enhanced green and red upconversion emissions in Er<sup>3+</sup>-doped boro-tellurite glass containing gold nanoparticles. *Journal of Molecular Structure*, 1079, 347-352.**

**ABSTRACT:**

Increasing the cross-section of upconversion emissions from the rare earth ions doped materials is a challenging issue. In this work, we report on the enhancement of the up-converted emissions of Er<sup>3+</sup>-doped boro-tellurite glasses containing gold nanoparticles which have been prepared by a conventional melt-quench technique. Seven absorption bands and three emission lines are observed using the UV–Vis–IR and photoluminescence spectroscopic techniques, respectively. Red emission is enhanced up to 30 times in a sample having 1 wt% of Au nanoparticles. The presence of the gold nanoparticles with average size of  $\sim 5.74\ \text{nm}$  is confirmed by transmission electron microscopy and corresponding surface plasmon band is observed at 630 nm in a singly-doped Au-nanoparticles embedded glass sample. A model to determine the enhancement factor of the emissions is suggested which could not describe the phenomenon for high concentrations of nanoparticles. Enhancement is attributed to the increased local field around the metal, and the results are discussed in details.

**WEB URL:** <http://www.sciencedirect.com/science/article/pii/S0022286014008709>

**89. Javed, M. S., Dai, S., Wang, M., Xi, Y., Lang, Q., Guo, D., & Hu, C. (2015). Faradic redox active material of Cu<sub>7</sub>S<sub>4</sub> nanowires with a high conductance for flexible solid state supercapacitors. *Nanoscale*, 7(32), 13610-13618.**

**ABSTRACT:**

The exploration of high Faradic redox active materials with the advantages of low cost and low toxicity has been attracting great attention for producing high energy storage supercapacitors. Here, the high Faradic redox active material of Cu<sub>7</sub>S<sub>4</sub>-NWs coated on a carbon fiber fabric (CFF) is directly used as a binder-free electrode for a high performance flexible solid state supercapacitor. The Cu<sub>7</sub>S<sub>4</sub>-NW-CFF supercapacitor exhibits excellent electrochemical performance such as a high specific capacitance of 400 F g<sup>-1</sup> at the scan rate of 10 mV s<sup>-1</sup> and a high energy density of 35 Wh kg<sup>-1</sup> at a power density of 200 W kg<sup>-1</sup>, with the advantages of a light weight, high flexibility and long term cycling stability by retaining 95% after 5000 charge–discharge cycles at a constant current of 10 mA. The high Faradic redox activity and high conductance behavior of the Cu<sub>7</sub>S<sub>4</sub>-NWs result in a high pseudocapacitive performance with a relatively high specific energy and specific power. Such a new type of pseudocapacitive material of Cu<sub>7</sub>S<sub>4</sub>-NWs with its low cost is very promising for actual application in supercapacitors.

**WEB URL:**

<http://pubs.rsc.org/en/content/articlelanding/2015/nr/c5nr03363b/unauth#!divAbstract>

**90. Çetin, S. A., & BESIII Collaboration. (2015). Study of chi (c) decaying into phi k\*(892)(k) over-bar. *Physical Review D*. 91/11. 112008.**

**ABSTRACT:**

Using a data sample of 106 million psi(3686) events collected with the BESIII detector operated at the BEPCII storage ring, we study for the first time the decays chi(c) ->

$\phi(KSK \pm K-0 \pi(-/+))$  and  $\chi(cJ) \rightarrow \phi K+K-\pi(0)$  in the E1 radiative transition  $\psi(3686) \rightarrow \gamma \chi(cJ)$ . The decays are dominated by the three-body decay  $\chi(cJ) \rightarrow \phi K^*(892)(K) \overline{K}$ . We measure branching fractions for this reaction via the neutral and charged  $K^*(892)$  and find them consistent with each other within the expectation of isospin symmetry. In the  $K(K) \overline{K} \pi$  invariant mass distribution, a structure near the  $K^*(892)(K) \overline{K}$  mass threshold is observed, and the corresponding mass and width are measured to be  $1412 \pm 4(\text{stat}) \pm 8(\text{sys}) \text{ MeV}/c^2$  and  $\Gamma = 84 \pm 12(\text{stat}) \pm 40(\text{sys}) \text{ MeV}$ , respectively. The observed state favors an assignment to the  $h(1)(1380)$ , considering its possible  $J(PC)$  and comparing its mass, width and decay mode to those reported in the Particle Data Group.

**WEB URL:** <http://openaccess.dogus.edu.tr/handle/11376/1866>

**91. Farooq, M., Imran, A., Alam, S., Naseem, S., Riaz, S., & Shaukat, S. F. (2015). Friction and Wear Assessment of Yttria Stabilised Zirconia Thermal Barrier Coatings Produced by Plasma Spraying Method. *JOURNAL OF FACULTY OF ENGINEERING & TECHNOLOGY*, 22(1), xx-xx.**

**ABSTRACT:**

Wear and friction behaviour of yttria stabilised zirconia coatings are very sensitive to the structure of the material and test parameters such as temperature, applied load, sliding speed, and environment. The present study describes the friction, and sliding wear behaviours of plasma sprayed yttria stabilized zirconia coating ( $ZrO_2$ -8wt.% $Y_2O_3$  (YSZ) deposited on a stainless steel substrate with NiAl bond coat. Tribological properties of the coating were assessed under lubrication condition at loads of 4N and 8N. The frictional behaviour of coating was assessed at a constant temperature of 50°C, while wear characteristics of the coating were investigated at 50°C and 100°C. The experimental results of this study showed a slight decrease in frictional coefficient with increasing load. However, the coating wear rate was slightly increased with increasing

load and temperature. The coating wear mainly involved materials transferred from the counter body and pulling-out from the coating material.

**WEB URL:** <http://111.68.103.26/journals/index.php/jfet/article/view/509>

**92. Farooq, A. Imran, S. Alam, S. F. Shaukat, R. Farooq. (2015). Thermal Barrier Coatings (TBC) for Energy Efficient Systems. *JPICHE* 43(1). 1-4.**

**ABSTRACT:**

Thermal barrier coatings (TBC) is being applied very successfully in a variety of systems in energy, defense, gasturbine engines and innovative ceramic materials sectors for the improved efficiencies. Zirconia yttria (ZrO Y O ) coating deposited by plasma spray method is one of the best TBC techniques. A widespread research 2. 2 3 has been carried out to explore the effect of stabilizer on the performance of ZrO thermal barrier coatings. The 2 morphology, thermal behavior and other characteristics have been determined, using the latest techniques. It has been observed that the porosity content is homogeneously distributed and pore size is of micro level in TBC. It has been revealed that, in case of less porosity in TBC, it do not affect the hardness values but certainly it is affected by the phase change in coating. The region close to the coating showed the plastic deformation, while analyzing the samples microscopically. The validation of grain size has also been noticed in the coating region, which might be due to the overheating the samples, while coating.

**WEB URL:**

<http://www.piche.org.pk/journal/index.php?journal=jpiche&page=article&op=view&path%5B%5D=212&path%5B%5D=234>

**93. Asif,. M (2015). Theoretical Calculation of Plasma Thermal Energy Using the Solution of Equilibrium Problem. *Journal of Nuclear and Particle Physics*,5(6)97-100.**

**ABSTRACT:**

In this work we presented the plasma thermal energy by using the solution of equilibrium problem with Lithium limiter for circular cross-section HT-7 tokamak. For

this, the poloidal beta was obtained by analytical solution of the Grad-Shafranov equation (GSE) and then the plasma thermal energy is calculated. It is observed, the plasma thermal energy obtained from the analytical solution of GSE by using liquid lithium limiter is larger than that using graphite limiter, which shows that the plasma performance was improved.

**WEB URL:** <http://article.sapub.org/10.5923.j.jnpp.20150506.01.html>

**94. M. Asif (2015). Dependence of Effective Edge Safety Factor on the Energy Confinement Time by Using Equilibrium Problem. *Journal of Nuclear and Particle Physics* 5(5),93-95.**

**ABSTRACT:**

In this work we present the dependence of effective edge safety factor on the energy confinement time with Lithium limiter for circular cross-section HT-7 tokamak. For this purpose, the Shafranov parameter was obtained from analytical solution of GSE. Therefore, effective edge safety factor is calculated. Then we can find the plasma energy confinement time. It is observed, the maximum energy confinement time relate to the low values of effective edge safety factor  $(2.6 \langle q_{\text{eff}}(a) \rangle^3)$ .

**WEB URL:** <http://article.sapub.org/10.5923.j.jnpp.20150505.02.html>

**95. Ellahi, M., Rafique, M. Y., Ishtiaque, S., Ali, M. F., & Memon, J. (2015). Study on the Effects of Epoxy Resin Based Polymer Dispersed Liquid Crystal Films Using Polythiol Group (-SH) as Hardener and Catalyst. *Materials Focus*, 4(3), 197-201.**

**ABSTRACT:**

The present work has been performed to investigate the effects of the structure of epoxy resin based polymer dispersed liquid crystal (PDLC) films using polythiol group (-SH) as hardener and as well as catalyst with 4-cyano-4'-pentylbiphenyl (5CB) liquid crystal. In this study we have observed two types of system. In first system, using polythiol group (-SH) as excessive hardener Pentaerythritol-tetrakis-3-

mercaptopropionate (PERTMP), the morphology of the PDLC films were strongly influenced with alkoxy(-OR) chain length epoxy resin to the formation of crack growth PDLC films. The excessive hardener PERTMP also effects the electrooptical properties with varied driving voltage. In second system, using the catalyst Triethyleneglycol dimercaptan (TEGDM) effects the Liquid Crystal domain size and electro-optical properties of PDLC films. The liquid crystal device (LCD) parameters tester to determine the electro-optical properties of the PDLC films and observe the microstructure of the polymer matrix taking away the LC component under scanning electron microscopy (SEM). Furthermore, experimental results showed that with different amounts of TEGDM catalyst reduce the heat curing time of PDLC films from 5 hours to 3 hours, which leads to low energy consumption in LC display technology in second system. On the other hand in first system, polythiol group fractured the PDLC films continuously with changing driving voltage dramatically. Meanwhile, it is examined that by adjusting the mol% of excessive hardener, catalyst and LC content we can possess good electro-optical properties with a low energy efficient method for preparing PDLC display films.

**WEB URL:**

<http://www.ingentaconnect.com/content/asp/mf/2015/00000004/00000003/art00005>

# DEPARTMENT OF STATISTICS

## Journal Contents

1. Sanaullah, A., Noor-ul-Amin, M., & Hanif, M. (2015). Generalized exponential-type ratio-cum-ratio and product-cum-product estimators for population mean in the presence of non-response under stratified two-phase random sampling. *Pakistan Journal of Statistics*, 31(1)71-91

### **ABSTRACT:**

In this paper, generalized exponential-type estimators have been proposed for estimating the finite population mean of study variable using information on two auxiliary variables in the presence of non-response under stratified two-phase random sampling. The expressions for the bias and mean square error (MSE) of proposed estimators have been derived in two different situations of non-response. Theoretical comparisons of proposed estimators have been made with modified forms of Hansen and Hurwitz (1946), ratio and product estimators to the stratified two-phase sampling method. An empirical study has also been carried out to demonstrate the performances of proposed estimators.

### **WEB URL:**

<http://web.b.ebscohost.com/abstract?direct=true&profile=ehost&scope=site&authtype=crawler&jrnl=10129367&AN=102250771&h=u4Bogi8NGyCi0oUW%2fSOeMBaB%2b6GQomUbxOK4vJ2cSfg%2biVzOexPYBN%2bBDhfEiFqzjrtkpeVc78RjNtzJPCNw6g%3d%3d&crI=c&resultNs=AdminWebAuth&resultLocal=ErrCrlNotAuth&crlhashWebURL=login.aspx%3fdirect%3dtrue%26profile%3dehost%26scope%3dsite%26authtype%3dcrawler%26jrnl%3d10129367%26AN%3d102250771>

**2. Ismail, M. Hanif, M. & Shahbaz. M.Q (2015) Generalized estimators for population mean in the presence of non-response for two-phase sampling. *Pakistan Journal of Statistics* 31(1) 295-306.**

Abstract not found

**3. Shah, F. T., Shamail, S., & Akhtar, A., N. (2015). Lean quality improvement model for quality practices in software industry in Pakistan. *Journal of Software: Evolution and Process*, 27(4), 237-254.**

**ABSTRACT:**

Implementation of quality and achieving quality culture in small and medium software houses (SMSH) have been a subject of discussion among the industry. The existing software process improvement frameworks are too heavy for SMSH. There is a need of lean quality models that will help SMSH in establishing quality culture with minimal effort and resources. The objective of this research study is to map the environment and culture of SMSH in Pakistan towards quality improvement and process improvement by implementing total quality management philosophy. A lean quality improvement model (LQIM) consisting of four quality constructs and 10 quality practices has been proposed. The LQIM is validated using good fit indices in structural equation modeling. At the end, implementation of the proposed LQIM is explained using the Deming's philosophy of plan, do, check, act cycle for continuous process improvement.

**WEB URL:** <http://onlinelibrary.wiley.com/doi/10.1002/smr.1709/abstract>

**4. Jabeen, R., Sanaullah, A., & Hanif, M. Efficient Class Of Exponential Estimators For Population Mean In Two-Stage Cluster Sampling. *Pakistan Journal of Statistics*.31(6) 683-696.**

**ABSTRACT:**

In this study, two-stage cluster sampling has been considered for estimating population mean of study variable. The proposed class of efficient estimators is the exponential

function of single auxiliary variable. The mean square error (MSE) and bias equations have been derived for the proposed class of exponential estimators. Some conditions have been identified for which the proposed class of estimators is more efficient than the simple combined type two-stage estimator, Srivastva and Garg (2009) and Jabeen et al. (2014). An empirical study has also been carried out in order to demonstrate the performance of the proposed estimators.

**WEB URL:**

[https://www.researchgate.net/profile/Aamir\\_Sanaullah/publication/272823591\\_EFFICIENT\\_CLASS\\_OF\\_EXPONENTIAL\\_ESTIMATORS\\_FOR\\_POPULATION\\_MEAN\\_IN\\_TWO-STAGE\\_CLUSTER\\_SAMPLING/links/54f04e6a0cf2495330e58121.pdf](https://www.researchgate.net/profile/Aamir_Sanaullah/publication/272823591_EFFICIENT_CLASS_OF_EXPONENTIAL_ESTIMATORS_FOR_POPULATION_MEAN_IN_TWO-STAGE_CLUSTER_SAMPLING/links/54f04e6a0cf2495330e58121.pdf)

**5. Hussain, I., Faisal, M., Shad, M. Y., Hussain, T., & Ahmed, S. (2015). Assessment of spatial models for interpolation of elevation in Pakistan. *International Journal of Global Warming*, 7(3), 409-422.**

**ABSTRACT:**

Elevation has major impact on the climate change. Interpolation of elevation at any location in Pakistan may be useful for predicting environmental parameters such as precipitation, temperature, humidity and wind speed. The locations with low elevations are more effecting global warming as compared with locations at high elevation. Present study interpolates the amount of elevation at unobserved locations using: 1) model-based ordinary kriging; 2) model-based Bayesian kriging with constant trend; 3) model-based Bayesian kriging with varying trend; 4) spatial artificial neural network. Prediction maps of elevation for complete domain are estimated along with prediction standard deviation. The results of suggested methods are compared with means of leave one take others cross validation method. It is observed from cross validation method that model-based Bayesian kriging with constant trend performs better than the other methods of predicting the amount of elevation in Pakistan.

**WEB URL:** <http://www.inderscienceonline.com/doi/abs/10.1504/IJGW.2015.069371>

**6. Mubarak, N., Hussain, I., Faisal, M., Hussain, T., Shad, M. Y., AbdEl-Salam, N. M., & Shabbir, J. (2015). Spatial Distribution of Sulfate Concentration in Groundwater of South-Punjab, Pakistan. *Water Quality, Exposure and Health*, 7(4), 503-513.**

***ABSTRACT:***

Sulfate causes various health issues for human if on average daily intake of sulfate is more than 500 mg from drinking-water, air, and food. Moreover, the presence of sulfate in rainwater causes acid rains which has harmful effects on animals and plants. Food is the major source of sulfate intake; however, in areas of South-Punjab, Pakistan, the drinking-water containing high levels of sulfate may constitute the principal source of intake. The spatial behavior of sulfate in groundwater is recorded for South-Punjab province, Pakistan. The spatial dependence of the response variable (sulfate) is modeled by using various variograms models that are estimated by maximum likelihood method, restricted maximum likelihood method, ordinary least squares, and weighted least squares. The parameters of estimated variogram models are utilized in ordinary kriging, universal kriging, Bayesian kriging with constant trend, and varying trend and the above methods are used for interpolation of sulfate concentration. The *K*-fold cross validation is used to measure the performances of variogram models and interpolation methods. Bayesian kriging with a constant trend produces minimum root mean square prediction error than other interpolation methods. Concentration of sulfate in drinking water within the study area is increasing to the Northern part, and health risks are really high due to poor quality of water.

***WEB URL:*** <http://link.springer.com/article/10.1007/s12403-015-0165-7>

**7. Hussain, I., Mubarak, N., Shabbir, J., Hussain, T., & Faisal, M. (2015). Spatial interpolation of sulfate concentration in groundwater including covariates using Bayesian hierarchical models. *Water Quality, Exposure and Health*, 7(3), 339-345.**

**ABSTRACT:**

Sulfate is a key parameter for water quality and is commonly used in manufacturing of fertilizers, soaps, glass, papers, and common household items. If sulfate quantity is more than a threshold, it is hazardous for health. In the present paper, we use Bayesian kriging with external drift and Gaussian spatial predictive process model to analyze the spatial behavior of response variable (Sulfate). Different informative and non-informative priors are utilized to estimate the correlation parameters. The performance of these models are compared by means of twofold cross validation with deviance information criterion, and root mean square prediction as criterion. In summary, the inclusion of covariates plays an important role in minimizing the mean square prediction error. Bayesian kriging with external drift performs better than Gaussian spatial predictive process. The predictive distribution of Bayesian kriging with external drift is also applicable for interpolation of sulfate concentration at unobserved locations.

**WEB URL:** <http://link.springer.com/article/10.1007/s12403-014-0154-2>

**8. Sanaullah, A., Noor-ul-amin, M., Hanif, M., & Singh, R. (2015). Generalized Exponential Chain Estimators Using Two Auxiliary Variables For Stratified Sampling With Non-Response. *Science International*, 27(2).901-915.**

**ABSTRACT:**

In this paper, some generalized exponential chain ratio and chain product type estimators have been proposed for finite population mean in the presence of non-response in stratified two-phase sampling when means of the auxiliary variables are not available. The expressions for the bias and mean square error (MSE) of proposed estimators have been derived for two different situations of non-responses. Theoretical comparisons for proposed class of exponential estimators have been made with Hansen and Hurwitz (1946), stratified two-phase ratio and stratified two-phase product estimators. An empirical study has also been carried out to demonstrate the performances of the estimators.

**WEB URL:**

[https://www.researchgate.net/profile/Aamir\\_Sanaullah/publication/272795441\\_Generalized\\_Exponential\\_Chain\\_Estimators\\_using\\_Two\\_Auxiliary\\_Variables\\_for\\_Stratified\\_Sampling\\_with\\_Non-Response/links/54ef02680cf2e55866f3d995.pdf](https://www.researchgate.net/profile/Aamir_Sanaullah/publication/272795441_Generalized_Exponential_Chain_Estimators_using_Two_Auxiliary_Variables_for_Stratified_Sampling_with_Non-Response/links/54ef02680cf2e55866f3d995.pdf)

**9. Hussain, T., & Younis, A. (2015). Quality Management Practices And Organizational Performance: Moderating Role Of Leadership. *Science International*, 27(1) 57-522**

**ABSTRACT:**

This paper is intended to explore the synergic impact of leadership in cultivating the organizational performance outcomes of quality management practices. The main purpose of this research study is to investigate the impact of quality management practices on organizational performance through moderating role of leadership in pharmaceutical industry of Pakistan. A survey was conducted using a structured questionnaire to collect data. The population of study was comprised of pharmaceutical firms located in Lahore, Punjab those were listed on the Pakistan Pharmaceutical Manufacturers Association. The results show that implementation of quality management practices plays an important role among pharmaceutical firms' performance. Direct multiple regression model of organizational performance identified three quality management practices, customer focus, continuous improvement, and benchmarking, as significant predictors of organizational performance. Further, a moderation analysis between three significant predictors and an organizational performance revealed that leadership has strong and significant moderating role. It is inferred that the success of quality management programs is actually stimulated with enthusiastic involvement of leadership.

**WEB URL:**

<http://web.a.ebscohost.com/abstract?direct=true&profile=ehost&scope=site&authtype=crawler&jrnl=10135316&AN=102199574&h=IscmBLL1hUi9HyW9ad6sTbOnDwbb%2bmBKLHfHD7DVEQcn29QqYQxp3h8%2bU5FKFgGDAOr0mbvLy0CzbkbRHMhELw%3d%3d&c>

rl=c&resultNs=AdminWebAuth&resultLocal=ErrCrINotAuth&crlhashWeb  
URL=login.aspx%3fdirect%3dtrue%26profile%3dehost%26scope%3dsite%26authype%3  
dcrawler%26jrnl%3d10135316%26AN%3d102199574

**10. Shah, F.T. . Khan, A. Imam and M. Sadiqa. (2015) Impact of service quality on customer satisfaction of banking sector employees: a study of lahore, Punjab, Vidyabharati International Interdisciplinary Research Journal, 4(1) 54-60.**

**ABSTRACT:**

Customer satisfaction and service quality both are most widely studied constructs. Organizations are working hard to provide the quality of service to their customers in order to attain their satisfaction and loyalty. This study was destined to find the impact of service quality on customer satisfaction in banking sector employees of Lahore region. This study was a cross-sectional study and questionnaire used was adopted from empirical studies. Finding showed that there exists a significant positive relationship between service quality and customer satisfaction. Study revealed that the respondents have responded in disagreement to the quality of services provided to the customers, which in turn, definitely affected the customer satisfaction. Poor quality of service is being provided to customers who show a poor customer satisfaction. Data was analyzed using reliability statistics, correlation and regression analysis. Future recommendations were also presented in this study.

**WEB URL:** <http://www.viirj.org/vol4issue1/9.pdf>

**11. Mansoor, S., Shah, F. T., ur Rehman, A., & Tayyaba, A. (2015). Impact of Training and Development on Organization Performance with Mediating Role of Intention to Quit as Human Resource Quality Cost. *European Online Journal of Natural and Social Sciences*, 4(4), 787.**

**ABSTRACT:**

The study is focused on the analysis of the impact of the training and development efforts in the Small and Medium Enterprises of Pakistan on the intention of employees to leave the organization considering it as an expense and the wastage of time and resources by the organization. The study will also evaluate the ultimate impact of the intentions of the employees on the performance of the organization. The salary based employees of the organizations having 5 – 250 employees have been selected on the basis of stratified sampling technique for the data collection purposes. Out of 600 questionnaires distributed, 290 were returned and 278 were used for the study. The relationship of training and development and organization performance has been found to be positively mediated by the intention of employees to quit the organizations. The positive relationship might exist due to the number of other factors like inflation, less job opportunities existing in the Pakistani context. The study will be highly significant for the practitioners in the SMEs, shifting their focus towards the increased training and development efforts.

**WEB URL:**

<http://search.proquest.com/openview/3e90e32f4d1829a2b404fcbc26d28e3b/1?pq-origsite=gscholar&cbl=2029677>

**12. Shahzad,, N M., Asghar, Z., Shehzad, F., & Shahzadi, M. (2015). Parameter Estimation of Power Function Distribution with TL-moments. *Revista Colombiana de Estadística*, 38(2), 321-334.**

**ABSTRACT:**

Accurate estimation of parameters of a probability distribution is of immense importance in statistics. Biased and imprecise estimation of parameters can lead to erroneous results. Our focus is to estimate the parameter of Power function distribution accurately because this density is now widely used for modelling various types of data. In this study, L-moments, TLmoments, LL-moments and LH-moments of power function distribution are derived. In addition, the coefficient of variation, skewness and kurtosis

are obtained by method of moments, L-moments and TL-moments. Parameters of the density are estimated using linear moments and compared with method of moments and MLE on the basis of bias, root mean square error and coefficients through simulation study. L-moments proved to be superior for the parameter estimation and this conclusion is equally true for different parametric values and sample size.

**WEB URL:** <http://www.scielo.org.co/pdf/rce/v38n2/v38n2a01.pdf>

**13.Rashid, R., ul Amin, M. N., & Hanif, M. (2015). Exponential Estimators for Population Mean Using the Transformed Auxiliary Variables. *Appl. Math*,9(4), 2107-2112.**

**ABSTRACT:**

This paper deals with exponential ratio-cum-ratio and product-cum-product type estimators using transformed auxiliary variables under simple random sampling without replacement. The proposed estimators are useful for estimating the finite population mean. The development of estimators is based on the information of two transformed auxiliary variables. The generalized form of the proposed estimator has been developed and the special cases are discussed. The bias and mean square error expressions of the proposed estimators are derived up to the first order of approximation. An empirical study has been carried out to compare the efficiency of proposed estimators with some available estimators in literature. An improvement has been reflected in terms of mean square error (MSE).

**WEB URL:** <http://cpaindex.naturalspublishing.com/files/published/23tgsas0x17732.pdf>

# MISCELLANEOUS

## Journal Papers

1. Abbas, H. W., Shafique, M., Qadeer, F., Moin ud Din, N., Ahmad, R., & Saleem, S. S. (2015). Impact of Perceptions of Organizational Politics on Employees' Job Outcomes: The Moderating Role of Self-Efficacy and Personal Political Skills. *Science International*, 27(3). 2729-2734.

**ABSTRACT:**

Organizational politics within the organization is considered as a source of stress and dissatisfaction among employees. Many organizations are working to eradicate organizational politics within them, but most of them are unsuccessful to eliminate this epidemic phenomenon. By using data from 101 employees from different organizations in Lahore-Pakistan, this study reviews the relationship between perception of organizational politics and job attitudes (OC, JS and IL). This study also examines the role of self-efficacy and personal political skills in moderating the relationship between organizational politics and job outcomes. The results of the study imply that perception of organizational politics has significant negative effects on organizational commitment and job satisfaction and a positive but insignificant relationship with intention to leave. Personal political skill and self-efficacy moderates the relationship between POP & job outcomes. Politically skilled employees with high level of self-efficacy remain committed even when the POP is high within the organization. Moreover, self-efficacy does not moderate the relationship between POP and job satisfaction.

**WEB URL:** [http://papers.ssrn.com/sol3/papers.cfm?abstract\\_id=2631403](http://papers.ssrn.com/sol3/papers.cfm?abstract_id=2631403)

2. Masood, M., Shafique, M., Ahmad, R., & Mansoor, M. Y. (2015). The Impact of Upward Influence Strategies on Performance Ratings: Using Social Network as Moderator. *Sci. Int.(Lahore)*, 27(3), 2945-2952.

**ABSTRACT:**

Subordinates frequently employ specific influence strategies in their attempt to obtain rewards and recognition from their supervisors. This is a descriptive study that explains and examines the impact of upward influence strategies on performance rating with a moderating effect of social capital. The sample is taken from hotel industry employees where supervisors, being the targets are influenced by their subordinates. The findings suggest that upward influence strategies have a significant impact on performance ratings. Moreover, results also indicate that while using social network as moderator, upward influence strategies have a more significant impact on performance ratings. Practical implications, contributions and limitations of the study are also described.

**WEB URL:** [http://papers.ssrn.com/sol3/papers.cfm?abstract\\_id=2635144](http://papers.ssrn.com/sol3/papers.cfm?abstract_id=2635144)

**3. Fatima, M., Shafique, M., Qadeer, F., & Ahmad, R. (2015). HR Practices and Employee Performance Relationship in Higher Education: Mediating Role of Job Embeddedness, Perceived Organizational Support and Trust. *Pakistan Journal of Statistics and Operation Research*, 11(3), 421-439.**

**ABSTRACT:**

The purpose of this paper is to find out the impact of Human Resource practices on employee performance. Job embeddedness, Perceived organizational support and Trust were taken as mediators and they were investigated for their mediation effect on the relationship between human resource practices and employee performance. Organizational citizenship behavior and task performance were taken as two dimensions of Employee Performance. Data was collected through questionnaires from faculty members of seven campuses of a Public sector University in Pakistan. Results support that job embeddedness, perceived organization support and trust have partial or full mediation role for Human Resource Practices-Performance relationship of teaching faculty of Higher Education sector.

**WEB URL:** [http://papers.ssrn.com/sol3/papers.cfm?abstract\\_id=2672948](http://papers.ssrn.com/sol3/papers.cfm?abstract_id=2672948)

**4. Shafique, M., Ahmad, R., Saleem, S. S., & Qadeer, F. (2015). Work Family Conflicts and its Impact on Attitude of Motorway Patrolling Officers: Moderating Role of Embeddedness. *Vidyabharati International Interdisciplinary Research Journal*, 4(2), 129-141.**

**ABSTRACT:**

This study is aimed to examine the impact of work family conflicts on job satisfaction level of employees which is an important and most studied attitudinal antecedent of employees' outcomes. Mitigation role of both facets of job embeddedness have also been investigated for this relationship which has not been focused in previous research. This study is unique in a way that it has considered family specific perspective and contemporary construct 'embeddedness' simultaneously that ultimately shape and influence job satisfaction level on employees. In this correlational and cross-sectional study data was collected from patrolling officers of Motorway Police, Punjab, Pakistan. The analysis proved negative correlation of work family conflicts with job satisfaction and moderating role of organization embeddedness has its support from the data. Relationship of family work conflict and community embeddedness has no support in this study that needs to be investigated in future research. HR professionals of today' business organizations must work toward work life balance strategies and should consider organizational embeddedness as one of the options to dissipate family conflict caused due to extra work demands.

**WEB URL:** [http://papers.ssrn.com/sol3/papers.cfm?abstract\\_id=2718848](http://papers.ssrn.com/sol3/papers.cfm?abstract_id=2718848)

## Author Index

### A

- A. Khan et al, 51  
A. Rauf, 84  
A., Hussain, T, 81  
A., Khan,, 80, 81, 103, 104, 121, 123, 246  
A.A. Chaudhry, 84  
A.S. Khan, 84  
Abassi, A. S, 129, 136  
Abbas, F, 141  
Abbas, G, 116, 195, 207, 215, 241, 249, 251  
Abbas, H, 232, 292  
Abbas, N, 25  
Abbas, S, 3  
Abbasi, A. S, 131  
Abbasi, M, 47  
Abd El-Salam, N. M, 123  
AbdEl-Salam, N. M, 285  
Abdullah, M. A, 33  
Abid, S. A, 46  
Abid,. M K. S, 212  
Abid1, M, 211  
Ablikim,. M, 219, 224, 225, 257, 258, 259, 260, 261, 262, 263, 264, 269, 270, 271, 272  
Achasov, M. N, 219, 224, 225, 257, 258, 259, 260, 261, 263, 264, 269, 270, 271, 272  
Adnan, F, 134  
Afaq, A, 226  
Afza, T, 129, 169, 170, 171, 173, 174, 175  
Afzaal, M, 33  
Afzaal, S, 76  
Afzal, M, 126, 217, 227, 250, 255  
Afzal., H, 50  
Agarwal, R. P, 209, 210  
Ahmad, A, 33, 265  
Ahmad, E, 45  
Ahmad, F, 4, 5, 6, 42, 51  
Ahmad, H, 209  
Ahmad, I, 105  
Ahmad, K, 73  
Ahmad, M, 13, 70, 215, 233, 241, 243, 251  
Ahmad, M. A, 215  
Ahmad, M. M, 13, 70  
Ahmad, P, 101, 104  
Ahmad, R., 83, 237, 292, 293, 294  
Ahmad, S, 77, 203  
Ahmad, W, 241  
Ahmad, Z, 29, 35, 51  
Ahmed, A, 248  
Ahmed, E, 250, 274  
Ahmed, F., Hussain, 95  
Ahmed, K, 144, 152  
Ahmed, O. H, 212  
Ahmed, S, 285  
Ahn, S, 234, 235, 256  
Ai, X. C, 219, 224, 225, 257, 258, 259, 260, 261, 263, 264, 269, 270, 271, 272  
Ain, Q, 77  
Aisha, A. Q, 165  
Ajmal, M, 16  
Akhtar, A, 153  
Akhtar, A., N., 284  
Akhtar, J, 29  
Akhtar, M. N, 215, 241, 243, 244, 245, 248, 251, 252, 253, 254  
Akhtar, N. A, 29  
Akhtar, N. M, 233  
Akhter, P, 10, 12, 36  
Akhter, W, 153, 158  
Akram, M, 176, 228  
Akram, N, 157, 247, 248  
Al Khuraif, A. A, 75  
Al Mamun, 146  
Alam, A, 175  
Alam, S. F, 279  
Al-Amiery, A. A, 252  
Albayrak, O, 219, 224, 225, 257, 258, 259, 260, 261, 263, 264, 269, 270, 271, 272  
Albrecht, M, 219, 224, 225, 257, 258, 259, 260, 261, 263, 264, 269, 270, 271, 272  
Ali, A, 128, 247  
Ali, I, 241, 243, 244  
Ali, J, 121, 246  
Ali, K, 55, 180, 181, 182, 206  
Ali, M, 46, 220, 239, 281  
Ali, N, 29  
Ali, S, 195, 203  
Ali, Z, 23  
ALla, A, 251  
Alia, I, 208  
Alias, A. N, 264  
Alkanhal, M. A, 119  
Alonso, G. A, 74  
Alvi, F, 248  
Alwi, H, 53, 54

**Ambrose, D. J.**, 219, 224, 225, 257, 258, 259, 260, 261, 263, 264, 269, 270, 271, 272  
**Amin, M.**, 101, 283, 291  
**Amin, N.**, 27, 28, 31, 227, 255  
**Amin, N. S.**, 27, 28, 31  
**Amin, Y. M.**, 101, 104  
**Amir, H.**, 155, 165, 167  
**Amir-ud-Din, R.**, 164  
**Amjad, R. J.**, 216, 226, 231, 242, 253, 264, 265, 276  
**Amjed, N.**, 266  
**Andreescu, S.**, 77, 85, 95  
**Anis, O.**, 141  
**Anjum, M. W.**, 18, 19  
**Anjum, S.**, 236  
**Anwar, I.**, 180, 181, 203  
**Anwar, M. S.**, 76, 87, 118, 119  
**Anwar, S.**, 148  
**Arain, M. B.**, 98  
**Arshad, M.**, 117  
**Arshad, S.**, 179, 194, 209, 210, 213, 214  
**Arshad, Z.**, 43  
**Asghar, Z.**, 290  
**Ashiq, M. N.**, 244  
**Ashraf, M.**, 113, 120  
**Ashraf, R.**, 60  
**Ashraf, S.**, 177, 194, 204  
**Asif, A.**, 209  
**Asif, M.**, 49, 50, 101, 121, 222, 233, 246, 275  
**Asif, M.**, 280  
**Aslam, M. N.**, 266  
**Atif, M.**, 251  
**Atiq, S.**, 107, 118, 119  
**Awais, M. N.**, 55  
**Awan, M. A.**, 3  
**Awan, M. S.**, 101, 121, 222  
**Ayub, K.**, 84, 117  
**Azam, M. T.**, 78, 83  
**Azhari, C. H.**, 254  
**Aziz, S.**, 65  
**Azmat, I.**, 226

## B

**Bahadori, A.**, 34  
**Baig, M. M. Z.**, 61, 62, 63, 64  
**Baig, M. Z.**, 71  
**Baig, S.**, 53  
**Bains, A. S.**, 273  
**Bajda, M.**, 95, 113, 120  
**Bajodah, A.**, 53  
**Bajwa, U. I.**, 44

**Balaji, N.**, 235, 256, 257  
**Bandulasena, H.**, 4  
**Bano, N.**, 156  
**Baron, G. V.**, 18  
**Basavarajappa, S.**, 75  
**Basharat, B.**, 172  
**Bashir, A.**, 161  
**Bashir, M.**, 105, 220, 228, 230  
**Bashir, S.**, 112, 228  
**Batool, F.**, 186  
**Bazmi, A. A.**, 30  
**Bazmi, A. A.**, 34, 79  
**Behery, E. E.**, 230  
**Belic, M.**, 184, 189  
**BESIII Collaboration.**, 236, 259, 266, 267, 268, 271, 272, 278  
**Bhand, S.**, 99  
**Bhar, P.**, 204  
**Bhat, A. H.**, 33  
**Bhatti, A. A.**, 190  
**Bhatti, K. A.**, 275  
**Bhatti, M.**, 188  
**Bhutto, A. W.**, 34  
**Bibi, S.**, 135  
**Bilal, K.**, 165  
**Biswas, A.**, 184  
**BISWAS, A.**, 189  
**Bodla, M. A.**, 169, 173  
**Borhani, M. R.**, 29  
**Bouoiyour, J.**, 133  
**Bueken, B.**, 19  
**Bulbul, G.**, 85  
**Bülbul, G.**, 95  
**Bustam, M. A.**, 89, 97, 102, 110, 116, 125  
**Butt, S. I.**, 182

## C

**Cao, H.**, 239  
**Carvalho, H. F.**, 91  
**Catanante, G.**, 92, 99, 100  
**Çetin, S. A.**, 236, 267, 268, 272, 278  
**Champagne, D. L.**, 122  
**Chattopadhyay, S.**, 185, 186, 196, 202  
**Chaudhry, A. A.**, 77, 88, 111  
**Chaudhry, M.**, 39, 40  
**Chaudhry, S.**, 40, 47  
**Chaudhry, S. R.**, 40  
**Cheema, I. Z.**, 212  
**Chen, G.**, 24, 43  
**Chen, L.**, 43, 221

**Chighoub, F**, 208  
**Choi, K. H.**, 14, 15, 55  
**Choudary, M. A.**, 105  
**Cianca, E.**, 55  
**Couck, S.**, 18  
**Cox, R. J.**, 126  
**Crudden, C. M.**, 115  
**Cunningham, J.**, 85

## D

**D. M., Barbosa,** 91  
**D., Chen, Y.**, 96  
**D., Faryal,** 83  
**Dai, S.**, 221, 277  
**Damalas, C. A.**, 132, 137, 149, 150, 151  
**Damas-Souza,** 91  
**Danielsson, B.**, 275  
**Danish, R. Q.**, 173  
**Dawood, A.**, 228  
**Dawson, R.**, 247  
**de Camargo, A. S. S.**, 264  
**de Clippel, F.**, 18  
**De Sao Carlos, F.**, 221  
**De Vos, D. E.**, 19  
**Debnath, U.**, 186, 195  
**Del Valle, M.**, 107, 109  
**Deorsola, F. A.**, 11  
**Didden, J.**, 18  
**Dildar, I. M.**, 275  
**Din, M. I.**, 85, 112  
**Dominguez, R. B.**, 74  
**Dong, R.**, 7, 9, 20, 21, 22, 32  
**Dousti, M. R.**, 216, 226, 231, 242, 264, 276  
**Dovis, F.**, 55  
**Du, S.**, 250  
**Durgesh, B. H.**, 75

## E

**Edwards, C.**, 53, 54  
**Ehsan, F.**, 41, 138  
**Ehsan, S.**, 170  
**Ejaz, A.**, 117  
**Ellahi, M.**, 239, 281  
**Elsheikh, Y. A.**, 79  
**El-Taibany, W. F.**, 230

## F

**F., Afzal, A.**, 80  
**Faisal, M.**, 285, 286  
**Faisal,. A.**, 128  
**Fan, L.**, 217  
**Fang, L.**, 215  
**Farhani, S.**, 147  
**Farooq, A.**, 84, 90, 117, 162, 176, 279  
**Farooq, H.**, 212  
**Farooq, M.**, 278  
**Farooq, R.**, 37  
**Farooqi, Z. H.**, 125  
**Fatima, M.**, 155, 293  
**Fatima, S.**, 63, 68, 69  
**Fatima,. S.**, 66  
**Fatima. S.**, 68  
**Fazli, S. K.**, 60  
**Fazli, S.K.**, 71  
**Ferroli, R. B.**, 219, 224, 225, 257, 258, 259, 260, 261, 263,  
264, 269, 270, 271, 272  
**Fino, D.**, 8, 11

## G

**Gaaz, T. S.**, 252  
**Gao, Y.**, 15, 108, 239  
**Ghaffar, A.**, 119  
**Ghafoor, I.**, 107  
**Ghauri, M.**, 29  
**Ghauri, T. K.**, 153  
**Gholamreza Z.**, 30  
**Gilani, M. A.**, 84, 113, 114, 117  
**Gilanie, G.**, 45  
**Gonfa, G.**, 89, 94, 97, 116  
**Gong, W. X.**, 262  
**Guo, D.**, 221, 277  
**Gushikem, Y.**, 93  
**Guzman, J. V.**, 184

## H

**Habib, A.**, 31, 80  
**Habib, Z.**, 48  
**Haider, A.**, 159  
**Haider, W.**, 106, 111  
**Hamayun, M. T.**, 53, 54  
**Han, J. I.**, 26  
**Hanif, M.**, 283, 284, 287, 291  
**Haq, N. U.**, 16

Harijan, K, 34  
Hashmi, I, 3  
Haslenda H, 30  
Hassan, A, 116  
Hassan, H, 153  
Hassan, M. U, 233  
Hassan, S, 43, 161  
Hassan, S. U, 43  
Hayat, A, 74, 77, 85, 92, 95, 99, 100, 106, 107, 109, 111, 228  
Hong, W. P, 228, 239  
Hudon, M, 172  
Hurain, S. S, 31  
Husnain, M. I. U, 159  
Husnine, S. M, 206  
Hussain, 7, 8, 9, 10, 11, 12, 20, 21, 22, 23, 24, 31, 32, 36, 39, 40, 43, 45, 46, 47, 81, 125, 181, 188, 211, 212, 223, 234, 235, 241, 242, 250, 256, 257, 262, 274, 285, 286, 288  
Hussain, F, 45, 250, 274  
Hussain, H, 23  
Hussain, I, 43, 223, 285, 286  
Hussain, M, 7, 8, 9, 10, 11, 12, 20, 21, 22, 24, 32, 36, 46, 181, 188, 212  
Hussain, S. A, 39, 40, 47  
Hussain, S. M, 31  
Hussain, T, 125, 262, 285, 286, 288  
Hussnain, A, 237

## I

I. Rehma, 84  
I. U., & Wong, F. S, 82  
I., Afzal, 81  
Idrees, F, 153  
Idrees, M, 223, 233, 237  
Idris, M, 58  
Idris, S, 58  
Iftikhar, M. A, 46  
Ihsan, M, 98  
Ijaz, K, 88  
Ikram, M, 105  
Imran, A, 172, 278  
Imran, S, 279  
Inayat, A., 13  
Iqbal, A, 242, 253, 265  
Iqbal, B, 77  
Iqbal, F, 15, 108  
Iqbal, J, 15, 23, 108  
Iqbal, S, 121, 246  
Iqbal, Z, 23

Irfan, A, 116  
Irshad, M, 247  
Ishaque, M, 244  
Ishrat, S, 101, 222  
Islam, A, 33  
Islam, M, 244, 249  
Islam, M. U, 244  
Islam, S, 204  
Ismail, M, 283  
Ismail, Z, 33

## J

Jabeen, G, 37  
Jabeen, M, 249  
Jabeen, R, 284  
Jabeen, S, 47  
Jalil, A, 46, 163  
Jamal, A, 80  
Jamil, M, 220, 228, 239, 240, 241  
Jamil, T, 33  
Janjua, N. K, 249  
Javaid F, 167  
Javaid, I, 182  
Javaid, M, 167, 181, 188  
Javaid, M. F, 167  
Javed, M. S, 221, 277  
Javed, Q. U. A, 232  
Javed, S, 179, 194, 205  
Javed- S, 210  
Javid, M. A, 227, 255  
Jawad, A, 178, 184, 185, 186, 187, 189, 191, 192, 195, 196, 198, 199, 200, 201, 202, 204, 205  
Jawad, A, 197  
Jemaa, M. M. B, 139, 140  
Jiang, L, 7, 9, 20, 21, 22, 32  
Jibeen, T, 58, 66, 67, 68  
Jończyk, J, 95  
Jung, Y. D, 228, 239, 240

## K

Kadhun, A. A. H, 252  
Kaleem, M, 40, 82  
Kamran, M. A, 232  
Kandil, M, 148  
Kanwal, F. N, 85  
Kanwal, S, 205  
Karamat, N, 244  
Karim, S. A, 254

**Karimov, H. A,** 212  
**Kashif, A,** 181  
**Kerre, E,** 177, 204  
**Khaleeq-ur-Rahman,** 275  
**Khalid, M,** 49, 50, 180, 253  
**Khalil,** 211  
**Khan, A,** 4, 5, 17, 18, 19, 23, 37, 53, 75, 77, 78, 80, 81, 82,  
83, 88, 90, 96, 101, 102, 110, 116, 121, 123, 124, 125,  
168, 169, 213, 222, 241, 246, 289  
**Khan, A. A,** 37, 121, 241, 246  
**Khan, A. L,** 17, 18, 19  
**Khan, A. U,** 4, 5, 37, 96  
**Khan, A. Z,** 23  
**Khan, F. U.,,** 96  
**Khan, H,** 79, 123  
**Khan, I. U,** 120  
**Khan, K. A,** 182  
**Khan, M,** 15, 67, 68, 78, 103, 108, 123, 132, 137, 149, 150,  
151, 155, 157, 159, 165, 233, 243, 244  
**Khan, M. A,** 67, 68, 103, 243, 244  
**Khan, M. I,** 15, 108, 123  
**Khan, N. I,** 88  
**Khan, R. A,** 79  
**Khan, S,** 33, 42, 126, 234, 256  
**Khan, S. A,** 42  
**Khan, S. M,** 33  
**Khan, U,** 80, 93, 104  
**Khan, Z,** 13, 15, 25, 96, 108  
**Khandaker, M. U,** 101, 104  
**Khattak, N. S,** 80  
**Khraief, N,** 139, 140  
**Khurram, N,** 155, 159  
**Kim, H,** 15, 25, 257  
**Kim, H. C,** 15  
**Kim, H. T,** 25  
**Kim, J,** 40  
**Kim, S,** 234, 235, 256  
**Koppenwallner, M,** 114  
**Kubota, L. T,** 93  
**Kwon, G. D,** 234, 235, 256  
**Kyophilavong, P,** 148, 162

## L

**L. Shahzadi,** 84  
**Lakhvi, M. H,** 69  
**Latif, H,** 236, 253  
**Lau, K. K,** 4, 6  
**Le, A. H. T,** 235, 256  
**Lee, M,** 4  
**Lee, Y,** 15, 257

**Lee, Y. J,** 257  
**Lee, Y. W,** 15  
**Li, D,** 24  
**Lima, R. B,** 250  
**Ling, C. H,** 152  
**Ling, T. C,** 39, 40  
**Liu, Y,** 9, 32  
**Lock, S. S. M,** 4, 6  
**Loganathan, N,** 129, 141, 143  
**Long, W,** 144  
**Lu, X. Z,** 39  
**Lund, P. D,** 217  
**Lupulescu, V,** 209, 210  
**Luqman K. M,** 167  
**Luqman, K,** 167

## M

**M Yar,,** 84  
**M. R. A., Hussain,** 88  
**Ma, Y,** 217  
**Mahalik, M. K,** 141  
**Mahmood, A,** 104, 118  
**Mahmood, H,** 150, 155, 157, 232, 253  
**Mahmood, H. Z,** 150, 155, 157  
**Mahmood, K,** 228, 244  
**Mahmood, N,** 76, 87, 90  
**Mahmood, S. A,** 184  
**Mahmood, Z,** 160  
**Mahraz, Z. A. S,** 276  
**Majeed, A,** 189  
**Malik, A,** 223  
**Malik, M. E,** 156  
**Malik, S,** 172  
**Mallick, H,** 141  
**Man, Z,** 5, 79, 102, 110, 123, 125  
**Manan, A,** 80, 104  
**Manan, A., Rahman,** 80  
**Mansoor, M. Y,** 293  
**Mansoor, S,** 289  
**Manzoor, A,** 40  
**Manzoor, F,** 121, 246  
**Maqbool, K,** 194, 209, 214  
**Martens, J. A,** 17  
**Marty, J. L,** 74, 92, 99, 100, 106, 107, 109, 111  
**Masood, M,** 293  
**Masood, S,** 148  
**Masood,, S,** 165  
**Matin, A,** 16  
**Maulud, A,** 5  
**Mazloun-Ardakani, M,** 35

Medley, G. J, 4  
Mehfooz. M, 63  
Mehmood, I, 160  
Mehmood, M, 105, 237  
Mehmood, M. S, 105  
Mehmood, S, 249  
Metz, J. R, 122  
Mian, S. A, 78  
Miller, M, 180  
Mir, M., 116  
Mirza, H. H, 174  
Mirza, H. T, 43  
Mirza, M. L, 85  
Mishra, R, 92, 99, 100, 107, 109  
Mishra, R. K, 92, 99, 100, 107  
Mohamad, A. B, 252  
Mohamad, N, 97  
Moin ud Din, N, 292  
Moshrefifar, M, 35  
Mubarak, N, 285, 286  
Mudassar M, 71  
Muddasir, M. A, 71  
Muhamad, R. B, 152  
Muhammad, B, 55  
Muhammad, N, 5, 15, 79, 89, 91, 93, 94, 96, 101, 102, 104,  
108, 110, 116, 123, 125, 126  
Muhammad, S, 23  
Muhammed, M, 94  
Mujahid, A, 81, 125  
Mujahid, N, 128  
Munawar., S, 59  
Muñoz, R, 74  
Murtaza, G, 230, 243, 244  
Mushtaq, N, 223  
Mustafa, G, 241  
Mustafa, M, 14, 15, 36  
Mutahir, S, 103  
Mutalib, M. I. A, 5, 79  
Muzaffar, A. T, 134

## N

N. Mahmood, 84  
Nadeem, M, 181, 223, 237  
Nadeem, M. F, 181  
Naeem, B, 156, 169  
Naim, H, 230  
Najeeb, M, 98  
Nambo, M, 115  
Naqvi, I. H, 134, 164  
Naqvi, Q. A, 119

Naqvi, S. M. I. H, 168, 169  
Naqvi, I. H, 128  
Naseem, S, 107, 278  
Naseer, M, 51  
Nasibi, M, 29, 35  
Nasir, H, 3  
Nasir, M, 23, 146  
Nasreen, S, 141, 148  
Nasrullah, A, 123, 125  
Naveed, A, 65  
Naveed, Z, 164  
Nawaz, A, 172  
Nawaz, M. H, 23  
Nawaz, T, 53  
Naz T, 50  
Nazeer, S. U, 169  
Nazir, M. S, 33, 171  
Nazir, S, 170  
Nguyen, D. K, 142  
Niaz, A, 98  
Ninomiya, I, 117  
Nisa, Z. U, 125  
Nishan, U, 73, 91, 93  
Noureen, I, 177, 190, 197  
Nur, O, 233

## O

O'regan, D. O. N. A. L, 209  
O'REGAN,. D. O. N. A. L, 210  
Ocaña, C, 100, 107, 109  
Othman, M, 46  
Özel, R. E, 77  
Ozturk, I, 147, 163

## P

Pakistan, I, 246  
Park, H, 235  
Park, Y. H, 25  
Pei, R, 24  
Piracha, A. H, 119  
Pirone, R, 11  
Piumetti, M, 8  
Polat, A, 144

## Q

Qadeer, F, 292, 293, 294  
Qadir, M. A, 112

Qaim, S. M, 266  
Qamar, M. A, 155  
Qamar., M. A, 165  
Qasim, A, 144  
Qasim, M, 161  
Qazi, I. A, 3  
Qureshi, K, 34

## R

Rafiq, M. A, 56  
Rafiq, M. N, 56  
Rafiq, S, 4, 5  
Rafique, A, 247  
Rafique, M. S, 228, 236  
Rafique, M. Y, 239, 281  
Rahaman, F, 204  
Rahim, A, 15, 73, 80, 91, 93, 98, 104, 108  
Rahman, M. M, 162  
Rahmat, G, 213  
Rais, E, 114  
Rajabi, J, 245  
Ramakrishnaiah, R, 75  
Ramay, S. M, 101, 118, 119, 222  
Rana, A. M, 250, 274  
Rana, M. E, 158  
Rani, S, 185, 186, 187, 191, 201  
Rasheed, A, 220, 228, 239, 240  
Rashid, F, 112  
Rashid, N, 26  
Rashid, R, 291  
Rashid, Y, 128  
Rashidi, M. M, 183  
Rasool, G, 41, 43, 48, 138  
Rathore, S, 46  
Ratyal, N. I, 44  
Rauf, A, 76, 87, 95  
Raza, I, 40, 47  
Raza, M. H, 40, 81, 125  
Raza, M. R, 245, 254  
Raza, M. T, 17  
Raza, R, 215, 217, 247, 248, 250, 274  
Raza, S. A, 142  
Raza, Y, 106, 111  
Raza, Z, 180, 181  
Razaq, A, 101, 121, 222, 223, 246  
Rehman, F, 4, 93  
Rehman, G. U, 75  
Rehman, I. U, 134, 144  
Rehman, M. S, 3, 26  
Rehman, M. S. U, 3

Rehman, S, 275  
Rehman, T. U, 120  
Riasat, A, 205  
Riasat. A, 210  
Riaz, S, 23, 107, 120, 243, 278  
Riazi, H. R, 35  
Rizvi, S. T. R, 180, 184, 195, 202, 203, 206, 207  
RIZVI, S. T. R, 189  
Rozina, C, 240  
Rufai, O. R, 273  
Russo, N, 8, 10, 11, 12, 36  
Ryan, J, 180

## S

S. Nisar, 223, 224, 238, 259  
S. Nisar et al, 217, 218  
S., Kadir, 88  
S., Muzzafar, 83  
S., Rehman, 82, 93  
S.A. Siddiqi, 84  
Sabahat, S, 249  
Sabir, A, 33  
Sabir, O, 46  
Sadiq, M. W, 168  
Sadiq. A, 50  
Saeed, U, 155, 159  
Saeid, A. B, 176  
Sahar, M. R, 216, 242, 264  
Sajid, M, 44  
Sakai, M, 48  
Salako, I. G, 192, 196  
Saleem, A, 130  
Saleem, M, 29, 80, 118, 119, 215, 248  
Saleem, S. S, 292, 294  
Salehi, M, 216  
Salimullah, M, 220, 240  
Salman, A, 159  
Sanaullah, A, 283, 284, 287  
Sandberg, M. O, 233  
Saracco, G, 10, 12  
Saracco, G, 36  
Saravanan, K. V, 56  
Sardar, A, 206, 207  
Sarpoushi, M. R, 29, 35  
Sattar, A, 232, 233, 236, 253  
Satti, S. L, 144  
Sbia, R, 129, 135  
Selmi, R, 133  
Shabbir, F, 47  
Shabbir, J, 285, 286

**Shad, M. Y**, 285  
**Shafiq, M**, 33  
**Shafique, M**, 292, 293, 294  
**Shah, A. T**, 77, 81, 85, 112, 125  
**Shah, F. T**, 284, 289  
**Shah, N**, 46  
Shah, F. T, 289  
**Shahbaz, M**, 41, 128, 129, 133, 134, 135, 138, 139, 140,  
141, 142, 143, 144, 145, 146, 147, 148, 152, 162, 163,  
174  
**Shahbaz. M.Q**, 283  
**Shaheen, F**, 157, 159  
**Shahid, R.,** 94  
**Shahid, M**, 211  
**Shahzad, K**, 29  
**Shahzad, S**, 76, 87, 95, 103, 113  
**Shahzad,,. N M**, 290  
**Shahzadi, L**, 80, 90  
**Shahzadi, M**, 290  
**Shaker, H**, 181, 212  
**Shakir, I**, 119, 244  
**Shamail, S**, 284  
**Shao, G**, 25  
Sharif F, 86  
**Sharif, A. M**, 97  
**Sharif, F**, 122  
**Sharif, M**, 187  
**Sharif, T**, 98  
**Shariff, A. M**, 6  
**Sharma, A**, 99  
**Shaukat, A**, 113, 120  
**Shaukat, R**, 279  
**Shaukat, S. F**, 236, 242, 278  
**Shaukat, S. F**, 215  
**Shehzad, F**, 290  
**Shehzad, K**, 125  
**Shehzaib, U**, 49, 50  
**Sheikh, R**, 25  
**Sherafatian-Jahromi, R**, 143  
**Sherin, L**, 15, 36  
**Shishesaz, M. R**, 29  
**Shuaib, A**, 275  
**Shuja, A**, 129, 131, 136  
**Shujaat, S**, 36  
**Shum, K. P**, 176  
**Siddiqi, S. A**, 76, 83, 87, 90, 107, 118, 119, 237  
**Siddique, M. S**, 69  
**Siddiqui, G. U**, 14  
**Singh, R**, 287  
**Smith, J. D**, 115  
**Sohag, K**, 146

**Sohail, A**, 179, 183, 192, 194, 208, 209, 214  
**Solarin, S. A**, 135, 145  
**Sree, S. P**, 17  
**Steenbergen, P. J**, 122  
**Strålfors, P**, 233  
**Stroosma, O**, 54  
**Sulong, A. B**, 245, 252, 254  
**Sultan, M**, 33

## T

**Tabassum, S**, 84, 114  
**Tabraiz, A**, 188  
**Tabraiz, A**, 211  
**Tahir, B**, 28  
**Tahir, M**, 27, 28, 31, 138  
**Taj, I. A**, 44  
**Tariq, H**, 58  
**Tariq, M**, 105  
**Tayyaba, A**, 289  
**Tiwari, A. K**, 133, 138, 143  
**Tomescu, I**, 179, 182  
**Toprak, M. S**, 94  
**Toufiq, A. M**, 232  
**Treur, J**, 45

## U

**U. H., Kong**, 96  
**Uddin, G. S**, 146, 162  
**Uddin, M. J**, 183  
**Ul Hasan, K**, 233  
**Ul-Haq, N**, 31  
**Ullah, A**, 23  
**Ullah, H**, 45, 73, 250  
**Ullah, M**, 247, 250, 274  
**Ullah, M. K**, 247  
**Ullah, N**, 103, 113  
**Ullah, S**, 23, 46, 89, 97  
**Ullah, Z**, 102, 110  
**Umair, M**, 45  
**Umair, T**, 167  
**ur Rehman, A**, 204, 289  
**ur Rehman, I**, 77, 87, 90  
**ur Rehman, M. J**, 244  
**Usman, A.**, 101, 236  
**Usman, A. R**, 101  
**Usman, M**, 153, 172  
**uz Zaman, W**, 81  
**Uzarewicz-Baig**, 114

**V**

**Vankelecom, I. F.**, 17, 18, 19  
**Vasilescu, A.**, 107, 109  
**Vermoortele, F.**, 19  
**Vranjes, J.**, 220, 230

**W**

**Waheed, S.**, 178, 187, 193  
**Wajid, F.**, 212  
**Wajid, H. A.**, 211  
**Wan, P.**, 96  
**Wang, F. P.**, 232  
**Wang, M.**, 221, 277  
**Wang, X.**, 221  
**Wang, Y.**, 24  
**Warsi, M. F.**, 243, 244  
**Waseem, F.**, 72  
**Waseem, F.**, 66  
**Wilhelm, R.**, 84, 114  
**Willander, M.**, 233, 275  
**Wu, G.**, 7, 9, 20, 21, 22, 24, 32, 116  
**Wu, P.**, 7, 9, 20, 21

**X**

**Xi, Y.**, 221, 277  
**Xiu, Z.**, 9, 32

**Y**

**Yang, B. S.**, 14

**Yang, H.**, 239, 262  
**Yang, W.**, 7, 9, 20, 21, 22, 32  
**Yaqoob, M. Z.**, 119  
**Yaqub, A.**, 249  
**Yar, M.**, 76, 87, 90, 95, 103, 113, 115, 117, 120, 223  
**Yasin, T.**, 33, 105  
**Yi, J.**, 234, 257  
**Younis, A.**, 288  
**Younis, M.**, 184, 189, 195, 202, 203, 206, 207  
**Yousaf, M.**, 227, 255  
**Yu, H. W.**, 262  
**Yu, Z.**, 20, 21  
**Yunus, U.**, 16  
**Yusup, S.**, 13

**Z**

**Z. A. Qureshi.**, 84  
**Zabidi, Z. M.**, 264  
**Zada, A.**, 213  
**Zafar, S.**, 181  
**Zahid, H.**, 159, 161  
**Zahid, Z.**, 181  
**Zaman, A.**, 164  
**Zaman, M. I.**, 98  
**Zhang, L.**, 126  
**Zhang, S.**, 24  
**Zhou, Q.**, 184, 189, 207  
**Zhu, B.**, 250  
**Zhu, B.**, 217  
**Zimmerman, W. B.**, 4  
**Zubair, M.**, 177, 178, 187, 190, 191, 193, 197, 205, 207  
**Zubair, H. M.**, 59

## **Library Information Services**

COMSATS Institute of Information Technology

Defense Road, Off Raiwind Road, Lahore

Ph. 042 111 001 007 Ext. 855, 856

Email: [library@ciitlahore.edu.pk](mailto:library@ciitlahore.edu.pk)